

**PHARMACOMETRICS AND METABOLONOMICS OF SELECTED CHIRAL
FLAVONOIDS**

By

JAIME A. YÁÑEZ

A dissertation submitted in partial fulfillment of
the requirements for the degree of
DOCTOR OF PHILOSOPHY

WASHINGTON STATE UNIVERSITY

Department of Pharmaceutical Sciences

MAY 2008

To the faculty of Washington State University:

The members of the Committee appointed to examine the
dissertation/thesis of JAIME A. YÁÑEZ find it satisfactory and recommend that it be accepted.

Chair

ACKNOWLEDGMENTS

There have been many people that have contributed to the research presented in this thesis. First and foremost, I would like to express my deepest gratitude to my thesis advisor, Dr. Neal M. Davies, for his exceptional guidance, scientific expertise, and encouragement over my graduate at Washington State University. Thanks for keeping me focused, for your patience and advice, and for allowing me to learn from my mistakes and be a better scientist and a better human being.

Special thanks to my Ph.D. committee: Dr. Catherine Elstad, Dr. Arash Hatefi, and Dr. Preston Andrews for encouragement and support in helping me with the preparation of this thesis. I appreciate their excellent guidance.

I also acknowledge all the professors who taught the different classes during my graduate studies, and to the ones that I served as their teaching assistant (TA): Dr. Black, Dr. Elstad, Dr. Lindsey, Dr. Meadows, Dr. Meier, Dr. Quock, and Dr. Vorderstrasse. Thanks for your guidance and for allowing me to learn from your teaching skills.

I wish to thank all my colleagues in the lab: Connie M. Remsberg, Jody Takemoto, Karina Vega-Villa, Esteban Mejía-Meza, Nicole D. Miranda, Jinna Navas, and Dr. Yusuke Ohgami. Thanks for your moral support, friendship, and for listening when I just needed to talk and for sharing a smile when the stress reached harsh levels. Special thanks to past lab members: Dr. Xiao Wei (Shirley) Teng, Dr. Chie Fukuda, Dr. Kathryn Roupe for all their time and patience in teaching me analytical and cell culture techniques. I would also like to acknowledge Dr. M. Laird Forrest for boosting my work ethic and for showing me that it is worthy to go the extra mile at work. Special thanks to Dr. Huimin Lin for her invaluable research support answering

random questions. Special thanks to Dr. Glen S. Kwon, Dr. Steve Martinez, Dr. Chuck Benbrook, Dr. Carolina Torres, Dr. David McCormick, Dr. Canming Xiao, Kelly Hughes, Cara Temple, Margaret (Peggy) Collier, and Kinta Serve for their invaluable contribution during different research projects and manuscript preparation.

Thanks to Paul Winkler from Shimadzu for having time to reply emails and phone calls when the HPLC and LC-MS decided to give up on me. Thanks to Sarah McCord for helping me find obscure citations and research papers.

I acknowledge the support of my graduate research awards: the Sue Harriet Monroe Mullen Graduate Cancer Fellowship, the Dorothy Otto Kennedy Scholarship Fund, the Darden Holzer Memorial Scholarship, the Travel Award for Best Abstract from the Pharmacokinetics, Pharmacodynamics and Drug Metabolism (PPDM) Section of the American Association of Pharmaceutical Sciences (AAPS), the Graduate Student Travel Grant, the Sigma Xi Undergraduate Scholar Award, and the Graduate School Scholar Award from Washington State University, and a teaching assistantship from the Department of Pharmaceutical Sciences of Washington State University.

I also acknowledge the financial support of the Organic Center, Shimadzu Scientific, the Washington Tree Fruit Research Commission, Vetri-Science® Laboratories of Vermont, the Wisconsin Alumni Research Foundation, National Institutes of Health, RS Medical, the IMPACT Center, the Center for Sustainable Agriculture and Natural Resources Bio-Ag Program, the American Cancer Society, the Summer Undergraduate Research Fellowship (SURF) Program at Washington State University, the American Society for Pharmacology and Experimental Therapeutics (ASPET), and Merck Frosst.

Special thanks to Patty Murphy, Paula Marley, Donna Sienkiewicz, Pat Ager, Jerry Emerson, Sarah Kohler, and Jan Brossman for always having your doors open and helping me find the answers I needed.

Last but not least, I would like to thank my grandparents and my uncles. Thanks for the phone calls, the emails, and the conversations on the internet to remind me that you always will be there no matter how far away we might be. Thanks for believing in me and for allowing me to make my dreams come true. This thesis is dedicated to the loving memory of my mother: Lillian Emperatriz Farfán Azpilcueta, who spent all her life teaching me how to believe in myself, and how to keep enjoying life no matter how harsh it turns to be. Thank you.

PHARMACOMETRICS AND METABOLONOMICS OF SELECTED CHIRAL
FLAVONOIDS

Abstract

By Jaime A. Yáñez, Ph.D.
Washington State University
May 2008

Chair: Neal M. Davies

Flavonoids are naturally occurring compounds found in a wide range of plant sources. They exhibit potent anti-cancer, anti-inflammatory, and anti-oxidant activities. Flavanones are a sub-class of flavonoids that present a unique structural characteristic of chirality. The scope of this thesis is centered on these three selected flavanones: hesperetin, naringenin, and eriodictyol. These compounds have been well characterized as achiral entities overlooking their enantiospecific pharmacokinetics and pharmacodynamics.

Simple, stereoselective, accurate, reproducible and isocratic high-performance liquid chromatography (HPLC) methods were developed and validated for the first time for the quantification of hesperetin, naringenin, and eriodictyol enantiomers. These novel methods were applied to assess the pharmacokinetic parameters of these compounds and their content in various fruit juices.

The stereospecific pharmacokinetic parameters following intravenous administration of hesperetin, naringenin, and eriodictyol in male Sprague Dawley rats were characterized and modeled using WinNonlin® pharmacokinetic software. Each flavanone underwent extensive glucuronidation and was predominantly eliminated via non-renal routes. Differences in pharmacokinetic parameters were observed between enantiomers. All three flavanones were

highly distributes into tissues and were moderately extracted by the liver. The detectable serum half-lives of these compounds appears to be relatively short. However, utilizing urinary concentration-time data, much longer elimination half-lives were revealed. The stereospecific content of these compounds in citrus fruit juices exhibited a predominance of the glycoside form and the S(-)-enantiomer and (2S)-epimer of the studied flavanones.

Hesperetin, naringenin, eriodictyol and their corresponding glycosides: hesperidin, naringin, and eriodictyol were tested in several *in vitro* models. It was observed that these compounds exhibit concentration-dependant anti-inflammatory properties, cyclooxygenase-1 and -2 (COX-1 and -2) inhibitory activity, anti-cancer activity, anti-oxidant capacity, anti-adipogenic activity, and inflammatory bowel disease activity. The aglycones were more active than the glycosides, and the activity varied from one another and was dependent on differences in methoxy, and hydroxyl moiety substitutions and glycosylation patterns. Individual enantiomers exhibited activity in an anti-cancer study although this activity was not always additive.

The pharmacodynamic activity of hesperetin, hesperidin, naringenin, and naringin was determined in an experimental model of ulcerative colitis using a novel detection method of phenol red excretion. The oral administration of these selected flavanones reduced the colonic damage in this experimental model. The results parallel the *in vitro* activity indicating that these compounds are bioactive natural products that should undergo further experimental scrutiny.

TABLE OF CONTENTS

ACKNOWLEDGEMENTS	iii
ABSTRACT	vi
LIST OF TABLES	xx
LIST OF FIGURES	xiii
PUBLICATIONS IN SUPPORT OF THIS THESIS	xxx
ABBREVIATIONS AND SYMBOLS	xxxiii

Chapter 1

Literature Review and Background

1.1 Introduction	1-1
1.2 Structure, Formation, Synthesis and Sources of Flavonoids	1-2
1.2.1 Structure	1-2
1.2.2 Formation	1-28
1.2.3 Synthesis and Sources	1-30
1.3 Methods of Analysis and Separation of Chiral Flavanones	1-33
1.3.1 Chromatographic Methods of Separation of Enantiomers	1-36
1.3.1.1 Direct Methods of Analysis: Chiral Stationary Phases (CSP)	1-36
1.3.1.1.1 Chiral Polymer Phases	1-36
1.3.1.1.1.1 Polysaccharide-Derived Columns	1-36
1.3.1.1.1.2 Cyclodextrin and “Mixed” Cyclodextrin Columns	1-39
1.3.1.1.2 Chiral Mobile Phase Additives	1-41
1.3.1.2 Indirect Methods of Analysis: Chiral Derivatization Techniques	1-43
1.3.1.3 Racemization, Enantiomerization and Epimerization	1-44

1.3.1.4 Advantages and Disadvantages of Current Methods	1-47
1.3.2 Flavanones	1-49
1.3.2.1 Dihydrowogonin	1-49
1.3.2.2 Dihydrooroxylin A	1-49
1.3.2.3 Eriocitrin and Eriodictyol	1-49
1.3.2.4 Flavanone	1-51
1.3.2.5 Hesperidin and Hesperetin	1-53
1.3.2.6 Homoeriodictyol	1-55
1.3.2.7 Hydroxyflavanone, 2'-	1-56
1.3.2.8 Hydroxyflavanone, 4'-	1-56
1.3.2.9 Hydroxyflavanone, 6-	1-56
1.3.2.10 Isosakuranetin	1-57
1.3.2.11 Liquiritigenin	1-57
1.3.2.12 Methoxyflavanone, 4'-	1-58
1.3.2.13 Methoxyflavanone, 5-	1-58
1.3.2.14 Methoxyflavanone, 6-	1-58
1.3.2.15 Methoxyflavanone, 7-	1-59
1.3.2.16 Naringin and Naringenin	1-59
1.3.2.17 Narirutin	1-63
1.3.2.18 Neoeriocitrin	1-64
1.3.2.19 Neohesperidin	1-64
1.3.2.20 Pinocembrine	1-65
1.3.2.21 Pinostrobin	1-65

1.3.2.22 Prunin	1-65
1.3.2.23 Sakuranetin	1-66
1.3.2.24 Taxifolin	1-66
1.3.3 Conclusions	1-66
1.4 Hesperidin and Hesperetin	1-67
1.4.1 Anti-Fungal, Anti-Bacterial, and Anti-Viral Activity	1-68
1.4.2 Anti-Inflammatory Activity	1-69
1.4.3 Anti-Oxidant Activity	1-71
1.4.4 Anti-Cancer Activity	1-72
1.4.5 Cyclooxygenase-1 and -2 Inhibitory Activity	1-74
1.4.6 Anti-Adipogenic Activity	1-75
1.4.7 Other Reported Activities	1-76
1.5 Naringin and Naringenin	1-76
1.5.1 Anti-Fungal, Anti-Bacterial, and Anti-Viral Activity	1-77
1.5.2 Anti-Inflammatory Activity	1-79
1.5.3 Anti-Oxidant Activity	1-80
1.5.4 Anti-Cancer Activity	1-81
1.5.5 Cyclooxygenase-1 and -2 Inhibitory Activity	1-85
1.5.6 Anti-Adipogenic Activity	1-85
1.5.7 Cardioprotective Effects	1-86
1.5.8 Effect on Cytochrome P450	1-86
1.5.9 Other Reported Activities	1-89
1.6 Eriocitrin and Eriodictyol	1-91

1.6.1	Anti-Bacterial Activity	1-92
1.6.2	Anti-Inflammatory Activity	1-92
1.6.3	Anti-Oxidant Activity	1-92
1.6.4	Anti-Cancer Activity	1-94
1.6.5	Cyclooxygenase-1 and -2 Inhibitory Activity	1-95
1.6.6	Other Reported Activities	1-95
1.7	Pharmacokinetics and Metabolism of Racemic Hesperidin, Hesperetin, Naringin, Naringenin, Eriocitrin, and Eriodictyol	1-96
1.8	Objectives	1-100
Chapter 2		
Stereospecific Method Development and Validation of Hesperetin, Naringenin, and Eriodictyol		
2.1	Introduction	2-104
2.2	Background	2-105
2.3	Methods	2-106
2.3.1	Chemicals and Reagents	2-106
2.3.2	Chromatographic System and Conditions	2-106
2.3.3	Stock and Working Standard Solutions	2-107
2.3.4	Sample Preparation	2-108
2.3.5	Precision and Accuracy	2-108
2.3.6	Recovery	2-109
2.3.7	Freeze-Thaw and Bench-Top Stability	2-109

2.3.8	Data Analysis	2-110
2.4	Results and Discussion	2-110
2.4.1	Chromatography	2-110
2.4.1.1	Hesperetin	2-110
2.4.1.2	Naringenin	2-112
2.4.1.3	Eriodictyol	2-113
2.4.2	Linearity and Limit of Quantification (LOQ)	2-117
2.4.2.1	Hesperetin	2-117
2.4.2.2	Naringenin	2-117
2.4.2.3	Eriodictyol	2-118
2.4.3	Precision, Accuracy and Recovery	2-118
2.4.3.1	Hesperetin	2-118
2.4.3.2	Naringenin	2-119
2.4.3.3	Eriodictyol	2-121
2.4.4	Stability	2-122
2.4.4.1	Hesperetin	2-122
2.4.4.2	Naringenin	2-122
2.4.4.3	Eriodictyol	2-123
2.5	Conclusions	2-123

Chapter 3

Pre-Clinical Stereospecific Pharmacokinetics of Hesperetin, Naringenin, and Eriodictyol in Rats and their Content in Selected Fruit Juices

3.1 Introduction	3-124
3.2 Background	3-125
3.3 Methods	3-129
3.3.1 Chemicals and Reagents	3-129
3.3.2 Animals and Surgical Procedures	3-130
3.3.3 Pharmacokinetic Study	3-131
3.3.4 Serum and Urine Sample Preparation for HPLC Analysis	3-132
3.3.5 Fruit Juice Analysis	3-133
3.3.6 HPLC Chromatography	3-134
3.3.6.1 Hesperetin Stereospecific Quantification	3-134
3.3.6.2 Naringenin Stereospecific Quantification	3-135
3.3.6.3 Eriodictyol Stereospecific Quantification	3-136
3.3.7 LC/MS Analysis	3-136
3.3.8 Pharmacokinetic Analysis	3-137
3.3.9 Statistical Analysis	3-139
3.4 Results	3-139
3.4.1 Stereospecific Pharmacokinetics of Hesperetin, Naringenin, and Eriodictyol	3-139
3.4.2 Stereospecific Quantification of Hesperidin, Hesperetin, Naringin, Naringenin, Eriocitrin, and Eriodictyol in Fruit Juices	3-151
3.5 Discussion and Conclusions	3-156

Chapter 4

***In Vitro* Pharmacodynamics of Racemic Hesperidin, Hesperetin, Naringin, Naringenin, Eriocitrin and Eriodictyol**

4.1 Introduction	4-163
4.2 Background	4-164
4.3 Methods	4-179
4.3.1 Anti-Inflammatory Properties	4-179
4.3.1.1 Chemicals and Reagents	4-179
4.3.1.2 Cell Culture	4-180
4.3.1.3 Cell Subculture and Cell Number	4-180
4.3.1.4 Anti-Inflammatory Model	4-182
4.3.1.5 Cell Viability	4-182
4.3.1.6 Relevance of the Selected Inflammatory Mediators in the <i>In Vitro</i> Model of Osteoarthritis	4-183
4.3.1.7 Nitric Oxide (NO) Determination	4-186
4.3.1.8 Prostaglandin E ₂ (PGE ₂) Determination	4-186
4.3.1.9 Sulphated Glycosaminoglycan (sGAG) Determination	4-186
4.3.1.10 Matrix Metalloproteinase-3 (MMP-3) Determination	4-187
4.3.1.11 Tumor Necrosis Factor- α (TNF- α) Determination	4-187
4.3.1.12 Statistical Analysis	4-187
4.3.2 Cyclooxygenase-1 and -2 (COX-1 and COX-2) Inhibitory Activity	4-188
4.3.2.1 Description of the Assay	4-188

4.3.2.2	COX Inhibitory Screening	4-189
4.3.2.2.1	Pre-Assay Preparation	4-189
4.3.2.2.2	COX Reactions	4-189
4.3.2.2.3	Performing the Assay	4-190
4.3.2.2.4	Plate Incubation, Developing and Reading	4-191
4.3.3	Inflammatory Bowel Activity	4-191
4.3.3.1	Chemicals and Reagents	4-191
4.3.3.2	Cell Culture	4-191
4.3.3.3	Cell Subculture	4-192
4.3.3.4	Cell Number	4-193
4.3.3.5	Inflammatory Bowel Model	4-193
4.3.4	Anti-Adipogenic Activity	4-194
4.3.4.1	Description of the Assay	4-194
4.3.4.2	Chemicals and Reagents	4-195
4.3.4.3	Cell Culture	4-196
4.3.4.4	Cell Subculture	4-196
4.3.4.5	Differentiation Procedure and Treatment	4-197
4.3.4.6	Lipid Droplet Staining and Quantification	4-198
4.3.5	Anti-Cancer Activity	4-198
4.3.5.1	Chemicals and Reagents	4-198
4.3.5.2	Enantiomer Separation	4-199
4.3.5.3	Cell Culture	4-199
4.3.5.4	Cell Subculture	4-200

4.3.5.5	Cell Number	4-201
4.3.5.6	Alamar Blue Assay	4-202
4.3.5.7	Data Analysis	4-203
4.3.6	Anti-Oxidant Capacity	4-203
4.3.6.1	Chemicals and Reagents	4-203
4.3.6.2	Stock Solutions	4-204
4.3.6.3	Biological Material and Separation of Lipophilic and Hydrophilic Fractions	4-205
4.3.6.4	Enzymatic Hydrolysis	4-207
4.3.6.5	Anti-Oxidant Capacity using a Modified 2,2'-azino-bis(3-ethylbenzthiazoline-6- sulphonic acid (ABTS) Method	4-208
4.3.6.6	Liquid Chromatography-Mass Spectrometry-Electro Spray Ionization (LC-MS- ESI) Analysis	4-209
4.3.6.7	Statistical Analysis	4-210
4.4	Results and Discussion	4-210
4.4.1	Anti-Inflammatory Properties	4-210
4.4.1.1	Cell Viability	4-210
4.4.1.2	Nitric Oxide (NO)	4-211
4.4.1.2.1	Nitrite Levels	4-211
4.4.1.2.2	Nitrate Levels	4-213
4.4.1.3	Prostaglandin E ₂ (PGE ₂)	4-215
4.4.1.4	Sulphated Glycosaminoglycan (sGAG)	4-217
4.4.1.5	Matrix Metalloproteinase-3 (MMP-3)	4-219

4.4.1.6	Tumor Necrosis Factor- α (TNF- α)	4-221
4.4.2	Cyclooxygenase-1 and -2 (COX-1 and COX-2) Inhibitory Activity	4-223
4.4.3	Inflammatory Bowel Activity	4-228
4.4.4	Anti-Adipogenic Activity	4-230
4.4.4.1	Hesperidin and Hesperetin	4-230
4.4.4.2	Naringin and Naringenin	4-231
4.4.4.3	Eriocitrin and Eriodictyol	4-232
4.4.5	Anti-Cancer Activity	4-234
4.4.5.1	Hesperidin and Hesperetin	4-234
4.4.5.2	Naringin and Naringenin	4-234
4.4.5.3	Eriocitrin and Eriodictyol	4-235
4.4.5.4	Determination of Inhibitory Concentration at 50% (IC ₅₀) values	4-236
4.4.5.5	Flavanone Enantiomers	4-237
4.4.6	Anti-Oxidant Capacity	4-241
4.4.6.1	Hesperidin and Hesperetin	4-241
4.4.6.2	Naringin and Naringenin	4-242
4.4.6.3	Eriocitrin and Eriodictyol	4-243
4.4.6.4	Comprehensive Anti-Oxidant Method	4-245
4.4.6.4.1	Percent Hydrolysis of Glycosides	4-245
4.4.6.4.2	LC-MS-ESI Analysis	4-246
4.4.6.4.3	Anti-Oxidant Capacity of Pure Compounds	4-249
4.4.6.4.4	Anti-Oxidant Capacity of Apples	4-251
4.5	Conclusions	4-253

5.4.1	Methods	5-269
5.4.1.1	Stock Solutions Preparation	5-269
5.4.1.2	Treatment and Induction of Colitis	5-269
5.4.1.3	Phenol Red Excretion	5-270
5.4.1.4	Macroscopic Scoring	5-270
5.4.1.5	Statistical Analysis	5-271
5.5	Results and Discussion	5-271
5.5.1	Non-Invasive Method for Assessing Experimental Colitis <i>In Vivo</i> and <i>Ex Vivo</i>	5-271
5.5.2	Application of the Experimental Colitis Model to Flavanones	5-280
 Chapter 6		
Conclusions and Future Directions		
6.1	Summary	6-284
6.2	Future Directions	6-290
References	R-294

LIST OF TABLES

Table 1-1: Comprehensive list of naturally occurring chiral flavanones	1-4
Table 1-2: Comprehensive list of naturally occurring chiral 3-hydroxyflavanones or dihydroflavonols	1-8
Table 1-3: Comprehensive list of chiral flavanones and 3-hydroxyflavanones having complex substituents	1-11
Table 2-1. Within- and between-day precision and accuracy of the assay for hesperetin (HT) enantiomers in rat urine	2-119
Table 2-2. Recovery of hesperetin enantiomers from rat urine	2-119
Table 2-3. Within- and between-day precision and accuracy of the assay for naringenin (N) enantiomers in rat urine	2-120
Table 2-4. Recovery of naringenin enantiomers from rat urine	2-120
Table 2-5. Stereospecific within- and between-day precision and accuracy of the assay for eriodictyol (E) in rat urine	2-121
Table 2-6. Stereospecific recovery of eriodictyol from rat urine	2-121
Table 3-1. Stereospecific pharmacokinetics of hesperetin, naringenin, and eriodictyol in serum after IV administration in rats (20 mg/kg)	3-143
Table 3-2. Stereospecific pharmacokinetics of hesperetin, naringenin, and eriodictyol in urine (and percentage change between serum and urine pharmacokinetic parameters assuming the serum parameters represent 100%) after IV administration in rats (20 mg/kg)	3-150
Table 3-3. Stereospecific hesperidin and hesperetin content (mg per 100 mL juice) in various commercial fruit juices	3-153

Table 3-4. Stereospecific naringin and naringenin content (mg per 100 mL juice) in various commercial fruit juices	3-154
Table 3-5. Stereospecific eriocitrin and eriodictyol content (mg per 100 mL juice) in various commercial fruit juices	3-155
Table 4-1: IC ₅₀ values of deracoxib and flavanones for nitrite reduction	4-213
Table 4-2: IC ₅₀ values of deracoxib and flavanones for nitrate reduction	4-215
Table 4-3: IC ₅₀ values of deracoxib and flavanones for Prostaglandin E ₂ (PGE ₂) reduction	4-217
Table 4-4: IC ₅₀ values of deracoxib and flavanones for Sulfated Glycosaminoglycans (sGAG) reduction	4-219
Table 4-5: IC ₅₀ values of deracoxib and flavanones for Matrix Metalloproteinase-3 (MMP-3) reduction	4-221
Table 4-6: IC ₅₀ values of deracoxib and flavanones for Tumor Necrosis Factor- α (TNF- α) reduction	4-223
Table 4-7: IC ₅₀ values of ibuprofen and flavanones for COX-1 inhibition	4-225
Table 4-8: IC ₅₀ values of ibuprofen, etodolac, and flavanones for COX-2 inhibition	4-227
Table 4-9: IC ₅₀ values of the different flavanones for Prostaglandin E ₂ (PGE ₂) reduction	4-230
Table 4-10: IC ₅₀ values of the different flavanones for Oil Red O Stained Material (OROSM) reduction	4-233
Table 4-11: IC ₅₀ values (μ g/ml) of the racemic hesperetin, naringenin, and eriodictyol, and 5-fluorouracil (5-FU) as positive control across different cancer cell lines	4-238

Table 4-12: IC ₅₀ (µg/ml) and anti-radical efficiency values (AE) (µg/ml) ⁻¹ values of the racemic hesperetin, naringenin, and eriodictyol, and α-tocopherol as positive control	4-245
Table 4-13: Trolox® equivalent anti-oxidant capacity (TEAC) expressed as mM Trolox® of phloridzin, phloretin, quercitrin, rutin, and quercetin before enzymatic hydrolysis (BEH) and after enzymatic hydrolysis (AEH)	4-250
Table 4-14: Trolox® equivalent anti-oxidant capacity (TEAC) expressed as mM Trolox® of apples before enzymatic hydrolysis (BEH) and after enzymatic hydrolysis (AEH). Total is the sum of the hydrophilic, lipophilic, and insoluble fractions	4-253
Table 5-1: Criteria for macroscopic scoring of colonic damage	5-264
Table 5-2. Primer Sequences for Rat Quantitative Polymerase Chain Reaction (QPCR)	5-268

LIST OF FIGURES

Figure 1-1: Spatial disposition of the enantiomers of chiral flavanones	1-2
Figure 1-2: Chemical structure of the chiral 3-hydroxyflavanones or dihydroflavonols	1-3
Figure 1-3: Phenylpropanoid pathway and chalcone synthesis	1-28
Figure 1-4: Synthetic Pathway of chiral flavanones and other flavonoid derivatives ..	1-29
Figure 1-5: Relationship between flavanones, isoflavonoids, stilbenes, lignans and other flavonoid derivatives formation	1-30
Figure 1-6: Structures of (A) hesperetin, (B) naringenin and (C) eriodictyol	1-33
Figure 1-7: Structure of hesperidin. *Denotes chiral center	1-67
Figure 1-8: Structure of naringin. *Denotes chiral center	1-77
Figure 1-9: Structure of eriocitrin. *Denotes chiral center	1-91
Figure 2-1: Representative chromatograms, of (A) drug-free urine, (B) urine containing hesperetin enantiomers each with concentration of 1.0 µg/ml and the internal standard (IS), and (C) 6 hour rat urine sample containing hesperetin enantiomers and the IS	2-110
Figure 2-2: Representative chromatograms, of (A) drug-free urine, (B) urine containing naringenin enantiomers each with concentration of 10 µg/ml and the internal standard (IS), and (C) 8 h rat urine sample containing naringenin enantiomers and the IS	2-112
Figure 2-3: Representative chromatograms of (A) drug-free urine, (B) urine containing eriodictyol with concentration of 10 µg/ml and the internal standard (IS), (C) 10 h rat urine sample containing eriodictyol and the IS after oral ingestion of lemonade	2-114

- Figure 2-4:** Representative chromatograms of thyme (*Thymus vulgaris*) containing predominantly S(-)-eriodictyol2-115
- Figure 3-1.** Concentration-time profile in serum plot of hesperetin (R(+)-hesperetin (□), R(+)-hesperetin glucuronide (■), S(-)-hesperetin (Δ), and S(-)-hesperetin glucuronide (▲)) after IV administration of racemic hesperetin (20 mg/kg) to rats3-140
- Figure 3-2.** Concentration-time profile in serum plot of hesperetin (R(+)-naringenin (□), R(+)-naringenin glucuronide (■), S(-)-naringenin (Δ), and S(-)-naringenin glucuronide (▲)) after IV administration of racemic naringenin (20 mg/kg) to rats3-141
- Figure 3-3.** Concentration-time profile in serum plot of eriodictyol (R(+)-eriodictyol (□), R(+)-eriodictyol glucuronide (■), S(-)-eriodictyol (Δ), and S(-)-eriodictyol glucuronide (▲)) after IV administration of racemic eriodictyol (20 mg/kg) to rats3-141
- Figure 3-4.** Rate of urinary excretion plot of hesperetin (R(+)-hesperetin (□), R(+)-hesperetin glucuronide (■), S(-)-hesperetin (Δ), and S(-)-hesperetin glucuronide (▲)) after IV administration of racemic hesperetin (20 mg/kg) to rats3-147
- Figure 3-5.** Rate of urinary excretion plot of naringenin (R(+)-naringenin (□), R(+)-naringenin glucuronide (■), S(-)-naringenin (Δ), and S(-)-naringenin glucuronide (▲)) after IV administration of racemic naringenin (20 mg/kg) to rats3-148
- Figure 3-6.** Rate of urinary excretion plot of eriodictyol (R(+)-eriodictyol (□), R(+)-eriodictyol glucuronide (■), S(-)-eriodictyol (Δ), and S(-)-eriodictyol glucuronide (▲)) after IV administration of racemic eriodictyol (20 mg/kg) to rats3-148
- Figure 4-1:** Schematic of the methodology of the novel comprehensive anti-oxidant activity method4-206

- Figure 4-2:** The number of viable canine chondrocytes following treatment of the different flavanones4-211
- Figure 4-3:** Nitrite production (means \pm SEM) in the cell culture medium from canine chondrocytes 72 h after the addition of the different flavanones and deraxocib as positive control at concentrations 1-250 μ g/ml with inteleukin-1 β (IL-1 β) (100 μ L of 100 ng/ml)4-212
- Figure 4-4:** Nitrate production (means \pm SEM) in the cell culture medium from canine chondrocytes 72 h after the addition of the different flavanones and deraxocib as positive control at concentrations 1-250 μ g/ml with IL-1 β (100 μ L of 100 ng/ml)4-214
- Figure 4-5:** Prostaglandin E₂ (PGE₂) production (means \pm SEM) in the cell culture medium from canine chondrocytes 72 h after the addition of the different flavanones and deraxocib as positive control at concentrations 1-250 μ g/ml with IL-1 β (100 μ L of 100 ng/ml)4-216
- Figure 4-6:** Sulfated glycosaminoglycans (sGAG) production (means \pm SEM) in the cell culture medium from canine chondrocytes 72 h after the addition of the different flavanones and deraxocib as positive control at concentrations 1-250 μ g/ml with IL-1 β (100 μ L of 100 ng/ml)4-218
- Figure 4-7:** Matrix metalloproteinase-3 (MMP-3) production (means \pm SEM) in the cell culture medium from canine chondrocytes 72 h after the addition of the different flavanones and deraxocib as positive control at concentrations 1-250 μ g/ml with IL-1 β (100 μ L of 100 ng/ml)4-220

Figure 4-8: Tumor necrosis factor- α (TNF- α) production (means \pm SEM) in the cell culture medium from canine chondrocytes 72 h after the addition of the different flavanones and deracoxib as positive control at concentrations 1-250 μ g/ml with IL-1 β (100 μ L of 100 ng/ml)4-222

Figure 4-9: Cyclooxygenase-1 (COX-1) activity (means \pm SEM) after the addition of the different flavanones and ibuprofen as positive control at concentrations 1-250 μ g/ml4-224

Figure 4-10: Cyclooxygenase-2 (COX-2) activity (means \pm SEM) after the addition of the different flavanones, ibuprofen and etodolac as positive control at concentrations 1-250 μ g/ml4-226

Figure 4-11: Cyclooxygenase-2 (COX-2) to cyclooxygenase-1 (COX-1) ratio (means \pm SEM) of the different flavanones, ibuprofen and etodolac as positive control at concentrations 1-250 μ g/ml4-228

Figure 4-12: Prostaglandin E₂ (PGE₂) production (means \pm SEM) in the cell culture medium from colorectal adenocarcinoma (HT-29) cells after the addition of the different flavanones at concentrations 1-250 μ g/ml with TNF- α (100 μ L of 100 ng/ml)4-229

Figure 4-13: Effects of flavanones on oil red O stained material (OROSM) in 3T3-L1 pre-adipocytes. 3T3-L1 pre-adipocytes were harvested 8 days after the initiation of differentiation and were stained with oil red O (A). Cells were treated with 0–250 μ g/ml of hesperidin or hesperetin (B) for 72 h at 37°C in a humidified 5% carbon dioxide (CO₂) incubator4-231

Figure 4-14: Effects of flavanones on oil red O stained material (OROSM) in 3T3-L1 pre-adipocytes. 3T3-L1 pre-adipocytes were harvested 8 days after the initiation of differentiation and were stained with oil red O. Cells were treated with 0–250 µg/ml of naringin or naringenin for 72 h at 37°C in a humidified 5% CO₂ incubator4-232

Figure 4-15: Effects of flavanones on oil red O stained material (OROSM) in 3T3-L1 pre-adipocytes. 3T3-L1 pre-adipocytes were harvested 8 days after the initiation of differentiation and were stained with oil red O. Cells were treated with 0–250 µg/ml of eriocitrin or eriodictyol for 72 h at 37°C in a humidified 5% CO₂ incubator4-233

Figure 4-16: Effects of hesperidin (A) and hesperetin (B) in the viability of different cancer cell lines (means ± SEM)4-234

Figure 4-17: Effects of naringin (A) and naringenin (B) in the viability of different cancer cell lines (means ± SEM)4-235

Figure 4-18: Effects of eriocitrin (A) and eriodictyol (B) in the viability of different cancer cell lines (means ± SEM)4-235

Figure 4-19: Effects of collected hesperetin enantiomers (A), naringenin enantiomers (B), and eriodictyol enantiomers (C) in the viability of hepatoma (HepG2) cells (means ± SEM)4-239

Figure 4-20: Trolox® equivalent anti-oxidant capacity (TEAC) of hesperidin and hesperetin (means ± SEM)4-242

Figure 4-21: Trolox® equivalent anti-oxidant capacity (TEAC) of naringin and naringenin (means ± SEM)4-243

- Figure 4-22:** Trolox® equivalent anti-oxidant capacity (TEAC) of eriocitrin and eriodictyol (means \pm SEM)4-244
- Figure 4-23:** Chromatogram of (A) standard mixture of phenolic compounds (10 μ g/ml of each compound) and daidzein (internal standard, IS) by liquid chromatography (LC) (280 nm) (B) red delicious apple skin. 1=Gallic acid, 2=Catechin, 3=Chlorogenic acid, 4=epicatechin, 5=quercetin-3-rutinoside (rutin), 6=quercetin-3-rhamnoside (quercitrin), 7=phloridzin, 8=daidzein (IS), 9=quercetin, and 10=phloretin4-247
- Figure 4-24:** Concentrations of (A) quercitrin, (B) rutin, (C) quercetin, (D) phloridzin, and (E) phloretin in conventional and organic apples skin and flesh before enzymatic hydrolysis (BEH) and after enzymatic hydrolysis (AEH)4-248
- Figure 4-25:** Trolox® equivalent anti-oxidant capacity (TEAC) expressed as mM Trolox® of phloridzin, phloretin, quercitrin, rutin, and quercetin before enzymatic hydrolysis (BEH) and after enzymatic hydrolysis (AEH)4-250
- Figure 4-26:** Trolox® equivalent anti-oxidant capacity (TEAC) expressed as mM Trolox® of apples before enzymatic hydrolysis (BEH) and after enzymatic hydrolysis (AEH)4-252
- Figure 5-1:** Typical calibration curve of phenol red in urine5-267
- Figure 5-2:** Macroscopic colonic damage score after administration of TNBS to rats (n=5, Mean \pm SEM)5-271
- Figure 5-3:** Phenol red excretion in urine of rats over time (n=5, Mean \pm SEM)5-272
- Figure 5-4:** Oral and rectal administration of phenol red to rats with colitis (n=5, Mean \pm SEM)5-272

- Figure 5-5:** Excretion of ^{51}Cr -EDTA in urine of rats treated with indomethacin 10 mg/kg 24 h post-dose (n=5, Mean +/- SEM)5-273
- Figure 5-6:** Excretion of phenol red in urine of rats treated with indomethacin 10 mg/kg 24 h post-dose (n=5, Mean \pm SEM)5-273
- Figure 5-7:** Effects of 5-ASA and dexamethasone on macroscopic damage score after acute colitis (n=5, Mean \pm SEM)5-274
- Figure 5-8:** Effects of 5-ASA and dexamethasone on phenol red excretion in acute colitis (n=5, Mean \pm SEM)5-274
- Figure 5-9:** Macroscopic colonic damage of colitis in rats (n=5, Mean \pm SEM)5-275
- Figure 5-10:** Effects of reactivation of experimental colitis on urinary excretion of oral phenol red excretions (n=5, Mean \pm SEM)5-276
- Figure 5-11.** Exacerbation of experimental colitis in by diclofenac (n=5, Mean \pm SEM)5-276
- Figure 5-12.** Effects of diclofenac on experimental colitis and urinary excretion of oral administered phenol red (n=5, Mean \pm SEM)5-277
- Figure 5-13.** Mitochondrial oxidative deoxyribonucleic acid (DNA) damage in rat colonic tissue after administration of trinitrobenzene sulphonic acid (TNBS) and protection with various pharmacological agents (n=3, Mean \pm SD)5-278
- Figure 5-14.** Macroscopic colonic damage score of rats treated with dexamethasone (10 mg/kg), or racemic flavanones (20 mg/kg) 24 h post-colitis induction with TNBS (n=5, Mean \pm SEM)5-281

Figure 5-15. Excretion of phenol red in urine of rats treated with dexamethasone (10 mg/kg), or racemic flavanones (20 mg/kg) 24 h post-colitis induction with TNBS (n=5, Mean \pm SEM)

.....5-282

PUBLICATIONS IN SUPPORT OF THIS THESIS

Papers Published

Yáñez JA, Andrews PK, Davies NM. Methods of Analysis and Separation of Chiral Flavonoids. *Journal of Chromatography B: Analytical Technologies in the Biomedical and Life Sciences* 2007; 848(2):159-181. Review.

Yáñez JA, Remsberg CM, Miranda ND, Vega-Villa KR, Andrews PK, Davies NM. Pharmacokinetics of Selected Chiral Flavonoids: Hesperetin, Naringenin, and Eriodictyol in Rats and their Disposition in Fruit Juices. *Biopharmaceutics and Drug Disposition* 2007; In press.

Yáñez JA, Miranda NM, Remsberg CM, Ohgami Y, Davies NM. Stereospecific high-performance liquid chromatographic analysis of eriodictyol in urine. *Journal of Pharmaceutical and Biomedical Analysis* 2007; 43(1):255-262

Yáñez JA, Teng XW, Roupe KA, Davies NM. Alternative Methods for Assessing Experimental Colitis In Vivo and Ex Vivo. *Journal of Medical Sciences* 2006; 6(3):356-365.

Yáñez JA, Davies NM. Stereospecific high-performance liquid chromatographic analysis of naringenin in urine. *Journal of Pharmaceutical and Biomedical Analysis* 2005; 39(1-2):164-169.

Yáñez JA, Teng XW, Roupe KA, Davies NM. Stereospecific high-performance liquid chromatographic analysis of hesperetin in biological matrices. *Journal of Pharmaceutical and Biomedical Analysis* 2005; 37(3):591-5.

Conference Abstracts

Yáñez JA, Ohgami Y, Remsberg CM, Davies NM. Eriocitrin and Eriodictyol: Anti-Cancer Activity, Anti-Oxidant Capacity, and Stereospecific Disposition in Rats, Humans, and Lemonade. American Association of Pharmaceutical Sciences Annual Meeting, San Antonio, TX, October 29 - November 2, 2006. *The AAPS Journal* 2006;8(S2) Abstract M1351.

Yáñez JA, Miranda NM, Villa-Romero KS, Ohgami Y, Davies NM. Stereospecific Disposition and Anti-Cancer /Anti-Oxidant Activity of the Chiral Flavonoids Eriocitrin and Eriodictyol. The 15Pth World Congress of Pharmacology, International Union of Pharmacology (IUPHAR), Beijing, China, July 2-7, 2006. *Acta Pharmacologica Sinica* 2006:Supplement 1:219 Abstract P170068.

Yáñez JA, Fukuda C, Davies NM. Naringenin and Naringin: Anti-Cancer Activity and Stereospecific Disposition in Rats, Humans, and Citrus Fruit Juices. American Association of Pharmaceutical Sciences Annual Meeting, Nashville, TN, November 8, 2005. *The AAPS Journal* 2005;7(S2) Abstract T3262.

Yáñez JA, Fukuda C, Roupe KA, Davies NM. Hesperetin and Hesperidin: Anti-Cancer Activity and Stereospecific Disposition in Rats, Humans, and Citrus Fruit Juices. American Association of Pharmaceutical Sciences Annual Meeting, Nashville, TN, November 8, 2005. *The AAPS Journal 2005*:7(S2) Abstract T3264.

Yáñez JA, Roupe KA, Fukuda C, Teng XW, Davies NM. Stereospecific Disposition of the Chiral Flavonoids Hesperetin and Hesperidin in Rodents, Humans, and Citrus Fruit Juices. Canadian Society of Pharmaceutical Sciences Annual Meeting, Vancouver, British Columbia, June 9, 2004. *Journal of Pharmacy and Pharmaceutical Sciences 2004*; 7(2):76.

Manuscripts in Preparation

The following manuscripts are in preparation and intended to be submitted to *Journal of Agricultural and Food Chemistry*, *Phytotherapy Research*, and *Journal of Pharmaceutical Sciences*.

Yáñez JA, Andrews PK, Davies NM. A Comprehensive Method for Measuring Anti-Oxidant Activity: Application to Apples. In preparation from thesis, 2007.

Yáñez JA, Remsberg CM, Miranda ND, Vega-Villa KR, Andrews PL, Davies NM. *In Vitro* Anti-Inflammatory, Anti-Cancer, Anti-Adipogenic, and Anti-Oxidant Activity of Three Selected Flavanones: Hesperetin, Naringenin, Eriodictyol and their Corresponding Glycosides. In preparation from thesis, 2007.

Yáñez JA, Remsberg CM, Mejia-Meza EI, Takemoto JK, Vega-Villa KR, Davies NM. Amelioration of Experimental Colitis *In Vitro* and *In Vivo* by Three Structurally Similar Selected Flavanones: Hesperetin, Naringenin, Eriodictyol and their Corresponding Glycosides. In preparation from thesis, 2007.

ABBREVIATIONS AND SYMBOLS

3CLpro	3C-like cysteine protease
5-FU	5-fluorouracil
α	Alpha
A3G	Anthocyanidin-3-O-glucosyltransferase
AAPH	2,2'-azo-bis(2-amidinopropane)dihydrochloride
ABTS	2,2'-azinobis-(3-ethyl-benzothiazoline-6-sulfonic acid)
ACF	Aberrant crypt foci
AchE	Acetylcholinesterase
AChE:Fab'	Acetylcholinesterase:Fab' Conjugate
ACII	Adjuvant–carrageenan-induced inflammation
ADP	Adenosine diphosphate
AEH	After enzymatic hydrolysis
AgNOR	Silver-stained nucleolar-organizer-region-associated proteins
ANOVA	Analysis of variance
AOM	Azoxymethane
AP-1	Activator protein 1
APCI	Atmospheric pressure chemical ionization
ATP	Adenosine triphosphate
ATPase	Enzyme that catalyze the decomposition of (ATP)
AUC	Area under the curve
β	Beta
Bak	Bcl-2 homologous antagonist killer

Bax	Bcl-2 associated X protein
Bcl-2	B-cell lymphoma 2
BEH	Before enzymatic hydrolysis
BHP	Butyl hydroperoxide
BUdR	5-bromodeoxyuridine
BW	Body weight
C	Carbon
C4H	Cinnamate 4-hydroxylase
Caco-2	Colon adenocarcinoma cell line
CASP3	Caspase-3
CAT	Catalase
CCl ₄	Carbon tetrachloride
CD-1	Cluster of differentiation-1
CDK	Cyclin-dependent kinases
CHI	Chalcone isomerase
CHP	Cumene hydroperoxide
ChS	Chromone synthase
CL _h	Hepatic clearance
CL _r	Renal clearance
CL _{tot}	Total clearance
CO ₂	Carbon dioxide
CoA	Coenzyme A
CoASH	Coenzyme A

Conc.	Concentration
CoV	Coronavirus
COX	Cyclooxygenase
CS	Coumarin synthase
CSP	Chiral stationary phase
CTA	Cellulose triacetate
Cu	Copper
CTnT	Cardiac troponin T
CV	Coefficient of variation
CYP/CYP450	Cytochrome P450
DC	Dien conjugate
DNA	Deoxyribonucleic acid
DMEM	Dulbecco's modified Eagle's medium
DMEM/F-12	Dulbecco's modified Eagle's medium/nutrient mixture F-12 Ham
DMSO	Dimethyl sulfoxide
DPPH	1,1-diphenyl-2-picrylhydrazyl
DTT	Dithiothreitol
DW	Dry weight
ϵ	Epsilon
EC ₅₀	Half maximal effective concentration
ECG	Electrocardiogram
EDTA	Ethylenediaminetetraacetic acid
EGM-2	Epithelial growth medium

EIA	Enzyme immuno assay
ELISA	Enzyme-linked immunosorbent assay
ER	Estrogen receptor
ER α	Estrogen receptor alpha
ER β	Estrogen receptor beta
ESI	Electrospray ionization
F3D	Flavanone-3-dioxygenase
FDA	United States Food and Drug Administration
Fe	Iron
FS	Flavonol synthase
γ	Gamma
g	gram
GLUT4	Facilitated glucose transporter member 4
GPDH	Glycerol-3-phosphate dehydrogenase
GSH	Glutathione
GSHPx	Glutathione peroxidase
Gy	Gray, unit of radiation
h	hour
H ₂ O ₂	Hydrogen peroxide
HaCaT	Human keratinocyte cell line
HCl	Hydrochloric acid
HDA	Hydrogen-donating ability
HDL	High-density lipoprotein

HEPES	N-(2-hydroxyethyl) piperazine-N'-(2-ethane sulfonic acid)
HIV	Human immunodeficiency virus
HMACF	High multiplicity aberrant crypt foci
HPLC	High performance liquid chromatography
HSV	Herpes simplex virus
HUVEC	Human umbilical vein endothelial cells
IC ₅₀	Half maximal inhibitory concentration
ICAM-1	Intercellular adhesion molecule-1
ID ₅₀	Half maximal inhibitory dose
IFS	Isoflavonoid synthase
IκB	Nuclear factor of kappa light polypeptide gene enhancer in B-cells inhibitor
IκBα	Nuclear factor alpha of kappa light polypeptide gene enhancer in B-cells inhibitor
IL-1β	Interleukin-1 beta
IL-1Rα	Interleukin-1 receptor alpha
iNOS	Inducible nitric oxide synthase
i.p.	Intraperitoneal
IS	Internal standard
ISO	Isoproterenol
IV	Intravenous
κ	Kappa
k _e	Elimination rate constant

K4R	Kaempferol-4-reductase
LC	Liquid chromatography
LC-MS or LC/MS	Liquid chromatography couples with mass spectrometry
LDH	Lactate dehydrogenase
LDL	Low-density lipoprotein
LO	Leucocyanidin oxygenase
LOD	Limit of detection
LOQ	Limit of quantification
LPS	Lipopolysaccharide
LS	Lignan synthase
LTB ₄	Leukotriene B ₄
MAPK	Mitogen-activated protein kinase
MCCTA	Microcrystalline cellulose triacetate
MCP	Monocyte chemotactic protein
MeCD	6 ^A -N-allylamino-6 ^A -deoxy)permethylated β-cyclodextrin
MEKC	Micellar electrokinetic chromatography
MIC	Maximum inhibitory concentration
min	Minute
ml	Milliliter
mM	Millimol per liter
MMP	Matrix metalloproteinase
Mn	Manganese
MNAN	N-methyl-N-amyl nitrosamine

MNBNC	Binucleate cells bearing micronuclei
mRNA	Mitochondrial ribonucleic acid
MTT	3-(4,5-dimethylthiazol-2-yl)-2,5-diphenyltetrazolium bromide
MW	Molecular weight
NA	Not applicable
NaOH	Sodium hydroxide
NHEK	Normal human epidermal keratinocyte
NFκB	Nuclear factor-kappa B
NFS	Neoflavonoid synthase
ng/ml	Nanogram per milliliter
NO	Nitric oxide
NO ₂	Nitrite
NOS-2	Nitric oxide synthase 2
NSAID	Non-steroidal anti-inflammatory drug
NSV	Neurovirulent Sindbis strain
O ₂	Oxygen
OH	Hydroxyl group
OH-BBN	N-butyl-N-(4-hydroxybutyl)nitrosamine
ONOO ⁻	Peroxynitrite
OTM	Olive tail moment
PAL	Phenylalanine ammonia-lyase
PAR	Peak area ratio
PARP	Poly ADP-ribose polymerase

PBMC	Peripheral blood mononuclear cells
PBS	Phosphate buffer saline
Pf-3	Parainfluenza virus type 3
PG	Prostaglandin
pg	Picogram
PGE ₂	Prostaglandin E ₂
PGH ₂	Prostaglandin H ₂
pH	Power of hydrogen
PI3K	Phosphoinositide 3-kinase
Q	Hepatic blood flow
QPCR	Quantitative PCR
ROS	Reactive oxygen species
rpm	Revolutions per minute
RT	Retention time
RSD	Relative standard deviation
RSV	Respiratory syncytial virus
RT-PCR	Reverse transcriptase polymerase chain reaction
SAR	Structure-activity relationship
SARS	Severe acute respiratory syndrome
SD	Standard deviation
sec	Second
SEM	Standard error of the mean
SDC	Severely damaged cells

SDS	Sodium dodecyl sulfate
SFC	Supercritical fluid chromatography
sGAG	Sulfated glycosaminoglycans
SHC	Thiol group (SH) concentration
SOD	Superoxide dismutase
$t_{1/2}$	Half life
TBARS	Thiobarbituric acid reactive substances
TEAC	Trolox® equivalent anti-oxidant capacity
TFA	Trifluoroacetic acid
TNBS	Trinitrobenzenesulfonic acid
TNF- α	Tumor necrosis-alpha
TSC	Total scavenger capacity
μg	Microgram
μM	Micromol per liter
μl	Microliter
UV	Ultraviolet
USDA	United States Department of Agriculture
VCAM-1	Vascular cell adhesion molecule-1
V_{ss}	Volume of distribution at steady state
VEGF	Vascular endothelial growth factor
XLogP	Experimental octanol to water partition coefficient
Zn	Zinc

CHAPTER I Literature Review and Background

1.1 INTRODUCTION

The first segment of this chapter reviews the molecular structures, and natural sources of three specific flavanones: hesperetin, naringenin, and eriodictyol. Additionally, the current knowledge pertaining to the stereospecific methods of separation, the pharmacologically activity, and pharmacokinetic studies of these three chiral flavonoids are reviewed and evaluated in this chapter.

as diastereoisomers or epimers that have the opposite configuration at only one of two or more tetrahedral stereogenic centers present in the respective molecular entities.

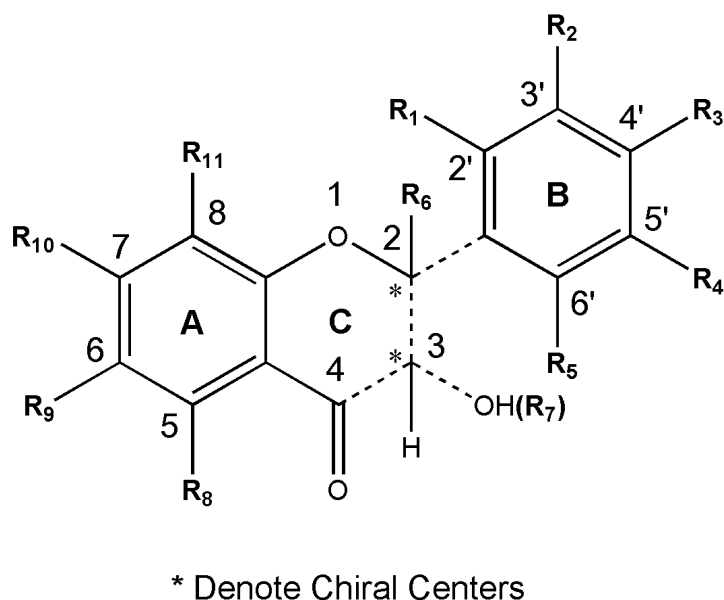


Figure 1-2: Chemical structure of the chiral 3-hydroxyflavanones or dihydroflavonols

The vast majority of chiral flavanones (Table 1-1, 1-2, and 1-3) can now be purchased from chemical companies, but they are almost exclusively available only as racemates (equivalent proportions of both enantiomers or epimers). To our knowledge there are only three stereochemically pure flavanones that are currently marketed and commercially available internationally. Eriodictyol is marketed as the pure S-(-)-enantiomer by Fluka (Buchs, Switzerland); however it has been demonstrated by Caccamese *et al.* that the marketed eriodictyol is indeed a R,S mixture of eriodictyol enantiomers (Caccamese *et al.*, 2005). Homoeriodictyol is marketed as the pure S-(-)-enantiomer by Indofine Chemical Company (Hillsborough, NJ), Extrasynthese (Genay, France), and ITI International Inc. (Miami, FL). Finally, taxifolin is marketed as the pure 2R, 3R-enantiomer by Alexis Biochemicals (San Diego, CA), Fluka (Buchs, Switzerland), and Extrasynthese (Genay, France).

Table 1-1: Comprehensive list of naturally occurring chiral flavanones

Chiral Flavanone	Other name(s)	R ₁	R ₂	R ₃	R ₄	R ₅	R ₆	R ₇	R ₈	R ₉
		2'	3'	4'	5'	3	5	6	7	8
Aervanone	Liquiritigenin-8-galactose	H	H	OH	H	H	H	H	OH	galactose
Alpinetin	7-hydroxy-5-methoxyflavanone	H	H	H	H	H	OCH ₃	H	OH	H
Ampelopsin	3,5,7,3',4',5'-hexahydroxyflavanone, Dihydromyricetin	H	OH	OH	OH	OH	OH	H	OH	H
Aromadendrin	3,5,7,4'-tetrahydroxyflavanone, 2,3-dihydrokaempferol	H	H	OH	H	OH	OH	H	OH	H
Artocarpanone	5,2',4'-trihydroxy-7-methoxyflavanone	OH	H	OH	H	H	OH	H	OCH ₃	H
Carthamidin	4',5,6,7-tetrahydroxyflavanone	H	H	OH	H	H	OH	OH	OH	H
Cryptostrobin	5,7-dihydroxy-8-methylflavanone	H	H	H	H	H	OH	H	OH	CH ₃
Cyrtominetin	5,7,3',4'-tetrahydroxy-6,8-dimethylflavanone	H	OH	OH	H	H	OH	CH ₃	OH	CH ₃
Cyrtopterinetin	6,8-dimethyl-4',5,7-trihydroxyflavanone	H	H	OH	H	H	OH	CH ₃	OH	CH ₃
Desmethoxymatteucinol	5,7-dihydroxy-6,8-dimethylflavanone	H	H	H	H	H	OH	CH ₃	OH	CH ₃
Didymin	Isosakuranetin-7-O-rutinoside, Neoponcirin	H	H	OCH ₃	H	H	OH	H	O-rutinoside	H
Didymocarpin	7-hydroxy-5,6,8-trimethoxyflavanone	H	H	H	H	H	OCH ₃	OCH ₃	OH	OCH ₃
Dihydrokaempferide	3,5,7-trihydroxy-4'-methoxyflavanone	H	H	OCH ₃	H	OH	OH	H	OH	H
Dihydrooroxylin A	5,7-dihydroxy-6-methoxyflavanone	H	H	H	H	H	OH	OCH ₃	OH	H
Dihydorobinetin	3,7,3',4',5'-pentahydroxyflavanone	H	OH	OH	OH	OH	H	H	OH	H
Dihydrotectochrysin	5-hydroxy-7-methoxyflavanone	H	H	H	H	H	OH	H	OCH ₃	H
Dihydrowogonin	5,7-dihydroxy-8-methoxyflavanone	H	H	H	H	H	OH	H	OH	OCH ₃
Dimethoxyflavanone	7,8-dimethoxyflavanone	H	H	H	H	H	H	H	OH	OH

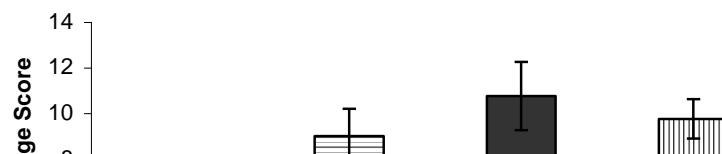


Table 1-1 Cont'd: Comprehensive list of naturally occurring chiral flavanones

Chiral Flavanone	Other name(s)	R ₁	R ₂	R ₃	R ₄	R ₅	R ₆	R ₇	R ₈	R ₉
		2'	3'	4'	5'	3	5	6	7	8
Isosakuranetin	5,7-dihydroxy-4'-methoxyflavanone, Acacetin, Linarigenin	H	H	OCH ₃	H	H	OH	H	OH	H
Kanakugin	5,6,7,8-tetramethoxyflavanone	H	H	H	H	H	OCH ₃	OCH ₃	OCH ₃	OCH ₃
Lawinal	5,7-dihydroxy-6-formyl-8-methylflavanone	H	H	H	H	H	OH	CHO	OH	CH ₃
Liquiritigenin	7,4'-dihydroxyflavanone	H	H	OH	H	H	H	H	OH	H
Liquiritin	Liquiritigenin-4'-O-glucoside	H	H	O-glucose	H	H	H	H	OH	H
Matteucinol	5,7-dihydroxy-6,8-dimethyl-4'-methoxyflavanone, 4'-methylfarrerol	H	H	OCH ₃	H	H	OH	CH ₃	OH	CH ₃
Methoxyflavanone, 4'	4'-methoxyflavanone	H	H	OCH ₃	H	H	H	H	H	H
Methoxyflavanone, 5	5-methoxyflavanone	H	H	H	H	H	OCH ₃	H	H	H
Methoxyflavanone, 6	6-methoxyflavanone	H	H	H	H	H	H	OCH ₃	H	H
Methoxyflavanone, 7	7-methoxyflavanone, 7-hydroxyflavanone methylether	H	H	H	H	H	H	H	OCH ₃	H
Naringenin	5,7,4'-trihydroxyflavanone	H	H	OH	H	H	OH	H	OH	H
Naringin	Naringenin-7-O-neohesperidoside	H	H	OH	H	H	OH	H	O-neohesperidose	H
Narirutin	Naringenin-7-O-rutinoside, Isonaringenin	H	H	OH	H	H	OH	H	O-rutinoside	H
Neohesperidin	Eriodictyol-7-O-neohesperidoside	H	H	OH	OH	H	OH	H	O-neohesperidose	H
Neohesperidin	Hesperetin-7-O-neohesperidoside	H	OH	OCH ₃	H	H	OH	H	O-neohesperidose	H
Persicogenin	5,3'-dihydroxy-7,4'-dimethoxyflavanone	H	OH	OCH ₃	H	H	OH	H	OCH ₃	H
Pinobanksin	3,5,7-trihydroxyflavanone	H	H	H	H	OH	OH	H	OH	H
Pinocembrin	5,7-dihydroxyflavanone	H	H	H	H	H	OH	H	OH	H
Pinocembrin-7-methylether	5-hydroxy-7-methoxyflavanone	H	H	H	H	H	OH	H	OCH ₃	H

Table 1-1 Cont'd: Comprehensive list of naturally occurring chiral flavanones

Chiral Flavanone	Other name(s)	R ₁	R ₂	R ₃	R ₄	R ₅	R ₆	R ₇	R ₈	R ₉
		2'	3'	4'	5'	3	5	6	7	8
Pinocembrin dimethylester	5,7-dimethoxyflavanone	H	H	H	H	H	OCH ₃	H	OCH ₃	H
Pinostrobin	5-hydroxy-7-methoxyflavanone, pinocembrin-7-methylether	H	H	H	H	H	OH	H	OCH ₃	H
Poncirin	Isosakuranetin-7-O-neohesperidoside	H	H	OCH ₃	H	H	OH	H	O-neohesperidose	H
Prunin	Naringenin-7-O-glucoside	H	H	OH	H	H	OH	H	O-glucose	H
Sakuranetin	5,4'-dihydroxy-7-methoxyflavanone	H	H	OH	H	H	OH	H	OCH ₃	H
Strobopinin	5,7-dihydroxy-6-methylflavanone	H	H	H	H	H	OH	CH ₃	OH	H
Strobopinin-7-methylether	5-hydroxy-6-methyl-7-methoxyflavanone	H	H	H	H	H	OH	CH ₃	OCH ₃	H
Taxifolin	3,5,7,3',4'-pentahydroxyflavanone, 2,3-dihydroquercetin	H	OH	OH	H	OH	OH	H	OH	H
Taxifoliol	(2R)-taxifolin, Distylin	H	OH	OH	H	OH	OH	H	OH	H
Trimethoxyflavanone	5,7,8-trimethoxyflavanone	H	H	H	H	H	OCH ₃	H	OCH ₃	OCH ₃
Trimethoxyflavanone	5,7-dihydroxy-3',4',5'-trimethoxyflavanone	H	OCH ₃	OCH ₃	OCH ₃	H	OH	H	OH	H

Table 1-2: Comprehensive list of naturally occurring chiral 3-hydroxyflavanones or dihydroflavonols.

Chiral 3-hydroxyflavanone or dihydroxyflavonol	Other name(s)	R ₁	R ₂	R ₃	R ₄	R ₅	R ₆	R ₇	R ₈	R ₉	R ₁₀	R ₁₁
		2'	3'	4'	5'	6'	2	3	5	6	7	8
Ampelopsin	3,5,7,3',4',5'- hexahydroxyflavanone, Dihydromyricetin	H	OH	OH	OH	H	H	OH	OH	H	OH	H
Aromadendrin	3,5,7,4'- tetrahydroxyflavanone, 2,3-dihydrokaempferol	H	H	OH	H	H	H	OH	OH	H	OH	H
Aromadendrin-3-O- glucose	5,7,4'- trihydroxyflavanone-3- O-glucose	H	H	OH	H	H	H	O-glucose	OH	H	OH	H
Aromadendrin-4'- methyl ether	3,5,7,-trihydroxy-4'- methoxyflavanone	H	H	OCH ₃	H	H	H	OH	OH	H	OH	H
Aromadendrin-4'-O- xylose	3,5,7- trihydroxyflavanone-4'- O-glucose	H	H	O-glucose	H	H	H	OH	OH	H	OH	H
Aromadendrin-7-O- glucose	3,5,4'- trihydroxyflavanone-7- O-glucose	H	H	OH	H	H	H	OH	OH	H	O-glucose	H
Aromadendrin-7,4'- dimethyl ether	3,5-dihydroxy-7,4'- methoxyflavanone	H	H	OCH ₃	H	H	H	OH	OH	H	OCH ₃	H
Aromadendrin-7,4'- dimethyl ether-5-O- glucose	3-hydroxy-7,4'- methoxyflavanone-5-O- glucose	H	H	OCH ₃	H	H	H	OH	O-glucose	H	OCH ₃	H
Astilbin	5,7,3',4'- tetrahydroxyflavanone- 3-O-rhamnose, Taxifolin-3-O- rhamnose	H	OH	OH	H	H	H	O-rhamnose	OH	H	OH	H
Cedeodarin	3,5,7,3',4'- pentahydroxy-6- methylflavanone	H	OH	OH	H	H	H	OH	OH	CH ₃	OH	H
Cedrin	3,5,7,3',4',5'- hexahydroxy-6- methylflavanone, 6- methylhydromyricetin	H	OH	OH	OH	H	H	OH	OH	CH ₃	OH	H

Table 1-2 Cont'd: Comprehensive list of naturally occurring chiral 3-hydroxyflavanones or dihydroflavonols

Chiral 3-hydroxyflavanone or dihydroxyflavonol	Other name(s)	R ₁	R ₂	R ₃	R ₄	R ₅	R ₆	R ₇	R ₈	R ₉	R ₁₀	R ₁₁
		2'	3'	4'	5'	6'	2	3	5	6	7	8
Cedrinoside	3,5,7,4',5'- pentahydroxy-6- methylflavanone-3'-O- glucose, Cedrin-3'-O- glucose	H	O- glucose	OH	OH	H	H	OH	OH	CH ₃	OH	H
Dihydrokaempferide	3,5,7-trihydroxy-4'- methoxyflavanone	H	H	OCH ₃	H	H	H	OH	OH	H	OH	H
Dihydromyricetin-5'- methyl ether-4'-O- rhamnose	3,5,7,3'-tetrahydroxy-5'- methylflavanone-4'-O- rhamnose	H	OH	O- rhamnose	OCH ₃	H	H	OH	OH	H	OH	H
Dihydorobinetin	3,7,3',4',5'- pentahydroxyflavanone	H	OH	OH	OH	H	H	OH	H	H	OH	H
Dihydromorin	3,5,7,2',4'- pentahydroxyflavanone	OH	H	OH	H	H	H	OH	OH	H	OH	H
Engelitin	5,7,4'- trihydroxyflavanone-3- O-rhamnose	H	H	OH	H	H	H	O-rhamnose	OH	H	OH	H
Fustin	3,7,3',4'- tetrahydroxyflavanone, 2,3-dihydrofisetin	H	OH	OH	H	H	H	OH	H	H	OH	H
Fustin-3-O-methyl	7,3',4'-trihydroxy-3-O- methylflavanone	H	OH	OH	H	H	H	OCH ₃	H	H	OH	H
Fustin-8-hydroxy	3,7,8,3',4'- pentahydroxyflavanone, 8-hydroxyfustin	H	OH	OH	H	H	H	OH	H	H	OH	OH
Garbanzol	3,7,4'- dihydroxyflavanone	H	H	OH	H	H	H	OH	H	H	OH	H
Pinobanksin	3,5,7- trihydroxyflavanone	H	H	H	H	H	H	OH	OH	H	OH	H
Pinobanksin dimethyl ether	3-hydroxy-5,7- dimethoxyflavanone	H	H	H	H	H	H	OH	OCH ₃	H	OCH ₃	H
Sepinol	3,7,3',5'-tetrahydroxy- 4'-methoxyflavanone, Dihydorobinetin-4'- methyl ether	H	OH	OCH ₃	OH	H	H	OH	H	H	OH	H

Table 1-2 Cont'd: Comprehensive list of naturally occurring chiral 3-hydroxyflavanones or dihydroflavonols

Chiral 3-hydroxyflavanone or dihydroxyflavonol	Other name(s)	R ₁	R ₂	R ₃	R ₄	R ₅	R ₆	R ₇	R ₈	R ₉	R ₁₀	R ₁₁
		2'	3'	4'	5'	6'	2	3	5	6	7	8
Taxifolin	3,5,7,3',4'- pentahydroxyflavanone, 2,3-dihydroquercetin	H	OH	OH	H	H	H	OH	OH	H	OH	H
Taxifolin-3-O- galactose	5,7,3',4'- tetrahydroxyflavanone- 3-O-galactose	H	OH	OH	H	H	H	O-galactose	OH	H	OH	H
Taxifolin-3-O- glucose	5,7,3',4'- tetrahydroxyflavanone- 3-O-glucose	H	OH	OH	H	H	H	O-glucose	OH	H	OH	H
Taxifolin-3-O-methyl	5,7,3',4'-tetrahydroxy- 3-methylflavanone, 3- O-methyltaxifolin	H	OH	OH	H	H	H	OCH ₃	OH	H	OH	H
Taxifolin-3,5-di-O- rhamnose	7,3',4'- trihydroxyflavanone- 3,5-di-O-rhamnose	H	OH	OH	H	H	H	O-rhamnose	O-rhamnose	H	OH	H
Taxifolin-3'-O- glucose	3,5,7,4'- tetrahydroxyflavanone- 3'-O-glucose	H	O- glucose	OH	H	H	H	OH	OH	H	OH	H
Taxifolin-7-O- galactose	3,5,3',4'- tetrahydroxyflavanone- 7-O-galactose	H	OH	OH	H	H	H	OH	OH	H	O-galactose	H
Taxifoliol	(2R,3R)-taxifolin, Distylin	H	OH	OH	H	H	H	OH	OH	H	OH	H
Tetrahydroxyflavano- ne	3,5,7,2'-tetrahydroxy-5'- methoxyflavanone	OH	H	H	OCH ₃	H	H	OH	OH	H	OH	H
Trihydroxyflavanone	3,5,4'-trihydroxy-6,7- methoxyflavanone	H	H	OH	H	H	H	OH	OH	OCH ₃	OCH ₃	H

Table 1-3: Comprehensive list of chiral flavanones and 3-hydroxyflavanones having complex substituents.

Chiral Flavanone	Other name(s)	Structure
Anastatin-A		
Anastatin-B		
Bavachinin-A	4'-hydroxy-7-methoxy-6-(3-methyl-2-butenyl)-flavanone, Bavachinin	
Brosimacutin-A	7,4'-dihydroxy-8-(2,3-dihydroxy-3-methylbutyl)flavanone	

Table 1-3 Cont'd: Comprehensive list of chiral flavanones and 3-hydroxyflavanones having complex substituents

Chiral Flavanone	Other name(s)	Structure
Brosimacutin-E		
Cajaf flavanone	5,4'-dihydroxy-6-prenyl-6',6'-dimethylpyrano-(2',3',7,8)-flavanone	
Diprenylflavanone	7,4'-dihydroxy-6,8-diprenylflavanone	
Diprenylflavanone	7-hydroxy-6,8-diprenylflavanone	

Table 1-3 Cont'd: Comprehensive list of chiral flavanones and 3-hydroxyflavanones having complex substituents

Chiral Flavanone	Other name(s)	Structure
Dorsmanin-F		
Dorsmanin-G		
Emoroidenone		
Epimedokoreanin-A		

Table 1-3 Cont'd: Comprehensive list of chiral flavanones and 3-hydroxyflavanones having complex substituents

Chiral Flavanone	Other name(s)	Structure
Flemichin-A		
Flemichin-D	5,2',4'-trihydroxy-6'',6''-dimethylpyrano(2'',3'',7,6)-8-prenylflavanone	
Flemichin-E		
Flemiflavanone-A	5,7,2'-trihydroxy-4'-methoxy-6,8-dimethylflavanone	

Table 1-3 Cont'd: Comprehensive list of chiral flavanones and 3-hydroxyflavanones having complex substituents

Chiral Flavanone	Other name(s)	Structure
Flemiflavanone-B	6,8-dihydroxy-7-(5-hydroxygeranyl)-flavanone	
Formylallylflavanone	5,7-dihydroxy-8-(β -methyl- β -hydroxy-formylallyl)-flavanone	
Geranylflavanone, 8	5,7-dihydroxy-8-geranylflavanone	
Glabranin	5,7-dihydroxy-8-prenylflavanone	

Table 1-3 Cont'd: Comprehensive list of chiral flavanones and 3-hydroxyflavanones having complex substituents

Chiral Flavanone	Other name(s)	Structure
Glabranin, 7-methyl-	5-hydroxy-7-methoxy-8-prenylflavanone, 7-methyl-glabranin	
Glabatephrin		
Isolonchocarpin	6'',6''-dimethyl-(2'',3'',7,8)-pyranoflavanone	
Isolonchocarpin, 3-hydroxy-	3-hydroxy-6'',6''-dimethyl-(2'',3'',7,8)-pyranoflavanone	

Table 1-3 Cont'd: Comprehensive list of chiral flavanones and 3-hydroxyflavanones having complex substituents

Chiral Flavanone	Other name(s)	Structure
Isopentylnaringenin-7,4'-diglucoside	5-hydroxy-8-C-prenylflavanone-4',7-di-O-glucose	
Isosilybin	2-(2,3-dihydro-2-(4-hydroxy-3-methoxyphenyl)-3-(hydroxymethyl)-1,4-benzodioxin-6-yl)-3,5,7-trihydroxyflavanone	
Isouvaretin	5,7-dihydroxy-6-(2-hydroxybenzyl)-flavanone	
Lonchocarpol-C		

Table 1-3 Cont'd: Comprehensive list of chiral flavanones and 3-hydroxyflavanones having complex substituents

Chiral Flavanone	Other name(s)	Structure
Lonchocarpol-D		
Lonchocarpol-E		
Lupineol		
Lupiniol-A		

Table 1-3 Cont'd: Comprehensive list of chiral flavanones and 3-hydroxyflavanones having complex substituents

Chiral Flavanone	Other name(s)	Structure
Methylallylflavanone	5,7-dihydroxy-8-(β -methyl- β -hydroxy-methylallyl)-flavanone	
Naphthoflavanone, α	7,8-benzoflavanone, α -Naphthoflavanone	
Naphthoflavanone, β	5,6-benzoflavanone, β -Naphthoflavanone	
Neocalixin		

Table 1-3 Cont'd: Comprehensive list of chiral flavanones and 3-hydroxyflavanones having complex substituents

Chiral Flavanone	Other name(s)	Structure
Nirurin	5,6,7,4'-Tetrahydroxy-8-(3-methyl-2-butenyl)flavanone-5-O-rutinoside	
Ovalichromene	6-methoxy-6''-dimethyl-(2'',3'',7,8)-pyranoflavanone	
Ovalichromene-A	6-methoxy-6''-dimethyl-(2'',3'',7,8)-pyrano-3',4'-methylenedioxyflavanone	
Ovalichromene-B	6'',6''-dimethyl-(2'',3'',7,8)-pyrano-3',4'-methylenedioxyflavanone	

Table 1-3 Cont'd: Comprehensive list of chiral flavanones and 3-hydroxyflavanones having complex substituents

Chiral Flavanone	Other name(s)	Structure
Ovaliflavanone-C	7-hydroxy-8-prenyl-3',4'-methylenedioxyflavanone	
Ovaliflavanone-D	7-hydroxy-6,8-diprenyl-3',4'-methylenedioxyflavanone	
Phellamurin		
Phellavin	3,5,7,4'-tetrahydroxy-6-(3-hydroxy-emethyl-butyl)-flavanone-7-O-glucose	

Table 1-3 Cont'd: Comprehensive list of chiral flavanones and 3-hydroxyflavanones having complex substituents

Chiral Flavanone	Other name(s)	Structure
Phellodensin-A		
Phellodensin-C		
Phellodensin-D		
Prenylnaringenin	5,7,4'-trihydroxy-8-C-prenylflavanone	

Table 1-3 Cont'd: Comprehensive list of chiral flavanones and 3-hydroxyflavanones having complex substituents

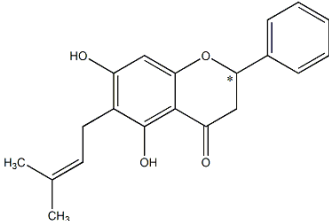
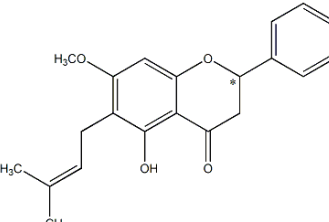
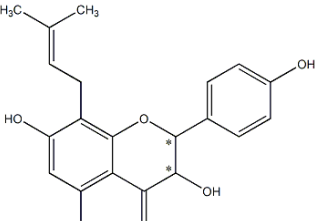
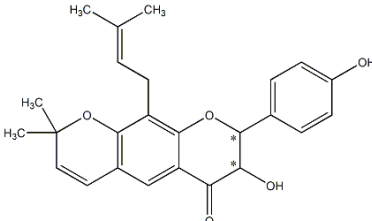
Chiral Flavanone	Other name(s)	Structure
Prenylpinocembrine, 6	5,7-dihydroxy-6-C-prenylflavanone, 6-prenylpinocembrine	
Prenylpinocembrine 7-methylether	5-hydroxy-7-methoxy-6-prenylflavanone, 6-prenylpinocembrine-7-methyl ether	
Prenylflavanone	3,5,7,4'-tetrahydroxy-8-prenylflavanone	
Prenylflavanone	3,5,4'-trihydroxy-6'',6''-dimethyl-(2'',3'',7,8)-pyrano-8-prenylflavanone	

Table 1-3 Cont'd: Comprehensive list of chiral flavanones and 3-hydroxyflavanones having complex substituents

Chiral Flavanone	Other name(s)	Structure
Prenylflavanone	5,3',4'-trihydroxy-7-methoxy-8-prenylflavanone	
Prenylflavanone	7-hydroxy-8-prenylflavanone	
Prenylpinocembrine, 8	5,7-dihydroxy-8-C-(β -Methyl- β -formylallyl)-flavanone, 8-prenylpinocembrine	
Prenylpinocembrine, 8	5,7-dihydroxy-8-C-(β -Methyl- β -hydroxymethylallyl)-flavanone, 8-prenylpinocembrine	

Table 1-3 Cont'd: Comprehensive list of chiral flavanones and 3-hydroxyflavanones having complex substituents

Chiral Flavanone	Other name(s)	Structure
Purpurin		
Pyranoflavanone	3,5,4'-trihydroxy-6'',6''-dimethyl-(2'',3'',7,8)-pyranoflavanone	
Pyranoflavanone	5-methoxy-6'',6''-dimethyl-(2'',3'',7,8)-pyranoflavanone	
Silybin	2-(2,3-dihydro-3-(4-hydroxy-3-methoxyphenyl)-2-(hydroxymethyl)-1,4-benzodioxin-6-yl)-3,5,7-trihydroxyflavanone, Silibinin, Silymarin	

Table 1-3 Cont'd: Comprehensive list of chiral flavanones and 3-hydroxyflavanones having complex substituents

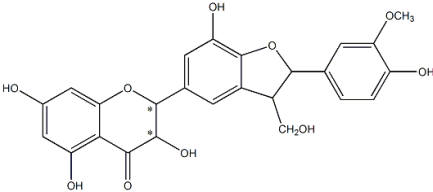
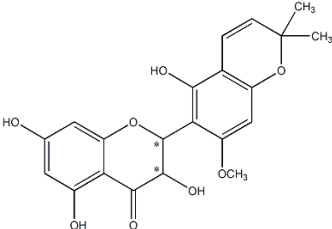
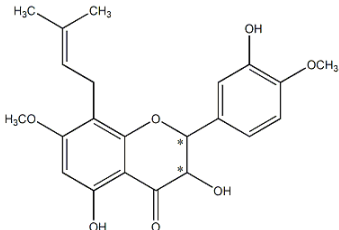
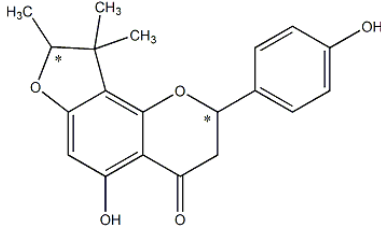
Chiral Flavanone	Other name(s)	Structure
Silychristin		
Sophoronol	3,5,7-trihydroxy-2'-methoxy-6'',6''-dimethyl-(2'',3'',4',3')-pyranoflavanone	
Tirumalin	3,5,3'-trihydroxy-7,4'-dimethoxy-8-prenylflavanone	
Ugonin-D		

Table 1-3 Cont'd: Comprehensive list of chiral flavanones and 3-hydroxyflavanones having complex substituents

Chiral Flavanone	Other name(s)	Structure
Uvaretin	5,7-dihydroxy-8-(2-hydroxybenzyl)-flavanone	
Uvarinol		
Velloeriodictyol		

1.2.2 Formation

Flavonoids are synthesized via the phenylpropanoid pathway and are derived from estrogen (Kodan *et al.* 2002). The phenylalanine structure from phenolic compounds is transformed to cinnamate by the enzyme phenylalanine ammonia-lyase (PAL). The cinnamate 4-hydroxylase (C4H) converts cinnamate to *p*-coumarate, and then an acetyl-CoA group is added by the CoA ligase enzyme to yield cinnamoyl-CoA. Lastly, this product is transformed by chalcone synthase to yield a general chalcone structure. Stilbenoids are synthesized in much the same fashion except for the C4H enzymatic step (Figure 1-3).

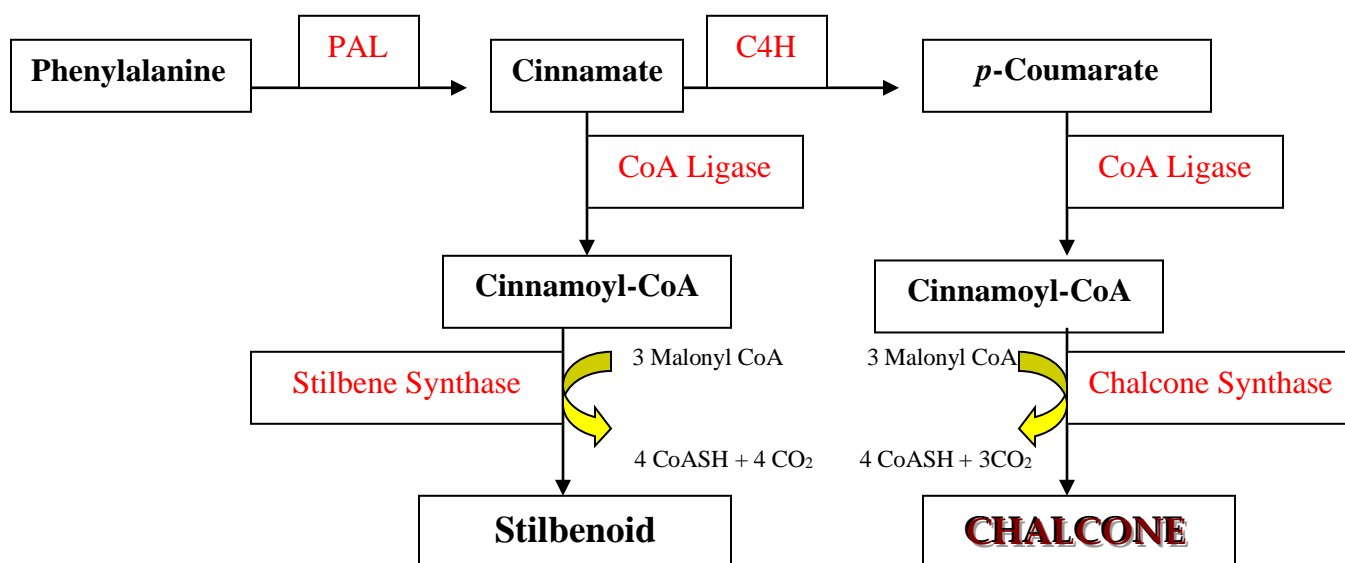


Figure 1-3: Phenylpropanoid pathway and chalcone synthesis

The chalcone structure is further metabolized by the chalcone isomerase (CHI) to the general chiral flavanone structure. From the general chiral flavanone structure, the other derivatives namely: dihydroflavonols, flavonols, flavones, flavan-3-ols, flavan-3,4-diols, isoflavonoids, and neoflavonoids are further metabolized by a well characterized enzymatic-derived process (Figure 1-4). Anthocyanidins and anthocyanins are derived from flavan-3,4-

diols by leucocyanidin oxygenase (LO) and anthocyanidins-3-O-glucosyltransferase respectively. Chromones are synthesized from isoflavonoids through the chromone synthase (ChS), while lignans and coumarins are derived from neoflavonoids by lignan synthase (LS) and coumarin synthase (CS) respectively (Figure 1-4).

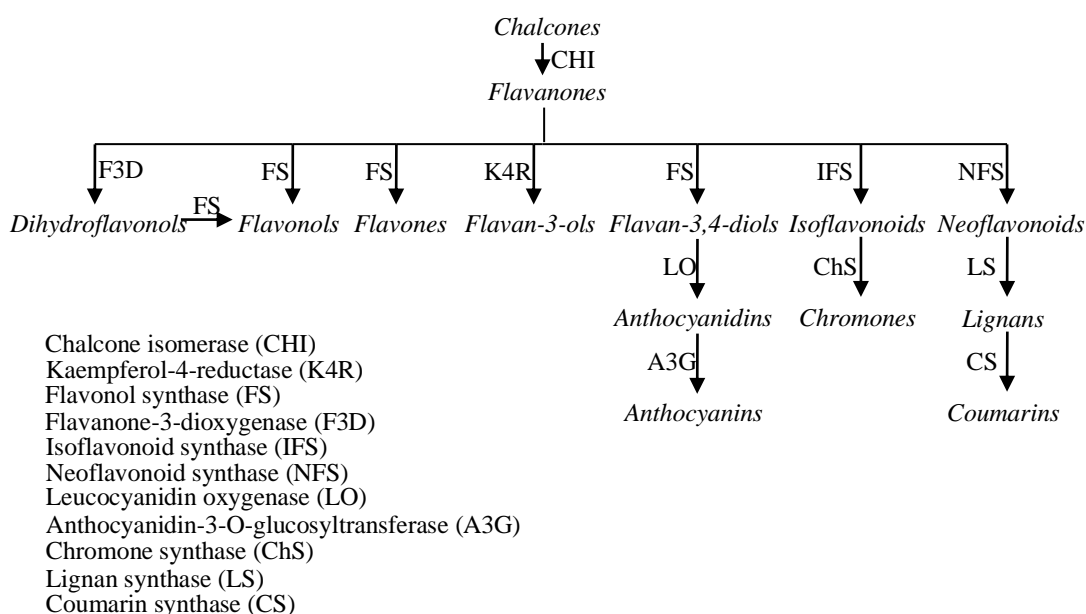


Figure 1-4: Synthesis pathway of chiral flavanones and other flavonoid derivatives

In addition to flavanone, other small natural compounds found in a wide variety of food and plant sources exist. These compounds, namely flavonoids, isoflavonoids, and lignans, have generated much scientific interest in their potential clinical applications in the possible dietary prevention of different diseases. Flavanones, stilbenes, lignans, isoflavonoids and other flavonoid derivatives are similar in structure and provide host-protective purposes. They share the common parent compound, estrogen, in their synthesis and are differentiated based on key structural differences, specific plant hosts, and the environment (Figure 1-5).

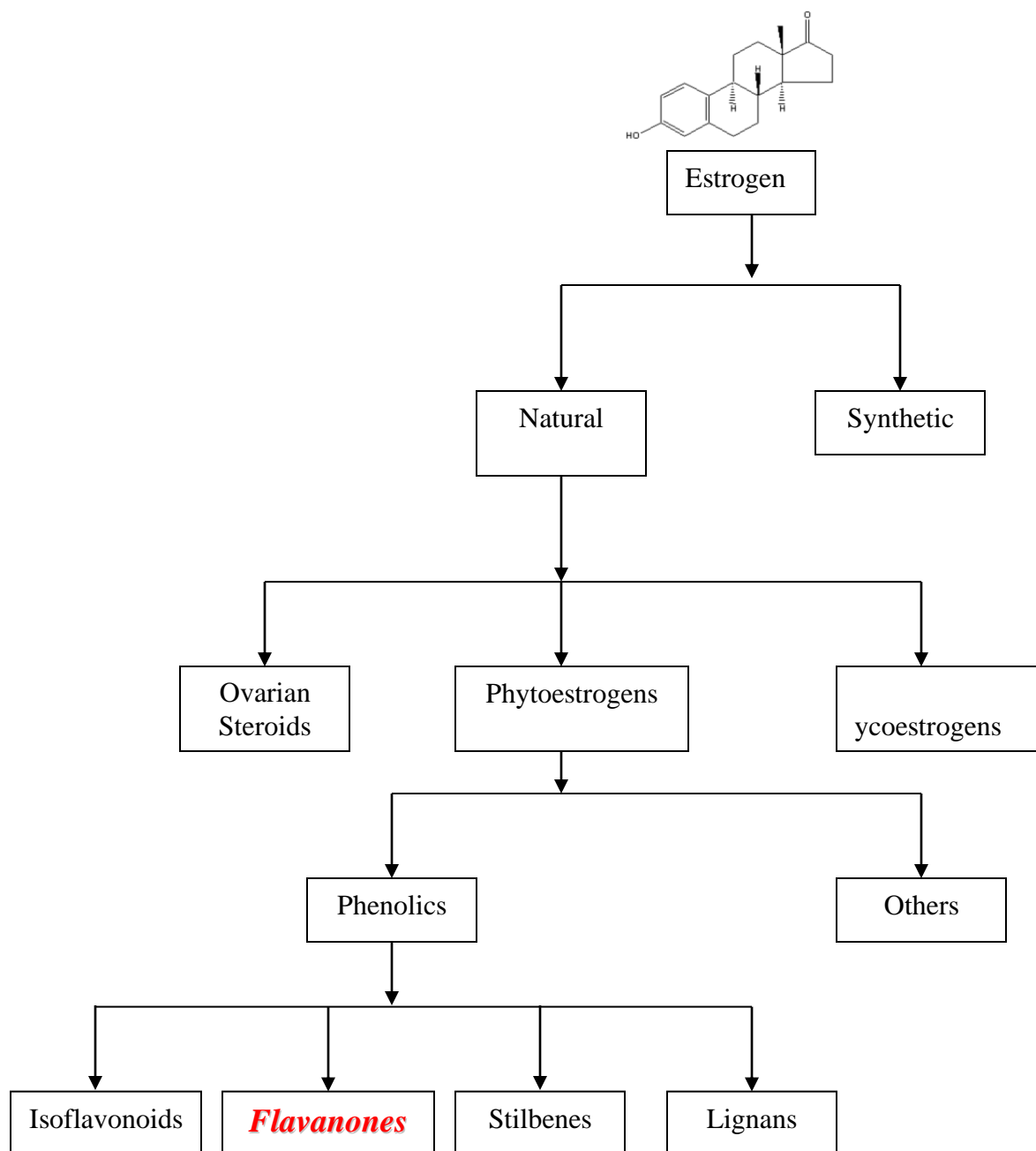


Figure 1-5: Relationship between flavanones, isoflavonoids, stilbenes, lignans and other flavonoid derivatives formation.

1.2.3 Synthesis and Sources

In 1936, Professor Szent-Györgyi reported the isolation of a substance that was a strong reducing agent acting as a cofactor in the reaction between peroxidase and ascorbic acid. This

substance was initially given the name “vitamin P”; this substance has been subsequently categorized as the flavonoid rutin. Professor Szent-Györgyi’s seminal investigations identified rutin and reported its isolation from both lemons and red pepper (Szent-Györgyi, 1936). Since this time, more than other 4,000 flavonoids have being identified and studied. Flavonoids are a group of polyphenolic compounds of low molecular weight (Haslam, 1998) that present a common benzo- γ -pyrone structure (Cook *et al.*, 1996). They are categorized into various subclasses including flavones, flavonols, flavanones, isoflavanones, anthocyanidins, and catechins. The average human diet contains a considerable amount of flavonoids, the major dietary sources of which include fruits (i.e. orange, grapefruit, apple, and strawberry), vegetables (i.e. onion, broccoli, green pepper, and tomato), soybeans and a variety of herbs (Moon *et al.*, 2006; Scalbert *et al.*, 2005). Due to the constant and significant intake of these compounds in our diet, the United States Department of Agriculture (USDA) has created a database that contains the reported average content of these compound in different foodstuffs (USDA, 2003). Among the classes of flavonoids, flavanones have been defined as citrus flavonoids (Kawaii *et al.*, 1999b; Nielsen *et al.*, 2002; USDA, 2003) due to their almost unique presence in citrus fruits (Ameer *et al.*, 1996; Benavente-Carcia *et al.*, 1997; Brevik *et al.*, 2004; Caccamese *et al.*, 2003; Caristi *et al.*, 2003; Erlund *et al.*, 2001; Gil-Izquierdo *et al.*, 2004; Middleton *et al.*, 1994; Miyake *et al.*, 2006; Miyake *et al.*, 2000; Montanari *et al.*, 1998; Wilcox *et al.*, 1999). However, flavanones have been also reported in tomatoes (Bugianesi *et al.*, 2002; Le Gall *et al.*, 2003; Stewart *et al.*, 2000; Szent-Györgyi, 1936), peanuts (Daigle *et al.*, 1988; Krause *et al.*, 1991a) and some herbs such as mint (Manach *et al.*, 2003), gaviota tarplant (Krause *et al.*, 1991a; Proksch *et al.*, 1984), yerba santa (Geissman, 1940; Krause *et al.*, 1991a), and thyme (Krause *et al.*, 1991a; van den Broucke *et al.*, 1982).

Flavonoids in general have been studied for more than 70 years in *in vivo* and *in vitro* systems. They have been shown to exert potent anti-oxidant capacities (Benavente-Carcia *et al.*, 1997; Formica *et al.*, 1995; Le Gall *et al.*, 2003; Pietta, 2000; van Acker *et al.*, 2000) in some instances stronger than α -tocopherol (vitamin E) (Miyake *et al.*, 1997). They have been also shown to exhibit beneficial effects on capillary permeability and fragility (Benavente-Carcia *et al.*, 1997; Bocco *et al.*, 1998; Cao *et al.*, 1997; Chen *et al.*, 1997; Cook *et al.*, 1996; Di Carlo *et al.*, 1999; Harborne *et al.*, 2000; Marin *et al.*, 2002; Pietta, 2000; Rice-Evans *et al.*, 1996; Ruzsnyak *et al.*, 1936), to have anti-platelet (Benavente-Carcia *et al.*, 1997; Bocco *et al.*, 1998; Cao *et al.*, 1997; Chen *et al.*, 1997; Cook *et al.*, 1996; Di Carlo *et al.*, 1999; Formica *et al.*, 1995; Harborne *et al.*, 2000; Marin *et al.*, 2002; Pietta, 2000; Rice-Evans *et al.*, 1996), hypolipidemic (Bok *et al.*, 1999; Borradaile *et al.*, 1999; Formica *et al.*, 1995; Santos *et al.*, 1999; Shin *et al.*, 1999), anti-hypertensive (Erlund *et al.*, 2001; Formica *et al.*, 1995; Hertog *et al.*, 1993), anti-microbial (Formica *et al.*, 1995), anti-viral (Benavente-Carcia *et al.*, 1997; Bocco *et al.*, 1998; Cao *et al.*, 1997; Chen *et al.*, 1997; Cook *et al.*, 1996; Di Carlo *et al.*, 1999; Formica *et al.*, 1995; Harborne *et al.*, 2000; Kaul *et al.*, 1985; Marin *et al.*, 2002; Pietta, 2000; Rice-Evans *et al.*, 1996; Wang *et al.*, 1998), anti-allergenic (Middleton, 1998), anti-ulcerogenic (Formica *et al.*, 1995), cytotoxic (Formica *et al.*, 1995), anti-neoplastic (Ameer *et al.*, 1996; Caccamese *et al.*, 2003; Formica *et al.*, 1995; Fotsis *et al.*, 1997; Knekt *et al.*, 1997; So *et al.*, 1996; Stefani *et al.*, 1999; Tanaka *et al.*, 1997b; Yang *et al.*, 1997), anti-inflammatory (Benavente-Carcia *et al.*, 1997; Bocco *et al.*, 1998; Cao *et al.*, 1997; Chen *et al.*, 1997; Cook *et al.*, 1996; Di Carlo *et al.*, 1999; Formica *et al.*, 1995; Harborne *et al.*, 2000; Marin *et al.*, 2002; Pietta, 2000; Rice-Evans *et al.*, 1996), anti-atherogenic (Formica *et al.*, 1995; Samman *et al.*, 1999), and anti-hepatotoxic (Formica *et al.*, 1995) activities.

As shown in Table 1-1, 1-2, and 1-3 there are multiple chiral flavanones; however, they have been generally thought of as achiral entities and their chiral nature in many cases has not been recognized or denoted. Furthermore, the USDA database reports these compounds as achiral entities and uses the aglycone terminology (hesperetin, naringenin, and eriodictyol) interchangeably with the glycosides (hesperidin, naringin, and eriocitrin) (USDA, 2003). Thus, one purpose of this introductory chapter is to describe the different methods of analysis and separation of the various chiral flavanones, and to review in detail the applications in current pharmaceutical research of three selected flavanones: hesperetin, naringenin, and eriodictyol that are the focus of this thesis (Figure 1-6).

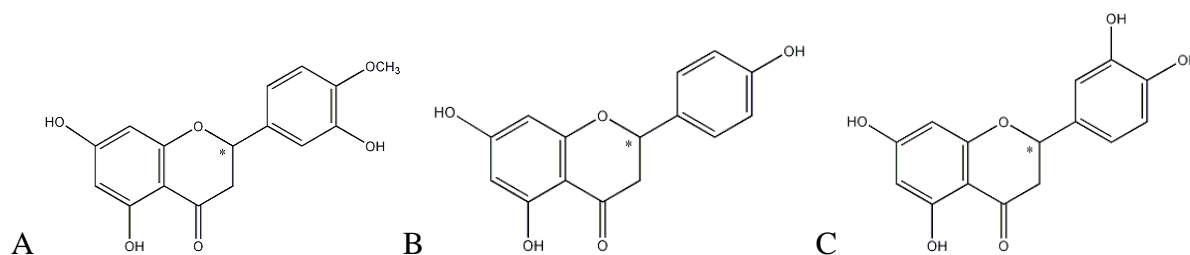


Figure 1-6: Structures of (A) hesperetin, (B) naringenin and (C) eriodictyol. *Denotes chiral center.

1.3 METHODS OF ANALYSIS AND SEPARATION OF CHIRAL FLAVANONES

The importance of stereospecific pomological disposition and content of racemic flavanones has been recognized and reported in the last 20 years. Most of these investigations report the quantification of a variety of flavanones in citrus fruit juices and herbs (Caccamese *et al.*, 2003; Gel-Moreto *et al.*, 2003; Gel-Moreto *et al.*, 2001; Krause *et al.*, 1991a; Krause *et al.*, 1991b; Li *et al.*, 1998c), or report the separation of flavanones on different stationary phases (Asztemborska *et al.*, 2003; Chankvetadze *et al.*, 1996; Ficarra *et al.*, 1995; Krause *et al.*, 1988; Krause *et al.*, 1990a; Krause *et al.*, 1990b; Kusuno *et al.*, 2002; Ng *et al.*, 2002; Okamoto *et al.*, 1987a; Okamoto *et al.*, 1986a). There is a paucity of investigations detailing

the importance of stereospecific pharmacokinetics and pharmacodynamics of chiral flavanones. Of these investigations, only one manuscript reports the human urinary excretion of four different flavanones (liquiritigenin, naringenin, dihydrowogonin, and dihydroroxylin A) after ingestion of different herbal products (Li *et al.*, 1998a; Li *et al.*, 1998b; Li *et al.*, 1998c), unfortunately this report didn't employ pharmacological and pharmacokinetic analysis and modeling.

It has been reported that some chiral flavanones are stereochemically unstable depending on the substitution pattern of various functional groups around the stereogenic centre. When non-enzymatic inversion occurs causing the formation of a racemate it is termed racemization, while enantiomerization is the reversible interconversion of enantiomers. For compounds with more than one stereogenic center, a process called epimerization can occur when there is a change of configuration at a single chiral center (Wistuba *et al.*, 2006). The racemization process, which is characterized by a process reaching equilibrium between the two enantiomers is facilitated by temperature, moisture, solvent, pH, among other factors (Srinivas, 2004). In addition, flavanones with a free hydroxyl group in the position 4' (equivalent to R₃ in Figure 1-1) (i.e. naringenin and eriodictyol) may racemize easier than flavanones with a methoxy group on that position (i.e. hesperetin and isosakuranetin) (Miles *et al.*, 1988). Non-stereospecific assay methods cannot interpret the stability of enantiomers nor the pharmacokinetics of an individual enantiomer and any results using achiral assays could be misleading in determining concentration dependence of each enantiomer of a racemic flavonoid xenobiotic in terms of efficacy or toxicity.

To our knowledge, there has been no report on examining the pharmacokinetics, anti-cancer, or anti-inflammatory activity of the individual enantiomers of chiral flavanones.

However, there is one report where the S and R enantiomers of naringenin were studied for their inhibition of cyclosporine A oxidase activity in human liver microsomes, which is a cytochrome P450 3A4-dependent activity. Interestingly, no enantioselectivity or significant inhibitory activity were demonstrated for either (R)- or (S)-naringenin or a mixture of epimers of naringin (Caccamese *et al.*, 2005).

Importantly, it should be recognized that other classes of flavonoids including isoflavonoids can also demonstrate chirality in some of their individual members. Legumes are a rich source of isoflavones that may have pharmacological properties. The isoflavone reductase enzyme reduces achiral isoflavones to chiral isoflavones during the biosynthesis of chiral pterocarpan phytoalexins. Red clover for instance synthesizes (-)-maackiain, garden pea synthesizes predominantly (+)-pisatin, and alfalfa (-)-medicarpin (Delslerone *et al.*, 1992; Paiva *et al.*, 1994). The soy isoflavonoids daidzein and the red clover isoflavonoid formentin are stereospecifically converted to the chroman metabolite S-(-)-equol by microbial flora of the gastrointestinal tract (Muthyala *et al.*, 2004; Setchell *et al.*, 2005; Wang *et al.*, 2005a). In addition, daidzein and genestein are both reduced to racemic (+/-) dihydrodaidzein and (+/-) dihydrogenestein respectively (Wang *et al.*, 2005b). In addition, 2-hydroxyformononetin is reduced to R and S vestitone and subsequently to (+)-medicarpin in peanut and (-)-medicarpin in alfalfa through pterocarpan synthase which can differ between plant varieties (Allen *et al.*, 2000). Furthermore, due to their possible therapeutic uses scientists and pharmaceutical companies are now employing flavanones as potential lead compounds and synthesizing a variety of derivatives such as chiral dihydrofuroflavones (Lantz *et al.*, 2004).

Thus, there is a need for stereospecific assay methods for the quantitation and effective isolation of pure flavonoid enantiomers for pharmacometric and metabolomic studies in *in*

vivo and *in vitro* models. This stereospecific analytical methodology can provide valuable information to enantiospecifically understand how these xenobiotics are metabolized in plant, human, and animal models and to be able to better understand their disposition, pharmacological activity, as well as therapeutic and toxic effects.

1.3.1 Chromatographic methods of separation of enantiomers

The separation, resolution, and analysis of enantiomers have generally been accomplished through the formation of diastereoisomers either transiently or covalently. Diastereoisomers have different physicochemical properties in an achiral environment and thus they can be separated on an achiral chromatographic column through differential interaction and retention. Racemic flavonoid resolution has generally been accomplished by chromatographic enantiospecific resolution through temporary formation of diastereoisomers on a chemically bonded chiral stationary phase (CSP) with an achiral mobile phase.

1.3.1.1 Direct Methods of Analysis: Chiral Stationary Phases (CSP)

A number of different CSPs have been utilized to resolve and separately quantify the enantiomers of chiral flavonoids including: chiral polymer phases. These chiral polymer phases can be further sub-divided into Polysaccharide-Derived Columns, and Cyclodextrin and “Mixed” Cyclodextrin Columns

1.3.1.1.1 Chiral Polymer Phases

1.3.1.1.1.1 Polysaccharide-Derived Columns

A variety of chiral columns employing synthetic polysaccharides particularly D-cellulose esters to which a variety of terminal groups are attached have been employed. Resolution of flavanone enantiomers by HPLC utilizing polysaccharide derivatives such as cellulose trans-tris (4-phenylazaphenylcarbamate) columns were first established in the 1980's (Okamoto *et al.*,

1986a). This was followed by separation on cellulose tris (3,5-dimethylphenylcarbamate) columns (Okamoto *et al.*, 1987b; Okamoto *et al.*, 1986b). Unsubstituted flavanone can be easily separated on cellulose mono and disubstituted carbamates including cellulose-4-substituted triphenylcarbamate derivatives, cellulose chloro-substituted triphenyl carbamate, and cellulose methyl-substituted triphenylcarbamate supported in silica gel (Okamoto *et al.*, 1987a). Hesperetin has been successfully separated in a validated reverse-phase HPLC method and a commercially available Chiralpak AD-RH tris (3,5-dimethylphenylcarbamate) derivative of amylose column (Yanez *et al.*, 2005d).

The chiral recognition of microcrystalline triacetate may involve inclusion complexation. Three commercially available columns of microcrystalline cellulose triacetate were able to resolve several flavanones including naringenin, hesperetin, eriodictyol, homoeriodictyol, pinocembrine, and isosakuranetin (Krause *et al.*, 1988). For instance, Chiralcel OA is a commercially available cellulose triacetate column coated on macroporous silica gel (Krause *et al.*, 1990a). The seminal work on separation of some racemic flavanones was accomplished on microcrystalline cellulose triacetate supported on non-macroporous silica gel diol (Krause *et al.*, 1990a). This CSP employed in normal (apolar) phase using gradient elution was found to be superior to a commercially available cellulose triacetate columns for separation of polyhydroxylated flavanones particularly the 5,7-dihydroxy substituted on ring A (i.e. pinocembrine, isosakuranetin, naringenin, eriodictyol, homoeriodictyol, and hesperetin). Normal phase chromatography was far superior to reverse (polar) elution to separate flavanone enantiomers. In addition, flavanone glycosides could also be resolved together with their aglycones and this was applied to analysis of naringenin enantiomers in tomato skin (Krause *et*

al., 1990a). The performance of a Chiralcel OA column also indicated that 5- and 7-methoxyflavanone could be resolved as well as naringenin (Ficarra *et al.*, 1995).

The Chiralcel OD column is a macroporous silica gel coated with cellulose tris (3,5-dimethylphenylcarbamate), which has demonstrated ability to separate a variety of flavanone derivatives including (i.e. flavanone (Krause *et al.*, 1989; Krause *et al.*, 1990b), 4'- and 6-methoxyflavanone (Krause *et al.*, 1989; Krause *et al.*, 1990b), 5-methoxyflavanone; 2'- or 6-hydroxyflavanone; pinostrobin (Krause *et al.*, 1990b); and 7-methoxyflavanone (Ficarra *et al.*, 1995)). A small clinical study involved the administration of the Chinese herbal medicines Daisiko-to and Shosaiko-to to human subjects and analyzed the urine post-administration, resolving several polysubstituted flavanones including liquiritigenin, naringenin, dihydrowogonin, and dihydrooxylin A (Li *et al.*, 1998a; Li *et al.*, 1998b; Li *et al.*, 1998c). Chiralcel OD can also separate and resolve naringin epimers during grapefruit maturation (Caccamese *et al.*, 2003). The Chiralcel OD-RH (tris-3,5-dimethylphenylcarbamate) column has demonstrated the ability to resolve naringenin enantiomers in an isocratic reverse phase in a validated assay in biological matrices (Yanez *et al.*, 2005a). Chiralcel OD in normal phase has been utilized for the direct separation of epimers of the glycosides narirutin, hesperidin, neohesperidin, and naringin (Uchiyama *et al.*, 2005), and the aglycones naringenin, hesperetin, eriodictyol, and pinocembrin (Caccamese *et al.*, 2005). The 2,3,4-tris-O-(3,5-dimethylphenylcarbamoyl) CSP demonstrated the ability to resolve flavanone (Kusuno *et al.*, 2002). The Chiralcel OC column (tris-phenylcarbamate) has been demonstrated to resolve flavanone as well as 4'-, 5-, and 6-methoxyflavanone and homoeriodictyol (Ficarra *et al.*, 1995). Furthermore, the Chiralcel OJ column (tris 4-methylphenyl-benzoate ester) can resolve flavanone, 4'-, 5-, and 6-methoxyflavanone, eriodictyol, and hesperetin (Ficarra *et al.*, 1995).

In addition, chiral columns employing amylose esters such as amylose tris (3,5-dimethylphenylcarbamate) and tris (3,5-dichlorophenylcarbamate) supported on silica gel have demonstrated the ability to resolve flavanone (Okamoto *et al.*, 1987a). The amylose tris (3,5-dimethylphenylcarbamate) column Chiralpak IA has the advantage of being an immobilized chiral stationary phase instead of a silica gel supported stationary phase enabling a wider range of solvents to be employed as the mobile phase. Furthermore, it has also been shown to have the ability to resolve hesperidin, neohesperidin, narirutin, and naringin (Uchiyama *et al.*, 2005).

Chiralpak OP (+) is based on macroporous silica gel coated with poly (diphenyl-2-pyridylmethylmethacrylate). The separation of flavanone, 5-, 6-, and 4'-methoxyflavanone were achieved on this column (Krause *et al.*, 1990b). ChiraSpher is a small-pore silica gel chiral polymer (poly-N-acryloyl-(S)-phenylalanine ethyl ester), with this the separation of flavanone, 2'-, 4'-, and 6-hydroxyflavanone, 4'-, 5-, and 6-methoxyflavanone, and pinostrobin have been described although naringenin and naringenin tribenzoate were not separated (Krause *et al.*, 1990b). The use of a Chiralpak AS-H (tris (S)-1-phenylethylcarbamate) to separate naringenin, eriodictyol, hesperetin, and pinocembrine has recently been reported (Caccamese *et al.*, 2005). Furthermore, a Chiralcel AD column has also been reported to separate naringenin (Caccamese *et al.*, 2005).

1.3.1.1.2 Cyclodextrin and “Mixed” Cyclodextrin Columns

Cyclodextrins are cyclic oligomers of α -D-glucose bonded through α -(1,4) linkages. In this group of CSP columns, there is another group that consists of β -cyclodextrin bonded phase type columns, from which the silica-supported cyclodextrin columns are available. Cyclobond I is a β -cyclodextrin column made up of cyclic glucoamyloses that have been found to separate flavanone, 2'- and 6-hydroxyflavanone as well as the 4'- and 6-methoxyflavanone (Krause *et*

al., 1990b). Acetylating the 3-hydroxyl groups on the mouth of the cyclodextrin molecule introduces further binding sites and an acetylated Cyclobond I column can resolve several flavanones including: flavanone, 2'- and 6-hydroxyflavanone as well as 6-methoxyflavanone (Krause *et al.*, 1990b). In addition, the Cyclobond I column can resolve several flavanone glycosides including prunin, naringin, narirutin and neohesperidin. The flavanones with 7-O-neohesperidose sugars attached were better resolved (i.e. naringin and neohesperidin) (Krause *et al.*, 1991b). Recently, Cyclobond I 2000 has been utilized to baseline separate naringin, neohesperidin, and separate narirutin and hesperidin (Asztemborska *et al.*, 2006).

Columns utilizing cyclodextrin bonded silica as well as cellulose-coated silica gel have been successfully employed. Silica coated with a 2-hydroxy-3-methacryloyloxypropyl β -cyclodextrin-co-N-vinylpyrrolidone copolymer has been successfully utilized in reverse phase mode to resolve flavanone and monosubstituted flavanones such as 6- and 7-methoxyflavanones and 6-hydroxyflavanone (Carbonnier *et al.*, 2005). Ureido-bonded methylated β -cyclodextrin CSP columns can also separate flavanone; 5-, 6- and 7-methoxyflavanone; hesperetin; naringenin; and taxifolin (Ng *et al.*, 2002).

New dichloro-, dimethyl- and chloromethylphenylcarbamate derivatives of α , β , γ -cyclodextrin were prepared as CSPs using normal phase liquid chromatography resolved flavanone. In particular 2,5- and 3,4-dichlorophenylcarbamates of β -cyclodextrin as CSPs provided better resolution than dimethylphenylcarbamate derivatives (Chankvetadze *et al.*, 1996). Enantioseparation of various flavanones on mono (6^A-N-allylamino-6^A-deoxy)permethylated β -cyclodextrin (MeCD) covalently bonded to silica gel in the reverse phase has been reported (Lai *et al.*, 2004). More recently column coupling with achiral reverse phase chromatography has been utilized to separate the flavanone glycosides. For this, a β -

cyclodextrin column is coupled with mass spectrometry operated with negative ion electrospray ionization, which has been utilized to separate and detect eriocitrin, hesperidin, and neohesperidin enantiomers, and applied to their analysis in citrus fruit juices (Aturki *et al.*, 2004).

1.3.1.1.2 Chiral Mobile Phase Additives

The addition of an optically active molecule to the mobile phase can facilitate separation of enantiomers on conventional stationary phases. Separation of flavonoids through the addition of cyclodextrins to the mobile phase is a rational approach given the effectiveness of CSP cyclodextrin columns. The interaction of the chiral additive with the enantiomers facilitated the formation of transient diastereomers. These diastereomeric pairs have different physicochemical properties and thus may distribute differentially between the adsorbing achiral stationary phase and the organic mobile phase. Capillary electrophoresis can be operated in various modes and the separation of several flavanone-7-O-glycosides (naringin, prunin, narirutin, hesperidin, neohesperidin, and eriocitrin) by chiral capillary electrophoresis was accomplished by a variety of cyclodextrin mobile phase additives in borate buffer at a pH range of 8-10 (Gel-Moreto *et al.*, 2001). There is no generally applicable cyclodextrin for flavonoid glycosides separation and therefore assays must be developed individually; however, naturally occurring β and γ cyclodextrin and neutral cyclodextrin derivatives such as DM- β -cyclodextrin, HP- β -cyclodextrin, and charged derivatives CM- β -cyclodextrin and CE- β -cyclodextrin were all successful as chiral selectors (Gel-Moreto *et al.*, 2001). These methods were subsequently applied to examine flavanone-7-O-glycosides in citrus fruit (Gel-Moreto *et al.*, 2003).

A recent publication (Wistuba *et al.*, 2006) demonstrated the stereospecific separation of many flavanones and flavanone-7-O-glycosides with capillary electrophoresis by adding cyclodextrins or cyclodextrin derivatives as chiral selectors to the background electrolyte. The ionizability of flavanones at high pH requires an anionic cyclodextrin derivative such as carboxymethylcyclodextrin, and sulfatocyclodextrin as buffer selectors. While a buffer system at pH 7 containing neutral cyclodextrins does not appear to possess enantiomeric discrimination (Wistuba *et al.*, 2006). It appears that the pH strongly influences the stereospecific separation and that methyl-carboxymethyl and hydroxypropyl- γ -cyclodextrin leads to a better resolution than the corresponding β -cyclodextrin, while sulfato- γ -cyclodextrin provided no separation of the examined flavanones (Wistuba *et al.*, 2006).

Separation of some chiral flavanones by micellar electrokinetic chromatography (MEKC) has also been accomplished (Asztemborska *et al.*, 2003). γ -cyclodextrin and sodium cholate were used as chiral mobile phase additives. Sodium cholate when used above at critical micelle point concentration forms chiral micelles and was effective at separating flavanone glycosides due to a sugar micelle interaction, while the use of cyclodextrin was more effective in separating flavanone aglycones.

Using MEKC, the glycoside neohesperidin was baseline separated while naringin was not. For the aglycones examined, the best resolution was for hesperetin although again baseline resolution was not achieved (Asztemborska *et al.*, 2003). A more recent investigation demonstrates that micellar electrokinetic chromatography with a) sodium cholate or b) sodium cholate plus cyclodextrins or cyclodextrin derivatives or c) sodium dodecyl sulfate (SDS) plus cyclodextrin or cyclodextrin derivatives as a chiral surfactants/selectors can be employed for the epimeric separation of flavanone 7-O-glycosides (Wistuba *et al.*, 2006). Flavanone

aglycones are not separable into their respective enantiomers with sodium cholate alone; however, by adding sodium dodecyl sulfate (SDS) to a buffer system containing certain γ -cyclodextrins enantioseparation can be obtained. No stereospecific separation was demonstrated for other bile salts such as sodium deoxycholate and sodium taurocholate; however, baseline separation for neohesperidin and naringin was achieved and this separation was dependent on concentration of sodium cholate and pH of the mobile phase (Wistuba *et al.*, 2006).

Separation of several flavanone glycosides and aglycones including eriocitrin, hesperidin, hesperetin, naringin, naringenin, narirutin, neohesperidin, flavanone, 2'- and 6'-hydroxyflavanone, and 6-methoxyflavanone in citrus fruit juices was accomplished by capillary electrophoresis using sulfobutyl ether β -cyclodextrin as the chiral selector (Aturki *et al.*, 2003).

Cyclosophoraoses are unbranched cyclic (1 \rightarrow 2)- β -D-glucans oligosaccharides. Highly sulfated cyclosophoraoses or neutral cyclosophoraoses were successfully applied as chiral additives with SDS for the separation of isosakuranetin and neohesperidin in micellar electrokinetic chromatography (Park *et al.*, 2005).

1.3.1.2 Indirect Methods of Analysis: Chiral Derivatization Techniques

One of the first reports of HPLC separation of flavanone glycosides was in 1980 (Galensa *et al.*, 1980). It was suggested that both naringin and narirutin could be acetylated with equal portions of pyridine and acetic anhydride and resolved at low temperatures 0-5° C (Galensa *et al.*, 1980). In the mid-1980's there was some initial separation of prunin (naringenin-7-O-glucoside) using benzoylated derivatives to separate the epimers in *Prunus callus* (sweet cherries) (Treutter *et al.*, 1985), oranges and grapefruit (Siewek *et al.*, 1985). The separation of

prunin benzoate and naringin benzoate on Cyclobond I columns has also been reported (Krause *et al.*, 1991b). There is also mention in the literature of derivatization of naringenin to naringenin tribenzoate and separation on a Chiralcel OD column. However, naringenin enantiomers were not resolved suggesting that the hydroxyl groups present in naringenin hinder chiral recognition on this stationary phase (Krause *et al.*, 1990b).

1.3.1.3 Racemization, Enantiomerization and Epimerization

A feature that can exist with some chiral xenobiotics is a lack of configurational stability. Some chiral flavanoids undergo non-enzymatic interconversion of one stereoisomeric form into another. When isomerization occurs causing the formation of a racemate it is termed racemization. Racemization is the process of an enantioenriched substance becoming a mixture of enantiomeric forms and thus the formation of a racemate from a pure enantiomer. Alternatively stated, racemization is the conversion of one enantiomer into a 50:50 mixture of the two enantiomers of a substance. Racemization is normally associated with the loss of optical activity over a period of time since 50:50 mixtures of enantiomers are optically inactive, while enantiomerization is the reversible interconversion of enantiomers. For epimers when diastereoisomerization occurs by the change of configuration at a single chiral center, the process is called epimerization (Wistuba *et al.*, 2006).

For example, S-(-)-naringenin racemizes within 3 h in a water/methanol solvent (Krause *et al.*, 1991a). The importance of temperature and pH-dependent epimerization or enantiomerization barriers of many flavanone-7-O-glycosides (ie naringin, narirutin, neohesperidin and prunin) as well as flavanones (homoeriodictyol and naringenin) have been recently examined (Wistuba *et al.*, 2006).

The importance of enantiomerization and epimerization in stereospecific chromatography is evident when this occurs during separation on a chiral stationary phase as there are some characteristics of the eluting peaks such as peak broadening, peak coalescence, and plateau formation that suggest interconversion of the enantiomers or epimers under those conditions (Wistuba *et al.*, 2006). For instance, it has been demonstrated for some flavanones (i.e. naringenin and homoeriodictyol) as well as some flavanone-7-O-glycosides (ie narirutin, naringin, neohesperidin, and prunin) under basic conditions of high pH (9-11) a visually evident temperature dependent plateau is apparent between the peaks of the respective enantiomers and epimers (Wistuba *et al.*, 2006).

Non-enzymatic inversion of xenobiotics is important in the pharmaceutical manufacturing process and has implications for the shelf-life of a drug and the economic feasibility of the stereoresolution. Non-enzymatic inversion can also occur during the stereospecific chromatographic procedures. Racemization may also occur in physiological fluids such as the acidic environment of the stomach.

The biogenic mechanism of epimerization during the maturation of the fruit has been studied by several investigators (Gaffield, 1970; Gaffield *et al.*, 1975). Naringin is present at very high quantities in young grapefruit and as the fruit increases in size there is a decrease in naringin content as ripening occurs following a characteristic sigmoid pattern (Gaffield *et al.*, 1975). Naringin is essentially in the 2S-epimeric form in immature fruits and it is believed that it is produced by enzymatic cyclization of its precursor chalcone glycoside. However, the findings of Wistuba *et al.* (Wistuba *et al.*, 2006) suggests that chalcones were not detected in dynamic electrophoretic studies of the interconversion of flavanones. Further studies are required to clarify intermediates involved in enantiomerization and epimerization.

During fruit enlargement 2S naringin is stored in fruit vesicles and undergoes non-enzymatic racemization at the C-2 position leading to the production of 2S and 2R naringin. This phenomena appears to be independent of plant habitat and may also affect taste perception (Gaffield, 1970; Gaffield *et al.*, 1975).

Demonstration of racemization or epimerization may have profound consequences for the development of stereochemically pure flavanones as a pharmaceutical/nutraceutical entity. A better understanding of the factors facilitating such interconversions may greatly aid their development by identifying this feature at an early stage and thereby reducing pharmacological and bioanalytical workload. Regulatory agencies such as the United States Food and Drug Administration (FDA) are increasingly asking for evidence regarding this phenomena following administration of racemates or single enantiomer drug candidates (FDA, 1992). Racemization could lead to variability in both the pharmacokinetics and pharmacodynamics of chiral xenobiotics and have implications for preclinical screening and for safety evaluation and be a source of variability in response. As racemization may occur for some stereoisomeric flavanones, an examination of pharmacokinetics and pharmacodynamics of both *in vitro* and *in vivo* after administration of the racemates and the enantiomers or epimers is necessary. For instance, it has been observed that after oral administration of traditional Chinese medicines Daisaiko-to and Shosaiko-to to healthy volunteers, dihydrowogonin and dihydroroxylin were predominantly excreted as S-enantiomers while naringenin was excreted as R,S mixture in urine (Li *et al.*, 1998c). Therefore, the need to have stereospecific methods of analysis is warranted to study their biological activity and monitor the xenobiotic development process (Caldwell, 1996; Crossley, 1992).

Furthermore, it is prudent for the analyst to avoid any environment that may epimerize or racemize the chiral centre of the flavanone. This would be for example the use of extreme alkaline or acidic conditions or elevated temperatures. For instance naringenin plateau formation can be observed at pH 9-11 but not under neutral (pH 7.0) or acidic (pH 2.5) conditions (Wistuba *et al.*, 2006). A hydroxyl group at position 4' of ring B is a common structural feature of flavanones that undergo enantiomerization or epimerization except for neohesperidin (Wistuba *et al.*, 2006). Naringin, prunin and narirutin all undergo epimerization with the type of saccharide attached on ring A having minimal influence on the interconversion; however, flavanone 7-O-glucosides appear to be more prone to inversion than their respective aglycones. In this recent investigation only naringenin and homoeriodictyol were demonstrated to enantiomerize under the conditions examined (Wistuba *et al.*, 2006). A recent investigation using stopped-flow HPLC, dynamic HPLC and enantioselective HPLC determined that the rate constants of diastereomerization were about eight times higher for naringin and narirutin than for hesperidin and neohesperidin (Asztemborska *et al.*, 2006). The rate of diastereomerization between neohesperidoses and corresponding rutinosides were not significantly different. Interestingly, the rate of diastereomerization of naringin was ~10 times faster using the dynamic HPLC than using a stop-flow method. At present the intermediates involved in this enantiomerization and epimerization process have not been clearly delineated and the reasons for differences in the rate and extent of these processes within and between each flavonoid require further detailed study.

1.3.1.4 Advantages and Disadvantages of Current Methods

All of these methods of analysis may have certain advantages and disadvantages. Some disadvantages might include long run times that make routine analysis of large volumes of

samples impractical. In addition, many columns and methods that have shown stereospecific separation are not yet commercially available. The choice of commercial chiral columns are increasing, however, the costs of the columns can also be prohibitive and the mobile phase composition can be rather limited with CSPs. In the case of some CSP HPLC columns, they can only be used with non-aqueous solvents and this requires judicious removal of water from biological samples to retain optimal column efficiency.

On the other hand, the ultimate advantage of chiral separation methods over achiral methods include a more thorough understanding of the pharmacokinetics of flavanones and the determination of safe and effective dosing regimens. In the case of racemic flavanones or stereochemically pure flavanones this requires knowledge of the *in vivo* behavior of the enantiomers and epimers. Awareness and appreciation in the drug development process of conformational stability of chiral compounds may have significant bearing on the pharmaceutical, pharmacokinetic, and pharmacodynamic data. Stereospecific analysis methods can enable the study of enantiomerization/epimerization and racemization. Putative differences in therapeutic or adverse effects of the enantiomers would be abolished by rapid interconversion *in vivo* and render the development of stereochemically pure enantiomers ineffective. In the development of stereochemical pure compounds and racemates, chirality must be taken into account *ab initio* in the development process. Many publications report the applicability of CSPs to resolve different chiral flavanones; however, there are still comparatively few published and validated chiral assays in biological matrices.

Finally, the lack of availability of optically pure enantiomers and epimers renders evaluation of configurational stability of chromatographic methods complicated. Regardless of the method of resolution the possibility of non-enzymatic inversion during the assay and

biological extraction must be recognized early on in the development and validation process for any new stereospecific assay. The commercial availability of pure enantiomers and epimers from chemical companies to facilitate assay validation and examination of configurational stability would be beneficial to the analyst. A more thorough understanding of fruit regulation and growth also may allow extraction of enantioenriched epimers and enantiomers. Further chemical characterization and synthesis of pure enantiomers to serve as assay standards would greatly assist the analyst in the development of stereospecific analytical methodology (Gaffield, 1970; Giorgio *et al.*, 2004).

1.3.2 Flavanones

1.3.2.1 Dihydrowogonin

The enantiomers of dihydrowogonin were resolved on a Chiralcel OD column in normal phase and its presence was detected in post-administrative urine predominantly in the S form in patients administered some Asian herbal medicines (Li *et al.*, 1998a; Li *et al.*, 1998b; Li *et al.*, 1998c).

1.3.2.2 Dihydrooroxylin A

Dihydrooroxylin A was resolved into its respective enantiomers on a Chiralcel OD column under normal phase conditions and its presence predominantly in the S enantiomer was detected in post-administrative urine of patients administered with some Asian herbal medicines (Li *et al.*, 1998a; Li *et al.*, 1998b; Li *et al.*, 1998c).

1.3.2.3 Eriocitrin and Eriodictyol

Eriocitrin ((+/-)-5,7,3',4'-tetrahydroxyflavanone 7-O-rutinoside) is a chiral flavanone-7-O-glycoside present in lemons, tamarinds and other citrus fruits, as well as in mint, oregano, fennel, thyme, and rose hip. Eriocitrin was successfully resolved into its epimers using a

variety of cyclodextrin mobile phase additives and capillary electrophoresis although baseline resolution was not obtained (Gel-Moreto *et al.*, 2001). It has been suggested that eriocitrin is found equally as 2R and 2S in lemons (Gel-Moreto *et al.*, 2003). Multi-dimensional liquid chromatography through the use of carboxylated β -cyclodextrin columns coupled to mass spectrometry demonstrated that lemon juices contain eriocitrin epimers in approximately equal amounts (Caccamese *et al.*, 2005). Separation of eriocitrin by capillary electrophoresis using sulfobutyl ether β -cyclodextrin as the selector demonstrated that in citrus fruit juices ~50:50 2S/2R epimers was also evident (Aturki *et al.*, 2003).

After consumption, the sugar moiety is rapidly cleaved off the parent flavanone glycoside eriocitrin in the gastrointestinal tract and liver to leave the aglycone bioflavonoid eriodictyol ((+/-)-5,7,3',4'-tetrahydroxyflavanone). Three commercially available columns of microcrystalline cellulose triacetate (MCCTA) were able to resolve eriodictyol isomers (Krause *et al.*, 1988). Eriodictyol could be resolved under reverse and normal phase conditions on modified MCCTA (Krause *et al.*, 1991a; Krause *et al.*, 1990a). Eriodictyol was determined in peanut hull (*Arachis hypogaea*), gaviota tarplant (*Hemizonia increscens*) and thyme (*Thymus vulgaris*) to be predominantly in the S-(-) configuration (Krause *et al.*, 1991a). A recent study that employed the commercially available Chiralcel OD and Chiralpak AS-H separated eriodictyol enantiomers under normal-phase HPLC. The authors obtained baseline resolution with the Chiralpak-AS-H, but not with Chiralcel OD, however, the method was not validated in biological matrices (Caccamese *et al.*, 2005). The Chiralcel OJ column (tris 4-methylphenyl-benzoate ester) can resolve eriodictyol (Ficarra *et al.*, 1995). In my thesis studies I have recently validated a method for the separation of eriodictyol enantiomers under reversed-phase HPLC utilizing the Chiralcel OJ-RH, a cellulose tris (4-methylbenzoate)

column (Yanez *et al.*, 2006a) (Chapter II). This method is a stereoselective, isocratic, reversed-phase high-performance liquid chromatography (HPLC) method that has been successfully applied for the determination of the enantiomers of eriodictyol and its application to *in vivo* kinetic studies, determine enantiomers in lemons, limes, and lemonade, peanut hulls and thyme and to separately isolate enantiomers for further pharmacological testing (Yanez *et al.*, 2006b). The enantiomeric separation of eriodictyol by capillary electrophoresis using the various cyclodextrins as selectors demonstrated separation with the best resolution of $R_s = 1.61$ with carboxymethyl- β -cyclodextrin (Wistuba *et al.*, 2006). The combined use of the surfactant SDS to a buffer system containing γ -cyclodextrin or hydroxypropyl- γ -cyclodextrin using micellar electrokinetic chromatography demonstrated separation for both and baseline separation for the later (Wistuba *et al.*, 2006).

1.3.2.4 Flavanone

Resolution of flavanone enantiomers by HPLC was first established utilizing the polysaccharide derivatives cellulose trans-tris(4-phenylazaphenylcarbamate) columns (Okamoto *et al.*, 1986a). This was followed by separation on cellulose tris(3,5-dimethylphenylcarbamate) columns (Okamoto *et al.*, 1987b; Okamoto *et al.*, 1986b). The Chiralcel OD column is a macroporous silica gel coated with cellulose tris (3,5-dimethylphenylcarbamate) has demonstrated ability to separate flavanone (Ficarra *et al.*, 1995; Krause *et al.*, 1989; Krause *et al.*, 1990b). While Chiralcel OC, OA and OJ columns can also resolve flavanone (Ficarra *et al.*, 1995). In addition, the Chiralpak AD-RH can effectively baseline resolve flavanone enantiomers (Davies *et al.* unpublished observations).

Unsubstituted flavanone can be easily separated on cellulose mono and disubstituted carbamates including cellulose-4-substituted triphenylcarbamate derivatives, cellulose chloro-

substituted triphenyl carbamate, and cellulose methyl-substituted triphenylcarbamate supported in silica gel (Okamoto *et al.*, 1987a). Also the 2,3,4-Tris-O-(3,5-dimethylphenylcarbamoyl) CSP demonstrated the ability to resolve flavanone (Kusuno *et al.*, 2002).

The resolution of flavanone has been demonstrated on silica coated with a (2-hydroxy-3-methacryloyloxypropyl β -cyclodextrin-co-N vinylpyrrolidone) copolymer that has been successfully employed in reverse-phase mode (Carbonnier *et al.*, 2005). In addition, reasonable enantioseparation of flavanone ($R_s = 1.31$) on mono (6^A-N-allylamino-6^A-deoxy)permethylated β -cyclodextrin (MeCD) covalently bonded to silica gel in the reverse phase has been reported (Lai *et al.*, 2004). Cyclobond I is a β -cyclodextrin column made up of cyclic glucoamyloses that have been demonstrated to separate flavanone enantiomers (Krause *et al.*, 1990b). The acetylated Cyclobond I column (Krause *et al.*, 1990b), and the ureido-bonded methylated β -cyclodextrin column (Ng *et al.*, 2002) can also effectively resolve flavanone.

In addition chiral columns employing amylose esters such as amylose tris (3,5-dimethylphenylcarbamate) and tris (3,5-dichlorophenylcarbamate) supported on silica gel have shown ability to resolve flavanone (Okamoto *et al.*, 1987a). Chiralpak OP (+) is based on macroporous silica gel coated with poly(diphenyl-2-pyridylmethylmethacrylate) and has been reported to separate flavanone enantiomers (Krause *et al.*, 1990b). ChiraSpher is a small-pore silica gel chiral polymer (poly-N-acryloyl-(S)-phenylalanine ethyl ester) that has demonstrated the separation of flavanone (Krause *et al.*, 1990b).

Separation of flavanone by capillary electrophoresis using sulfobutyl ether β -cyclodextrin as the selector was also accomplished although baseline resolution was not obtained (Aturki *et al.*, 2003).

1.3.2.5 Hesperidin and Hesperetin

Hesperidin (+/-3,5,7-trihydroxy-4'-methoxyflavanone 7-rhamnoglucoside) is a chiral flavanone-7-O-glycoside consumed in oranges, grapefruit, and other citrus fruits and herbal products. Recently, the use of chiral mobile phase additives of β -cyclodextrin, hydroxypropyl β -cyclodextrin and capillary electrophoresis were found to separate hesperidin epimers although baseline resolution was not observed (Gel-Moreto *et al.*, 2001). Hesperidin has been suggested to be in an epimeric ratio between 90:10 and 97:3 with the 2S epimer predominating in lemons and 95:5 ratio in sweet orange and mandarin juice (Gel-Moreto *et al.*, 2003). Multi-dimensional liquid chromatography through the use of β -cyclodextrin columns coupled to mass spectrometry demonstrated that fruit juices contain hesperidin epimers predominantly in the 2S epimer (Aturki *et al.*, 2004). In orange/sour orange cross freshly squeezed juice, hesperidin was almost exclusively in the 2S epimer (92%) and in lemon juices (96%) (Aturki *et al.*, 2004). In a recent study, hesperidin was separated using normal-phase HPLC in commercial hesperidin and herbal medicine samples and although the 2S epimer predominated there was significant 2R hesperidin present in some samples (Uchiyama *et al.*, 2005). Finally, baseline separation of hesperidin and hesperetin by capillary electrophoresis using sulfobutyl ether β -cyclodextrin as the selector was accomplished and 2S hesperidin predominated in lemon and orange juice (Aturki *et al.*, 2003). Furthermore, the baseline separation of hesperidin by capillary electrophoresis using carboxymethyl- β -cyclodextrin as the selector has also been accomplished (Wistuba *et al.*, 2006).

The rutinose sugar moiety is rapidly cleaved off the parent flavanone glycoside hesperidin to leave the aglycone bioflavonoid hesperetin (+/-3,5,7-trihydroxy-4'-methoxyflavanone), also a chiral flavonoid. There are just a few reports where hesperetin enantiomers were

separated although baseline resolution and separation were poor and validation was not undertaken. Ng *et al.* employed multipleureido-covalent bonded methylated β -cyclodextrin columns supported on silica gel (Ng *et al.*, 2002), while Krause and Galensa used multiple microcrystalline cross-linked acetylcellulose (MCCTA) columns (Krause *et al.*, 1988). Hesperetin could also be resolved under reverse and normal phase conditions on modified MCCTA (Krause *et al.*, 1990a). Unfortunately, these columns are not commercially available, and separation was poor with no baseline resolution and quantification was not validated in biological matrices or applied to pharmacokinetics studies. Hesperetin could be separated using γ -cyclodextrin as a mobile phase additive and micellar electrokinetic chromatography; however, baseline resolution was not obtained (Asztemborska *et al.*, 2003). Baseline enantioseparation of hesperetin ($R_s = 1.88$) on mono (6^A-*N*-allylamino-6^A-deoxy)permethylated β -cyclodextrin (MeCD) covalently bonded to silica gel in the reverse phase has been reported (Lai *et al.*, 2004). Nevertheless, there is a recent study that employed the commercially available Chiralcel OD and Chiralpak AS-H, for the separated of hesperetin enantiomers under normal-phase HPLC, the authors obtained baseline resolution with the Chiralcel AS-H column only, but the method was not validated in biological matrices (Caccamese *et al.*, 2005). The Chiralcel OJ column (tris 4-methylphenyl-benzoate ester) can resolve hesperetin (Ficarra *et al.*, 1995). I have developed the only validated method for the separation of hesperetin enantiomers under reversed-phase HPLC on a Chiralpak AD-RH column and successfully applied this to *in vivo* pharmacokinetic studies and citrus fruit analysis (Yanez *et al.*, 2005c) (Chapter II) during the course of my studies. The enantiomeric separation of hesperetin by capillary electrophoresis using the various cyclodextrins as selectors demonstrated separation with the best resolution of $R_s = 3.65$ with methyl- γ -cyclodextrin and

baseline resolution with sulfato- β -cyclodextrin (Wistuba *et al.*, 2006). The combined use of the surfactant SDS to a buffer system containing γ -cyclodextrin or hydroxypropyl- γ -cyclodextrin using micellar electrokinetic chromatography demonstrated separation for both and baseline separation for the former (Wistuba *et al.*, 2006). A recent study, (Asztemborska *et al.*, 2006) demonstrated separation of hesperidin on Cyclobond 1 2000 column in reverse phase and its application to assessment of freshly squeezed and commercial orange juice. The ratio of 2S/2R hesperidin is much higher in fresh (17.9) than in processed juice (3.2-4.6) (Asztemborska *et al.*, 2006).

1.3.2.6 Homoeriodictyol

Three commercially available columns of microcrystalline cellulose triacetate (CTA I, CTA II, and CTA III available from Merck, Darmstadt, Germany) were able to resolve homoeriodictyol (Krause *et al.*, 1988). It could be resolved under reverse and normal phase conditions on modified MCCTA (Krause *et al.*, 1990a). In yerba santa (*Eriodictyon glutinosum*), homoeriodictyol was determined to be predominantly in the S-(-) configuration (Krause *et al.*, 1991a). Furthermore, it can be resolved on a Chiralcel OC column under normal phase conditions (Ficarra *et al.*, 1995). Finally, separation was achieved using micellar electrokinetic chromatography with γ -cyclodextrin as a mobile phase additive although baseline resolution was not obtained (Asztemborska *et al.*, 2003). In addition, the enantiomeric separation of homoeriodictyol by capillary electrophoresis using the various cyclodextrins as selectors demonstrated separation with the best resolution of $R_s = 6.47$ with methyl- γ -cyclodextrin and suitable baseline resolution with hydroxypropyl- γ -cyclodextrin ($R_s = 2.22$) and sulfato- β -cyclodextrin ($R_s = 1.82$) (Wistuba *et al.*, 2006). The combined use of the surfactant SDS to a buffer system containing γ -cyclodextrin or hydroxypropyl- γ -cyclodextrin

using micellar electrokinetic chromatography demonstrated separation for both and baseline separation for the later (Wistuba *et al.*, 2006). Furthermore, other members of the laboratory have recently developed a method to separate this chiral flavanone employing the Chiralcel OJ-RH column (Vega-Villa *et al.*, 2007).

1.3.2.7 Hydroxyflavanone, 2'-

Different columns have being reported to separate 2'-hydroxyflavanone including: Chiralcel OD, ChiraSpher, Cyclobond I, and acetylated Cyclobond I (Krause *et al.*, 1990b). However, baseline resolution was not obtained by capillary electrophoresis using sulfobutyl ether β -cyclodextrin as the selector (Aturki *et al.*, 2003).

1.3.2.8 Hydroxyflavanone, 4'-

The separation of 4'-hydroxyflavanone has been described using ChiraSpher, a small-pore silica gel chiral polymer made of poly-N-acryloyl-(S)-phenylalanine ethyl ester (Krause *et al.*, 1990b). In addition, reasonable enantioseparation of 4'-hydroxyflavanone ($R_s = 0.93$) on mono (6^A-N-allylamino-6^A-deoxy)permethylated β -cyclodextrin (MeCD) covalently bonded to silica gel in the reverse phase has been reported (Lai *et al.*, 2004). The enantiomeric separation of 4'-hydroxyflavanone by capillary electrophoresis using the various cyclodextrins as selectors demonstrated separation with the best resolution of $R_s = 1.39$ with methyl-sulfato- β -cyclodextrin (Wistuba *et al.*, 2006).

1.3.2.9 Hydroxyflavanone, 6-

Different columns have being reported to separate 6-hydroxyflavanone including: Chiralcel OD, ChiraSpher, Cyclobond I, and acetylated Cyclobond I (Krause *et al.*, 1990b). In addition, near baseline enantioseparation of 6'hydroxy flavanone ($R_s = 1.45$) on mono (6^A-N-allylamino-6^A-deoxy)permethylated β -cyclodextrin (MeCD) covalently bonded to silica gel in

the reverse phase has been reported (Lai *et al.*, 2004). However, baseline resolution was not obtained by capillary electrophoresis using sulfobutyl ether β -cyclodextrin as the selector (Aturki *et al.*, 2003).

1.3.2.10 Isosakuranetin

One commercially available column made of microcrystalline cellulose triacetate (CTA II available from Merck, Darmstadt, Germany) was able to resolve isosakuranetin (Krause *et al.*, 1988). It could also be resolved under reverse and normal phase conditions on modified MCCTA (Krause *et al.*, 1990a). Isosakuranetin could be separated using γ -cyclodextrin as a mobile phase additive and micellar electrokinetic chromatography; however, baseline resolution was not obtained (Asztemborska *et al.*, 2003). More recently using highly sulphated cyclosophoraoses as chiral mobile phase additives with SDS using micellar electrokinetic chromatography allowed the resolution of isosakuranetin enantiomers (Park *et al.*, 2005). A follow-up study of the enantiomeric separation of isosakuranetin by capillary electrophoresis using the various cyclodextrins as selectors demonstrated separation with the best resolution of $R_s = 3.43$ with sulfato- β -cyclodextrin and baseline resolution with carboxymethyl- γ -cyclodextrin ($R_s = 2.11$) and methyl- γ -cyclodextrin ($R_s = 2.05$) (Wistuba *et al.*, 2006). The combined use of the surfactant SDS to a buffer system containing γ -cyclodextrin ($R_s = 1.78$) or hydroxypropyl- γ -cyclodextrin ($R_s = 1.49$) using micellar electrokinetic chromatography demonstrated good separation for both (Wistuba *et al.*, 2006). Furthermore, current members of the laboratory lead by Karina Vega-Villa are validating a method to separate this chiral flavanone enantiomers using the Chiralpak AD-RH column (Vega-Villa *et al.* unpublished observations).

1.3.2.11 Liquiritigenin

Liquiritigenin was resolved into its respective enantiomers on a Chiralcel OD column in normal phase and its presence was detected in post-administrative urine of patients administered herbal medicines predominantly in the S enantiomer (Li *et al.*, 1998a; Li *et al.*, 1998b; Li *et al.*, 1998c).

1.3.2.12 Methoxyflavanone, 4'-

Different columns have been reported to separate 4'-methoxyflavanone including: Chiralcel OD (Krause *et al.*, 1989; Krause *et al.*, 1990b), Chiralpak OP (+), ChiraSpher, Cyclobond I (Krause *et al.*, 1990b), Chiralcel OC and Chiralcel OJ (Ficarra *et al.*, 1995).

1.3.2.13 Methoxyflavanone, 5-

5-methoxyflavanone has been separated using different columns, such as: Chiralcel OD (Ficarra *et al.*, 1995; Krause *et al.*, 1990b), Chiralpak OP (+), ChiraSpher, acetylated Cyclobond I (Krause *et al.*, 1990b), ureido-bonded methylated β -cyclodextrin (Ng *et al.*, 2002), Chiralcel OC, Chiralcel OJ, and Chiralcel OA (Ficarra *et al.*, 1995).

1.3.2.14 Methoxyflavanone, 6-

6-methoxyflavanone has been separated using different columns, such as: Chiralcel OD (Krause *et al.*, 1989; Krause *et al.*, 1990b), Chiralcel OC, Chiralcel OJ (Ficarra *et al.*, 1995), Chiralpak OP (+), ChiraSpher, Cyclobond I (Krause *et al.*, 1990b), and ureido-bonded methylated β -cyclodextrin (Ng *et al.*, 2002). Separation of 6-methoxyflavanone by capillary electrophoresis using sulfobutyl ether β -cyclodextrin as the selector was accomplished although baseline resolution was not obtained (Aturki *et al.*, 2003). It has also been resolved using a silica coated with a (2-hydroxy-3-methacryloyloxypropyl β -cyclodextrin-co-N-vinylpyrrolidone) copolymer in reverse-phase mode (Carbonnier *et al.*, 2005). In addition,

reasonable enantioseparation of 6-methoxy flavanone ($R_s = 1.31$) on mono (6^A-*N*-allylamino-6^A-deoxy)permethylated β -cyclodextrin (MeCD) covalently bonded to silica gel in the reverse phase has been reported (Lai *et al.*, 2004).

1.3.2.15 Methoxyflavanone, 7-

7-methoxyflavanone has been separated using different columns, such as: Chiralcel OA, Chiralcel OD (Ficarra *et al.*, 1995), and ureido-bonded methylated β -cyclodextrin (Ng *et al.*, 2002). It has also been resolved using a silica coated with a (2-hydroxy-3-methacryloyloxypropyl β -cyclodextrin-co-N vinylpyrrolidone) copolymer in reverse-phase mode (Carbonnier *et al.*, 2005). In addition, baseline enantioseparation of 7-methoxyflavanone ($R_s = 2.28$) on mono (6^A-*N*-allylamino-6^A-deoxy)permethylated β -cyclodextrin (MeCD) covalently bonded to silica gel in the reverse phase has been reported (Lai *et al.*, 2004).

1.3.2.16 Naringin and Naringenin

Naringin ((+/-)-4',5,7-trihydroxyflavanone 7-rhamnoglucoside) is a chiral flavanone-7-O-glycoside present in citrus fruits, tomatoes, cherries, oregano, beans, and cocoa (Exarchou *et al.*, 2003; Ho *et al.*, 2000; Hungria *et al.*, 1992; Minoggio *et al.*, 2003; Sanchez-Rabaneda *et al.*, 2003; Wang *et al.*, 1999). After consumption, the neohesperidose sugar moiety is rapidly cleaved off the parent compound in the gastrointestinal tract and liver to leave the aglycone bioflavonoid naringenin. The ratio between the amount of naringenin and naringin varies among different food products. For instance, citrus fruits contain higher amounts of the glycoside naringin, while tomatoes have higher amounts of the aglycone naringenin (Yanez *et al.*, 2005b). Naringin was acetylated and separated on an achiral column (Galensa *et al.*, 1980). A Cyclobond I column can also resolve naringin epimers (Krause *et al.*, 1991b). Only about 2% of naringin is in the 2R configuration in immature freshly squeezed grapefruit, while ripe

grapefruit contained 66% 2S and 34% 2R naringin, and grapefruit from a commercial source 60% 2S and 40% 2R (Krause *et al.*, 1991b). A CSP using MCCTA in normal phase provided resolution in a tomato ketchup sample (Krause *et al.*, 1990a). The Chiralcel OD column can separate naringin in albedo grapefruit and examine epimer changes during grapefruit maturation using normal phase isocratic HPLC (Caccamese *et al.*, 2003). The stereochemistry of naringin changes with the diameter of fruit with greater concentrations of S-naringin in the smallest diameter of grapefruit (Caccamese *et al.*, 2003). A recent report using β -cyclodextrin, dimethyl- β -cyclodextrin, and hydroxypropyl β -cyclodextrin as mobile phase additives in capillary electrophoresis resolved the epimers of naringin although baseline resolution was not obtained (Gel-Moreto *et al.*, 2001). Naringin could be separated using sodium cholate as a mobile phase additive under micellar electrokinetic chromatography; however, baseline resolution was not obtained (Asztemborska *et al.*, 2003) although a follow-up study demonstrated pH dependent baseline resolution (Wistuba *et al.*, 2006). The S:R ratio in sour oranges and marmalade made from sour oranges was 60:40, while in immature grapefruits both naringenin enantiomers were detected, and the S enantiomer clearly predominated and decreased as the fruit matured (Gel-Moreto *et al.*, 2003). The use of carboxylated β -cyclodextrin columns in reverse phase demonstrated that Jaffa grapefruit juices contain naringin epimers mainly in the 2S form (Aturki *et al.*, 2004). In freshly squeezed red grapefruit juice, 56% of the naringin was in the 2S form whereas lower percentage of the 2S epimer was found in commercial white and red grapefruit juice (Aturki *et al.*, 2004). A Chiralpak IA column was also able to separate naringin directly under normal phase isocratic conditions although baseline resolution was not obtained (Uchiyama *et al.*, 2005). Finally, separation of naringin and naringenin by capillary electrophoresis using sulfobutyl ether β -cyclodextrin as

the selector was accomplished and grapefruit juice was determined to be essentially 50:50 in naringin epimers (Aturki *et al.*, 2003). A more recent study reported the enantiomeric separation of naringenin by capillary electrophoresis using the various cyclodextrins as selectors and demonstrated separation with the best resolution of $R_s = 4.85$ with hydroxypropyl- γ -cyclodextrin and baseline resolution with methyl- γ -cyclodextrin ($R_s = 3.81$), carboxymethyl- γ -cyclodextrin ($R_s = 2.26$), and sulfato- β -cyclodextrin ($R_s = 3.63$) (Wistuba *et al.*, 2006). The combined use of the surfactant SDS to a buffer system containing γ -cyclodextrin or hydroxypropyl- γ -cyclodextrin or sulfato- β -cyclodextrin using micellar electrokinetic chromatography demonstrated separation for all and baseline separation ($R_s = 1.72$) for γ -cyclodextrin (Wistuba *et al.*, 2006). Finally, the Cyclobond I 2000 column has been shown to demonstrate baseline resolution of naringin in reverse phase.

Three commercially available columns of microcrystalline cellulose triacetate (CTA I, CTA II, and CTA III available from Merck, Darmstadt, Germany) were able to resolve naringenin (Krause *et al.*, 1988). A commercially available cellulose triacetate column coated on macroporous silica gel (Chiralcel OA, Daicel) separated naringenin enantiomers in normal phase although baseline resolution was not obtained (Ficarra *et al.*, 1995; Krause *et al.*, 1990a). A microcrystalline cellulose triacetate (MCCTA) coated on 7 μ m Nucleosil diol, and depolymerized MCCTA using normal and reverse phase provided baseline resolution. A CSP using MCCTA in normal phase provided resolution in a tomato sample demonstrating the presence of both enantiomers (Krause *et al.*, 1990a). A CSP using cellulose triacetate in normal phase in thyme samples demonstrated stereospecific disposition of the S(-)- enantiomer and both enantiomers in a tomato ketchup sample (Krause *et al.*, 1990a). Naringenin was also resolved into respective enantiomers on a Chiralcel OD column in normal phase and its

presence was detected in post-administrative urine of patients administered herbal medicines predominantly in the S enantiomer (Li *et al.*, 1998a; Li *et al.*, 1998b; Li *et al.*, 1998c). The utility of the Chiralcel OD column was also demonstrated by others (Caccamese *et al.*, 2005).

There are, however, a couple of reports demonstrating that micellar electrokinetic chromatography with chiral γ -cyclodextrin as a mobile phase additive (Asztemborska *et al.*, 2003), and multi-dimensional liquid chromatography coupled with mass spectroscopy (Aturki *et al.*, 2004) can separate naringenin enantiomers. However, baseline resolution and separation was not evident (Asztemborska *et al.*, 2003), and quantification was not validated in biological matrices (Asztemborska *et al.*, 2003; Aturki *et al.*, 2004). Ureido-bonded methylated β -cyclodextrin CSP columns can also separate naringenin (Ng *et al.*, 2002).

There was a report by Geiser *et al.* at Pittcon 2000 reporting the use of supercritical fluid chromatography (SFC) with the analytical column Chiralpak AD-RH to separate the enantiomers of naringenin. Using a Chiralpak AD-RH column with HPLC I failed to demonstrate baseline resolution for the analysis of naringenin in biological matrices. However, I was successful in naringenin separation with the commercially available Chiralcel OD-RH column, and this is the only validated direct assay method for stereospecific analysis of naringenin enantiomers in the literature (Yanez *et al.*, 2005a) (Chapter II). There is also a recent study that employed the commercially available Chiralpak AS-H (an amylose-derived column) for the separation of naringenin under normal-phase HPLC, the authors obtained baseline resolution but the method was not validated in biological matrices (Caccamese *et al.*, 2005). Furthermore, there is a recent study that reported separation of naringenin enantiomers using the ChiralPak AD-H column using APCI for normal-phase LC/MS chiral analysis (Cai *et al.*, 2007). Our method is a stereoselective, isocratic, reversed-phase high-performance liquid

chromatography (HPLC) method that has been successfully validated and applied to the determination of the enantiomers of naringenin and its application to disposition in tomato fruit and *in vivo* kinetic studies (Torres *et al.*, 2006; Torres *et al.*, 2005; Yanez *et al.*, 2005b). Furthermore, naringenin stereospecific disposition in pears, strawberries, sweet cherries, apples, and apple products has recently been determined (Davies *et al.* unpublished observations).

1.3.2.17 Narirutin

Narirutin was first separated indirectly by derivatization through acetylation and separation on an achiral column (Galensa *et al.*, 1980). In addition, Cyclobond I column can resolve narirutin directly and has shown a higher concentration of 2S narirutin than 2R narirutin in grapefruit juice but equal 2R and 2S concentrations in sweet orange juice (Krause *et al.*, 1991b). The use of the mobile phase additives γ -cyclodextrin and dimethyl- β -cyclodextrin demonstrated ability to separate the epimers of narirutin, although baseline resolution was not obtained (Gel-Moreto *et al.*, 2001). Narirutin was approximately 50:50 in sweet orange juice (Gel-Moreto *et al.*, 2003). The use of carboxylated β -cyclodextrin columns in reverse phase demonstrated that grapefruit and orange juice contain narirutin epimers in approximately equal amounts (Aturki *et al.*, 2004). Separation of narirutin by capillary electrophoresis using sulfobutyl ether β -cyclodextrin as the selector was accomplished and suggested that 2S was slightly higher in grapefruit but equal to 2R in oranges (Aturki *et al.*, 2003). The pH dependent separation of sulfobutyl ether β -cyclodextrin has been verified by a more recent publication (Wistuba *et al.*, 2006). Narirutin was separated using normal-phase HPLC in commercial herbal medicine samples using a Chiralpak IA column with the 2S epimer predominating ~60-

80% (Uchiyama *et al.*, 2005). A recent investigation, failed to achieve baseline resolution of narirutin on a Cyclobond I 2000 column (Asztemborska *et al.*, 2006).

1.3.2.18 Neoeriocitrin

The resolution of neoeriocitrin epimers using hydroxypropyl β -cyclodextrin as a chiral mobile phase additive in borate buffer with capillary electrophoresis was reported (Gel-Moreto *et al.*, 2003). Neoeriocitrin was further determined to be ~50:50 ratio in sour orange juice (Gel-Moreto *et al.*, 2003). A recent investigation using β -cyclodextrin as a chiral selector in capillary electrophoresis demonstrated poor resolution ability ($R_s = 0.35$) (Wistuba *et al.*, 2006).

1.3.2.19 Neohesperidin

The Cyclobond I column can resolve neohesperidin directly and it has been demonstrated that the presence of 2S neohesperidin predominates in marmalade processed from bitter oranges (*Citrus aurantium*) (Krause *et al.*, 1991b). A recent investigation, also achieve baseline resolution of neohesperidin on a Cyclobond I 2000 column (Asztemborska *et al.*, 2006). The resolution of neohesperidin was accomplished using natural, neutral and charged cyclodextrins as mobile phase additives using capillary electrophoresis (Gel-Moreto *et al.*, 2001; Wistuba *et al.*, 2006). The baseline resolution using hydroxypropyl- β -cyclodextrin and dimethyl- β -cyclodextrin and β -cyclodextrin was reported (Gel-Moreto *et al.*, 2001). The separation on neohesperidin on carboxylated β -cyclodextrin, permethylated β -cyclodextrin and acetylated β -cyclodextrin columns in reverse phase was also suggested (Aturki *et al.*, 2004). In addition, carboxymethyl- β -cyclodextrin can baseline resolve neohesperidin (Wistuba *et al.*, 2006). Neohesperidin could be separated using sodium cholate as a mobile phase additive in micellar electrokinetic chromatography with baseline resolution obtained (Asztemborska *et al.*, 2003;

Wistuba *et al.*, 2006). Neohesperidin was predominant in sour orange juice in the 2S form (Gel-Moreto *et al.*, 2003), and it could be separated using normal-phase HPLC in commercial herbal medicine samples using a Chiralpak IA column (Uchiyama *et al.*, 2005). More recently the separation of neohesperidin has being demonstrated using highly sulphated cyclodextrins as chiral mobile phase additives with SDS under micellar electrokinetic chromatography (Park *et al.*, 2005).

1.3.2.20 Pinocembrine

Three commercially available columns of microcrystalline cellulose triacetate were able to resolve pinocembrine (Krause *et al.*, 1988). It could also be resolved under reverse and normal phase conditions on modified MCCTA (Krause *et al.*, 1990a). Pinocembrine could be separated on both Chiralcel OD and Chiralpak AS-H columns, although baseline resolution was not obtained (Caccamese *et al.*, 2005).

1.3.2.21 Pinostrobin

It could be resolved utilizing the Chiralcel OD and ChiraSpher column (Krause *et al.*, 1990b). Pinostrobin could also be separated using γ -cyclodextrin as a mobile phase additive and micellar electrokinetic chromatography; however, baseline resolution was not obtained (Asztemborska *et al.*, 2003). The enantiomeric separation of pinostrobin by capillary electrophoresis using the various cyclodextrins as selectors demonstrated separation with the best resolution of $R_s = 1.44$ with methyl- γ -cyclodextrin (Wistuba *et al.*, 2006).

1.3.2.22 Prunin

Separation of prunin using benzoylated derivatives and reverse phase HPLC demonstrate stereospecific disposition in sweet cherries (Treutter *et al.*, 1985), oranges and grapefruit (Siewek *et al.*, 1985). In addition, the Cyclobond I column can resolve prunin and has

demonstrated its presence almost exclusively in the 2S-epimer in immature grapefruit (Gel-Moreto *et al.*, 2003; Krause *et al.*, 1991b). Finally, the use of mobile phase additives containing β -cyclodextrin and dimethyl- β -cyclodextrin demonstrated their ability to separate prunin epimers, although baseline resolution was not obtained (Gel-Moreto *et al.*, 2001). Recent investigations using sulfato- β -cyclodextrin as a chiral selector in capillary electrophoresis demonstrated excellent baseline separation of prunin epimers (Wistuba *et al.*, 2006).

1.3.2.23 Sakuranetin

Our laboratory has been successful in separating sakuranetin baseline resolution and current members of the laboratory are working in the validation of this chiral flavanone utilizing the Chiralpak AD-RH column (Takemoto *et al.* unpublished observations).

1.3.2.24 Taxifolin

Ureido-bonded methylated β -cyclodextrin CSP columns can separate taxifolin but not to baseline resolution (Ng *et al.*, 2002). However, our laboratory has recently being able to separate taxifolin utilizing the Chiralcel OJ-RH with baseline resolution (Vega-Villa *et al.* unpublished observations).

1.3.3 Conclusions

Over the last several decades a number of methods and techniques have been developed for the analysis of chiral flavanones by scientific researchers from a number of disciplines. The direct chromatographic approach has dominated this field of investigation with resolution being achieved through chiral polymer phases of oligosaccharides and their derivatives. Indirect derivatization methods have been very limited and mostly observational. There has been an increase use of chiral mobile phase additives in recent years often coupled to capillary electrophoresis. Since the seminal work in this field of Krause and Galensa in the 1980's there

has been increased awareness and interest in developing the techniques to separately analyze chiral flavanoids. It is apparent that the importance of enantiomerization and epimerization needs to be examined when developing assays for chiral flavanones. There remains a lack of stereospecific assays published in the literature for a plethora of chiral flavanones. There also remains very few validated stereospecific assays in biological matrices for the majority of compounds in this class, however, ongoing investigations in laboratories throughout the world are in progress and are rapidly advancing our stereospecific knowledge of this important class of compounds and applying this knowledge to biological applications.

1.4 HESPERIDIN AND HESPERETIN

Hesperidin ((+/-) 3,5,7-trihydroxy-4'-methoxyflavanone 7-rhamnoglucoside) $C_{28}H_{34}O_{15}$, MW 610.56 g/mol, experimental octanol to water partition coefficient (XLog P) value of -1.1 (Figure 1-7), is a chiral flavanone-7-O-glycoside consumed in oranges and other citrus fruits and herbal products (Yanez *et al.*, 2005d). The rutinose sugar moiety is rapidly cleaved off the parent compound to leave the aglycone bioflavonoid hesperetin (+/--3,5,7-trihydroxy-4'-methoxyflavanone) $C_{16}H_{14}O_6$, MW 302.28 g/mol, XLog P value of 2.174 (Figure 1-6A), also a chiral flavonoid. There is current interest in the medical use of bioflavonoids including hesperetin in the treatment of a variety of cancers and vascular diseases (Garg *et al.*, 2001).

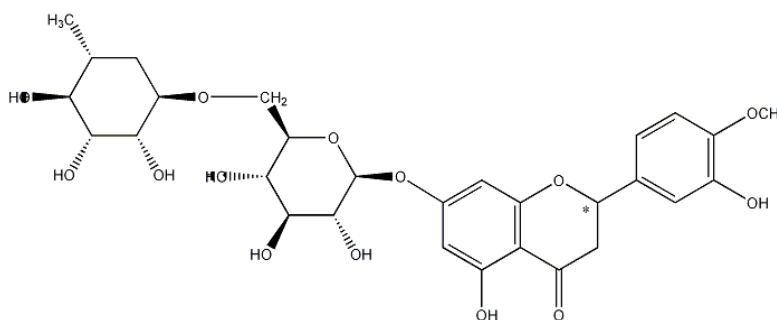


Figure 1-7: Structure of hesperidin. *Denotes chiral center.

1.4.1 Anti-Fungal, Anti-Bacterial, Anti-Viral Activity

Hesperidin extracted from grapefruit (*Citrus paradise* Macf., Rutaceae) seed and pulp ethanolic extracts has been related to have anti-bacterial and anti-fungal activity against 20 bacterial and 10 yeast strains (Cvetnic *et al.*, 2004). The level of anti-microbial effects was assessed employing an *in vitro* agar assay and standard broth dilution susceptibility test. It was observed that hesperidin exhibits strong anti-microbial activity against *Salmonella enteritidis* (Minimal Inhibitory Concentration – MIC of 2.06% extract concentration – m/V), while its activity against other bacteria and yeasts ranged from 4.13% to 16.5% m/V (Cvetnic *et al.*, 2004). Furthermore, hesperidin has also been observed to have protective effects in infected mice with Encephalomyocarditis (EMC) virus and *Staphylococcus aureus* that were administered with hesperidin before or co-administered with the lethal viral-bacterial dose (Panasiak *et al.*, 1989).

In the case of the aglycone, hesperetin, it has been shown to have MIC >20 µg/ml against *Helicobacter pylori*. However, neither hesperetin nor other flavonoids and phenolic acids inhibited the urease activity of *Helicobacter pylori* (Bae *et al.*, 1999). Furthermore, hesperetin has shown to be an effective *in vitro* agent against severe acute respiratory syndrome (SARS) (or similar) coronavirus (CoV) infections (De Clercq, 2006). Hesperetin inhibits the SARS-CoV replication by interacting with the spike (S) glycoprotein (S1 domain) in the host cell receptor and fusing the S2 domain with the host cell membrane activating the replicase polyproteins by the virus-encoded proteases (3C-like cysteine protease (3CLpro) and papain-like cysteine protease) and other virus-encoded enzymes such as the NTPase/helicase and RNA-dependent RNA polymerase. The blocking of the S1 may play an important role in the immunoprophylaxis of SARS (De Clercq, 2006). Similar activities have also been observed for

hesperetin against the replication of the neurovirulent Sindbis strain (NSV) having a 50% inhibitory doses (ID₅₀) of 20.5 µg/ml. However its glycoside, hesperidin did not have inhibitory activity indicating the possibility that the rutinose moiety of flavanones blocks the antiviral effect (Paredes *et al.*, 2003). Nevertheless, hesperetin has also been reported to be effective against the replication of herpes simplex virus type 1 (HSV-1), polio-virus type 1, parainfluenza virus type 3 (Pf-3), and respiratory syncytial virus (RSV) in *in vitro* cell culture monolayers employing the technique of viral plaque reduction (Kaul *et al.*, 1985).

1.4.2 Anti-Inflammatory Activity

The inflammatory process involves a series of events encompassed by numerous stimuli such as: infectious agents, ischemia, antigen–antibody interactions, chemical, thermal or mechanical injury. The inflammatory responses has been characterized to occur in three distinct phases, each apparently mediated by different mechanisms: an acute phase characterized by local vasodilatation and increased capillary permeability, a subacute phase characterized by infiltration of leukocyte and phagocyte cells, and a chronic proliferative phase, in which tissue degeneration and fibrosis occur (Rotelli *et al.*, 2003). Different animal models have been developed to study the different phases of an inflammatory response. In the case of testing acute inflammatory response, the carrageenan-induced paw edema in mice (Sugishita *et al.*, 1981), and the xylene induced ear edema (Young *et al.*, 1989) are widely employed. Methods to test the proliferative phase (granuloma formation) include the cotton pellet granuloma model (Meier *et al.*, 1950). Another model that allows the assessment of acute and chronic inflammation is the adjuvant–carrageenan-induced inflammation (ACII) model to induce adjuvant arthritis (Mizushima *et al.*, 1972). Hesperidin and hesperetin were tested under these models, and it was observed that only hesperetin had a positive effect in

reducing the carrageenan-induced paw edema in mice by 48% and 29% after 3 and 7 hours post-inflammatory insult (Rotelli *et al.*, 2003). In the case of the xylene induced ear edema model both hesperidin and hesperetin had a positive effect by reducing the edema by 45% and 44% respectively (Rotelli *et al.*, 2003). Similar observations were observed in the cotton pellet granuloma whereas hesperidin and hesperetin inhibited granuloma formation by 30% and 28% respectively (Rotelli *et al.*, 2003). In the case of the adjuvant–carrageenan-induced inflammation (ACII) model, hesperidin exhibited activity in the acute phase (day 6) by causing a reduction in paw edema of 52% and exhibited a more moderate reduction in the chronic phase (7-21 days) by reducing the paw edema by 36, 44, 47, 38, and 31% at 7, 8, 10, 12, and 16 days post-inflammatory insult, respectively (Rotelli *et al.*, 2003). Different mechanisms to elucidate how hesperidin, hesperetin, and other polyphenols might carry their anti-inflammatory activity have been proposed. Among these it has been observed that after carrageenan injection there is an initial release of histamine and serotonin during the first 1.5 h with a posterior release of kinin between 1.5 and 2.5 h, followed with a release of prostaglandins until 5 hours (Di Rosa *et al.*, 1971; Vinegar *et al.*, 1976; Vinegar *et al.*, 1982). Thus, it is believed that these hesperidin and hesperetin might be involved with a variety of steps during the development of inflammation.

Other studies have reported that hesperidin downregulates the LPS-induced expression of different proinflammatory (TNF-alpha, IL-1 beta, IL-6) and anti-inflammatory mediators (IL-12) cytokines as well as cytokines (KC, MCP-1 and MIP-2), while enhancing the production of other anti-inflammatory cytokines (IL-4 and IL-10) (Yeh *et al.*, 2007). In this study mice were challenged with intratracheal lipopolysaccharide (100 µg) 30 min before with treatment hesperidin (200 mg/kg oral administration) or vehicle. After 4 and 24 h, bronchoalveolar

lavage fluid was collected observing that hesperidin significantly reduced the total leukocyte counts, nitric oxide production, and iNOS expression (Yeh *et al.*, 2007). These results correlate with *in vitro* studies that have demonstrated that hesperidin suppresses the expression of IL-8 on A549 cells and THP-1 cells, the expression of TNF-alpha, IL-1 beta, and IL-6 on THP-1 cells, the expression of ICAM-1 and VCAM-1 (responsible for cell adhesion) on A549 cells. The suppression of these inflammatory mediators is regulated by NF- κ B and AP-1, which are activated by I κ B and MAPK pathways indicating that hesperidin might interact within these pathways to exert its anti-inflammatory activity (Yeh *et al.*, 2007).

1.4.3 Anti-Oxidant Activity

Hesperidin and its aglycone, hesperetin have been assessed in various *in vitro* chemical anti-oxidant models (cell-free bioassay systems). It has been observed that both hesperidin and hesperetin exhibited similar patterns of 1,1-diphenyl-2-picrylhydrazyl (DPPH) radical scavenging activities (Cho, 2006). Similar results have been reported elsewhere for hesperidin anti-oxidant capacity in similar efficacy of Trolox® (positive control) (Wilmsen *et al.*, 2005). Furthermore, hesperetin alone has been reported to effectively scavenge peroxynitrite (ONOO⁻) in a concentration-dependant manner. Peroxynitrite (ONOO⁻) is a reactive oxidant formed from superoxide (*O₂⁻) and nitric oxide (*NO), that can oxidize several cellular components, including essential protein, non-protein thiols, DNA, low-density lipoproteins (LDL), and membrane phospholipids (Kim *et al.*, 2004).

Both hesperidin and hesperetin have also been assessed for their anti-oxidant capacity *in vivo*. It has been observed that hesperidin (25 mg/kg body weight p.o.) offers protection against lung damage induced by a subcutaneous injection of nicotine at a dosage of 2.5 mg/kg body weight for 5 days a week. Hesperidin treatment resulted in a decreased level of all the marker

enzymes, the recovery of the *in vivo* anti-oxidant status back to near baseline level (Balakrishnan *et al.*, 2007a), and different matrix metalloproteinases (MMPs) were downregulated (Balakrishnan *et al.*, 2007b). Hesperidin (60 mg/kg body weight/day p.o for 9 days) has also been shown to increase the free SH-group concentration (SHC), hydrogen-donating ability (HDA), and natural scavenger capacity and to decrease the hepatic malonaldehyde content and dien conjugate (DC) in male Wistar albino rats with alimentary-induced fatty livers (Rapavi *et al.*, 2007). Furthermore, hesperidin in the same animal models has been reported to increase both the total scavenger capacity (TSC) and the activity of superoxide dismutase (SOD) in liver homogenates, and to induce slight changes in the Cu, Zn, Mn and Fe content of liver homogenates (Rapavi *et al.*, 2006). Similar results were observed for hesperidin (100 and 200 mg/kg p.o for one week) in CCl₄-induced oxidative stressed rats, whereas the thiobarbituric acid reactive substances (TBARS) decreased and the glutathione (GSH) content, superoxide dismutase (SOD), and catalase (CAT) levels increased in liver and kidney homogenates (Tirkey *et al.*, 2005). In the case of hesperetin, it was observed to be a potent anti-oxidant, inhibiting lipid peroxidation initiated in rat brain homogenates by Fe²⁺ and L-ascorbic acid. Hesperetin was found to protect primary cultured cortical cells against the oxidative neuronal damage induced by H₂O₂ or xanthine and xanthine oxidase. In addition, it was shown to attenuate the excitotoxic neuronal damage induced by excess glutamate in the cortical cultures (Cho, 2006).

1.4.4 Anti-Cancer Activity

In vitro tests have shown that hesperidin reduces the proliferation of many cancer cells (Zheng *et al.*, 2002). For instance, hesperidin (100 µM) has been shown to reduce cell viability $65 \pm 0.05\%$ of human colon cancer cells, SNU-C4 based in 3-(4,5-dimethylthiazol-2-yl)-2,5-

diphenyltetrazolium bromide (MTT) assay (Park *et al.*, 2007). It was proposed that hesperidin treatment decreased the expression of B-cell CLL/lymphoma 2 (BCL2) mRNA, and increased the expression of BCL2-associated X protein (BAX) and of the apoptotic factor caspase3 (CASP3) inducing apoptosis (Park *et al.*, 2007). Another study, less mechanistic in nature, observed that hesperidin and hesperetin at smaller concentrations (1 μ M) inhibit the neoplastic transformation of C3H 10T1/2 murine fibroblasts induced by the carcinogen 3-methylcholanthrene (Franke *et al.*, 1998).

Hesperetin has been reported to affect the proliferation and growth of a human breast carcinoma cell line, MDA-MB-435 with an IC_{50} of 22.5 μ g/ml and to exhibit low cytotoxicity (> 500 μ g/ml for 50% cell death) (So *et al.*, 1996). Furthermore, hesperetin has also been reported to significantly inhibit cell proliferation of MCF-7 cells in a concentration-dependent manner by causing cell cycle arrest in the G1 phase. In the G1-phase, hesperetin downregulates the cyclin-dependent kinases (CDKs) and cyclins, while upregulating p21(Cip1) and p27(Kip1) in MCF-7 cells. Hesperetin also decreases CDK2 and CDK4 together with cyclin D. In addition, hesperetin increases the binding of CDK4 with p21(Cip1) but not p27(Kip1) or p57(Kip2), indicating that the regulation of CDK4 and p21(Cip1) may participate in the anti-cancer activity pathway of hesperetin in MCF-7 cells (Choi, 2007).

The $Apc^{Min/+}$ mouse model and the azoxymethane (AOM) rat model are the main animal models used to study the effect of dietary agents on colorectal cancer (Corpet *et al.*, 2002). Different chemopreventive agents in the AOM rat model have been analyzed (Corpet *et al.*, 2003; Corpet *et al.*, 2002) and it was observed that hesperidin and hesperetin-rich foods are able to suppress colon adenocarcinoma and/or consistently inhibit adenoma and ACF in several independent rat studies (Corpet *et al.*, 2002; Franke *et al.*, 2002; Miyagi *et al.*, 2000; Tanaka *et*

al., 2000; Yang *et al.*, 1997). Other animal studies have reported that hesperidin has the capacity to inhibit tumor initiation and promotion in CD-1 mice skin. Subcutaneous application of hesperidin did not inhibit 7,12-dimethylbenz(a)anthracene-induced tumor initiation but did inhibit 12-O-tetradecanoyl-13-phorbol acetate-induced tumor promotion (Berkarda *et al.*, 1998). Furthermore, male ICR mice that were N-butyl-N-(4-hydroxybutyl)nitrosamine (OH-BBN) (500 µg/ml)-induced for urinary-bladder tumors were fed with hesperidin (1 mg/ml), diosmin (1 mg/ml), and combination (4.9 mg/ml diosmin and 0.1 mg/ml hesperidin) for 8 weeks. It was observed that hesperidin and diosmin alone or in combination significantly reduced the frequency of bladder carcinoma and preneoplasia. Also a significant decrease in incidence of bladder lesions and cell-proliferation activity estimated by enumeration of silver-stained nucleolar-organizer-region-associated proteins (AgNORs) and by the 5-bromodeoxyuridine (BUdR)-labeling index was observed (Yang *et al.*, 1997). However, other research groups have observed that hesperidin (100 µg/ml) and diosmin (100 µg/ml) alone or in combination (900 µg/ml diosmin and 100 µg/ml hesperidin) provide no pathological alterations during the initiation and post-initiation phases of esophageal carcinogenesis initiation with N-methyl-N-amyl nitrosamine (MNAN) in male Wistar rats (Tanaka *et al.*, 1997a).

1.4.5 Cyclooxygenase-1 and -2 Inhibitory Activity

Hesperidin has been assessed for its inhibitory effect on lipopolysaccharide (LPS)-induced over-expression of cyclooxygenase-2 (COX-2), inducible nitric oxide synthase (iNOS) proteins, over-production of prostaglandin E₂ (PGE₂) and nitric oxide (NO) using mouse macrophage cells. Treatment with hesperidin suppressed production of PGE₂, nitrogen dioxide (NO₂), and expression of iNOS protein. In the case of COX-2, hesperidin did not affect the protein levels expressed. Thus, hesperidin has been reported to be a COX-2 and iNOS

inhibitor, which may explain its anti-inflammatory and anti-tumorigenic efficacies *in vivo* (Sakata *et al.*, 2003). Furthermore, hesperetin and hesperidin in the concentration range 250-500 μM have been shown to potently inhibit the LPS-induced expression of the COX-2 gene in RAW 264.7 cells, also demonstrating the anti-inflammatory activity of these compounds. The ability of hesperetin and hesperidin to suppress COX-2 gene expression has been suggested to possibly be a consequence of their anti-oxidant activity (Hirata *et al.*, 2005).

1.4.6 Anti-Adipogenic Activity

Obesity is biologically characterized at the cellular level to be an increase in the number and size of adipocytes differentiated from fibroblastic pre-adipocytes in adipose tissue. It has been reported that hesperidin inhibits the formation of 3T3-L1 pre-adipocytes by 11.1%. Apoptosis assays indicate that hesperidin increased apoptotic cells in a time- and concentration-dependent manner. Treatment of cells with hesperidin also decreased the mitochondrial membrane potential in a time and dose-dependant manner. The cell apoptosis/necrosis assay demonstrated that hesperidin increased the number of apoptotic cells, but not necrotic cells. Hesperidin treatment of cells caused a significant time- and concentration-dependent increase in the caspase-3 activity. Western blot analysis indicated that treatment of hesperidin also markedly down-regulated poly ADP-ribose polymerase (PARP) and Bcl-2 proteins, and activated caspase-3, Bax, and Bak proteins. These results indicate that hesperidin efficiently inhibits cell population growth and induction of apoptosis in 3T3-L1 pre-adipocytes (Hsu *et al.*, 2006). Furthermore, in the same *in vitro* model hesperidin has been recently reported to inhibit intracellular triglyceride and glycerol-3-phosphate dehydrogenase (GPDH) activity by $40.2 \pm 3.2\%$ and $37.9 \pm 4.6\%$ respectively (Hsu *et al.*, 2007).

1.4.7 Other Reported Activities

Hesperidin and its aglycone hesperetin have been shown to have a very weak estrogenic effect, and its regular use can alleviate certain symptoms related with menopause and dysmenorrhea (Klinge *et al.*, 2003; Philp, 2003). For instance, in a controlled clinical study 94 menopausal women with hot flashes were given a daily formula for one month containing 900 mg hesperidin, 300 mg hesperidin methyl chalcone, and 1,200 mg vitamin C. After one month of treatment, the symptoms of hot flashes were completely relieved in 53 percent and reduced in 34 percent of the women (Smith, 1964).

1.5 NARINGIN AND NARINGENIN

Naringin ((+/-) 4',5,7-trihydroxyflavanone 7-rhamnoglucoside) $C_{27}H_{32}O_{14}$, MW 580.53 g/mol, XLogP value of -1 (Figure 1-8) is a chiral flavanone-7-O-glycoside present in citrus fruits, tomatoes, cherries, oregano, beans, and cocoa (Exarchou *et al.*, 2003; Ho *et al.*, 2000; Hungria *et al.*, 1992; Minoggio *et al.*, 2003; Sanchez-Rabaneda *et al.*, 2003; Wang *et al.*, 1999). After consumption, the neohesperidose sugar moiety is rapidly cleaved off the parent compound in the gastrointestinal tract and liver to leave the aglycone bioflavonoid naringenin ((+/-) 4',5,7-trihydroxyflavanone) $C_{15}H_{12}O_5$, MW 272.25 g/mol, XLogP value of 2.211 (Figure 1-6B). The ratio between the amount of naringenin and naringin varies among different food products. For instance, citrus fruits contain higher amounts of the glycoside naringin, while tomatoes have higher amounts of the aglycone naringenin (Minoggio *et al.*, 2003).

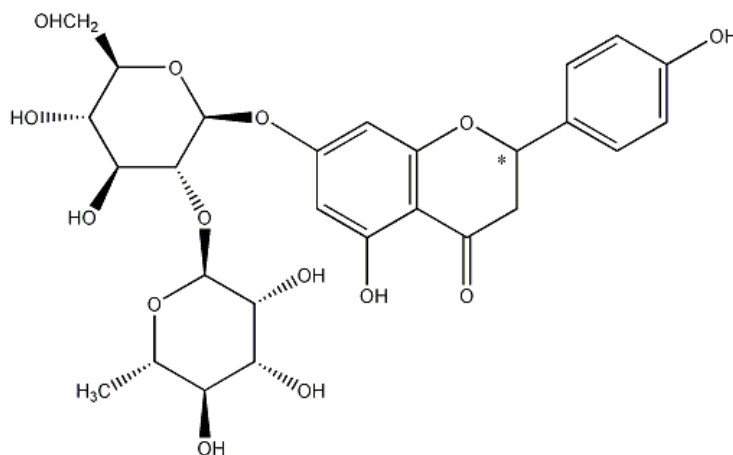


Figure 1-8: Structure of naringin. *Denotes chiral center.

1.5.1 Anti-Fungal, Anti-Bacterial, and Anti-Viral Activity

Naringin present in grapefruit (*Citrus paradise* Macf., Rutaceae) seed and pulp ethanolic extracts has been related to have anti-bacterial and anti-fungal activity against multiple bacteria, fungi, and yeast strains (Cvetnic *et al.*, 2004; el-Gammal *et al.*, 1986). Naringin was assessed employing an *in vitro* agar assay and standard broth dilution susceptibility test and it was observed that it exhibited the strongest anti-microbial effect against *Salmonella enteritidis* (Minimal Inhibitory Concentration – MIC of 2.06% extract concentration – m/V) and a MIC ranging from 4.13% to 16.5% m/V for the other tested bacteria and yeasts (Cvetnic *et al.*, 2004). Similar results have been reported for naringin present in Argentine Tagetes (Asteraceae) (Tereschuk *et al.*, 2004) and in *Drynaria quercifolia* (Ramesh *et al.*, 2001).

Naringenin isolated from ethanol extracts of Propolis from four different regions of Turkey and Brazil exhibited to have minimum inhibitory concentrations (MIC) values ranged from 4 to 512 $\mu\text{g/ml}$ for all the analyzed bacterial strains. Death was observed within 4 h of incubation for *Peptostreptococcus anaerobius* and *micros*, *Lactobacillus acidophilus* and *Actinomyces naeslundii*, while 8 h for *Prevotella oralis* and *Prevotella melaninogenica* and *Porphyromonas gingivalis*, 12 h for *Fusobacterium nucleatum*, 16 h for *Veillonella parvula* (Koru *et al.*, 2007).

Similar results were found for naringenin-rich ethanol extracts of Propolis having MIC values of 2 µg/ml for *Streptococcus sobrinus* and *Enterococcus faecalis*, 4 µg/ml for *Micrococcus luteus*, *Candida albicans* and *C. krusei*, 8 µg/ml for *Streptococcus mutans*, *Staphylococcus aureus*, *Staphylococcus epidermidis* and *Enterobacter aerogenes*, 16 µg/ml for *Escherichia coli* and *C. tropicalis* and 32 µg/ml for *Salmonella typhimurium* and *Pseudomonas aeruginosa* (Uzel *et al.*, 2005). Similar MIC values have been observed for naringenin isolated from the capitula of *Helichrysum compactum* (Suzgec *et al.*, 2005). Naringenin has also been shown to have MIC >20 µg/ml against *Helicobacter pylori*. However, neither naringenin nor other flavonoids and phenolic acids inhibited the urease activity of *Helicobacter pylori* (Bae *et al.*, 1999).

Naringenin have also been reported to have anti-viral activity. For instance, naringenin exhibited an inhibitory effect on the replication of the Sindbis neurovirulent strain (NSV) having a 50% inhibitory doses (ID₅₀) of 14.9 µg/ml. However its glycoside, naringin did not have inhibitory activity (Paredes *et al.*, 2003). Similar results were observed for naringin that was also ineffective on the replication of herpes simplex virus type 1 (HSV-1), polio-virus type 1, parainfluenza virus type 3 (Pf-3), and respiratory syncytial virus (RSV) in *in vitro* cell culture monolayers employing the technique of viral plaque reduction (Kaul *et al.*, 1985). Furthermore, naringenin has demonstrated activity against herpes simplex virus type 1 (HSV-1) and type 2 (HSV-2) infected Vero cells in a virus-induced cytopathic effect (CPE) inhibitory assay, plaque reduction assay, and yield reduction assay (Lyu *et al.*, 2005). However, both naringin and naringenin are ineffective in inhibiting poliovirus replication (Castrillo *et al.*, 1986).

1.5.2 Anti-Inflammatory Activity

Naringenin has been reported to have poor or no effect over different inflammatory mediators *in vitro*. For instance, naringenin was ineffective in inhibiting endothelial adhesion molecule expression or in attenuating expression of E-selectin and intercellular adhesion molecule 1 (ICAM-1), vascular cell adhesion molecule 1 (VCAM-1), and tumor necrosis factor alpha-induced adhesion molecule expression in human aortic endothelial cells (Lotito *et al.*, 2006). In another study, naringenin also exhibited virtually no effects on cytokines, metabolic activity or on the number of cells in the studied cell populations of stimulated human peripheral blood mononuclear cells (PBMC) by lipopolysaccharide (LPS) (Hougee *et al.*, 2005). Furthermore, the lack of ability of naringenin to inhibit the activity of NOS-2 has been reported; however, the induction of NOS-2 protein in LPS-treated J774.2 cell was evident by Western blotting techniques (Olszanecki *et al.*, 2002).

However, naringin has been reported to regulate certain inflammatory mediators and to possess anti-inflammatory activity. Naringin (10, 30 and 60 mg/kg i.p.) dose-dependently suppressed LPS-induced production of TNF-alpha in mice. To further examine the mechanism by which naringin suppresses LPS-induced endotoxin shock, an *in vitro* model, RAW 264.7 mouse macrophage cells was utilized. Naringin (1 mM) suppressed LPS-induced production of NO and the expression of inflammatory gene products such as inducible NO synthase (iNOS), TNF-alpha, inducible cyclooxygenase (COX-2) and interleukin-6 (IL-6) as determined by RT-PCR assay. Naringin was also found to have blocked the LPS-induced transcriptional activity of NF-κB in electrophoretic mobility shift assay and reporter assay. These findings suggest that suppression of the LPS-induced mortality and production of NO by naringin is due to inhibition of the activation of NF-κB (Kanno *et al.*, 2006a).

Similarly, a separate study assessed the effect of naringin in an endotoxin shock model based on *Salmonella* infection. Intraperitoneal (i.p.) infection with 10 CFU *Salmonella typhimurium* aroA caused lethal shock in lipopolysaccharide (LPS)-responder but not LPS-non-responder mice. Administration of 1 mg naringin 3 h before infection resulted in protection from lethal shock, similar to LPS-non-responder mice. The protective effect of naringin was time- and dose-dependent. Treatment with naringin resulted not only in a significant decrease in bacterial numbers in spleens and livers, but also in a decrease in plasma LPS levels. In addition, naringin markedly suppressed TNF-alpha and normalized the activated states of blood coagulation factors such as prothrombin time, fibrinogen concentration and platelet numbers caused by infection (Kawaguchi *et al.*, 2004).

1.5.3 Anti-Oxidant Activity

Different *in vitro* chemical and biological assays have reported that naringin and naringenin have considerable anti-oxidant properties. For instance, naringin has been reported to scavenge the 1,1-diphenyl-2-picrylhydrazyl (DPPH), 2,2'-azinobis-(3-ethyl-benzothiazoline-6-sulfonic acid) (ABTS) and nitric oxide (NO) radicals *in vitro* in a concentration-dependant manner (Rajadurai *et al.*, 2007a). Furthermore, naringin and naringenin have been assessed in the beta-carotene-linoleic acid, 1,1-diphenyl-2-picryl hydrazyl (DPPH), superoxide, and hamster low-density lipoprotein (LDL) *in vitro* models to measure their anti-oxidant activity. Using the beta-carotene-linoleate model, naringin (10 μ M) and naringenin (10 μ M) exhibited an 8% and 9% inhibition respectively. Whereas, both compounds demonstrated negative free radical scavenging activity using the DPPH method, and a 25% and 30% inhibition of superoxide radicals for naringin and naringenin respectively. Naringin and naringenin increased the lag time of LDL oxidation to 150 min (a 32% increase from baseline levels). Thus, indicating that

both compounds have significant *in vitro* anti-oxidant properties (Yu *et al.*, 2005). Furthermore, naringin has been reported to have a positive effect in iron-induced oxidative stress and in a variety of cellular processes like respiration and DNA synthesis. For this, HepG2 cells were treated with 0.5, 1, 2.5, and 5 mM naringin 1 h before exposure to 0.1, 0.25, 0.5, and 1 mM ferric iron. Pretreatment of HepG2 cells with naringin resulted in inhibition of lipid peroxidation, arrested the iron-induced depletion in the glutathione (GSH) concentration, and increased various antioxidant enzymes like glutathione peroxidase (GSHPx), catalase, and superoxide dismutase (SOD) (Jagetia *et al.*, 2004).

Naringin has also demonstrated anti-oxidant properties in different *in vivo* animal models. A comparison study between grapefruit juice and naringin reported that the total anti-oxidant activity of a quantity of red grapefruit juice was higher than that of naringin. Animals received a cholesterol-rich diet and after administration of naringin (0.46-0.92 mg p.o) or red grapefruit juice (1.2 ml), it was observed that diets supplemented with red grapefruit juice and to a lesser degree with naringin improved the plasma lipid levels and increased the plasma anti-oxidant activity (Gorinstein *et al.*, 2005).

1.5.4 Anti-Cancer Activity

Naringin and naringenin have been reported to have anti-cancer activities. For instance, naringenin has been reported to induce cytotoxicity in cell lines derived from cancer of the breast (MCF-7, MDA-MB-231), stomach (KATOIII, MKN-7), liver (HepG2, Hep3B, and Huh7), cervix (Hela, Hela-TG), pancreas (PK-1), and colon (Caco-2) as well as leukemia (HL-60, NALM-6, Jurkat, and U937). Naringenin-induced cytotoxicity was low in Caco-2 and high in leukemia cells compared to other cell lines. Naringenin dose-dependently induced apoptosis, with hypodiploid cells detected in both Caco-2 and HL-60 by flow cytometric analysis (Kanno

et al., 2005). Furthermore, naringenin at concentrations higher than 0.71 mM has been reported to inhibit cell proliferation of HT29 colon cancer cells (Frydoonfar *et al.*, 2003). While, naringin has been reported to induce cytotoxicity via apoptosis in mouse leukemia P388 cells, and to slightly increase the activities of anti-oxidant enzymes, catalase and glutathione peroxidase in these cells (Kanno *et al.*, 2004).

Naringin and naringenin have also been assessed for its effects on proliferation and growth of a human breast carcinoma cell line, MDA-MB-435. The concentration at which cell proliferation was inhibited by 50% (IC₅₀) was around 20 µg/ml for naringin and naringenin with low cytotoxicity (> 500 µg/ml for 50% cell death) (So *et al.*, 1996). It has been proposed two possible mechanisms that could modulate breast tumor growth, one via inhibition of aromatase (CYP19), and via interaction with the estrogen receptor (ER). Multiple *in vitro* studies confirmed that naringin and naringenin act as aromatase inhibitors potentially reducing tumor growth. It is thought that in the *in vivo* situation breast epithelial (tumor) cells communicate with surrounding connective tissue by means of cytokines, prostaglandins and estradiol forming a complex feedback mechanism. It has been reported that naringenin affects MCF-7 proliferation with an EC₅₀ value of 287 nM, and acts as an aromatase inhibitor with an IC₅₀ value of 2.2 µM. These results show that naringenin can induce cell proliferation or inhibit aromatase in the same concentration range (1-10 µM) (van Meeuwen *et al.*, 2007). The second proposed mechanism is related to the estrogen receptor (ER), and it has been observed that naringenin exerts an anti-proliferative effect only in the presence of ER α or ER β . Moreover, naringenin stimulation induces the activation of p38/MAPK leading to the pro-apoptotic caspase-3 activation and to the poly(ADP-ribose) polymerase cleavage in selected cancer cell lines. Notably, naringenin shows an anti-estrogenic effect only in ER α containing cells;

whereas in ER β containing cells, naringenin mimics the 17 β -estradiol effects. (Totta *et al.*, 2004). Nevertheless, naringenin mediated growth-arrest in MCF-7 breast cancer cells has also been observed. Naringenin was found to inhibit the activity of phosphoinositide 3-kinase (PI3K), a key regulator of insulin-induced GLUT4 translocation, as shown by impaired phosphorylation of the downstream signaling molecule Akt. Naringenin also inhibited the phosphorylation of p44/p42 mitogen-activated protein kinase (MAPK). Inhibition of the MAPK pathway with PD98059, a MAPK kinase inhibitor, reduced insulin-stimulated glucose uptake by approximately 60%. The MAPK pathway therefore appears to contribute significantly to insulin-stimulated glucose uptake in breast cancer cells (Harmon *et al.*, 2004).

In the case of human prostate cancer cells (PC3) stably transfected with activator protein 1 (AP-1) luciferase reporter gene, the maximum AP-1 luciferase induction is of about 3 fold over control after treatment with naringenin (20 μ M). At higher concentrations, naringenin demonstrated inhibition of AP-1 activity. The MTS assay for cell viability at 24 h demonstrated that even at a very high concentration (500 μ M), cell death was minimal for naringenin. Furthermore, induction of phospho-JNK and phospho-ERK activity was observed after a two hour incubation of PC3-AP1 cells with naringenin. However no induction of phospho-p38 activity was observed. Furthermore, pretreating the cells with specific inhibitors of C-Jun N-terminal kinases (JNK) reduced the AP-1 luciferase activity that was induced by naringenin while pretreatment with Mitogen-activated protein kinase (MEK) inhibitor did not affect the AP-1 luciferase activity (Gopalakrishnan *et al.*, 2006). It was also observed that naringenin induced apoptosis of human promyeloleukemia HL-60 cells by markedly promoting the activation of caspase-3, and slightly promoting the activation of caspase-9, but with no observed effect on caspase-8 (Kanno *et al.*, 2006b). The apoptosis-induced mechanism of

naringenin has also been linked with the activation of NF- κ B and the degradation of I κ B α , which has been observed in human promyeloleukemia HL-60 cells (Kanno *et al.*, 2006b), in human colon carcinoma HCT116 cells, and in human liver carcinoma HepG2 cells (Katula *et al.*, 2005).

Neoangiogenesis is required for tumor development and progression. Many solid tumors induce vascular proliferation by production of angiogenic factors, prominently vascular endothelial growth factor (VEGF). It has been reported that naringin has a significant inhibitory activity against VEGF at 0.1 μ M in MDA-MB-231 human breast cancer cells, and that glioma cells were similarly sensitive, with U343 more active than U118. Inhibition of VEGF release by naringin in these models of neoplastic cells suggests a novel mechanism for mammary cancer prevention (Schindler *et al.*, 2006).

Animal models have also demonstrated that grapefruit juice as well as the isolated citrus compound naringin can protect against azoxymethane (AOM)-induced aberrant crypt foci (ACF) by suppressing proliferation and elevating apoptosis through anti-inflammatory activities. Grapefruit juice suppressed aberrant crypt formation and high multiplicity ACF (HMACF) formation and expansion of the proliferative zone that occurs in the AOM-injected rats consuming the control diet. Grapefruit juice also suppressed elevation of both iNOS and COX-2 levels observed in AOM-injected rats consuming the control diet. Naringin suppressed iNOS levels in AOM-injected rats, no effect was observed with respect to COX-2 levels. Thus, lower levels of iNOS and COX-2 are associated with suppression of proliferation and upregulation of apoptosis, which may have contributed to a decrease in the number of HMACF in rats provided with naringenin. These results suggest that consumption of grapefruit juice or naringin may help to suppress colon cancer development (Vanamala *et al.*, 2006). Similar

inhibition in tumor growth and formation in sarcoma S-180-implanted mice have been reported for naringenin (Kanno *et al.*, 2005).

1.5.5 Cyclooxygenase-1 and -2 Inhibitory Activity

Naringenin has been assessed for its effects on nitric oxide (NO) and prostaglandin E₂ (PGE₂) production induced by lipopolysaccharide (LPS) in the macrophage cell line J774A.1. Naringenin (0.5-50 μM) was observed to be a significant inhibitor of NO production and this effect was concentration-dependent and significant at both 5 and 50 μM. A similar pattern was observed with the inhibitory effect of naringenin on LPS-induced PGE₂ release and COX-2 expression. Naringenin markedly decreased PGE₂ release and COX-2 expression in a concentration-dependent manner. Thus, naringenin inhibits iNOS and COX-2 expression and may be one of the important mechanisms responsible for their anti-inflammatory effects (Raso *et al.*, 2001).

1.5.6 Anti-Adipogenic Activity

A recent study has looked at the activity of naringin and naringenin and other flavonoids on pre-adipocyte cell population growth. The results demonstrated that the inhibition of naringin and naringenin on 3T3-L1 pre-adipocytes was 5.6% and 28.3% respectively. Apoptosis assays demonstrated that naringin and naringenin increased apoptotic cells in time- and concentration-dependent manner. Treatment of cells with naringin and naringenin also decreased the mitochondrial membrane potential in a time and dose-dependant manner. The cell apoptosis/necrosis assay demonstrated that both naringin and naringenin increased the number of apoptotic cells, but not necrotic cells. Naringin and naringenin treatment of cells caused a significant time- and dose-dependent increase in the caspase-3 activity. Western blot analysis indicated that treatment with both naringin and naringenin also markedly down-regulated

PARP and Bcl-2 proteins, and activated caspase-3, Bax, and Bak proteins. These results suggest that the glycoside naringin and the aglycone naringenin efficiently inhibit cell population growth and induction of apoptosis in 3T3-L1 pre-adipocytes (Hsu *et al.*, 2006). Furthermore, in this same *in vitro* model naringin and naringenin have been recently reported to inhibit intracellular triglyceride by $41.3 \pm 8.4\%$ and $39.4 \pm 7.8\%$ respectively, and also inhibit GPDH activity by $39.4 \pm 5.6\%$ and $35.7 \pm 1.4\%$ respectively (Hsu *et al.*, 2007).

1.5.7 Cardioprotective Effects

Naringin (10, 20 and 40 mg/kg, administered orally for 56 days) has been reported to decrease heart weight, blood glucose, serum uric acid, serum iron, levels of total proteins, and iron binding capacity, as well as to increase Na(+)/K(+) ATPase and to decrease the activities of Ca(2+) and Mg(2+) ATPase in the heart and the levels of glycoproteins in serum and the heart in an isoproterenol (85 mg/kg sc) (ISO)-induced myocardial infarction (MI) animal model (Rajadurai *et al.*, 2007a). Similar results have been observed for naringin reducing the levels of cardiac troponin T (cTnT), lactate dehydrogenase (LDH)-isoenzymes 1 and 2, cardiac marker enzymes, electrocardiographic (ECG)-patterns and lysosomal hydrolases (Rajadurai *et al.*, 2007b).

1.5.8 Effect on Cytochrome P450

Naringin and naringenin are the main flavanones present in grapefruit juice. These compounds have been shown to markedly augment the oral bioavailability of several drugs (Ho *et al.*, 2000). This effect was originally based on an unexpected observation from an interaction study between the dihydropyridine calcium channel antagonist, felodipine, and ethanol in which grapefruit juice was used to mask the taste of the ethanol (Arayne *et al.*, 2005). Naringenin has been reported to competitively inhibit CYP3A4 altering the bioavailability of

felodipine (Bailey *et al.*, 2000), most dihydropyridines, terfenadine, saquinavir (Eagling *et al.*, 1999), cyclosporin, midazolam, triazolam, quinine (Zhang *et al.*, 2000), verapamil (Yeum *et al.*, 2006), and one of the verapamil metabolites: norverapamil (Kim *et al.*, 2005), and this interaction may also occur with lovastatin, cisapride and astemizole (Guo *et al.*, 2000a; Guo *et al.*, 2000b).

Grapefruit juice contains a variety of flavonoid molecules, such as naringin, naringenin, Quercetin and kaempferol, and some non-flavonoid molecules such as 6',7'-dihydroxybergamottin, which are known to inhibit CYP3A4 activity *in vitro* (Chan *et al.*, 1998). These polyphenolic compounds are electron rich molecules and, therefore, are likely substrates for CYP3A4 and may inhibit the enzyme (Chan *et al.*, 1998). These molecules are known to interfere with intestinal CYP3A4 and hepatic CYP2A6, thereby lowering the biotransformation of several drugs and increasing their bioavailability (Runkel *et al.*, 1997). Earlier efforts to identify the inhibitory substance(s) present in grapefruit juice largely focused on naringin and quercetin. However, when administered to humans, both compounds failed to reproduce the inhibition of dihydropyridine metabolism caused by grapefruit juice (Bailey *et al.*, 1993a; Bailey *et al.*, 1993b). Edwards and Bernier (Edwards *et al.*, 1996b) have suggested that naringin and naringenin are not the primary inhibitory compounds in grapefruit juice, although results from rat and human liver microsomes demonstrate that naringenin and other flavonoids in grapefruit juice can inhibit the metabolism of dihydropyridine calcium antagonists (Guengerich *et al.*, 1990; Miniscalco *et al.*, 1992). In the continued quest to verify and identify the active inhibitor in grapefruit juice, 6',7'-dihydroxybergamottin, a furanocoumarin, was identified as a potent inhibitor of CYP3A4 activity (Edwards *et al.*, 1996a). This study was followed by another study that confirmed the presence of 6',7'-

dihydroxybergamottin as a major substance in grapefruit juice being responsible for enhanced oral availability of CYP3A4 substrates, although other furanocoumarins probably also contribute to this phenomena (Schmiedlin-Ren *et al.*, 1997). These results have been corroborated by others (Fukuda *et al.*, 1997) that reported similar findings of altered bioavailability. It has been suggested that hydrophilic components other than flavonoids, probably coumarin derivatives, are also responsible for the inhibitory effect of grapefruit juice. In another recent study, it was found that naringin alone was ineffective in causing the inhibition of the metabolism of 1,2-benzopyrone (coumarin) in humans, thereby concluding that the inhibitory effect of grapefruit juice may be modulated by naringenin (Runkel *et al.*, 1997). In view of the existing literature, it is apparent that the inhibition of first-pass metabolism by grapefruit juice probably involves the flavonoid naringenin and also furanocoumarins. Recent reviews on drug interactions with grapefruit juice are available elsewhere (Ameer *et al.*, 1997; Bailey *et al.*, 1998; Fuhr, 1998). Concern regarding the mechanism of inhibition of CYP3A enzymes by grapefruit juice has now centered on protein expression studies. In a recent study, it was reported a selective 62% down-regulation of CYP3A4 protein levels in small intestine epithelia (enterocytes) with no corresponding change in CYP3A4 mRNA levels (Lown *et al.*, 1997). In contrast, grapefruit juice did not alter hepatic CYP3A4 activity, colon levels of CYP3A5 or small bowel concentrations of P-glycoprotein, villin, CYP1A1 and CYP2D6. In another study, it was demonstrated that grapefruit juice induced a 2- to 5-fold increase in the ability of the P-glycoprotein pump to transport drugs such as vinblastine, cyclosporin, losartan, digoxin and fexofenadine across intestinal cell monolayers *in vitro* (Soldner *et al.*, 1999). However, drugs such as nifedipine and felodipine were not transported by P-glycoprotein in these cells and their passage through the monolayer was

unaffected by grapefruit juice, since these drugs are not P-glycoprotein substrates. Orange juice is also known to inhibit the activity of CYP3A enzymes; however, there is a large difference between grapefruit and orange juice in their enzyme inhibition potencies. The difference in potency may be accountable in part to lack of detectable naringin (Grundy *et al.*, 1998) and 6',7'-dihydroxybergamottin (Edwards *et al.*, 1996a) in orange juice. Perhaps this may partly explain why orange juice did not affect the bioavailability of orally administered nifedipine (Grundy *et al.*, 1998) or pranidipine, (Hashimoto *et al.*, 1998) whereas grapefruit juice significantly increased their bioavailability. Nevertheless, red wine, which also contains a complex mixture of flavonoids and other polyphenolic compounds, inhibits CYP3A4 activity *in vitro* (Chan *et al.*, 1998). Interestingly, white wine and its components do not apparently inhibit CYP3A4 activity (Chan *et al.*, 1998).

1.5.9 Other Reported Activities

Naringin has also been reported to have anti-genotoxic properties. Naringin was assessed in an *in vitro* biological model: bleomycin-induced genomic damage of cultured V79 cells. Exposure of V79 cells to bleomycin (50 µg/ml) induced a concentration dependent elevation in the frequency of binucleate cells bearing micronuclei (MNBNC) and a maximum number of MNBNCs. Treatment of cells with 1 mM naringin before exposure to different concentrations of bleomycin arrested the bleomycin-induced decline in the cell survival accompanied by a significant reduction in the frequency of micronuclei when compared with bleomycin treatment alone. The cell survival and micronuclei induction were found to be inversely correlated. The repair kinetics of DNA damage induced by bleomycin was evaluated by exposing the cells to 10 µg/ml bleomycin using single cell gel electrophoresis. Treatment of V79 cells with bleomycin resulted in a continuous increase in DNA damage up to 6 h post-bleomycin

treatment as evident by the migration of greater amounts of DNA into the tails (% tail DNA) of the comets and a subsequent increase in olive tail moment (OTM), an index of DNA damage. Treatment of V79 cells with 1 mM naringin reduced bleomycin-induced DNA damage and accelerated DNA repair as indicated by a reduction in % tail DNA and OTM with an increasing assessment time. A maximum reduction in the DNA damage was observed at 6 h post-bleomycin treatment, where it was 5 times lower than bleomycin alone (Jagetia *et al.*, 2007).

Other reported effects of naringin include protection against radiation-induced chromosome damage. For this naringin extracted from the ethyl acetate fraction of *Aphanamixis polystachya* was investigated on the radiation-induced chromosome damage in the bone marrow cells of Swiss albino mice exposed to various doses of gamma-radiation. The mice were divided into two groups, one group was exposed to 0, 1, 2, 3, 4 or 5 Gy of gamma-radiation, while another group received 7.5 mg/kg body weight (BW) of the ethyl acetate fraction of *Aphanamixis polystachya* 1 h before exposure to 0, 1, 2, 3, 4 or 5 Gy of gamma-radiation. Various asymmetrical chromosome aberrations were studied in the bone marrow cells of mice at 12, 24 or 48 h post-irradiation. Irradiation of mice to various doses of gamma radiation caused a dose dependent elevation in the frequency of aberrant cells and chromosome aberrations like chromatid breaks, chromosome breaks, dicentrics, acentric fragments and total aberrations at all the post-irradiation times studied. The maximum asymmetrical aberrations were scored at 24 h post-irradiation except chromatid breaks that were highest at 12 h post-irradiation. A maximum number of polyploid and severely damaged cells (SDC) were recorded at 24 h post-irradiation in the SPS plus irradiation group. Treatment of mice with 7.5 mg/kg BW of the naringin-rich ethyl acetate fraction of *Aphanamixis polystachya* before exposure to 1-5 Gy of whole body gamma-radiation significantly reduced the frequencies of aberrant cells and chromosomal

aberrations like acentric fragments, chromatid and chromosome breaks, centric rings, dicentrics and total aberrations at all post-irradiation scoring times. It can be observed from this study that the naringin-rich ethyl acetate fraction of *Aphanamixis polystachya* protects mouse bone marrow cells against radiation-induced chromosomal aberrations and this reduction in radiation-induced chromosome damage may be due to free radical scavenging and reduction in lipid peroxidation. The radioprotection caused by the naringin-rich ethyl acetate fraction of *Aphanamixis polystachya* is comparable to the protection demonstrated by naringin (Jagetia *et al.*, 2006).

1.6 ERIOCITRIN AND ERIODICTYOL

Eriocitrin ((+/-) -5,7,3',4-tetrahydroxyflavanone 7-O-ruinoside) C₂₇H₃₂O₁₅, MW 596.53 g/mol, XLogP value of -1.4 (Figure 1-9) is a chiral flavanone-7-O-glycoside present in lemons, tamarinds and other citrus fruits, as well as in mint, oregano, fennel thyme and rose hip (Dapkevicius *et al.*, 2002; Exarchou *et al.*, 2003; Gil-Izquierdo *et al.*, 2004; Hvattum, 2002; Kosar *et al.*, 2004; Parejo *et al.*, 2004; Sudjaroen *et al.*, 2005). After consumption, the neohesperidose sugar moiety is rapidly cleaved off the parent compound in the gastrointestinal tract and liver to leave the aglycone bioflavonoid eriodictyol ((+/-)-5,7,3',4'-tetrahydroxyflavanone) C₁₅H₁₂O₆, MW 288.25 g/mol, XLogP value of 1.837 (Figure 1-6C).

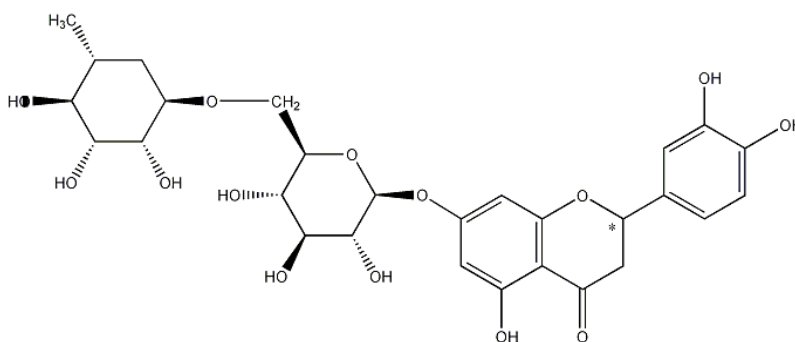


Figure 1-9: Structure of eriocitrin. *Denotes chiral center.

1.6.1 Anti-Bacterial Activity

Eriocitrin extracted from peppermint (*Mentha piperita* L.) leaves have demonstrated to have anti-microbial activities (McKay *et al.*, 2006). Furthermore, eriodictyol extracted from the leaves of *Rhus retinorrhoea* Steud, Ex Olive has exhibited moderate anti-malarial activity with an IC₅₀ 0.98 µg/ml against *Plasmodium falciparum* (W2 Clone) and weak activity against *P. falciparum* (D6 Clone) with an IC₅₀ of 2.8 µg/ml. Nevertheless, eriodictyol did not display any cytotoxicity (Ahmed *et al.*, 2001). However, eriodictyol isolated from *Gleditsia sinensis* Lam. spines demonstrated a lack of activity against *Xanthomonas vesicatoria* and *Bacillus subtilis* (Zhou *et al.*, 2007).

1.6.2 Anti-Inflammatory Activity

Eriodictyol extracted from *Thymus broussonetii* Boiss (Labiatae) leaves, a herbal drug used in Moroccan traditional medicine has been assessed using the croton oil ear test in mice and reported significant anti-inflammatory properties (Ismaili *et al.*, 2002). Furthermore, pretreatment of RAW 264.7 with eriodictyol inhibited TNF-α release in lipopolysaccharide (LPS)-stimulated macrophages. The potency of eriodictyol in inhibiting cytokine production was an IC₅₀ of less than 10 µM for TNF-α release. It was also observed that pretreatment of cells with eriodictyol decreased IκB-α phosphorylation and reduced the levels of IκB-α (Xagorari *et al.*, 2001).

1.6.3 Anti-Oxidant Activity

Eriocitrin and eriodictyol isolated from lemon (*Citrus limon*) juice exhibited a potent radical scavenging activity for 1,1-diphenyl-2-picrylhydrazyl (DPPH) and superoxide. Eriocitrin and eriodictyol were found to significantly suppress the expression of intercellular adhesion molecule-1 (ICAM-1) at 10 µM in human umbilical vein endothelial cells (HUVECs)

induced by necrosis factor-alpha (TNF- α) (Miyake *et al.*, 2007). Eriocitrin obtained from peppermint leaves (*Menthae x piperitae* folium) (total eriocitrin 38%) exhibited a strong antiradical activity (determined as DPPH* scavenging features). Eriocitrin also exhibited a strong anti-H₂O₂ activity (Sroka *et al.*, 2005). Similarly eriocitrin extracted from different *Mentha* species, varieties, hybrids, and cultivars was identified as the dominant radical scavengers in these extracts in an on-line high-performance liquid chromatography-1,1-diphenyl-2-picrylhydrazyl (HPLC-DPPH*) method (Kosar *et al.*, 2004). Furthermore, eriocitrin was reported to play a role as antioxidant *in vivo* in streptozotocin-induced diabetic rats. Diabetic rats were provided a diet which contained 0.2% eriocitrin. After the 28-d feeding period, the concentration of the thiobarbituric acid-reactive substance in the serum, liver, and kidney of diabetic rats administered eriocitrin significantly decreased as compared with that of the diabetic group. The levels of 8-hydroxydeoxyguanosine, which is exchanged from deoxyguanosine owing to oxidative stress, in the urine of diabetic rats administered eriocitrin significantly decreased as compared with that of the diabetic rat group. Eriocitrin also suppressed oxidative stress in the diabetic rats (Miyake *et al.*, 1998).

Eriodictyol isolated from the aerial parts from *Eysenhardtia subcoriacea* was assessed using an antioxidant activity assay-guided chemical analysis, using a rat pancreas homogenate model. The isolated eriodictyol demonstrated moderate radical scavenging properties against diphenylpicrylhydrazyl radical (DPPH) (Edenharder *et al.*, 2003; Narvaez-Mastache *et al.*, 2007) and reduced the glutathione levels in rat pancreatic homogenate (Narvaez-Mastache *et al.*, 2007). Furthermore, eriodictyol was assessed for its protective role against UV-induced apoptosis of human keratinocytes, the principal cell type of epidermis. The results demonstrated that eriodictyol had a positive effect on cell proliferation of human HaCaT

keratinocytes. Treatment with eriodictyol in particular resulted in significant suppression of cell death induced by ultraviolet (UV) light, a major skin-damaging agent. It was also observed that eriodictyol treatment apparently reduced the percentage of apoptotic cells and the cleavage of poly(ADP-ribose) polymerase, concomitant with the repression of caspase-3 activation and reactive oxygen species (ROS) generation. The anti-apoptotic and anti-oxidant effects of eriodictyol were also confirmed in UV-induced cell death of normal human epidermal keratinocyte (NHEK) cells suggesting that eriodictyol can be used to protect keratinocytes from UV-induced damage, implying the presence of a complex structure-activity relationship (SAR) in the differential apoptosis-modulating activities of eriodictyol and similar flavonoid compounds (Lee *et al.*, 2007).

1.6.4 Anti-Cancer Activity

Eriodictyol extracted from lemon fruit (*Citrus limon* BURM. f.) altered the DNA fragmentation of HL-60 cells when analyzed by flow cytometry. An apoptotic DNA ladder and chromatin condensation were observed in HL-60 cells when treated with eriodictyol (Ogata *et al.*, 2000). Eriodictyol was also assessed for its protective role against UV-induced apoptosis of human keratinocytes, the principal cell type of the epidermis. The results demonstrated that eriodictyol had a positive effect on cell proliferation of human HaCaT keratinocytes. Treatment with eriodictyol in particular resulted in significant suppression of cell death induced by ultraviolet (UV) light, a major skin-damaging agent. Eriodictyol treatment apparently reduced the percentage of apoptotic cells and the cleavage of poly(ADP-ribose) polymerase, concomitant with the repression of caspase-3 activation and reactive oxygen species (ROS) generation. The anti-apoptotic and anti-oxidant effects of eriodictyol were also confirmed in UV-induced cell death of normal human epidermal keratinocyte (NHEK) cells (Lee *et al.*,

2007). Eriodictyol also protected L-929 cells from TNF-induced cell death. The magnitude of protection and potentiation by eriodictyol was concentration-dependent and these effects were not altered when eriodictyol was added as much as 2 h after TNF treatment (Habtemariam, 1997). Eriodictyol possess anti-proliferative activities against several tumor and normal human cell lines. Eriodictyol has IC_{50} of 12, 10, 8.3, and 6.2 μ M in human lung carcinoma (A549), melanin pigment producing mouse melanoma (B16 melanoma 4A5), human T-cell leukemia (CCRF-HSB-2), and metastasized lymph node (TGBC11TKB) respectively (Kawaii *et al.*, 1999a).

1.6.5 Cyclooxygenase-1 and -2 Inhibitory Activity

Eriodictyol extracted from the methanol fraction of the stem bark of *Populus davidiana* demonstrated moderate inhibition against COX-1 only and exhibited suppressive effects on xanthine oxidase (XO) (Zhang *et al.*, 2006a).

1.6.6 Other Reported Activities

Eriodictyol also been reported to have anti-mutagenic activities in a model induced by tert-butyl hydroperoxide (BHP) or cumene hydroperoxide (CHP) in *Salmonella typhimurium* TA102 ($ID_{50} < 1 \mu$ mol per plate). These effects correlated with the radical scavenging activities of eriodictyol against peroxy radicals generated from 2,2'-azo-bis(2-amidinopropane)dihydrochloride (AAPH) as measured in the haemolysis test, and confirmed that in general eriodictyol is an effective radical scavenger. From these results it was concluded that in the *Salmonella*/reversion assay with strain TA102, anti-mutagenic activities of eriodictyol against the peroxide mutagens CHP and BHP are mainly caused by radical scavenging effects (Edenharder *et al.*, 2003).

1.7 PHARMACOKINETICS AND METABOLISM OF RACEMIC HESPERIDIN, HESPERETIN, NARINGIN, NARINGENIN, ERIOCITRIN, AND ERIODICTYOL

The importance of stereospecific disposition of racemic flavanones is slowly being recognized and reported in the biomedical literature. Most of these preliminary investigations report the quantification of a variety of flavanones in citrus fruit juices and herbs (Caccamese *et al.*, 2003; Gel-Moreto *et al.*, 2003; Krause *et al.*, 1991a; Krause *et al.*, 1991b; Li *et al.*, 1998c), or report the separation of flavanones on different stationary phases (Yanez *et al.*, 2007a). There is a paucity of investigations detailing the importance of stereospecific pharmacokinetics of chiral flavanones. Hesperetin, naringenin, eriodictyol and their corresponding glycosides (hesperidin, naringin, and eriocitrin) belong to this flavanone family (Yanez *et al.*, 2007a), but no stereospecific information on their pharmacokinetics has been reported. Non-stereospecific assay methods cannot interpret the time-course of an individual enantiomer and hence any interpretation based on achiral assay analysis could be misleading in determining concentration dependence of each enantiomer of a racemic flavonoid xenobiotic in terms of pharmacokinetics. For instance, most of the pharmacokinetic studies in humans after ingestion of different fruit juices or diets rich in fruits and vegetables only report the total amount excreted of different flavonoids in urine or the percentage of the dose excreted in urine (Ameer *et al.*, 1996; Brevik *et al.*, 2004; Choudhury *et al.*, 1999; Erlund *et al.*, 2001; Ishii *et al.*, 2000; Manach *et al.*, 2003; Manach *et al.*, 2005; Miyake *et al.*, 2000; Nielsen *et al.*, 2002). Out of these reports, only two studies by Manach *et al.* (Manach *et al.*, 2003) and Ishii *et al.* (Ishii *et al.*, 2000) report cumulative urinary excretion plots of hesperetin, naringenin, their glycosides, or glucuronidated metabolites. However, no further pharmacokinetic characterization was performed and urinary rate plots were not reported. Based on

pharmacokinetic theory, all the different pharmacokinetic parameters can also be derived from urinary data (Ritschel *et al.*, 2004; Shargel *et al.*, 2004). This raises a concern because most of the pharmacokinetic studies of different polyphenols in humans and rodents are based on serum or plasma data. Furthermore, different studies have reported that different polyphenols have relatively short half-lives. For instance, flavanones (i.e. hesperetin and naringenin) have been reported to have plasma elimination half-lives between 1 and 3 hours in humans (Erlund *et al.*, 2001; Manach *et al.*, 2005) and less than 20 minutes in rabbits (Hsiu *et al.*, 2002). Similar observations have been reported for flavanols (i.e. catechins) with plasma half lives of 2-3 hours (Balant *et al.*, 1979; Bell *et al.*, 2000; Chow *et al.*, 2001; Donovan *et al.*, 1999; Lee *et al.*, 2002; Lee *et al.*, 1995; Leenen *et al.*, 2000; Meng *et al.*, 2001; Richelle *et al.*, 1999; Schramm *et al.*, 2003; Ullmann *et al.*, 2003; Van Amelsvoort *et al.*, 2001) or up to 4-9 hours once milk is co-administered (Kimura *et al.*, 2002; Meng *et al.*, 2001; van het Hof *et al.*, 1998). The observations of short plasma half-life of these and other polyphenol sub-families have been recently presented in a review (Manach *et al.*, 2005). However, different studies have reported that certain polyphenols (stilbenes) would have longer urine half-lives (4.7-fold to 16-fold higher half-lives in urine compared to plasma half-lives) (Remsberg *et al.*, 2007; Roupe *et al.*, 2006). This discrepancy between plasma and urine half-life of different stilbenes was attributed to assay sensitivity limits that would most likely underestimate the overall half-life of these compounds. Underestimation of plasma half-life due to assay sensitivity limits has been reported before in the case of procainamide (Jamali *et al.*, 1988). In the report by Jamali *et al.* (Jamali *et al.*, 1988) an improved HPLC method was employed and it was observed that there was a significant 2-fold increase in plasma half-life compared to previous reports. Nevertheless, most of the pharmacokinetic studies only collected samples up to 24 hours post-

dose, which could underestimate the elimination phase and calculation of various pharmacokinetic parameters. Therefore, it is necessary to have improved analytical methods with higher detection limits that would allow detection of the polyphenol compound(s) of interest for longer than 24 hours. This would allow the assessment of the pharmacokinetics of hesperetin, naringenin, and eriodictyol enantiomers and/or hesperidin, naringin, and eriocitrin epimers as well as the determination of the stereospecific content in foodstuffs.

All three flavanones examined hesperetin, naringenin, and eriodictyol each undergoes glucuronidation upon intravenous administration, as determined by serum and urine concentrations and later verified by treating plasma and urine samples with β -glucuronidase. This *in vivo* data parallels *in vitro* metabolism findings in human and rat liver microsomes with these dietary flavonoids (Breinholt *et al.*, 2002; Nielsen *et al.*, 1998; Stevens *et al.*, 2001; Zhu *et al.*, 1998). Previous pharmacokinetic studies of these dietary flavonoids after oral ingestion of fruit juices have not been analyzed using chiral analytical techniques. For instance, hesperidin and hesperetin had been assessed after oral ingestion of orange juice by healthy human subjects (Erlund *et al.*, 2001; Kanaze *et al.*, 2007; Manach *et al.*, 2003). The pharmacokinetic studies after oral ingestion of orange juice suggested that racemic hesperetin had a plasma half-life of 2-3 hours, and that only 5% is excreted in urine (Erlund *et al.*, 2001; Kanaze *et al.*, 2007). These studies (Erlund *et al.*, 2001; Kanaze *et al.*, 2007; Manach *et al.*, 2003) also determined that hesperetin undergoes extensive glucuronidation after oral administration.

In the case of naringenin, its achiral pharmacokinetics have been studied after oral ingestion of orange juice, grapefruit juice (Erlund *et al.*, 2001), and tomato paste (Bugianesi *et al.*, 2002) showing that racemic naringenin has a short serum half life of 1-2 hours and that

after oral ingestion of orange juice only 1% of naringenin gets excreted in urine (Erlund *et al.*, 2001) and 7% in other study (Manach *et al.*, 2003). While 30% of naringenin gets excreted in urine after oral ingestion of grapefruit juice; however, the standard deviation of this measurement in the first study was 25.5% reducing the reliability of these results (Erlund *et al.*, 2001). Bugianesi *et al.* (Bugianesi *et al.*, 2002) assessed the bioavailability of naringenin from tomato paste in humans; however, half-life and fraction excreted unchanged in urine (f_e) values were not reported. The pharmacokinetics of intravenous-dosed racemic naringenin (25 mg/kg) in rabbits (2-3 kg weight) has been reported (Hsiu *et al.*, 2002). The authors report a short elimination phase half-life of only 17 ± 4 minutes, a low volume of distribution of 1.6 ± 0.4 L, and a high total clearance value of 0.16 ± 0.02 L/min. The authors also observe that naringenin undergoes significant glucuronidation and a higher concentration of the parent compound was detected in serum compared to the glucuronidated metabolite (Hsiu *et al.*, 2002).

Racemic eriodictyol has been studied after oral ingestion of eriocitrin (75 $\mu\text{mol/kg}$) via gastric intubation, as well as *ex vivo* everted gut studies to assess the intestinal absorption of eriocitrin (Miyake *et al.*, 2000). This study found that eriocitrin was not present in plasma samples of eriocitrin-treated rats, whereas significant concentrations of eriodictyol, homoeriodictyol, and hesperetin were determined 4 hours post-dose. This study was able to detect eriocitrin metabolites (eriodictyol, homoeriodictyol, hesperetin and their glucuronides) only up to 4 hours in plasma and up to 24 hours in urine. It was also observed that eriodictyol in the intestine is further metabolized to 3,4-dihydroxyhydrocinnamic acid (3,4-DHCA) (Miyake *et al.*, 2000). The same research group administered orally to humans flavonoid glycosides and aglycones extracted from lemon peel (Miyake *et al.*, 2006). This study also reported that eriocitrin undergoes sequential metabolism into eriodictyol, homoeriodictyol and

hesperetin and their corresponding glucuronidated and sulfated metabolites after the oral ingestion of the lemon peel extracts also suggesting that eriodictyol undergoes extensive phase II metabolism (Miyake *et al.*, 2006).

To our knowledge, there are no literature reports that have assessed the stereospecific pharmacokinetics of hesperetin, naringenin, and eriodictyol after intravenous administration of the pure racemates. Previous studies have focused only on the racemic mixtures and utilized achiral analysis after oral ingestion.

1.8 OBJECTIVES

Research characterizing the metabolism and pharmacokinetic parameters of different flavonoids and other polyphenols has shown that they are absorbed, distributed, and metabolized upon ingestion. Polyphenols are quickly biotransformed by the liver into glucuronidated metabolites following intestinal absorption and are excreted in the urine and bile. Furthermore, in some instances these compounds undergo extensive enterohepatic recirculation. It is also shown that humans can ingest and absorb pharmacologically active concentrations that have been shown to yield cardioprotective and chemoprotective activities. Hesperetin, naringenin, and eriodictyol are chiral flavonoids that are structurally similar to each other and possess varying degrees of potency across many assays and model systems *in vitro* and *in vivo*. It is evident that hydroxyl and methoxy moieties attached to the general flavanones structure produce these varying degrees of activity. Moreover, minute structural differences in chemical structure have the capacity to significantly change the metabolism and the pharmacokinetic parameters of these compounds. These flavanone compounds are attractive candidates for therapeutic development due to their apparent low toxicity and their anti-cancer and anti-inflammatory activities. For instance, scientists and pharmaceutical companies are

now employing flavanones as potential lead compounds and synthesizing a variety of derivatives such as chiral dihydrofuroflavones (Lantz *et al.*, 2004).

Despite encouraging research, there is a paucity of stereospecific pharmacokinetic data on the rate and extent of metabolism, elimination, and clearance of hesperetin, naringenin, and eriodictyol. There is a lack of investigations detailing the importance of stereospecific pharmacokinetics and pharmacodynamics of chiral flavanones. Of these investigations, only one reports the human urinary excretion of four different flavanones (liquiritigenin, naringenin, dihydrowogonin, and dihydrooroxylin A) after ingestion of different herbal products (Li *et al.*, 1998a; Li *et al.*, 1998b; Li *et al.*, 1998c), unfortunately pharmacokinetics analysis and modeling were not employed. To our knowledge there are no studies that have examined the pharmacokinetics, anti-cancer, or anti-inflammatory activity of the individual enantiomers of chiral flavanones. However, there is one report where the S and R enantiomers of naringenin were studied for the inhibition of cyclosporine A oxidase activity in human liver microsomes, which is a cytochrome P450 3A4-dependent activity. Interestingly, no enantioselectivity or significant inhibitory activity were demonstrated for either (R)- or (S)-naringenin or a mixture of epimers of naringin (Caccamese *et al.*, 2005).

Moreover, there are no data describing validated methods to stereospecifically quantify hesperetin, naringenin, and eriodictyol in biological matrices such as serum or urine. Thus, there is a need for stereospecific assay methods for the quantitation and effective isolation of pure flavonoid enantiomers for their pharmacometric study in *in vivo* and *in vitro* models. This stereospecific analytical methodology would provide valuable information to enantiospecifically understand how these xenobiotics are metabolized in plant, human, and animal models and to be able to better elucidate their disposition, pharmacological activity, as

well as therapeutic and toxic effects. These issues must be addressed in order to better assess whether these flavanones can be developed into feasible therapeutic agents. Therefore, the specific objectives of this project were:

- 1.) To develop and validate for the first time sensitive, specific, and stereoselective reverse phase high-performance liquid chromatography (RP-HPLC) assays in biological fluids for hesperetin, naringenin, and eriodictyol followed by verification using LC/MS (Chapter II).
- 2.) To characterize for the first time the stereospecific pharmacokinetic parameters of hesperetin, naringenin, and eriodictyol in a rat model and their stereospecific content in selected fruit juices qualitatively and quantitatively using newly developed sensitive, specific and stereoselective reverse phase high-performance liquid chromatography (RP-HPLC) assays and LC/MS for verification (Chapter III).
- 3.) To characterize the *in vitro* pharmacodynamics of racemic hesperidin, hesperetin, naringin, naringenin, eriocitrin, and eriodictyol. The anti-inflammatory properties were determined by measuring selected cytokines and other molecule markers of osteoarthritis, cyclooxygenase-1 and -2 inhibitory activity using a commercially available ELISA kit, anti-adipogenic activity using 3T3-L1 pre-adipocytes, gastrointestinal protective activity in an *in vitro* colitis model using HT-29 (colon adenocarcinoma) cells. Furthermore, their effect in cell viability was evaluated using different cancer cell lines, while their anti-oxidant capacity was evaluated using the ABTS method. Lastly, a novel and improved method for total anti-oxidant capacity was developed (Chapter IV).

- 4.) To develop new techniques to non-invasively assess inflammatory bowel disease and to further evaluate the *in vivo* gastrointestinal activity of racemic hesperidin, hesperetin, naringin, and naringenin in an experimental model of colitis in the rat (Chapter V).
- 5.) Conclusions and future directions (Chapter VI).

CHAPTER II Stereospecific Method Development and Validation of Hesperetin, Naringenin, and Eriodictyol

2.1 INTRODUCTION

This chapter describes the development of three simple, selective, accurate, reproducible, and stereospecific high-performance liquid chromatographic methods with ultraviolet detection for simultaneous separation of hesperetin, naringenin, and eriodictyol enantiomers in biological matrices. Details of the full validation of the reversed-phase HPLC assays in rat urine are reported in this chapter.

2.2 BACKGROUND

HPLC is considered to be the best and most widely used analytical tool in the separation and quantification of many classes of compounds including polyphenols (Dwyer *et al.*, 2002; Kelm *et al.*, 2005; Merken *et al.*, 2000). Reversed-phase HPLC was first employed in 1979 in the quantification of polyphenols and has since become the most commonly used technique in analysis of this class of compounds (Lea *et al.*, 1979). The widespread use of reversed-phase HPLC in the study of flavanoids and stilbenes has made possible meaningful comparisons of experimental results across laboratories. Moreover, reversed-phase HPLC has been shown to be a highly precise and sensitive method for the analysis of many compounds in biological fluids such as urine and serum. One advantage of employing reversed-phase HPLC in separating and quantifying a compound of interest is that it necessitates only a small quantity of sample. This is particularly useful when attempting to measure the concentrations of a drug and its possible metabolic or degradation products in rodent models because the sample size is frequently small (>0.5 ml).

There are just a few reports where hesperetin enantiomers have been separated although baseline resolution and separation were poor and assay validation was not undertaken (Chapter I). Even though there are several studies in the literature demonstrating separability of hesperetin, naringenin, and eriodictyol enantiomers, at the commencement of this research there were no validated stereospecific analytical methods to quantify these three chiral flavanones in biological matrices reported (Chapter I). Methods of analysis of hesperetin, naringenin, and eriodictyol enantiomers in biological fluids are necessary to study the kinetics of *in vitro* and *in vivo* metabolism and determine its concentration in foodstuffs. The purpose of this work was to develop and validate selective, stereospecific, and accurate isocratic reversed-

phase HPLC methods for the determination of hesperetin, naringenin, and eriodictyol in rat urine.

2.3 METHODS

2.3.1 Chemicals and Reagents

Racemic hesperidin, hesperetin, naringin, naringenin, 7-ethoxycoumarin, daidzein, etoposide, β -glucuronidase from *Escherichia coli* type IX-A, and β -glucuronidase from *Helix pomatia* type HP-2 were purchased from Sigma Chemicals (St. Louis, MO, USA). Racemic eriocitrin and eriodictyol were purchased from Indofine Chemical Company (Hillsborough, NJ, USA). HPLC grade acetonitrile, methanol, and water were purchased from J. T. Baker (Phillipsburg, NJ, USA). Phosphoric acid was from Aldrich Chemical Co. Inc. (Milwaukee, WI, USA). Minute Maid Orange Juice [®] was purchased from a local grocery. Rats were obtained from Charles River Laboratories. Ethics approval for animal experiments was obtained from Washington State University.

2.3.2 Chromatographic system and conditions

The HPLC system used was a Shimadzu HPLC (Kyoto, Japan), consisting of an LC-10ATVP pump, a SIL-10AF auto injector, a SPD-M10A VP spectrophotometric diodearray detector, and a SCL-10A VP system controller. Data collection and integration were accomplished using Shimadzu EZ Start 7.1.1 SP1 software (Kyoto, Japan). The analytical columns used were Chiralpak AD-RH, Chiralcel OD-RH, and Chiralpak OJ-RH for hesperetin, naringenin, and eriodictyol enantiomeric separation respectively. All the columns (150mm \times 4.6 mm i.d., 5- μ m particle size) are commercially available from Chiral Technologies Inc. (Exton, PA, USA).

Separation of hesperetin enantiomers was achieved using a mobile phase composed of acetonitrile, water and phosphoric acid (42:58:0.01, v/v/v), filtered and degassed under reduced pressure, prior to use. Separation was carried out isocratically at ambient temperature ($25 \pm 1^\circ\text{C}$), with 7-ethoxycoumarin as internal standard, and a flow rate of 0.8 ml/min with ultraviolet (UV) detection at 298 nm.

Naringenin enantiomers were separated using a mobile phase composed of acetonitrile, water and phosphoric acid (30:70:0.04, v/v/v), filtered and degassed under reduced pressure, prior to use. Separation was carried out isocratically at ambient temperature ($25 \pm 1^\circ\text{C}$), with daidzein and internal standard, and a flow rate of 0.4 ml/min, with ultraviolet (UV) detection at 292 nm.

Eriodictyol enantiomers were separated using a mobile phase composed of acetonitrile, water and phosphoric acid (20:80:0.04, v/v/v), filtered and degassed under reduced pressure, prior to use. Separation was carried out isocratically at ambient temperature ($25 \pm 1^\circ\text{C}$), with etoposide as internal standard, and a flow rate of 0.7 ml/min, with ultraviolet (UV) detection at 288 nm.

2.3.3 Stock and Working Standard Solutions

Twenty-five milligram of hesperetin, naringenin, and eriodictyol were accurately weighed on an analytical balance (AG245, Mettler) and dissolved separately with methanol in a 250 ml volumetric flask to make a stock standard solution with a racemic concentration of 100 $\mu\text{g/ml}$. A methanolic stock solution of the different internal standards (7-ethoxycoumarin, daidzein, and etoposide) was prepared similarly to a final concentration of 100 $\mu\text{g/ml}$. These solutions were protected from light and stored at -20°C between uses, for no longer than 3 months. Stereospecific calibration standards in urine were prepared daily from the stock

solutions of hesperetin, naringenin, or eriodictyol respectively by sequential dilution with blank rat urine, yielding a series of concentrations namely, 0.5, 1.0, 5.0, 10.0, 50.0 and 100.0 $\mu\text{g/ml}$ in three replicates.

Quality control (QC) samples were prepared from the stock solution of hesperetin, naringenin, or eriodictyol by dilution with blank rat urine to yield target concentrations of 0.5, 1.0, 5.0, 10.0, 50.0 and 100.0 $\mu\text{g/ml}$. The QC samples were divided into 0.1 ml aliquots in micro centrifuge tubes and stored at -70°C before use.

2.3.4 Sample Preparation

To the working standards or samples (0.1 ml), 100 μl of internal standard solution (100 $\mu\text{g/ml}$) was added into 2.0 ml Eppendorf tubes. The mixture was vortexed for 1 min (Vortex Genie-2, VWR Scientific, West Chester, PA, USA), and centrifuged at 5,000 rpm for 5 min (Beckman Microfuge centrifuge, Beckman Coulter, Inc., Fullerton, CA, USA). The supernatant was collected into 2.0 ml Eppendorf tubes and evaporated to dryness under compressed nitrogen gas. The residue was reconstituted with 400 μl of mobile phase, vortexed for 1 min and centrifuged at 5000 rpm for 5 minutes, the supernatant was transferred to HPLC vials and 150 μl of it was injected into the HPLC system.

2.3.5 Precision and Accuracy

The stereospecific within-run precision and accuracy of the replicate assays ($n = 6$) were tested by using six different concentrations of hesperetin, naringenin, or eriodictyol, namely 0.5, 1.0, 5.0, 10.0, 50.0 and 100.0 $\mu\text{g/ml}$. The between-run precision and accuracy of the assays were estimated from the results of six replicate assays of QC samples on six different days within one week. The precision was evaluated by the relative standard deviation (RSD). The

accuracy was estimated based on the mean percentage error of measured concentration to the actual concentration (Shah *et al.*, 1991).

2.3.6 Recovery

The stereospecific recovery for hesperetin, naringenin, and eriodictyol enantiomers from biological fluids was assessed ($n = 6$) at 0.5, 1.0, 5.0, 10.0, 50.0 and 100 $\mu\text{g/ml}$ and the recovery of the internal standard was evaluated at the concentration used in sample analysis (100 $\mu\text{g/ml}$). A known amount of compound or internal standard was spiked into 0.1 ml blank rat urine to give the above concentrations. The samples were treated as described under section 2.3.4 and analyzed by HPLC. The extraction efficiency was determined by comparing the peak areas of compound or internal standard to those of compound or internal standard solutions of corresponding concentration injected directly in the HPLC system without extraction.

2.3.7 Freeze-Thaw and Bench-Top Stability

The stereospecific freeze-thaw stability of hesperetin, naringenin, and eriodictyol was evaluated at three concentrations 1.0, 5.0 and 50 $\mu\text{g/ml}$, using QC samples. These samples were analyzed in triplicate without being frozen at first, and then stored at -70°C and thawed at room temperature ($25 \pm 1^{\circ}\text{C}$) for three cycles.

The stability of hesperetin, naringenin, and eriodictyol in reconstituted extracts during run-time in the HPLC auto-injector was investigated using pooled extracts from QC samples of three concentration levels 1.0, 5.0, and 50.0 $\mu\text{g/ml}$. Samples were kept in the sample rack of the auto-injector and injected into HPLC system every 4 h, from 0 to 24 h at the temperature of auto-injector ($26 \pm 1^{\circ}\text{C}$).

2.3.8 Data analysis

Stereospecific quantification was based on calibration curves constructed using peak area ratio (PAR) of hesperetin, naringenin, and eriodictyol to internal standard, against the respective hesperetin, naringenin, and eriodictyol concentrations using unweighed least squares linear regression.

2.4 RESULTS AND DISCUSSION

2.4.1 Chromatography

2.4.1.1 Hesperetin

Separation of hesperetin enantiomers and the internal standard in biological fluids was achieved successfully. There were no interfering peaks co-eluted with the compounds of interest (Figure 2-1A and 2-1C).

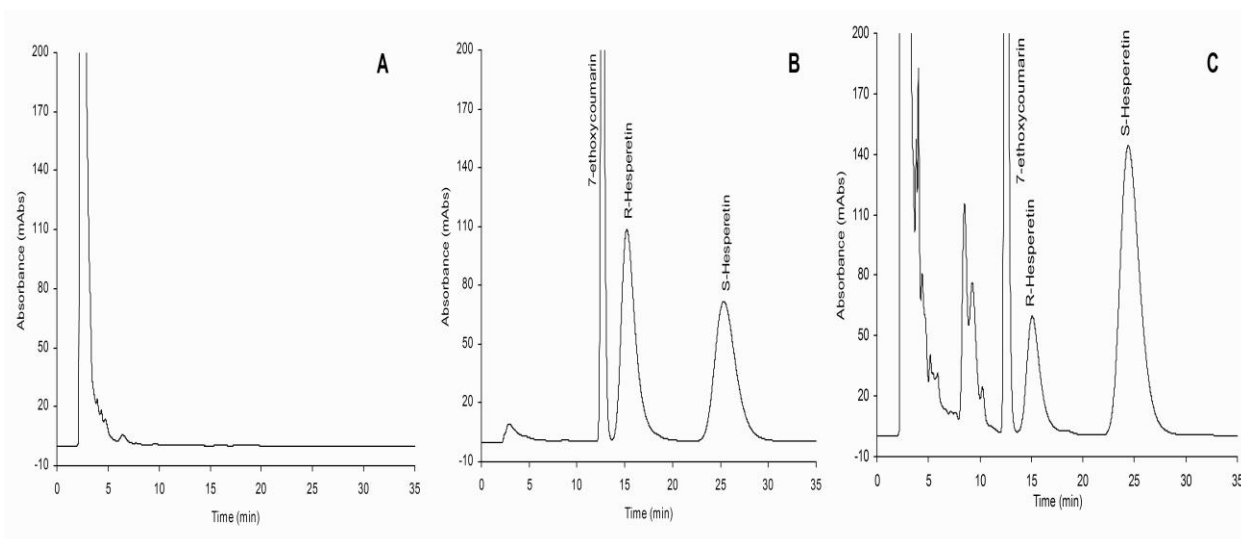


Figure 2-1: Representative chromatograms, of (A) drug-free urine, (B) urine containing hesperetin enantiomers each with concentration of 1.0 $\mu\text{g}/\text{ml}$ and the internal standard (IS), and (C) 6 hour rat urine sample containing hesperetin enantiomers and the IS.

The order of elution was determined by taking a 150 μL aliquot of lemon juice and subjecting it to 200 μL of *H. pomatia* Type-HP-2 enzyme (Erlund *et al.*, 2002). The

predominant enantiomer of hesperidin in lemon juice is in the S (-) configuration (Arakawa *et al.*, 1960; Gel-Moreto *et al.*, 2001). The retention times of R- and S-hesperetin were approximately 15 and 24 min, respectively (Figure 2-1B). The internal standard eluted at approximately 12 minutes.

The performance of the HPLC assay was assessed using the following parameters, namely peak shape and purity, interference from endogenous substances in biological fluid, linearity, limit of quantitation (LOQ), freeze-thaw stability, stability of reconstituted extracts, precision, accuracy and recovery. Various compositions of mobile phase were tested to achieve the best resolution between hesperetin enantiomers. For instance, the addition of phosphoric acid (0.01%) led to an improvement on the shape and sharpness of the peaks compared to a mobile phase without acid. Then, the amount of phosphoric acid was increased to 0.1%, which reduced the sharpness and resolution of the peaks. Also different mobile phase compositions were tested, the starting mobile phase was acetonitrile, water and phosphoric acid (40:60:0.01, v/v/v). Increasing the polarity (water) of the mobile phase increased the retention time. Thus, more acetonitrile was added in order to reduce the retention time to obtain an optimal mobile phase of acetonitrile, water and phosphoric acid (42:58:0.01, v/v/v). The amount of acetonitrile was not increased as the internal standard eluted near the solvent front affecting the reliability of the assay.

There are no other stereospecific assays of hesperetin published in the literature. The present assay is practical to use in pre-clinical and clinical applications of hesperetin where small sample volumes are obtained.

2.4.1.2 Naringenin

Separation of naringenin enantiomers and the internal standard in biological fluids was achieved successfully. There were no interfering peaks co-eluted with the compounds of interest (Figure 2-2A and 2-2C).

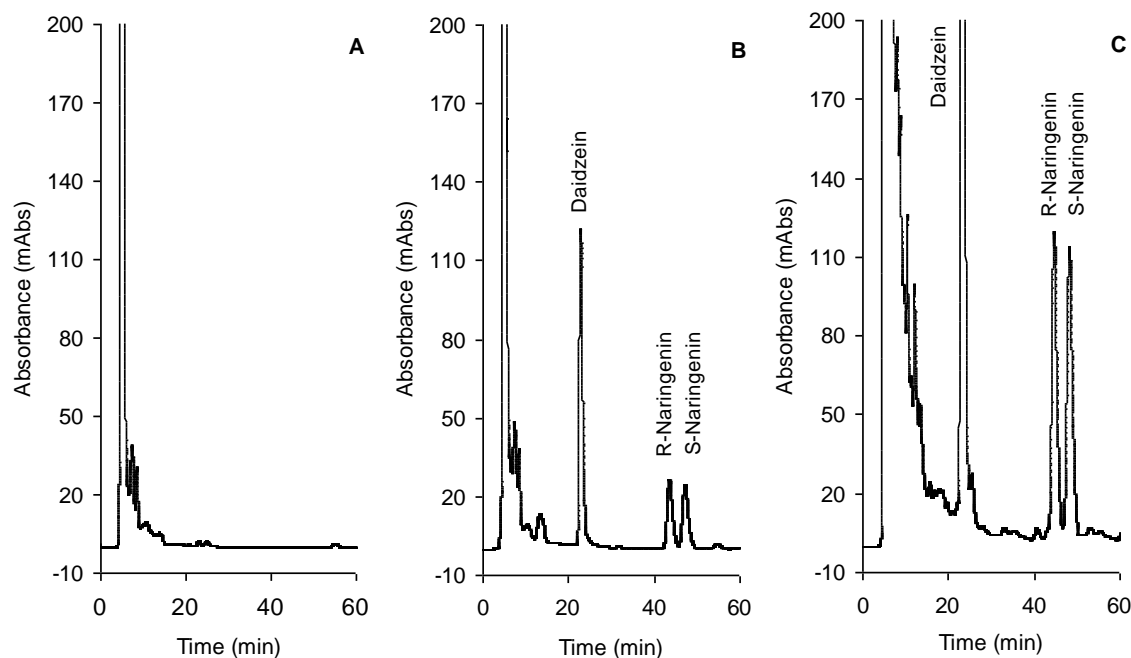


Figure 2-2: Representative chromatograms, of (A) drug-free urine, (B) urine containing naringenin enantiomers each with concentration of 10 $\mu\text{g/ml}$ and the internal standard (IS), and (C) 8 h rat urine sample containing naringenin enantiomers and the IS.

The order of elution was determined by taking a 150 μl aliquot of grapefruit juice and subjecting it to 200 μl of *H. pomatia* Type-HP-2 enzyme (Erlund *et al.*, 2001). The predominant enantiomer of naringin in grapefruit juice is in the S configuration (Aturki *et al.*, 2004; Krause *et al.*, 1991b). The retention times of R- and S- naringenin were approximately 43 and 47 min, respectively. The internal standard eluted at approximately 23 minutes (Figure 2-2B).

The performance of the HPLC assay was assessed using the following parameters, namely peak shape and purity, interference from endogenous substances in biological fluid,

linearity, limit of quantitation (LOQ), freeze-thaw stability, stability of reconstituted extracts, precision, accuracy and recovery. Various compositions of mobile phase were tested to achieve the best resolution between naringenin enantiomers.

The final mobile phase constitution is acetonitrile, water and phosphoric acid (30:70:0.04, v/v/v), this concentration enabled excellent separation. During assay development the amounts of phosphoric acid and the ratio between acetonitrile and water were tested at different concentration ratios. For instance, increasing the amount of phosphoric acid up to 0.1% reduces the sharpness and resolution of the peaks, thus 0.04% was found to be optimum. It was also observed that increasing the polarity of the mobile phase (water) increases the retention time. Thus, by increasing the amount of acetonitrile the retention times were reduced. However, increasing acetonitrile to concentrations greater than 30% eluted the peaks of the naringenin enantiomers too close to each other, and the internal standard too close to the solvent front. The retention times of the analytes were very sensitive to small changes in mobile phase composition on the Chiralcel OD-RH column.

The present assay is practical to use in pre-clinical and clinical applications of naringenin where small sample volumes are obtained.

2.4.1.3 Eriodictyol

Stereospecific separation of eriodictyol enantiomers and the internal standard in biological fluids was achieved successfully. There were no interfering peaks co-eluting with the compounds of interest (Figure 2-3A, 2-3B, and 2-3C).

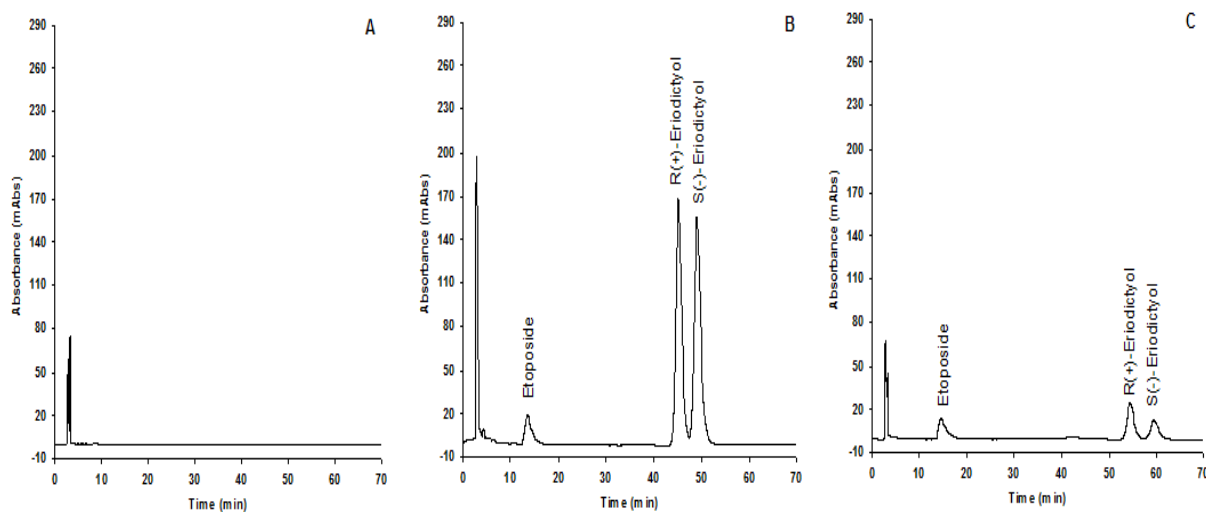


Figure 2-3: Representative chromatograms of (A) drug-free urine, (B) urine containing eriodictyol with concentration of 10 $\mu\text{g/ml}$ and the internal standard (IS), (C) 10 h rat urine sample containing eriodictyol and the IS after oral ingestion of lemonade.

The order of elution was determined by using the circular dichroism data reported by Caccamese *et al.* (Caccamese *et al.*, 2005). Under normal-phase conditions, the first enantiomer to be eluted is S(-)-eriodictyol (Ficarra *et al.*, 1995). Since we utilized reverse-phase conditions, the order of elution was reversed with the R(+)-eriodictyol being eluted first. To confirm this elution order, peanut hulls (*Arachis hypogaea*) and thyme (*Thymus vulgaris*) were analyzed since it has been previously reported that these two plants contain stereochemically enriched S(-)-eriodictyol (Krause *et al.*, 1991a). As shown in Figure 2-4, thyme contains predominantly S(-)-eriodictyol (96.35%) and this is the predominant second peak in order of elution. Therefore, the retention times of R- and S- eriodictyol were approximately 56 and 60 minutes, respectively. The internal standard eluted at approximately 16 minutes (Figure 2-3B). It was also observed that peanut hulls contain predominantly S(-)-eriodictyol, (97.16%).

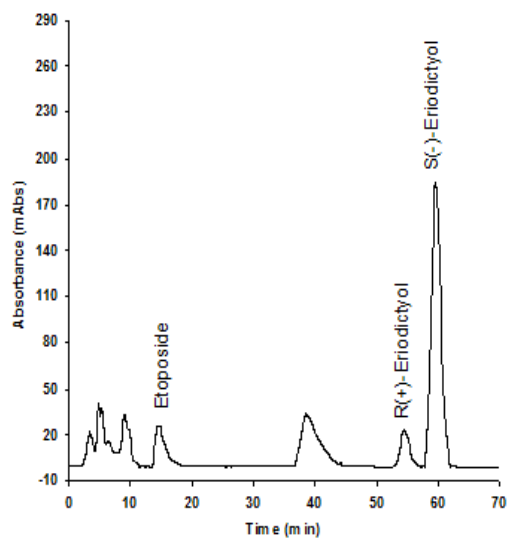


Figure 2-4: Representative chromatograms of thyme (*Thymus vulgaris*) containing predominantly S(-)-eriodictyol.

The performance of the HPLC assay was assessed using the following parameters, namely peak shape and purity, interference from endogenous substances in biological fluid, linearity, limit of quantitation (LOQ), freeze-thaw stability, stability of reconstituted extracts, precision, accuracy and recovery. Various compositions of mobile phase were tested to achieve the best stereospecific resolution of eriodictyol.

The final mobile phase constitution is acetonitrile, water, and phosphoric acid (20:80:0.04, v/v/v), this concentration was chosen because it was possible to attain baseline separation and no co-eluting peaks in fruit juices or biological matrices were evident. An optimization process was followed to attain this final mobile phase composition. The first mobile phase to be examined was acetonitrile water (50:50 v/v), but eriodictyol and etoposide did not adequately resolve. Subsequently, the amount of acetonitrile was reduced to 35% and two broad peaks were observed around 6 and 7 minutes without baseline resolution. As the two eriodictyol peaks were too close to the solvent front, and etoposide was not adequately

resolved further assay optimization was necessary. An increase in the polarity of the mobile phase, by increasing the concentration of water was employed to extend the elution time. Thus, the amount of water was increased from 65% to 80% and 90%. The initial mobile phase attempt simultaneously eluted etoposide, R(+)-, and S(-)-eriodictyol at 16, 56, and 60 minutes respectively. The second mobile phase also eluted etoposide, R(+)-, and S(-)-eriodictyol, but the elution times were higher: 29, 76, and 85 minutes respectively. The retention times of the analytes were very sensitive to small changes in mobile phase composition on the Chiralpak OJ-RH column. It was observed that with both mobile phases the peaks of eriodictyol were quite broad. For practical purposes and to reduce sample run-time, the first mobile phase was chosen. However, the peaks were still broad, thus the use of an acid was proposed as previously demonstrated for other flavonoids (Torres *et al.*, 2005; Yanez *et al.*, 2007c; Yanez *et al.*, 2005d). Initial testing of 0.15% trifluoroacetic acid (TFA) and 0.15% phosphoric acid ensued. Phosphoric acid improved the sharpness of the peaks to a greater extent than TFA. Therefore, phosphoric acid was explored in greater detail and ultimately its concentration was reduced to 0.1 and 0.04%. Phosphoric acid (0.04%) provided the best peak sharpness of the peaks of interest. Baseline resolution was attained, and there were no interfering co-eluting peaks observed with biological samples.

The choice of etoposide as internal standard was determined after extensive attempts with many other compounds such as naringenin and kaempferol. In the end we chose this internal standard because of the large difference in retention times which enables baseline separation of etoposide and eriodictyol and facilitates elution of other peaks of interest in fruits and vegetables without interfering with the peaks of interest. In addition, in some tissues and other biological matrices many interfering peaks make other internal standards impossible to

use. Naringenin originally offered good potential as internal standard, but this was also found to be present in many fruit samples and interfering peaks in urine were noted. Another suitable alternative was kaempferol, which was found to be present in the majority of fruit samples and eluted after S(-)-eriodictyol (around 79 minutes) making run times even longer.

The present assay is practical to use in pre-clinical applications of eriodictyol where small sample volumes are obtained.

2.4.2 Linearity and Limit of Quantification (LOQ)

2.4.2.1 Hesperetin

Linear relationships ($r^2 = 0.999$) were demonstrated between PAR of R- and S-hesperetin to the internal standard and the corresponding serum concentrations of hesperetin enantiomers over a range of 0.5 to 100 $\mu\text{g/ml}$. The mean regression lines from the validation runs was described by R-hesperetin ($\mu\text{g/ml}$) = $0.0392x + 0.311$ and S-hesperetin ($\mu\text{g/ml}$) = $0.0397x + 0.028$.

The LOQ of this assay was 0.5 $\mu\text{g/ml}$ in biological fluids with the corresponding between day relative standard deviation of 5.12 and 5.21% for R- and S-hesperetin respectively, and bias of 4.23 and 4.55% for R- and S-hesperetin respectively. The back-calculated concentration of QC samples was within the acceptance criteria.

2.4.2.2 Naringenin

Linear relationships ($r^2 = 0.999$) were demonstrated between PAR of R- and S-naringenin to the internal standard and the corresponding urine concentrations of naringenin enantiomers over a range of 0.5 to 100 $\mu\text{g/ml}$. The mean regression lines from the validation runs were described by R-naringenin ($\mu\text{g/ml}$) = $0.0439x + 0.0146$ and S-naringenin ($\mu\text{g/ml}$) = $0.0432x + 0.0129$.

The LOQ of this assay was 0.5 µg/ml in biological fluids with the corresponding between day relative standard deviation of 2.27 and 14.92% for R- and S-naringenin respectively and bias of 13.27 and 4.03% for R- and S-naringenin respectively. The back-calculated concentration of QC samples was within the acceptance criteria.

2.4.2.3 Eriodictyol

Linear relationships ($r^2 = 0.999$) were demonstrated between PAR of R(+)- and S(-)-eriodictyol to the internal standard and the corresponding urine concentrations of eriodictyol over a range of 0.5 to 100 µg/ml. The mean regression lines from the validation runs were described by R(+)-eriodictyol (µg/ml) = $0.0331x - 0.0080$ and S(-)-eriodictyol (µg/ml) = $0.0433x - 0.0049$.

The LOQ of this assay was 0.5 µg/ml in biological fluids with the corresponding between day relative standard deviation of 4.72 and 2.61% for R(+)- and S(-)-eriodictyol respectively and bias of 3.39 and -7.94% for R(+)- and S(-)-eriodictyol respectively. The back-calculated concentration of QC samples was within the acceptance criteria.

2.4.3 Precision, Accuracy and Recovery

2.4.3.1 Hesperetin

The within- and between-run precision (RSD) calculated during replicate assays ($n = 6$) of hesperetin enantiomers in rat urine was < 5% over a wide range of concentrations (Table 2-1). The intra- and inter-run bias assessed during the replicate assays for hesperetin enantiomers varied between 0.04 and 4.6% (Table 2-1).

Table 2-1. Within- and between-day precision and accuracy of the assay for hesperetin (HT) enantiomers in rat urine (n=3, Mean \pm SD).

Added	Enantiomer concentration ($\mu\text{g/ml}$)											
	Observed				RSD%				Bias %			
	Within-Day		Between-Day		Within-Day		Between-Day		Within-Day		Between-Day	
	R-HT	S-HT	R-HT	S-HT	R-HT	S-HT	R-HT	S-HT	R-HT	S-HT	R-HT	S-HT
0.5	0.49	0.49	0.49	0.49	4.51	4.43	5.12	5.21	2.45	2.49	4.23	4.55
1.0	1.00	1.01	1.02	1.01	3.21	3.21	3.25	3.33	1.81	1.82	3.31	3.32
5.0	5.01	5.02	5.01	5.10	2.10	2.11	2.01	4.02	0.50	0.52	0.74	0.75
10	9.97	9.99	9.99	10.01	1.71	1.54	1.51	2.94	3.30	3.31	1.05	1.08
50	24.89	25.00	24.92	25.03	1.92	1.80	2.21	2.43	3.32	3.34	2.15	2.12
100	50.01	49.98	50.01	49.98	3.41	3.62	3.51	3.52	0.05	0.05	0.04	0.04

These data indicated that the developed HPLC method is reproducible and accurate.

The mean extraction efficiency for hesperetin enantiomers from biological fluids varied from 98.2 to 98.7 % (Table 2-2). In addition, the recovery of 7-ethoxycoumarin was 97.1% at its concentration used in the assay. High recovery from biological fluids suggested that there was negligible loss of hesperetin enantiomers and 7-ethoxycoumarin during the protein precipitation process. Additionally the efficiencies of extraction of hesperetin enantiomers and 7-ethoxycoumarin were comparable.

Table 2-2. Recovery of hesperetin enantiomers from rat urine (n = 6, mean \pm SD).

Concentration ($\mu\text{g/ml}$)	Recovery % (Mean \pm SD)	
	R-hesperetin	S-hesperetin
1.0	98.2 \pm 1.1	98.6 \pm 1.3
5.0	98.5 \pm 1.2	98.5 \pm 1.2
50.0	98.7 \pm 1.3	98.7 \pm 0.9

2.4.3.2 Naringenin

The within- and between-run precision (RSD) calculated during replicate assays (n = 6) of naringenin enantiomers in rat urine was < 15% over a wide range of concentrations (Table

2-3). The intra- and inter-run bias assessed during the replicate assays for naringenin enantiomers varied between -3.77 and 13.27% (Table 2-3).

Table 2-3. Within- and between-day precision and accuracy of the assay for naringenin (N) enantiomers in rat urine (n = 6, mean, R.S.D., and Bias).

Added	Enantiomer concentration ($\mu\text{g/ml}$)											
	Observed				R.S.D. (%)				Bias (%)			
	Within-day		Between-day		Within-day		Between-day		Within-day		Between-day	
	R-N	S-N	R-N	S-N	R-N	S-N	R-N	S-N	R-N	S-N	R-N	S-N
0.5	0.54	0.56	0.57	0.52	6.13	0.52	2.27	14.92	8.87	12.74	13.27	4.03
1.0	1.06	1.09	1.07	1.03	6.26	7.53	0.68	9.35	6.35	9.35	6.86	2.57
5.0	5.08	5.12	4.81	4.88	2.64	3.19	4.67	5.28	1.55	2.33	-3.77	-2.42
10	10.31	10.35	10.18	10.27	1.69	1.97	1.60	1.46	3.14	3.55	1.81	2.75
50	48.95	48.63	50.97	50.81	0.52	0.64	2.91	2.87	-2.10	-2.74	1.93	1.63
100	100.53	100.62	99.49	99.65	0.07	0.16	0.67	0.66	0.53	0.62	-0.51	-0.35

These data indicated that the developed HPLC method is reproducible and accurate. The mean extraction efficiency for naringenin enantiomers from biological fluids varied from 102.78 to 118.05% (Table 2-4). In addition, the recovery of daidzein was 98.5% at its concentration used in the assay. High recovery from biological fluids suggested that there was negligible loss of naringenin enantiomers and during the protein precipitation process. Additionally the efficiencies of extraction of naringenin enantiomers and daidzein were comparable.

Table 2-4. Recovery of naringenin enantiomers from rat urine (n = 6, mean \pm SD).

Concentration ($\mu\text{g/ml}$)	Recovery (%) (Mean \pm S.D.)	
	R-naringenin	S-naringenin
0.5	117.4 \pm 5.3	122.4 \pm 3.8
1.0	118.1 \pm 0.1	121.0 \pm 0.1
5.0	106.8 \pm 0.6	106.4 \pm 0.5
10	107.8 \pm 2.1	108.0 \pm 2.3
50	109.9 \pm 0.1	110.0 \pm 0.1
100	103.3 \pm 2.4	102.8 \pm 2.4

2.4.3.3 Eriodictyol

The stereospecific within- and between-run precision (RSD) calculated during replicate assays (n = 6) of eriodictyol in rat urine was <12% over a wide range of concentrations (Table 2-5). The stereospecific intra- and inter-run bias assessed during the replicate assays for eriodictyol varied between -7.94 and 5.58% (Table 2-5).

Table 2-5. Stereospecific within- and between-day precision and accuracy of the assay for eriodictyol (E) in rat urine (n = 6, mean, R.S.D., and Bias).

Added	Eriodictyol concentration (µg/ml)											
	Observed				R.S.D. (%)				Bias (%)			
	Within-day		Between-day		Within-day		Between-day		Within-day		Between-day	
	R(+)-E	S(-)-E	R(+)-E	S(-)-E	R(+)-E	S(-)-E	R(+)-E	S(-)-E	R(+)-E	S(-)-E	R(+)-E	S(-)-E
0.5	0.53	0.47	0.52	0.46	11.37	1.80	4.72	2.61	5.58	-6.24	3.39	-7.94
1.0	1.03	1.02	1.01	1.01	6.30	2.78	2.80	4.13	2.98	1.77	1.04	1.07
5.0	5.06	4.99	5.02	5.11	0.40	0.19	0.91	3.51	1.13	-0.29	0.49	2.24
10	10.05	9.98	9.97	9.95	0.19	2.31	1.00	0.42	0.51	-0.20	-0.28	-0.47
50	49.64	50.28	49.91	49.96	0.61	0.95	0.50	1.21	-0.72	0.56	-0.17	-0.09
100	100.3	99.91	100.0	100.1	0.18	0.23	0.20	0.29	0.25	-0.09	0.03	0.09

These data indicated that the developed HPLC method is reproducible and accurate. The mean extraction efficiency for eriodictyol from biological fluids varied from 88.3 to 97.1% (Table 2-6).

Table 2-6. Stereospecific recovery of eriodictyol from rat urine (n = 6, (mean ± SD).

Concentration (µg/ml)	Recovery (%) (Mean ± S.D.)	
	R(+)-eriodictyol	S(-)-eriodictyol
0.5	97.1 ± 3.3	88.3 ± 0.8
1.0	104.8 ± 4.7	96.0 ± 1.7
5.0	101.0 ± 2.2	98.6 ± 0.7
10	100.1 ± 0.3	99.5 ± 2.9
50	98.9 ± 1.1	101.7 ± 0.3
100	100.3 ± 0.2	99.5 ± 0.3

In addition, the recovery of etoposide was 99.3% at its concentration used in the assay. High recovery from biological fluids suggested that there was negligible loss of eriodictyol and during the protein precipitation process. Additionally the efficiencies of extraction of eriodictyol and etoposide were comparable.

2.4.4 Stability

2.4.4.1 Hesperetin

No significant degradation was detected after the samples of racemic hesperetin in biological fluids following three freeze-thaw circles. The recoveries of R- and S-hesperetin were respectively from 98.5 to 99.9 % and 98.3 to 99.7% following three freeze-thaw cycles for hesperetin QC samples of hesperetin or 7-ethoxycoumarin. There was no significant decomposition observed after the reconstituted extracts of racemic hesperetin were stored in the auto-injector at room temperature for 24 h. The measurements were from 98.3 to 99.9% of the initial value for extracts of racemic hesperetin in biological fluids of 0.5, 1.0, 5.0, 10.0, 50.0 and 100.0 µg/ml respectively, during the storage in the auto injector at room temperature for 24 h.

2.4.4.2 Naringenin

No significant degradation was detected after the samples of racemic naringenin in biological fluids following three freeze-thaw circles. The recoveries of R- and S-naringenin were respectively from 99.52 to 108.35% and 84.83 to 107.71% following three freeze-thaw cycles for naringenin QC samples of naringenin or daidzein. There was no significant decomposition observed after the reconstituted extracts of racemic naringenin were stored in the auto-injector at room temperature for 24 h. The measurements were from 98.49 to 98.86% of the initial value for extracts of racemic naringenin in biological fluids of 0.5, 1.0, 5.0, 10.0,

50.0 and 100.0 µg/ml respectively, during the storage in the auto injector at room temperature for 24 h.

2.4.4.3 Eriodictyol

No significant degradation was detected after the samples of eriodictyol in biological fluids following three freeze-thaw circles. The recoveries of R(+)- and S(-)-eriodictyol were respectively from 98.81 to 101.75% and 99.41 to 103.71% following three freeze-thaw cycles for eriodictyol QC samples of eriodictyol or etoposide. There was no significant decomposition observed after the reconstituted extracts of eriodictyol were stored in the auto-injector at room temperature for 24 h. The measurements were from 99.22 to 99.80% of the initial value for extracts of eriodictyol in biological fluids of 0.5, 1.0, 5.0, 10.0, 50.0 and 100.0 µg/ml respectively, during the storage in the auto injector at room temperature for 24 h.

2.5 CONCLUSIONS

In summary, the developed HPLC assays are stereospecific, sensitive, reproducible and accurate and specific. The described methods allow for the separation of hesperetin, naringenin, and eriodictyol enantiomers and have been validated in rat urine but can also be applied to other biological matrices.

The performance of these HPLC assays have been evaluated using samples from rat urine for the following parameters; peak shape and purity, linearity, LOQ, LOD, stability, precision, accuracy, and recovery. Using these methods, large numbers of biological samples can be analyzed in a relatively short period of time.

CHAPTER III Pre-Clinical Stereospecific Pharmacokinetics of Hesperetin, Naringenin, and Eriodictyol in Rats and their Content in Selected Fruit Juices

3.6 INTRODUCTION

This chapter describes the stereospecific pharmacokinetic parameters of hesperetin, naringenin, and eriodictyol in Sprague-Dawley male rats as modeled using WinNonlin[®] pharmacokinetic software. Serum and urine samples of male rats were analyzed using validated HPLC methods and verified using liquid chromatography coupled with mass spectrometry with electro-spray ionization (LC-MS-ESI) following intravenous administration of each flavanone via jugular vein cannulas. The pharmacokinetic profiles of each selected flavanone are characterized and interpreted. Also, the stereospecific content of hesperetin, naringenin, eriodictyol and their corresponding glycosides (hesperidin, naringin, and eriocitrin) in selected fruit juices are reported.

3.7 BACKGROUND

The study of pharmacokinetics is a well-established discipline in pharmaceutical development and research. It is of utmost importance to understand the fate of a potential therapeutic compound in the body following administration in order to optimize its therapeutic use.

As described in great detail in chapter one, natural compounds such as flavanones boast many promising health benefits associated with their consumption. Despite numerous reports of their pharmacological activity in a variety of assays, there is a paucity of data that characterizes their stereospecific pharmacokinetic parameters. The stereospecific pharmacokinetics of hesperetin, naringenin, and eriodictyol must be established to elucidate definitive concentration-effect relationships.

The importance of stereospecific disposition of racemic flavanones is slowly being recognized and reported in the biomedical literature. Most of these preliminary investigations report the quantification of a variety of flavanones in citrus fruit juices and herbs (Caccamese *et al.*, 2003; Gel-Moreto *et al.*, 2003; Krause *et al.*, 1991a; Krause *et al.*, 1991b; Li *et al.*, 1998c), or report the separation of flavanones on different stationary phases (Yanez *et al.*, 2007a). There is a paucity of investigations detailing the importance of stereospecific pharmacokinetics and pharmacodynamics of chiral flavanones. Hesperetin, naringenin, eriodictyol and their corresponding glycosides (hesperidin, naringin, and eriocitrin) belong to this flavanone family (Yanez *et al.*, 2007a), but no stereospecific information on their pharmacokinetics, pharmacodynamics, or content in fruit juices have been reported.

The achiral pharmacokinetics of hesperetin, naringenin, eriodictyol, and their corresponding glycosides have been reported (Bugianesi *et al.*, 2002; Erlund *et al.*, 2001; Hsiu

et al., 2002; Kanaze *et al.*, 2007; Manach *et al.*, 2003; Miyake *et al.*, 2006; Miyake *et al.*, 2000) as well as their content in different fruits and fruit juices (2003). Furthermore, to our knowledge there are no studies that have properly assessed the urinary pharmacokinetics and/or disposition of these three chiral flavonoids or other polyphenols after oral ingestion of fruit juices or individual flavonoids in humans or rodents. For instance, most of the pharmacokinetic studies in humans after ingestion of different fruit juices or diets rich in fruits and vegetables only report the total amount excreted of different flavonoids in urine or the percentage of the dose excreted in urine (Ameer *et al.*, 1996; Brevik *et al.*, 2004; Choudhury *et al.*, 1999; Erlund *et al.*, 2001; Ishii *et al.*, 2000; Manach *et al.*, 2003; Manach *et al.*, 2005; Miyake *et al.*, 2000; Nielsen *et al.*, 2002). Out of these reports, only two studies by Manach *et al.* (Manach *et al.*, 2003) and Ishii *et al.* (Ishii *et al.*, 2000) report cumulative urinary excretion plots of hesperetin, naringenin, their glycosides, or glucuronidated metabolites. However, no further pharmacokinetic characterization was performed or urinary rate plots reported.

The different pharmacokinetic parameters of a compound provide very useful information to characterize xenobiotic disposition and predict how it will be absorbed, distributed, metabolized, and excreted by the body once ingested or administered via extravascular routes. For instance, the volume of distribution (V_d) of a drug is a hypothetical volume determined by the ratio of the amount of drug administered divided by the concentration quantified in the plasma. This ratio indicates the drug's affinity for tissue and plasma compartments. Drugs with low volumes of distribution signify that the drug administered has affinity for the plasma compartment and resides predominately in the plasma. High volume of distribution suggests that the drug prefers tissue and rapidly leaves the blood in favor of tissue compartments. The volume of distribution of a compound depends on its lipid

solubility, partition coefficient and protein binding. Half-life ($t_{1/2}$) is defined as the amount of time in hours that is necessary to decrease the drug concentration in serum or urine by one half. This parameter is dependent upon the volume of distribution and the clearance of the compound.

Clearance (CL_{tot}) is defined as the hypothetical volume of distribution (ml) of free drug that is cleared from the blood per minute through hepatic, renal, or other routes of elimination. The clearance indicates how efficient a specific organ is in removing drug present in the blood. It is determined by the ratio of the amount of drug administered divided by the total amount of drug exposure (Area Under the Curve). It is possible to determine the clearance of each individual organ. For example, to determine the renal clearance (CL_r), one would multiply the known total body clearance is multiplied by the amount of free, unmetabolized drug excreted in the urine. Organ clearance describes the ratio between the rate of drug elimination from the specific organ and the rate of drug entry into the specific organ. It is dependent upon the blood flow through the organ (Q) and the efficiency of the organ (ER) in extracting the drug from the blood. High clearance drugs are classified as drugs having high extraction ratios (ER), meaning the liver or kidney is highly efficient in metabolizing and/or eliminating the drug. High extraction drugs have clearance rates that approach the rate of blood flow and the clearance of such drugs are said to be limited by the rate of blood flow through the organ. Low extraction drugs signify that the liver on the first pass does not eliminate the drug and their clearance is dependant on intrinsic capacity of drug metabolizing enzymes.

Based on pharmacokinetic theory, all the different pharmacokinetic parameters can also be derived from urinary data (Ritschel *et al.*, 2004; Shargel *et al.*, 2004). This raises a concern because most of the pharmacokinetic studies of different polyphenols in humans and rodents

are based on serum or plasma data. Furthermore, different studies have reported that different polyphenols have relatively short half-lives. For instance, flavanones (i.e. hesperetin and naringenin) have been reported to have plasma elimination half-lives between 1 and 3 hours in humans (Erlund *et al.*, 2001; Manach *et al.*, 2005) and less than 20 minutes in rabbits (Hsiu *et al.*, 2002). Similar observations have been reported for flavanols (i.e. catechins) with plasma half lives of 2-3 hours (Balant *et al.*, 1979; Bell *et al.*, 2000; Chow *et al.*, 2001; Donovan *et al.*, 1999; Lee *et al.*, 2002; Lee *et al.*, 1995; Leenen *et al.*, 2000; Meng *et al.*, 2001; Richelle *et al.*, 1999; Schramm *et al.*, 2003; Ullmann *et al.*, 2003; Van Amelsvoort *et al.*, 2001) or up to 4-9 hours once milk is co-administered (Kimura *et al.*, 2002; Meng *et al.*, 2001; van het Hof *et al.*, 1998). The observations of short plasma half-life of these and other polyphenol sub-families have been recently presented in a review (Manach *et al.*, 2005). However, different studies have reported that certain polyphenols (stilbenes) would have longer urine half-lives (4.7-fold to 16-fold higher half-lives in urine compared to plasma half-lives) (Remsberg *et al.*, 2007; Roupe *et al.*, 2006). This discrepancy between plasma and urine half-life in different stilbenes is attributed to assay sensitivity limits that would most likely underestimate the overall half-life of these compounds. Underestimation of plasma half-life due to assay sensitivity limits has been reported previously in the case of procainamide (Jamali *et al.*, 1988). In the report by Jamali *et al.* (Jamali *et al.*, 1988) an improved HPLC method was employed and it was observed that there was a significant 2-fold increase in plasma half-life compared to previous reports. Nevertheless, most of the pharmacokinetic studies only collected samples up to 24 hours post-dose, which could underestimate the elimination phase and pharmacokinetic parameters. Therefore, it is necessary to have improved analytical methods with higher detection limits that would allow detection of the compound(s) of interest for longer than 24

hours. This would allow the assessment of the pharmacokinetics of hesperetin, naringenin, and eriodictyol enantiomers and/or hesperidin, naringin, and eriocitrin epimers as well as the determination of the stereospecific content in foodstuffs. To more thoroughly understand how these xenobiotics are metabolized in plant, human, and animal models and to be able to better understand or predict their disposition, pharmacological activity, as well as therapeutic and toxic effects, we have examined for the first time the stereoselective pharmacokinetics of three racemic flavanones in rat serum and urine as well as their stereospecific content in different fruit juices.

The main objective of this series of experiments described in this chapter is to characterize and compare the stereospecific pharmacokinetic parameters of hesperetin, naringenin, and eriodictyol employing chronic conscious catheterized male Sprague-Dawley rats. Another objective is to report the stereospecific content of these three flavanones and their corresponding glycosides (hesperidin, naringin, and eriocitrin).

3.8 METHODS

3.8.1 Chemicals and Reagents

Daidzein, 7-ethoxycoumarin, etoposide, β -glucuronidase from *Escherichia coli* type IX-A, β -glucuronidase from *Helix pomatia* type HP-2, halothane, and racemic hesperidin, hesperetin, naringin, and naringenin were purchased from Sigma (St. Louis, MO, USA). Racemic eriocitrin and eriodictyol were purchased from Indofine Chemical Company (Hillsborough, NJ, USA). HPLC grade acetonitrile and water were purchased from J. T. Baker (Phillipsburg, NJ, USA). Phosphoric acid was purchased from Aldrich Chemical Co. Inc. (Milwaukee, WI, USA). Silastic[®] laboratory tubing was purchased from Dow Corning Corporation, (Midland, MI, USA). Intramedic[®] polyethylene tubing was purchased from

Becton Dickinson Primary Care Diagnostics, Becton Dickinson and Company (Sparks, MD, USA). Monoject[®] 23 gauge (0.6 mm × 25 mm) polypropylene hub hypodermic needles were purchased from Sherwood Medical (St. Louis, MO, USA). Synthetic absorbable surgical sutures were purchased from Wilburn Medical US (Kernesville, NC, USA). Pasteurized, unsweetened (unless otherwise indicated), with no additives (besides ascorbic acid and/or salt) commercial conventional orange juice (Minute Maid[®] Premium, pulp free, not from concentrate, lot number SI 18:35A), white grapefruit juice (Ocean Spray[®], from concentrate, lot number CT8812120P WG), lemonade (Minute Maid[®], from concentrate, lot number TO82111), lime juice (Rose's[®] West India, sweetened, from concentrate, lot number WF30506F), apple juice (Martinelli's[®] Golden Apple, not from concentrate, lot number 312 03 0321), tomato juice (Campbell's[®], from concentrate, lot number CS 36Z4 18:56), and commercial organic orange juice (Organics O[™], no pulp, not from concentrate, lot number 1 06-10), white grapefruit juice (R.W. Knudsen Family[™], from concentrate, lot number 5 235 003 15:40), lemonade (Santa Cruz[®], from concentrate, lot number 035C02 07:13), lime juice (Stez[®] Key Lime, sweetened, from concentrate, lot number L05BB5 1038116), apple juice (R.W. Knudsen Family[™], not from concentrate, lot number 6 256 003 23:41), and tomato juice (Campbell's[®], from concentrate, lot number CS SDZ4 12:48) were obtained from local Safeway and Dissmores IGA grocery stores. Rats were obtained from Simonsen Labs (Gilroy, CA, USA). Ethics approval for animal experiments was obtained from Washington State University.

3.8.2 Animals and Surgical Procedures

Male Sprague-Dawley rats (200 - 240 g) were obtained from Simonsen Labs (Gilroy, CA, USA) and given food (Purina Rat Chow 5001) and water *ad libitum* in our animal facility

for at least 3 days before use. Rats were housed in temperature-controlled rooms with a 12 h light/dark cycle. The day before the pharmacokinetic experiment the right jugular veins of the rats were catheterized with sterile silastic cannula (Dow Corning, Midland, MI, USA) under halothane anesthesia. This involved exposure of the vessel prior to cannula insertion. After cannulation, the Intramedic PE-50 polyethylene tubing (Becton, Dickinson and Company, Franklin Lakes, NJ, USA) connected to the cannula was exteriorized through the dorsal skin. The cannula was flushed with 0.9% saline. The animals were transferred to metabolic cages and were fasted overnight. Animal ethics approval was obtained from The Institutional Animal Care and Use Committee at Washington State University, in accordance with "Principles of laboratory animal care" (NIH publication No. 85-23, revised 1985).

3.8.3 Pharmacokinetic Study

Eighteen (18) male Sprague Dawley rats (average weight: 220 g) were cannulated as described in the previous section. Each of the animals were placed in separate metabolic cages, allowed to recover overnight, and fasted for 12 h before dosing. On the day of experiment, the animals were dosed either intravenously with racemic hesperetin (20 mg/kg), racemic naringenin (20 mg/kg), or racemic eriodictyol (20 mg/kg) dissolved in 2% DMSO and 98% PEG-600 (n=6 for each treatment group). Animals received water *ad libitum* pre- and post-dosing, and food (Purina Rat Chow 5001) was provided 2 hour post-dosing. Racemic hesperetin (Galati *et al.*, 1994), naringenin (Choudhury *et al.*, 1999; Garg *et al.*, 2001), and eriodictyol (Crespy *et al.*, 2003; Minato *et al.*, 2003) at the dose of 20 mg/kg have previously been used in similar pharmacokinetic studies exhibiting pharmacological activity in preclinical studies. Serial blood samples (0.30 ml) were collected at 0, 1 min, 10 min, and 30 min, then 1, 2, 4, 6, 12, 24 h after intravenous administration. At 48, 72, and 96 h after intravenous (IV)

administration, 1.5 ml of blood was collected. At 120 h after intravenous (IV) administration, the animals were euthanized and exsanguinated collecting about 15 ml of blood. Immediately after all the blood collection time points (except the terminal point); the cannula was flushed with a replacement volume of 0.9% saline to replenish the collected blood volume. The samples were collected into regular polypropylene microcentrifuge tubes, centrifuged at 5,000 RPM for 5 min (Beckman Microfuge centrifuge, Beckman Coulter Inc., Fullerton, CA, USA), and the serum was collected. The serum was divided into two equal fractions into separate regular polypropylene microcentrifuge tubes labeled as free and total serum samples and stored at -70°C until further sample preparation for HPLC analysis and LC/MS validation. The serum fractions varied in volume, at the earlier points between 0-24 h the fractions were of 0.1 ml, at the posterior points between 48-96 h the fractions were of 0.3 ml and at the terminal point the fractions were of 3 ml to increase sensitivity. Urine samples were also collected at 0, 2, 6, 12, 24, 24, 48, 72, 96, and 120 h following flavonoid administration, the exact volumes were recorded and two equal aliquots were collected into separate regular polypropylene microcentrifuge tubes labeled as free and total urine samples and stored at -70°C until further sample preparation for HPLC analysis and LC/MS validation. The urine aliquots also varied in volume, at earlier points the aliquots were of 0.1 ml, and at terminal points the aliquots were of 2 ml to increase volume for drug extraction and improve assay sensitivity.

3.8.4 Serum and Urine Sample preparation for HPLC Analysis

Hesperetin (Matsumoto *et al.*, 2004; Yanez *et al.*, 2005d), naringenin (Choudhury *et al.*, 1999; Yanez *et al.*, 2005a), and eriodictyol (Miyake *et al.*, 2006; Yanez *et al.*, 2007c) have been shown previously to undergo phase II metabolism (predominantly glucuronidation) in plasma and urine after intravenous and/or oral dosing in rodents and humans. Thus, serum and

urine samples were run in duplicate with or without the addition of 40 μL of 500 U/ml β -glucuronidase from *Escherichia coli* type IX-A and incubated in a shaking water bath at 37°C for 2 h to liberate any glucuronide conjugates without decomposition of the parent compound (Yang *et al.*, 2002). The proteins present in the serum samples (as well as the enzyme in the total samples) were precipitated using 1 ml of ice-cold HPLC-grade acetonitrile, vortexed for 1 min (Vortex Genie-2, VWR Scientific, West Chester, PA, USA), and centrifuged at 5000 rpm for 5 min, the supernatant was transferred to new labeled 2 ml centrifuge tubes. The samples were evaporated to dryness under a constant flow of compressed nitrogen gas. The residue was reconstituted with 400 μL of mobile phase, vortexed for 1 min and centrifuged at 5000 rpm for 5 min, the supernatant was transferred to HPLC vials and 150 μL of it was injected into the HPLC system, the remaining volume was utilized for LC/MS validation. β -glucuronidase from *Escherichia coli* type IX-A cleaves specifically any glucuronidated metabolites back to the corresponding aglycones (hesperetin, naringenin, and eriodictyol). Therefore, the samples without enzymatic hydrolysis (free samples) were utilized to determine the concentration of the aglycones, whereas the samples with enzymatic hydrolysis (total samples) were utilized to determine the concentration of the aglycones originally present plus the concentration of the major glucuronidated metabolites converted to their respective aglycones by the cleavage action of the enzyme. Finally, by subtracting the free sample concentration from the total sample, the stereospecific concentration of the glucuronidated metabolites can be calculated.

3.8.5 Fruit Juice Analysis

The stereospecific content of the glycosides (hesperidin, naringin, and eriocitrin) and aglycones (hesperetin, naringenin, and eriodictyol) in fruit juices was quantified by HPLC and verified by LC/MS. Glycoside epimers were indirectly quantified in a 500 μL aliquot of fruit

juice with added 1 ml HPLC-grade H₂O, 110 μ L 0.78M sodium acetate acetic acid buffer (pH 4.8), 100 μ L 0.1M ascorbic acid, and 200 μ L crude preparation of *H. pomatia* type HP-2 followed by incubation for 17–24 h at 37°C (Erlund *et al.*, 2001). Subsequently the respective internal standard was added followed by 1 ml ice-cold acetonitrile to precipitate proteins. The mixture was vortexed for 1 min, and centrifuged at 5000 rpm for 5 min. The supernatant was collected into 15 ml poly-propylene tubes and evaporated to dryness under a constant flow of compressed nitrogen gas. The residue was reconstituted with 400 μ L of mobile phase, vortexed for 1 min and centrifuged at 5000 rpm for 5 min, the supernatant was transferred to HPLC vials and 150 μ L of it was injected into the HPLC system, the remaining volume was utilized for LC/MS validation. *H. pomatia* type-HP-2 is a β -glucuronidase that cleaves specifically the glycosylated sugar moiety of hesperidin, naringin, eriocitrin and other flavanones as previously described (Erlund *et al.*, 2001; Yanez *et al.*, 2005a; Yanez *et al.*, 2007c; Yanez *et al.*, 2005d). Therefore, the samples without enzymatic hydrolysis (free samples) were utilized to determine the concentration of the aglycones, whereas the samples with enzymatic hydrolysis (total samples) were utilized to determine the concentration of the aglycones originally present plus the concentration of the glycosides converted to aglycones by the cleavage action of the enzyme. Finally, by subtracting the free sample concentration from the total sample, the concentration of glycoside epimers can be calculated.

3.8.6 HPLC Chromatography

3.8.6.1 Hesperetin Stereospecific Quantification

For the quantification of hesperetin enantiomers, the HPLC system utilized was a Shimadzu HPLC (Kyoto, Japan), consisting of an LC-10ATVP pump, a SIL-10AF auto injector, a SPD-M10A VP spectrophotometric diodearray detector, and a SCL-10A VP system

controller. Data collection and integration were accomplished using Shimadzu EZ Start 7.1.1 SP1 software (Kyoto, Japan). The analytical column used was Chiralpak AD-RH column (150 mm × 4.6 mm i.d., 5 µm particle size, Chiral Technologies Inc., Exton, PA, USA). The mobile phase consisted of acetonitrile, water and phosphoric acid (42:58:0.01, v/v/v), filtered and degassed under reduced pressure, prior to use. Separation was carried out isocratically at ambient temperature ($25 \pm 1^\circ\text{C}$), and a flow rate of 0.8 ml/min, with ultraviolet (UV) detection at 298 nm, 7-ethoxycoumarin as internal standard, limit of detection (LOD) of 0.5 µg/ml, and CV% <6% as we have previously reported and validated (Yanez *et al.*, 2005d) (Chapter II). The previously reported and validated method employed 0.1 ml of serum or urine; thus, in order to significantly increase the sensitivity higher sample volumes were utilized in the terminal phase samples (posterior samples to 24 hours post IV dose). For instance, 0.3 ml of serum was employed in the 48-96 h samples, and 3 ml in the terminal sample (120 h). In the case of urine, 2 ml of urine was employed in the 48-120 h samples. This allowed for a significant increase in LOD (>100 fold) for the stereospecific quantification of hesperetin, naringenin, and eriodictyol.

3.8.6.2 Naringenin Stereospecific Quantification

The quantification of naringenin enantiomers was carried out utilizing a Shimadzu HPLC (Kyoto, Japan), consisting of an LC-10ATVP pump, a SIL-10AF auto injector, a SPD-M10A VP spectrophotometric diodearray detector, and a SCL-10A VP system controller. Data collection and integration were accomplished using Shimadzu EZ Start 7.1.1 SP1 software (Kyoto, Japan). The analytical column used was Chiralcel OD-RH column (150 mm × 4.6 mm i.d., 5 µm particle size, Chiral Technologies Inc., Exton, PA, USA). The mobile phase consisted of acetonitrile, water and phosphoric acid (30:70:0.04, v/v/v), filtered and degassed

under reduced pressure, prior to use. Separation was carried out isocratically at ambient temperature ($25 \pm 1^\circ\text{C}$), and a flow rate of 0.4 ml/min, with ultraviolet (UV) detection at 292 nm, daidzein as internal standard, limit of detection (LOD) of 0.5 $\mu\text{g/ml}$, and CV% <15% as we have previously reported and validated (Yanez *et al.*, 2005a) (Chapter II).

3.8.6.3 Eriodictyol Stereospecific Quantification

Eriodictyol enantiomers were quantified utilizing a Shimadzu HPLC (Kyoto, Japan), consisting of an LC-10ATVP pump, a SIL-10AF auto injector, a SPD-M10A VP spectrophotometric diodearray detector, and a SCL-10A VP system controller. Data collection and integration were accomplished using Shimadzu EZ Start 7.1.1 SP1 software (Kyoto, Japan). The analytical column used was Chiralpak OJ-RH column (150 mm \times 4.6 mm i.d., 5 μm particle size, Chiral Technologies Inc., Exton, PA, USA). The mobile phase consisted of acetonitrile, water and phosphoric acid (20:80:0.04, v/v/v), filtered and degassed under reduced pressure, prior to use. Separation was carried out isocratically at ambient temperature ($25 \pm 1^\circ\text{C}$), and a flow rate of 0.7 ml/min, with ultraviolet (UV) detection at 288 nm, etoposide as internal standard, limit of detection (LOD) of 0.5 $\mu\text{g/ml}$, and CV% <12% as we have previously reported and validated (Yanez *et al.*, 2007c) (Chapter II).

3.8.7 LC/MS Analysis

In order to verify the presence of hesperetin, naringenin, and eriodictyol glucuronides and the presence of hesperidin, naringin, and eriocitrin a Shimadzu LCMS-2010 EV liquid chromatograph mass spectrometer system (Kyoto, Japan) connected to the LC portion consisting of two LC-10AD pumps, a SIL-10AD VP auto injector, a SPD-10A VP UV detector, and a SCL-10A VP system controller was employed. Data analysis was accomplished using Shimadzu LCMS Solutions Version 3 software (Kyoto, Japan). The chromatographic

methods were slightly modified by replacing the phosphoric acid in the mobile phase by the same amount of formic acid, while the other conditions were kept the same. The mass spectrometer conditions consisted of a curved desolvation line (CDL) temperature of 200°C and a block temperature of 200°C. The CDL, interface, and detector voltages were -20.0 V, 4.5 kV, and 1.2 kV, respectively. Vacuum was maintained by an Edwards® E2M30 rotary vacuum pump (Edwards, UK). Liquid nitrogen (Washington State University Central Stores) was used as a source of nebulizer gas (1.5 L/min). In the negative-specific ion mode (SIM) the monitored single plot transitions (m/z) were: hesperetin 302→301, naringenin 272→271, eriodictyol 288→287, while the presence of a glucuronide was confirmed by an increase in m/z ratio of 176. Therefore, the single plot transitions (m/z) for the specific glucuronides were: hesperetin glucuronide 478→477, naringenin glucuronide 448→447, and eriodictyol glucuronide 464→463. The presence of the glycosides was verified by monitoring the single plot transitions (m/z): hesperidin 610→609, naringin 580→579, and eriocitrin 596→595.

3.8.8 Pharmacokinetic Analysis

Pharmacokinetic analysis was performed using data from individual rats for which the mean and standard error of the mean (SEM) were calculated for each group. The elimination rate constant (k_{el}) was estimated by linear regression of the serum concentrations in the log-linear terminal phase. In order to estimate the serum concentrations (C_0) immediately after IV dosing, a two-compartmental model was fitted to the serum concentration versus time data using WinNonlin® software (Ver. 5.1) (Pharsight Corporation, Mountain View, CA). The estimated C_0 was then used with the actual measured serum concentrations to determine the area under the serum concentration-time curve (AUC). The $AUC_{0-\infty}$ was calculated using the combined log-linear trapezoidal rule for data from time of dosing to the last measured

concentration, plus the quotient of the last measured concentration divided by k_{el} . Non-compartmental pharmacokinetic methods were used to calculate the different pharmacokinetic parameters in the terminal phase, namely mean residence time (MRT by dividing $AUMC_{0-\infty}$ by the $AUC_{0-\infty}$), total clearance (CL_{tot} by dividing dose by $AUC_{0-\infty}$) and volume of distribution (V_{ss} by multiplying dose by the $AUMC_{0-\infty}$ and dividing it by the square of $AUC_{0-\infty}$). Based on the cumulative urinary excretion, the fraction excreted in urine (f_e by dividing the total cumulative amount of flavonoid excreted in urine (ΣX_u) by the dose), renal clearance (CL_{renal} by multiplying f_e by CL_{tot}), hepatic clearance ($CL_{hepatic}$ by subtracting CL_{renal} from CL_{tot} , assuming that hepatic clearance is equivalent to non-renal clearance), extraction ratio (ER by dividing $CL_{hepatic}$ by hepatic flow (Q)) were calculated. The mean hepatic blood flow (Q) is approximately 3.22 L/h/kg (Davies *et al.*, 1993). Using the hematocrit in rat (Davies *et al.*, 1993) of 0.48, this yields a mean hepatic plasma flow of 1.74 L/h/kg. Therefore, the hepatic flow (Q) of 1.74 L/h/kg was employed.

In order to assess the pharmacokinetic parameters from urinary data, the urinary elimination rate constant (k_e) and half-life were first characterized employing non-compartmental pharmacokinetic methods using WinNonlin[®] software (Ver. 5.1) (Pharsight Corporation, Mountain View, CA). The other pharmacokinetic parameters were calculated employing pharmacokinetic principles (Ritschel *et al.*, 2004; Shargel *et al.*, 2004). For instance, the area under the curve from the time of dosing until the last sampling time (AUC_{0-t}) was calculated by dividing the initial concentration (C_0) by the urine elimination rate constant (k_e). The other pharmacokinetic parameters were calculated as described above but instead of employing serum elimination rate constant (k_{el}), urine elimination rate constant (k_e) was utilized.

3.8.9 Statistical Analysis

Compiled data were presented as mean and standard error of the mean (mean \pm SEM). Where possible, the data were analyzed for statistical significance using NCSS Statistical and Power Analysis software (NCSS, Kaysville, UT). Student's t-test was employed for unpaired samples with a value of $p < 0.05$ being considered statistically significant. Comparison among means were tested using General Linear Models (GLM) ANOVA followed by the Newman-Keuls multiple-comparison test with a value of $p < 0.05$ being considered statistically significant.

3.9 RESULTS

3.9.1 Stereospecific Pharmacokinetics of Hesperetin, Naringenin, and Eriodictyol

Linearity in the standard curves was demonstrated in the serum samples for the three chiral flavonoids over the concentration range studied, and chromatograms were free of interference from endogenous components. Total samples (incubated with β -glucuronidase from *Escherichia coli* Type IX-A) demonstrated the presence of at least one glucuronidated metabolite based on the increase in the aglycone parent compounds (hesperetin, naringenin and eriodictyol) concentrations after the enzymatic hydrolysis, which was assessed via HPLC and verified by LC/MS (hesperetin glucuronide m/z of 477, naringenin glucuronide m/z of 447, and eriodictyol glucuronide m/z of 463 in the negative-ion mode). Previous studies have reported that one or more glucuronidation sites predominate. For instance, after oral administration of hesperetin and hesperidin to rats it was observed that hesperetin-3'-O-glucuronide and hesperetin-7-O-glucuronide were present (Matsumoto *et al.*, 2004; Yamada *et al.*, 2006). In the case of naringenin, the major metabolites detected in rat urine after oral administration of naringenin or naringin (Zhang *et al.*, 2004) and in human plasma and urine after ingestion of

grapefruit juice (Davis *et al.*, 2006; Zhang *et al.*, 2004) were naringenin-4'-O-glucuronide and naringenin-7-O-glucuronide. However, in any of the cases it was not determined which of the glucuronidated metabolite isoforms was predominant.

The serum concentration vs. time profiles observed for hesperetin, naringenin, and eriodictyol demonstrated stereoselective disposition. For instance, R(+)-hesperetin (Figure 3-1), S(-)-naringenin (Figure 3-2), and R(+)-eriodictyol (Figure 3-3) achieved higher concentrations in serum compared to their enantiomeric antipodes.

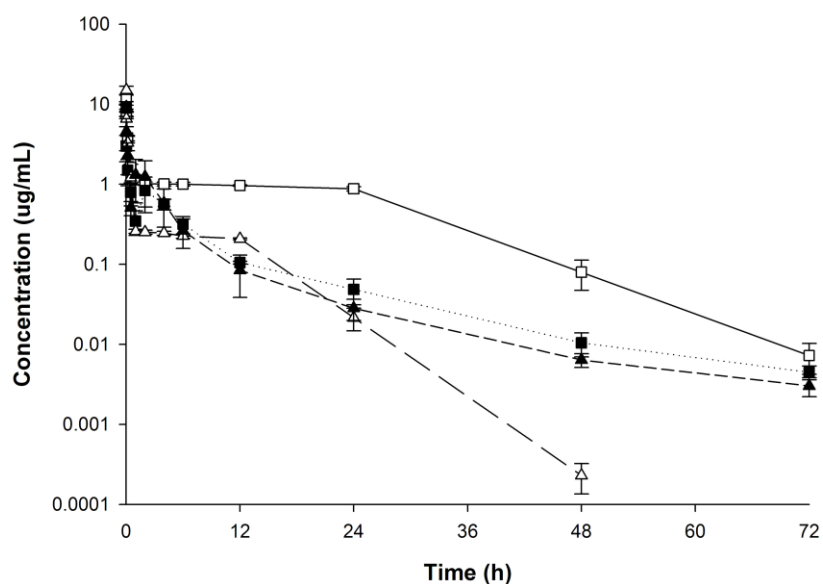


Figure 3-1. Concentration-time profile in serum plot of hesperetin (R(+)-hesperetin (□), R(+)-hesperetin glucuronide (■), S(-)-hesperetin (Δ), and S(-)-hesperetin glucuronide (▲)) after IV administration of racemic hesperetin (20 mg/kg) to rats (mean \pm SEM, n=6).

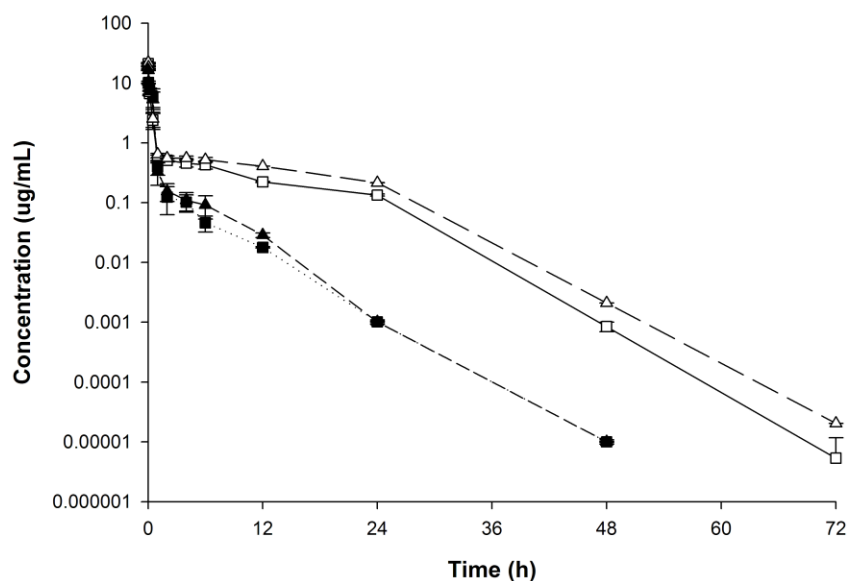


Figure 3-2. Concentration-time profile in serum plot of hesperetin (R(+)-naringenin (□), R(+)-naringenin glucuronide (■), S(-)-naringenin (Δ), and S(-)-naringenin glucuronide (▲)) after IV administration of racemic naringenin (20 mg/kg) to rats (mean \pm SEM, n=6).

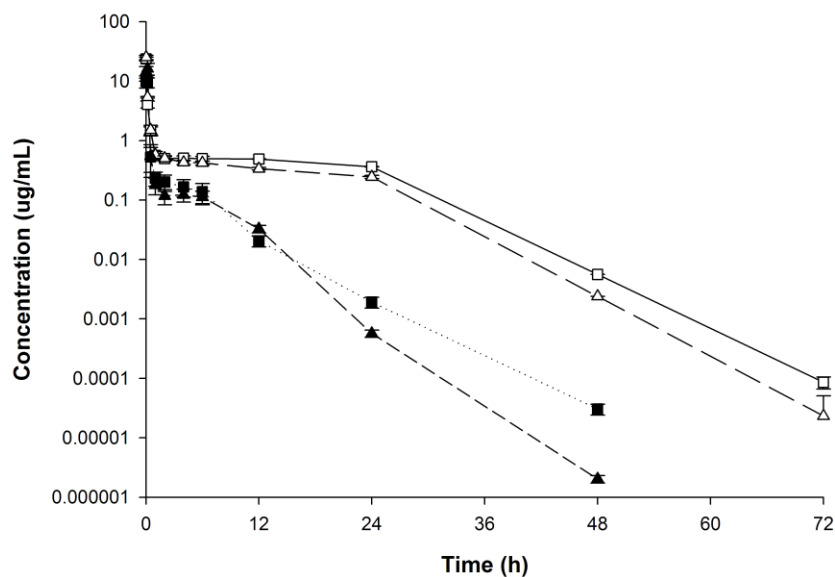


Figure 3-3. Concentration-time profile in serum plot of eriodictyol (R(+)-eriodictyol (□), R(+)-eriodictyol glucuronide (■), S(-)-eriodictyol (Δ), and S(-)-eriodictyol glucuronide (▲)) after IV administration of racemic eriodictyol (20 mg/kg) to rats (mean \pm SEM, n=6).

Independent of the enantiomeric form, the three flavonoids were characterized by a rapid decline in concentrations, representing a distribution phase (within the first hour) followed by steady concentrations up to 12 h and rapid elimination phase up to 72 hours (last time point at which all the compounds were detected, with the exception of S(-)-hesperetin that was only detected up to 48 hours, see Figure 3-1). The concentration-time profiles of the three flavonoids follow a biexponential pattern clearly indicating that the compounds do not reside within one central compartment. The elimination phase for the parent compounds was characterized with half-lives between 3-7 hours. In the case of hesperetin, R(+)-hesperetin was the only enantiomer to exhibit a significantly higher serum $t_{1/2}$ (6.989 ± 0.258 h) than its counterpart (3.727 ± 0.470 h) in serum (Table 3-1). In the case of naringenin and eriodictyol both enantiomers reported similar half-lives in serum, namely 3.400 ± 0.272 h for R(+)-naringenin and 3.648 ± 0.213 h for S(-)-naringenin; and 4.163 ± 0.361 h for R(+)-eriodictyol and 3.678 ± 0.250 h for S(-)-eriodictyol (Table 3-1).

The glucuronidated metabolites of hesperetin and naringenin exhibited similar concentration-profiles, while the R(+)-eriodictyol glucuronides reported stereospecific differences due to the observed higher concentrations than the S(-)-enantiomer glucuronide (Figure 3-1, 3-2, and 3-3) indicating possible differences in the rate-limiting process of elimination. In the case of hesperetin and naringenin glucuronidated metabolites, slight increases in concentration at 1-2 hours and 30 minutes were observed, respectively indicating the possibility of enterohepatic recycling (Figure 3-1 and 3-2). However, in the case of eriodictyol glucuronidated metabolites no indication of enterohepatic recycling was observed (Figure 3-3).

Table 3-1. Stereospecific pharmacokinetics of hesperetin, naringenin, and eriodictyol in serum after IV administration in rats (20 mg/kg) (mean \pm SEM, n=6). ^aDenotes statistical significant difference (P<0.05) between enantiomers.

Pharmacokinetic Parameter	R(+)-hesperetin	S(-)-hesperetin	R(+)-naringenin	S(-)-naringenin	R(+)-eriodictyol	S(-)-eriodictyol
AUC _{inf} ($\mu\text{g}\cdot\text{h}/\text{ml}$)	24.434 \pm 1.476	7.443 \pm 0.588 ^a	11.643 \pm 0.535	13.410 \pm 0.465 ^a	12.367 \pm 0.933	11.125 \pm 0.658
AUC _{72-inf} extrapolated (%)	0.747 \pm 0.012	2.680 \pm 0.029 ^a	3.422 \pm 0.082	2.748 \pm 0.093 ^a	2.706 \pm 0.047	3.465 \pm 0.056 ^a
V _{ss} (L/kg)	4.180 \pm 0.222	7.342 \pm 0.491 ^a	4.183 \pm 0.172	3.918 \pm 0.150	4.854 \pm 0.247	4.879 \pm 0.507
CL _{renal} (L/h/kg)	0.015 \pm 0.002	0.042 \pm 0.016	0.062 \pm 0.014	0.058 \pm 0.012	0.041 \pm 0.007	0.070 \pm 0.019
CL _{hepatic} (L/h/kg)	0.401 \pm 0.023	1.310 \pm 0.091 ^a	0.806 \pm 0.029	0.693 \pm 0.023 ^a	0.791 \pm 0.063	0.845 \pm 0.043
CL _{tot} (L/h/kg)	0.416 \pm 0.023	1.352 \pm 0.107 ^a	0.868 \pm 0.041	0.751 \pm 0.029 ^a	0.832 \pm 0.063	0.915 \pm 0.055
f _e (%)	3.771 \pm 0.548	3.047 \pm 0.916	6.869 \pm 1.393	7.542 \pm 1.489	5.070 \pm 0.989	7.342 \pm 1.754
k _{el} (h ⁻¹) serum	0.100 \pm 0.003	0.189 \pm 0.024 ^a	0.211 \pm 0.018	0.193 \pm 0.011	0.174 \pm 0.017	0.193 \pm 0.014
k _e (h ⁻¹) urine	0.028 \pm 0.001	0.027 \pm 0.001	0.040 \pm 0.008	0.038 \pm 0.007	0.016 \pm 0.002	0.015 \pm 0.001
T _{1/2} (h) serum	6.989 \pm 0.258	3.727 \pm 0.470 ^a	3.400 \pm 0.272	3.648 \pm 0.213	4.163 \pm 0.361	3.678 \pm 0.250
T _{1/2} (h) urine	25.202 \pm 1.072	25.943 \pm 0.652	12.404 \pm 2.439	12.769 \pm 2.508	46.688 \pm 7.000	47.385 \pm 3.646
MRT (h)	12.244 \pm 0.335	5.527 \pm 1.005 ^a	5.714 \pm 0.855	6.327 \pm 0.627	7.272 \pm 0.557	6.187 \pm 0.290
Extraction ratio (ER)	0.230 \pm 0.013	0.753 \pm 0.052 ^a	0.463 \pm 0.016	0.398 \pm 0.013 ^a	0.454 \pm 0.036	0.486 \pm 0.025

Non-compartmental analysis of the serum concentrations demonstrated significant difference in some pharmacokinetic parameters between hesperetin, naringenin, and eriodictyol enantiomers (Table 3-1). For instance, certain parameters such as AUC_{inf} , serum $t_{1/2}$, mean residence time (MRT) were stereoselective in favor of the R(+)-hesperetin enantiomer, while volume of distribution (V_{ss}), hepatic and total clearance, serum elimination rate constant (k_{el}), and extraction ratio were higher for the S(-)-enantiomer. In the case of naringenin, hepatic and total clearance, and extraction ratio were stereoselective in favor to the R(+)-naringenin enantiomer, while only AUC_{inf} was significantly higher for the S(-)-enantiomer. Nevertheless, no significant differences in the different pharmacokinetic parameters between eriodictyol enantiomers were observed indicating that eriodictyol enantiomers might be metabolized in a similar pattern (Table 3-1).

The differences in certain pharmacokinetic parameters between hesperetin and naringenin enantiomers demonstrate that these two flavonoids are stereospecifically metabolized. For instance, R(+)-hesperetin has a 3.2-fold higher AUC_{inf} , 1.9-fold higher serum $t_{1/2}$, and a 2.2-fold higher MRT than S(-)-hesperetin. On the other hand, S(-)-hesperetin exhibits a 1.7-fold higher V_{ss} , accompanied with a 3.3-fold higher values for both hepatic and total clearance, and a 3.2-fold higher extraction ratio than the R(+)-enantiomer. These results indicate that R(+)-hesperetin resides longer in the body and has a higher serum half-life. These differences may be partially attributed to the observed deeper penetration into tissues (higher V_{ss}) of S(-)-hesperetin, its higher clearance values, and higher extraction from the liver (higher extraction ratio). In the case of naringenin, the R(+)-enantiomer has a 1.2-fold and 1.6-fold higher values for hepatic and total clearance, respectively, accompanied with a 1.2-fold higher extraction ratio than the S(-)-enantiomer. On the other hand, S(-)-naringenin exhibits a 1.1-fold higher

AUC compared to the R(+)-enantiomer. These results indicated that both hesperetin enantiomers have similar mean residence times (MRT), and similar serum half-life. However, R(+)-naringenin has higher clearance values, and higher extraction from the liver (higher extraction ratio). In the case of eriodictyol, there were no significant differences between enantiomers in these parameters.

The physiological parameters of a rat of 0.25 kg body weight indicate that it has an average total blood volume of 13.5 ml and a total body water volume of 167 ml (Davies *et al.*, 1993). This translates in an average total blood volume of 54 ml/kg (0.054 L/kg) and a total water volume of 668 ml/kg (0.668 L/kg). For our compounds of interest, it was observed that the volume of distribution (V_{ss}) of R(+)-hesperetin and S(-)-hesperetin was 4.180 ± 0.222 L/kg and 7.342 ± 0.491 L/kg (Table 3-1). These V_{ss} values are significantly higher than the total blood volume (0.054 L/kg) and the total water volume (0.668 L/kg) indicating that both enantiomers are exiting the blood compartment and have deep penetration into tissues. The same can be stated of naringenin and eriodictyol enantiomers since they also have significantly large V_{ss} values. R(+)-naringenin has an observed V_{ss} of 4.183 ± 0.172 L/kg while S(-)-naringenin a V_{ss} of 3.918 ± 0.150 L/kg. Similarly R(+)-eriodictyol with a V_{ss} of 4.854 ± 0.247 L/kg and S(-)-eriodictyol a V_{ss} of 4.879 ± 0.507 L/kg. These similarly large volume of distribution (V_{ss}) values correlate with the lipophilic nature of these compounds (XLogP values of 2.174, 2.211, and 1.837 for hesperetin, naringenin, and eriodictyol, respectively), which might facilitate their preferential distribution to tissues.

Furthermore, the mean hepatic blood flow (Q) is approximately 3.22 L/h/kg (Davies *et al.*, 1993). Using the hematocrit in rat of 0.48 (Davies *et al.*, 1993), this yields a mean hepatic plasma flow of 1.74 L/h/kg. In the case of hesperetin, the CL_{tot} value for R(+)-hesperetin

(0.416 ± 0.023 L/h/kg) represents less than 25% than the hepatic plasma flow (1.74 L/h/kg), the CL_{tot} value for S(-)-hesperetin (1.352 ± 0.107 L/h/kg) is closer to the mean hepatic plasma flow indicating that S(-)-hesperetin is a high extraction compound (3.2-fold higher extraction ratio than the R(+)-enantiomer). For naringenin, the CL_{tot} value for R(+)-naringenin (0.868 ± 0.041 L/h/kg) and S(-)-naringenin (0.751 ± 0.029 L/h/kg) represent about 49% and 43%, respectively, of the hepatic plasma flow (1.74 L/h/kg) indicating that both enantiomers are medium extraction compounds with the R(+)-enantiomer cleared slightly more rapidly (1.2-fold higher extraction ratio). Similarly, the CL_{tot} value for R(+)-eriodictyol (0.832 ± 0.063 L/h/kg) and S(-)-eriodictyol (0.915 ± 0.055 L/h/kg) represent about 48% and 53%, respectively, of the hepatic plasma flow (1.74 L/h/kg) indicating that both enantiomers are also medium extraction compounds. It was also observed that the three flavonoids are predominately cleared via hepatic elimination (fraction excreted in urine, f_e of 3%, 7%, and 5-7% for both hesperetin, naringenin and eriodictyol enantiomers, respectively) (assuming that hepatic clearance is equivalent to non-renal clearance) (Table 3-1).

The glucuronidated metabolites of hesperetin, naringenin, and eriodictyol previously identified in serum were also detected in the urine samples (Figure 3-4, 3-5, and 3-6) and verified by LC/MS (hesperetin glucuronide m/z of 477, naringenin glucuronide m/z of 447, and eriodictyol glucuronide m/z of 463 in the negative ion mode). In the case of the three flavonoids it was observed that the terminal urine half-life was not significantly different between enantiomers. However, it was clearly observed that the urine half-life (12-47 hours among the three flavonoids) was significantly higher than the plasma half-life (3-7 hours among the three flavonoids). For instance, hesperetin exhibited serum half-lives of 6.989 ± 0.258 h and 3.727 ± 0.470 h for R(+)- and S(-)-hesperetin, respectively, while the urinary half-

lives for R(+)- and S(-)-hesperetin were 25.202 ± 1.072 h and 25.943 ± 0.652 h, respectively. In the case of naringenin, serum half-lives of 3.400 ± 0.272 h and 3.648 ± 0.213 h were observed for R(+)- and S(-)-naringenin, respectively, while the urinary half-lives for R(+)- and S(-)-naringenin were 12.404 ± 2.439 h and 12.769 ± 2.508 h, respectively. Similarly, the observed half-lives for R(+)- and S(-)-eriodictyol were 4.163 ± 0.361 h and 3.678 ± 0.250 h, respectively, while the urinary half-lives were 46.688 ± 7.000 h and 47.385 ± 3.646 h for R(+)- and S(-)-eriodictyol, respectively (Table 3-1).

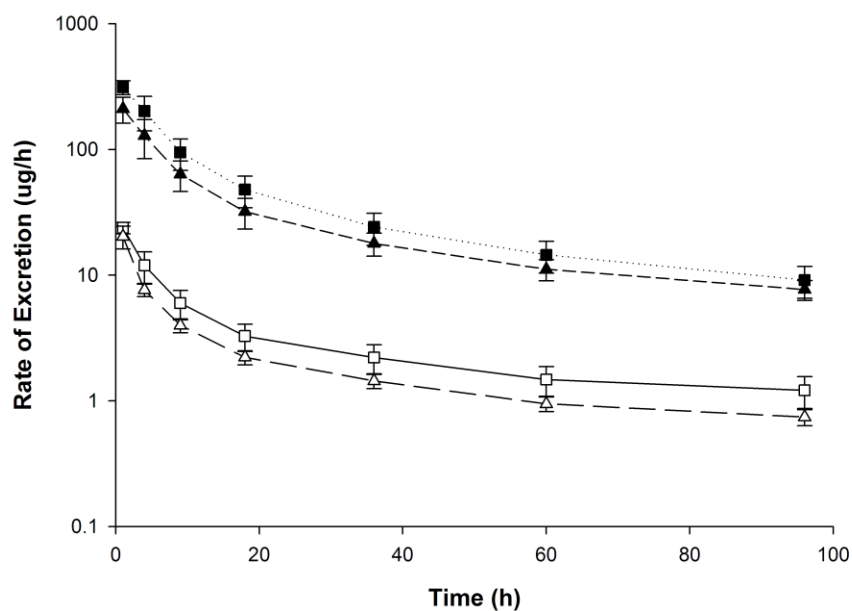


Figure 3-4. Rate of urinary excretion plot of hesperetin (R(+)-hesperetin (□), R(+)-hesperetin glucuronide (■), S(-)-hesperetin (△), and S(-)-hesperetin glucuronide (▲)) after IV administration of racemic hesperetin (20 mg/kg) to rats (mean \pm SEM, n=6).

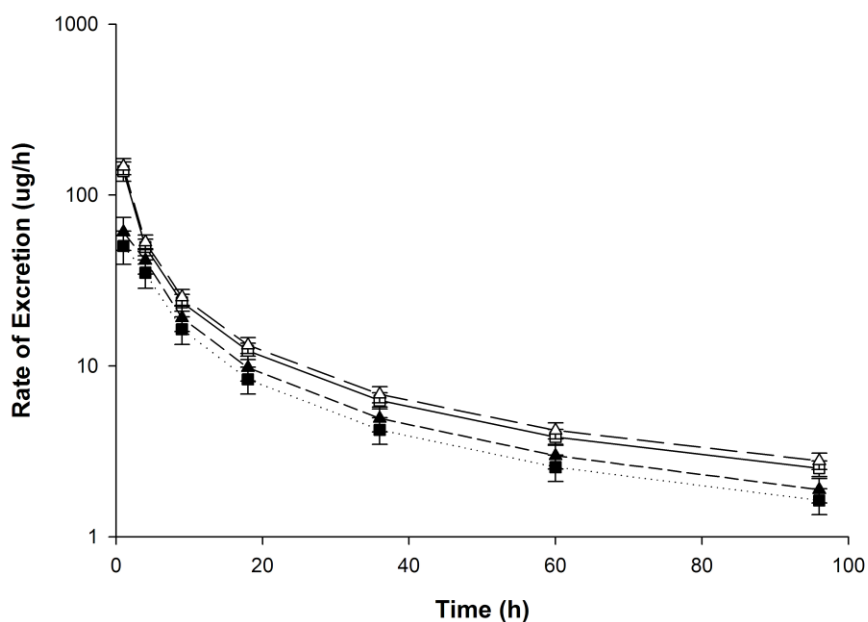


Figure 3-5. Rate of urinary excretion plot of naringenin (R(+)-naringenin (\square), R(+)-naringenin glucuronide (\blacksquare), S(-)-naringenin (Δ), and S(-)-naringenin glucuronide (\blacktriangle)) after IV administration of racemic naringenin (20 mg/kg) to rats (mean \pm SEM, n=6).

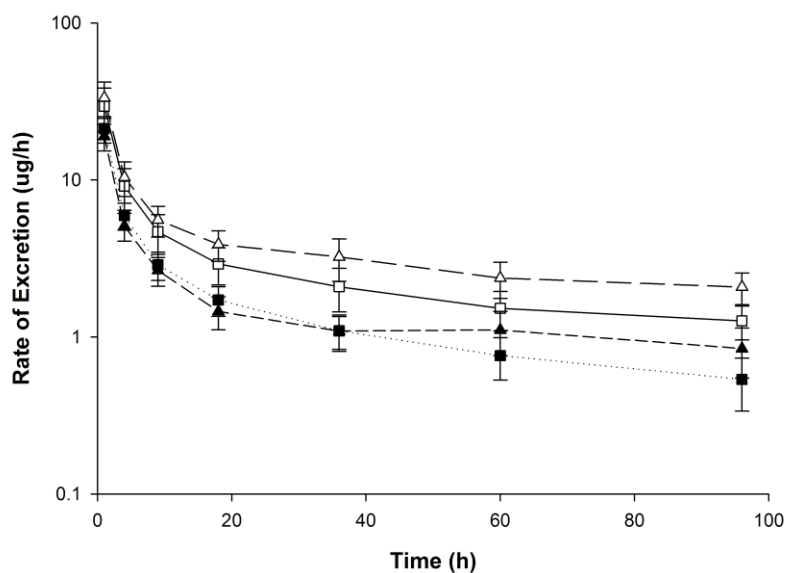


Figure 3-6. Rate of urinary excretion plot of eriodictyol (R(+)-eriodictyol (\square), R(+)-eriodictyol glucuronide (\blacksquare), S(-)-eriodictyol (Δ), and S(-)-eriodictyol glucuronide (\blacktriangle)) after IV administration of racemic eriodictyol (20 mg/kg) to rats (mean \pm SEM, n=6).

These pharmacokinetic in serum and urine half-life discrepancies suggest that the serum half-life is likely significantly underestimating the overall half-life of hesperetin, naringenin, and eriodictyol enantiomers due to assay sensitivity limits of each flavonoid in serum. These observations correlate with previous studies that have reported that certain stilbenes also have longer urine half-lives (4.7-fold to 16-fold higher half-lives in urine compared to plasma half-lives) (Remsberg *et al.*, 2007; Roupe *et al.*, 2006). Even though, there might be sensitivity issues with the employed methodology, the percentage of AUC extrapolated from the last time point (72 hours) to infinity (AUC_{72-inf}) is less than 3.5% (Table 3-1) indicating that more than 95% was effectively measured and employed for the calculation of the other pharmacokinetic parameters. Furthermore, it needs to be mentioned that the compounds of interest (hesperetin, naringenin, and eriodictyol) could be measured up to 72 hours in serum, while in urine they could be measured up to 120 hours. Thus, it is evident that urine is a better biological fluid to utilize in the determination of pharmacokinetic parameters because as it can be observed serum concentrations are at the limit of sensitivity and considerably underestimates the half-life of these compounds.

Therefore, the pharmacokinetic parameters determined by employing urine were calculated (Table 3-2). It can be observed that employing serum significantly underestimates AUC_{inf} , half-life, and MRT, while all the other parameters were overestimated. The volume of distribution (V_{ss}) did not significantly vary between serum and urine indicating that the changes in AUC_{inf} and $AUMC_{inf}$ were similar in both matrices ($V_{ss} = Dose * AUMC_{inf} / (AUC_{inf})^2$). Thus, urine provides more significant pharmacokinetic parameters indicating that these chiral flavonoids have long half-lives (12-48 h), very high volumes of distribution (4-9 L/kg) suggesting they considerably exit the blood compartment and distribute widely.

Table 3-2. Stereospecific pharmacokinetics of hesperetin, naringenin, and eriodictyol in urine (and percentage change between serum and urine pharmacokinetic parameters assuming the serum parameters represent 100%) after IV administration in rats (20 mg/kg) (mean \pm SEM, n=6). ^aDenotes statistical significant difference (P<0.05) between enantiomers.

Pharmacokinetic Parameter	R(+)-hesperetin	S(-)-hesperetin	R(+)-naringenin	S(-)-naringenin	R(+)-eriodictyol	S(-)-eriodictyol
AUC _{inf} (μ g*h/ml)	88.430 \pm 5.894 (361.91 \pm 24.12)	38.641 \pm 1.446 ^a (519.15 \pm 19.42)	51.593 \pm 5.133 (443.13 \pm 44.08)	56.799 \pm 3.553 (423.57 \pm 26.49)	142.083 \pm 24.926 (1148.90 \pm 201.55)	146.081 \pm 17.067 (1313.12 \pm 153.42)
V _{ss} (L/kg)	4.166 \pm 0.221 (99.67 \pm 5.28)	9.065 \pm 0.491 ^a (123.47 \pm 6.69)	4.173 \pm 0.211 (99.75 \pm 5.04)	3.919 \pm 0.184 (100.01 \pm 4.69)	4.853 \pm 0.246 (99.98 \pm 5.08)	4.878 \pm 0.507 (99.98 \pm 10.40)
CL _{renal} (L/h/kg)	0.004 \pm 0.001 (27.89 \pm 4.05)	0.006 \pm 0.001 (14.76 \pm 2.37)	0.015 \pm 0.001 (25.02 \pm 3.01)	0.016 \pm 0.001 (26.90 \pm 2.80)	0.004 \pm 0.001 (10.09 \pm 1.97)	0.006 \pm 0.002 (8.51 \pm 2.03)
CL _{hepatic} (L/h/kg)	0.111 \pm 0.007 (27.72 \pm 3.81)	0.254 \pm 0.010 ^a (19.39 \pm 2.34)	0.185 \pm 0.018 (22.98 \pm 1.46)	0.163 \pm 0.011 (23.55 \pm 1.88)	0.075 \pm 0.010 (9.49 \pm 2.50)	0.067 \pm 0.006 (7.94 \pm 2.47)
CL _{tot} (L/h/kg)	0.115 \pm 0.007 (27.73 \pm 1.71)	0.260 \pm 0.010 ^a (19.25 \pm 0.71)	0.201 \pm 0.018 (23.12 \pm 2.02)	0.179 \pm 0.011 (23.81 \pm 1.44)	0.079 \pm 0.011 (9.52 \pm 1.31)	0.073 \pm 0.008 (7.99 \pm 0.89)
f _e (%)	3.771 \pm 0.548	2.442 \pm 0.391	8.018 \pm 0.965	8.827 \pm 0.920	5.070 \pm 0.989	7.342 \pm 1.754
k ^e (h ⁻¹) urine	0.028 \pm 0.001 (28.00 \pm 1.26)	0.027 \pm 0.001 (14.29 \pm 0.81)	0.040 \pm 0.008 (18.96 \pm 1.25)	0.038 \pm 0.007 (19.69 \pm 0.48)	0.016 \pm 0.002 (9.19 \pm 1.07)	0.015 \pm 0.001 (7.77 \pm 0.72)
T _{1/2} (h) urine	25.202 \pm 1.072 (360.59 \pm 15.33)	25.943 \pm 0.652 (696.08 \pm 31.06)	12.404 \pm 2.439 (364.82 \pm 26.86)	12.769 \pm 2.508 (350.03 \pm 8.75)	46.688 \pm 7.000 (1121.50 \pm 168.16)	47.385 \pm 3.646 (1288.34 \pm 99.12)
MRT (h)	36.361 \pm 1.556 (296.98 \pm 12.71)	34.881 \pm 1.678 (631.16 \pm 30.37)	21.180 \pm 1.326 (370.65 \pm 23.20)	22.013 \pm 0.466 (347.94 \pm 7.36)	67.391 \pm 10.150 (926.71 \pm 139.57)	68.301 \pm 5.248 (1103.90 \pm 84.83)
Extraction ratio (ER)	0.064 \pm 0.004 (27.72 \pm 1.75)	0.146 \pm 0.006 ^a (19.39 \pm 0.78)	0.106 \pm 0.010 (22.98 \pm 2.20)	0.094 \pm 0.006 (23.55 \pm 1.59)	0.043 \pm 0.006 (9.49 \pm 1.28)	0.039 \pm 0.004 (7.94 \pm 0.77)

The most significant changes are the AUC_{inf} and clearance values (Table 3-2). Based on the low clearance values (0.07-0.27 L/h/kg) it can be observed that actually these xenobiotics are low extraction compounds (0.04-0.15). Interestingly, it was observed that there was stereospecificity in pharmacokinetic parameters only between hesperetin enantiomers, while naringenin and eriodictyol enantiomers exhibited similar parameters.

The total cumulative urinary excretion plots indicate that these three flavonoids undergo extensive phase II metabolism due to the significantly higher excretion of glucuronidated metabolites compared to the parent compounds. However, based on the low fraction excreted in urine (f_e values of 3%, 7%, and 5-7% for both hesperetin, naringenin and eriodictyol enantiomers, respectively), it can be presumed that these compounds will distribute from the systemic circulation into tissues (V_{ss} values of 4-9 L/kg) and eventually be eliminated via non-renal routes. Nevertheless, this is a dynamic system in which hesperetin, naringenin, and eriodictyol are rapidly being metabolized to different glucuronides. But despite the highly different solubility and lipophilicity nature of these compounds (parent and glucuronidated metabolites) it can be observed that they have similar rates of excretion (Figure 3-4, 3-5, and 3-6). This indicates that both forms undergo similar magnitude of apparent elimination (since their lines are parallel) indicating that the glucuronide conjugates are formation-rate limited and that their half-lives would be a reflection of the elimination of the parent flavonoids.

3.9.2 Stereospecific Quantification of Hesperidin, Hesperetin, Naringin, Naringenin, Eriocitrin, and Eriodictyol in Fruit Juices

The HPLC method has been applied to the stereospecific quantification of hesperetin, naringenin, and eriodictyol in conventional and organic orange, grapefruit, lemonade, lime, apple, and tomato juice. The glycosides hesperidin, naringin, and eriocitrin were quantified

indirectly via HPLC after enzymatic hydrolysis and verified by LC/MS before enzymatic hydrolysis by monitoring the single plot transitions (m/z): hesperidin 610→609, naringin 580→579, and eriocitrin 596→595).

Hesperetin, naringenin, and eriodictyol in some of these juices have been reported previously in the United States Department of Agriculture (USDA) Database for the Flavonoid Content of Selected Foods (USDA, 2003). This database reports only aglycones, but it is apparent based on our results, that the glycoside and aglycone terms are mistakenly used interchangeably.

Furthermore, the database is very limited in the number of flavonoids it contains and provides limited information. For instance, there is no information on the stereospecific flavanone content, and it was observed that the (2S)-epimers and S(-)-enantiomers of hesperidin, naringin, eriocitrin, hesperetin, naringenin, and eriodictyol were predominant in most of the juices examined. In some instances the organic fruit juices had higher concentrations of epimers and enantiomers than the conventional fruit juices (Table 3-3, 3-4, and 3-5). Among the juices examined, orange juice contained the highest concentration of (2R)- and (2S)-hesperidin (Table 3-3), while conventional and organic grapefruit juice contains the highest concentration of R(+)- and S(-)-hesperetin (Table 3-3), and (2R)- and (2S)-naringin (Table 3-4), while conventional and organic tomato juice reported the highest values in R(+)- and S(-)-naringenin (Table 3-4). In the case of (2R)- and (2S)-eriocitrin, and R(+)- and S(-)-eriodictyol similar values were observed between both lemonade and lime juice (Table 3-5).

Table 3-3. Stereospecific hesperidin and hesperetin content (mg per 100 ml juice) in various commercial fruit juices ($n=4$, mean \pm SEM). Racemic represent the sum of both preceding epimers or enantiomers, respectively. N/R = not reported. ^aDenotes statistical significant difference ($P<0.05$) between conventional and organic fruit juices. ^bDenotes statistical significant difference ($P<0.05$) between enantiomers in each fruit juice.

Juice	Hesperidin			USDA Database (2003)	Hesperetin			USDA Database (2003)
	(2R)-hesperidin	(2S)-hesperidin	Racemic		R(+)-hesperetin	S(-)-hesperetin	Racemic	
Conventional Orange Juice	20.06 \pm 0.342	299.9 \pm 5.429 ^b	320.0	N/R	0.895 \pm 0.014	0.788 \pm 0.013 ^b	1.683	3.610
Organic Orange Juice	11.65 \pm 0.112 ^a	170.4 \pm 3.084 ^{a,b}	182.0	N/R	0.893 \pm 0.111	0.695 \pm 0.011 ^{a,b}	1.588	N/R
Conventional Grapefruit Juice	1.696 \pm 0.018	18.29 \pm 0.165 ^b	19.99	N/R	0.907 \pm 0.014	0.707 \pm 0.011 ^b	1.614	3.420
Organic Grapefruit Juice	0.909 \pm 0.015 ^a	15.64 \pm 0.141 ^{a,b}	16.55	N/R	2.099 \pm 0.018 ^a	0.765 \pm 0.012 ^{a,b}	2.864	N/R
Conventional Apple Juice	1.075 \pm 0.011	1.281 \pm 0.013 ^b	2.356	N/R	0.729 \pm 0.012	0.721 \pm 0.011	1.450	N/R
Organic Apple Juice	2.749 \pm 0.023 ^a	4.462 \pm 0.034 ^{a,b}	7.211	N/R	1.150 \pm 0.012 ^a	1.615 \pm 0.017 ^{a,b}	2.765	N/R
Conventional Tomato Juice	0.717 \pm 0.011	0.942 \pm 0.015 ^b	1.659	N/R	0.687 \pm 0.011	0.701 \pm 0.011	1.389	N/R
Organic Tomato Juice	0.735 \pm 0.012	1.076 \pm 0.011 ^{a,b}	1.811	N/R	0.688 \pm 0.011	0.711 \pm 0.011	1.399	N/R

Table 3-4. Stereospecific naringin and naringenin content (mg per 100 ml juice) in various commercial fruit juices ($n=4$, mean \pm SEM). Racemic represent the sum of both preceding epimers or enantiomers, respectively. N/R = not reported. ^aDenotes statistical significant difference ($P<0.05$) between conventional and organic fruit juices. ^bDenotes statistical significant difference ($P<0.05$) between enantiomers in each fruit juice.

Juice	Naringin				Naringenin			
	(2R)-naringin	(2S)-Naringin	Racemic	USDA Database (2003)	R(+)-naringenin	S(-)-naringenin	Racemic	USDA Database (2003)
Conventional Orange Juice	2.611 \pm 0.022	4.798 \pm 0.047 ^b	7.409	N/R	0.017 \pm 0.001	0.036 \pm 0.001 ^b	0.053	1.470
Organic Orange Juice	1.398 \pm 0.018 ^a	2.510 \pm 0.025 ^{a,b}	3.908	N/R	0.009 \pm 0.001 ^a	0.020 \pm 0.001 ^{a,b}	0.029	N/R
Conventional Grapefruit Juice	13.97 \pm 0.036	18.65 \pm 0.060 ^b	32.62	N/R	0.077 \pm 0.002	0.031 \pm 0.059	0.108	20.06
Organic Grapefruit Juice	17.79 \pm 0.046 ^a	28.13 \pm 0.022 ^{a,b}	45.92	N/R	0.139 \pm 0.004 ^a	0.067 \pm 0.001 ^b	0.206	N/R
Conventional Apple Juice	0.020 \pm 0.001	0.045 \pm 0.002 ^b	0.065	N/R	0.018 \pm 0.001	0.031 \pm 0.001	0.050	N/R
Organic Apple Juice	0.010 \pm 0.001 ^a	0.089 \pm 0.001 ^{a,b}	0.099	N/R	0.019 \pm 0.001	0.024 \pm 0.001 ^{a,b}	0.043	N/R
Conventional Tomato Juice	0.616 \pm 0.019	0.609 \pm 0.023	1.225	N/R	0.693 \pm 0.022	0.759 \pm 0.029	1.452	N/R
Organic Tomato Juice	2.373 \pm 0.020 ^a	2.476 \pm 0.024 ^{a,b}	4.849	N/R	0.938 \pm 0.029 ^a	0.933 \pm 0.035 ^a	1.871	N/R

Table 3-5. Stereospecific eriocitrin and eriodictyol content (mg per 100 ml juice) in various commercial fruit juices ($n=4$, mean \pm SEM). Racemic represent the sum of both preceding epimers or enantiomers, respectively. ^aDenotes statistical significant difference ($P<0.05$) between conventional and organic fruit juices. ^bDenotes statistical significant difference ($P<0.05$) between enantiomers in each fruit juice.

Juice	Eriocitrin				Eriodictyol			
	(2R)-eriocitrin	(2S)-eriocitrin	Racemic	USDA Database (2003)	R(+)-eriodictyol	S(-)-Eriodictyol	Racemic	USDA Database (2003)
Conventional Lemonade	0.303 \pm 0.001	0.504 \pm 0.007 ^b	0.807	N/R	0.385 \pm 0.012	0.429 \pm 0.001 ^b	0.814	11.64
Organic Lemonade	2.347 \pm 0.002 ^a	6.457 \pm 0.074 ^{a,b}	8.804	N/R	2.391 \pm 0.002 ^a	0.384 \pm 0.005 ^{a,b}	2.775	N/R
Conventional Lime Juice	1.397 \pm 0.003	1.537 \pm 0.001 ^b	2.934	N/R	0.515 \pm 0.016	0.443 \pm 0.006 ^b	0.958	2.19
Organic Lime Juice	2.999 \pm 0.003 ^a	3.104 \pm 0.036 ^{a,b}	6.103	N/R	0.348 \pm 0.011 ^a	0.366 \pm 0.001 ^a	0.714	N/R

The values we report are in discrepancy with the USDA database; however, it is hard to make an effective comparison because the USDA database does not specify the source and variety or manufacturer of the fruit juices and the variability and validity of the employed assay methods are unknown. There are also some novel findings in these results with the detection of hesperidin, hesperetin, naringin, and naringenin found in apple juice for the first time.

3.10 DISCUSSION AND CONCLUSIONS

All three flavanones examined hesperetin, naringenin, and eriodictyol each undergoes glucuronidation upon intravenous administration, as determined by serum and urine concentrations and later verified by treating plasma and urine samples with β -glucuronidase. This *in vivo* data parallels the *in vitro* metabolism findings in human and rat liver microsomes with these dietary flavonoids (Breinholt *et al.*, 2002; Nielsen *et al.*, 1998; Stevens *et al.*, 2001; Zhu *et al.*, 1998). Previous pharmacokinetic studies of these dietary flavonoids after oral ingestion of fruit juices have not been analyzed using chiral analytical techniques. For instance, hesperidin and hesperetin have been assessed after oral ingestion of orange juice by healthy human subjects (Erlund *et al.*, 2001; Kanaze *et al.*, 2007; Manach *et al.*, 2003). The pharmacokinetic studies after oral ingestion of orange juice suggest that racemic hesperetin has a plasma half-life of 2-3 hours, and that only 5% is excreted in urine (Erlund *et al.*, 2001; Kanaze *et al.*, 2007). These studies (Erlund *et al.*, 2001; Kanaze *et al.*, 2007; Manach *et al.*, 2003) also determined that hesperetin undergoes extensive glucuronidation after oral administration. These results correlate with our present findings, of percentage of dose excreted in urine (f_e values of 3-4%) in the rat. However, the serum half-lives (3.7-7 h) calculated and urine half-lives (around 25 hours and actual better estimate) are higher than the previously reported (2-3 hours) (Erlund *et al.*, 2001). These differences might be attributed to

differences in sampling time, in the study by Erlund *et al.* (Erlund *et al.*, 2001) plasma and urine samples were collected up to 24 hours while in our study the last measurable point in serum was at 72 hours and in urine 120 h post-dose. Furthermore, there are considerable differences in the detection limits, in the study by Erlund *et al.* (Erlund *et al.*, 2001) the detection limit was 0.12 μM (0.036 $\mu\text{g/ml}$) while in our study the limit of detection was 0.0002 $\mu\text{g/ml}$ (0.2 ng/ml). Nevertheless, Erlund *et al.* (Erlund *et al.*, 2001) only reported the AUC_{0-24} but did not report the AUC_{inf} or the percentage of extrapolation from 24 to infinity making hard to know if the study was sufficient in time points to acquire for most of the administered dose. In our study the percentage of $\text{AUC}_{72-\text{inf}}$ extrapolated was $0.747 \pm 0.012\%$ and $2.680 \pm 0.029\%$ for R(+)- and S(-)-hesperetin, respectively (Table 3-1). Thus, it can be observed that our method was sufficient in the number of time points to represent more than 95% of the administered dose. Finally, the rat disposition kinetics may not quantitatively parallel human finding although preliminary studies performed in our laboratory indicate that the rat is a suitable model to study the pharmacokinetics of these flavanones (Davies *et al.* unpublished observations) and allometric scaling from rat to humans is possible.

In the case of naringenin, its achiral pharmacokinetics have been studied after oral ingestion of orange juice, grapefruit juice (Erlund *et al.*, 2001), and tomato paste (Bugianesi *et al.*, 2002) showing that racemic naringenin has a short serum half life of 1-2 hours and that after oral ingestion of orange juice only 1% of naringenin gets excreted in urine (Erlund *et al.*, 2001) and 7% in other study (Manach *et al.*, 2003). While 30% of naringenin gets excreted in urine after oral ingestion of grapefruit juice; however, the standard deviation of this measurement in the first study was 25.5% reducing the reliability of these results (Erlund *et al.*, 2001). Our results indicate that naringenin has a serum half-life of 3.40 ± 0.27 for R(+)-

naringenin and 3.65 ± 0.21 for S(-)-naringenin, urine half-life of 12.404 ± 2.439 for R(+)-naringenin and 12.769 ± 2.508 for S(-)-naringenin, and f_e values of around 7% for both enantiomers that are similar to the previous studies (Erlund *et al.*, 2001; Manach *et al.*, 2003). However, again our results reported higher serum and urine half-lives than previous results due to better sensitivity limits, longer sampling time, and known low percentage of extrapolation of AUC from 72 to infinity ($AUC_{72-\text{inf}}$) (Table 3-1). Bugianesi *et al.* (Bugianesi *et al.*, 2002) assessed the bioavailability of naringenin from tomato paste in humans; however, half-life or f_e values were not reported. The pharmacokinetics of intravenous-dosed racemic naringenin (25 mg/kg) in rabbits (2-3 kg weight) has been reported (Hsiu *et al.*, 2002). The authors report a short elimination phase half-life of only 17 ± 4 minutes, a low volume of distribution of 1.6 ± 0.4 L, and a high total clearance value of 0.16 ± 0.02 L/min. Our results in the rat are significantly different than these findings in the rabbit since we observed a longer half-life (around 3.5 h for both enantiomers), volumes of distribution of around 4 L/kg, and total clearance values between 0.7-0.9 L/h/kg. This discrepancy may be attributed to species differences in disposition and the lack of assay sensitivity as naringenin and its glucuronidated metabolite were detected only up to 90 minutes, and naringenin was still predominantly in the distribution phase, which would have biased the half-life and other pharmacokinetic parameter interpretations. The authors also observe that naringenin undergoes significant glucuronidation and similar to our results, a higher concentration of the parent compound was detected in serum compared to the glucuronidated metabolite (Hsiu *et al.*, 2002).

Racemic eriodictyol has been studied after oral ingestion of eriocitrin (75 $\mu\text{mol/kg}$) via gastric intubation, as well as *ex vivo* everted gut studies to assess the intestinal absorption of eriocitrin (Miyake *et al.*, 2000). This study found that eriocitrin was not present in plasma

samples of eriocitrin-treated rats, whereas significant concentrations of eriodictyol, homoeriodictyol, and hesperetin were determined 4 hours post-dose. Furthermore, similar to our investigations eriodictyol glucuronides were apparent in the plasma and urine (Figures 3-3 and 3-6). However, this study was able to detect eriocitrin metabolites (eriodictyol, homoeriodictyol, hesperetin and their glucuronides) only up to 4 hours in plasma and up to 24 hours in urine. It was also observed that eriodictyol in the intestine is further broken down to 3,4-dihydroxyhydrocinnamic acid (3,4-DHCA) (Miyake *et al.*, 2000). The same research group administered orally to humans flavonoid glycosides and aglycones extracted from lemon peel (Miyake *et al.*, 2006). This study also reported that eriocitrin undergoes sequential metabolism into eriodictyol, homoeriodictyol and hesperetin and their corresponding glucuronidated and sulfated metabolites after the oral ingestion of the lemon peel extracts also suggesting that eriodictyol undergoes extensive phase II metabolism (Miyake *et al.*, 2006).

To our knowledge, this is the first study that has assessed the stereospecific pharmacokinetics of hesperetin, naringenin, and eriodictyol after intravenous administration of the pure racemates. Previous studies have focused only on the racemic mixtures and utilized achiral analysis after oral ingestion. Our findings indicate that these three flavonoids have relatively short half-lives (3-7 h) in serum and long half-lives in urine (12-48 h) as shown previously with similar compounds (stilbenes) that belong to the same family of polyphenols (Remsberg *et al.*, 2007; Roupe *et al.*, 2006). This discrepancy between plasma and urine half-life in different stilbenes was attributed to assay sensitivity limits that would most likely underestimate the overall half-life of these compounds. Underestimation of plasma half-life due to assay sensitivity limits has been reported before in the case of procainamide (Jamali *et al.*, 1988). In the report by Jamali *et al.* (Jamali *et al.*, 1988) an improved HPLC method was

employed and it was observed that there was significant 2-fold increase in plasma half-life compared to previous reports. Nevertheless, most of the pharmacokinetic studies only collect samples up to 24 hours post-dose, which could underestimate the elimination phase and pharmacokinetic parameters. These discrepancies suggest that the serum half-life is likely significantly underestimating the overall half-life of hesperetin, naringenin, and eriodictyol enantiomers due to assay sensitivity limits in serum. Even though, there might be sensitivity issues with the employed methodology, the percentage of AUC extrapolated from the last time point (72 hours) to infinity (AUC_{72-inf}) is less than 3.5% (Table 3-1) indicating that more than 95% of the measured drug was effectively measured and employed for the calculation of the other pharmacokinetic parameters. Furthermore, it needs to be mentioned that the compounds of interest (hesperetin, naringenin, and eriodictyol) could be measured up to 72 hours in serum, while in urine they could be measured up to 120 hours. Thus, it is evident that urine is a better biological fluid to utilize in the determination of pharmacokinetic parameters because as it can be observed serum concentrations are at the limit of sensitivity and considerably underestimates the half-life of these compounds. Therefore, the pharmacokinetic parameters employing urine were calculated (Table 3-2). It can be observed that employing serum significantly underestimates AUC_{inf} , half-life, and MRT, while all the other parameters, except volume of distribution, were overestimated. The volume of distribution (V_{ss}) did not significantly vary between serum and urine indicating that the changes in AUC_{inf} and $AUMC_{inf}$ were similar in both matrices ($V_{ss} = Dose * AUMC_{inf} / (AUC_{inf})^2$). Thus, the pharmacokinetics and biodisposition of these compounds need to be reconsidered on the basis of their chirality and the finding that urine provides higher concentrations of these xenobiotics.

Furthermore, the large volumes of distribution (4-9 L/kg) of hesperetin, naringenin, and eriodictyol enantiomers are significantly larger than the total blood volume (0.054 L/kg) and the total water volume (0.668 L/kg) in the rat indicating that both enantiomers of these compounds are exiting the systemic circulation and distributing into tissues. These large volume of distribution (V_{ss}) values correlate with the lipophilic nature of these compounds (XLogP values of 2.174, 2.211, and 1.837 for hesperetin, naringenin, and eriodictyol, respectively), which facilitate their distribution to tissues. Based on the clearance values it can be observed that these three compounds are mainly excreted via non-renal routes (assuming that hepatic clearance is equivalent to non-renal clearance), which is also verified by their low fraction excreted in urine (f_e) values of 3-7% (Table 3-1). Based on these pharmacokinetic data, hesperetin, naringenin, and eriodictyol appear to be exiting the systemic circulation and apparently being distributed to the different tissues in the body (urine V_{ss} values of 4-9 L/kg and urine MRT values of 21-68 hours). The racemic mixtures of these flavonoids are known to undergo metabolic phase II reactions involving primarily conjugation with glucuronic acid (Erlund *et al.*, 2001; Hsiu *et al.*, 2002; Kanaze *et al.*, 2007; Manach *et al.*, 2003; Miyake *et al.*, 2006; Miyake *et al.*, 2000).

It was also observed that the fruit juices examined have stereospecific content of the glycoside epimers and of the aglycone enantiomers (Tables 3-3, 3-4, and 3-5) and that were statistically significant differences in some conventional juices from organic juices. Further exploration of the pharmacodynamics of chiral flavonoids and fruit juices has demonstrated health benefits in *in vitro* and *in vivo* models in our laboratory and further stereospecific clinical pharmacokinetic studies are ongoing in humans and animals after consumption of different fruits and fruit juices.

Based on these pharmacokinetic data, hesperetin, naringenin, and eriodictyol enantiomers appear to be distributing into tissues. The lumen of the intestine as well as the endothelial lining of the liver are exposed to the free, unchanged fraction of the administered flavanones prior to its biotransformation. With the known pharmacological properties of flavanones and other flavonoids, these selected compounds may be particularly useful in treating gastrointestinal and liver disorders such as ulcerative colitis, Crohn's disease, cirrhosis, hyperlipidemia, and hepatitis as they inherently associate with the gastrointestinal and hepatic systems.

Chapter IV In Vitro Pharmacodynamics of Racemic Hesperidin, Hesperetin, Naringin, Naringenin, Eriocitrin and Eriodictyol

4.1 INTRODUCTION

This chapter describes the *in vitro* anti-inflammatory properties, cyclooxygenase-1 and 2 inhibitory activities, inflammatory bowel activity, anti-adipogenic activity, anti-cancer activity, and anti-oxidant capacity of racemic hesperidin, hesperetin, naringin, naringenin, eriocitrin, and eriodictyol. The anti-inflammatory properties were assessed using an osteoarthritis model using canine chondrocytes after inflammatory insult using interleukin-1beta (IL-1 β) and measuring various inflammatory mediators released into the cell culture medium. The cyclooxygenase-1 and -2 inhibitory activities was measured employing a commercially available ELISA kit. The inflammatory bowel activity was measured using a colitis model in colon adenocarcinoma (HT-29) cells after inflammatory insult with tumor necrosis alpha (TNF- α) and measuring prostaglandin E₂ (PGE₂) levels using a commercially available ELISA kit. The anti-adipogenic activity was assessed using 3T3-L1 pre-adipocytes and subsequent staining for their production of fat droplets. The anti-cancer activity was assessed in selected cancer cell lines, utilizing the Alamar blue assay to quantify viable cancer cells present following flavanone treatment. Finally, a comprehensive anti-oxidant method was developed to account for the lipophilic, hydrophilic, glycoside and aglycone fractions of apple samples and of the selected flavanones. Where applicable, the IC₅₀ values of hesperidin, hesperetin, naringin, naringenin, eriocitrin, and eriodictyol in the different *in vitro* models were modeled using WinNonlin[®] pharmacodynamic software.

4.2 BACKGROUND

Inflammation is a complex process that involves a series of events encompassing numerous stimuli such as: infection, ischemia, antigen–antibody interactions, chemical, thermal or mechanical injury. The inflammatory responses has been characterized to occur in three distinct phases, each apparently mediated by different mechanisms: an acute phase characterized by local vasodilatation and increased capillary permeability, a subacute phase characterized by infiltration of leukocyte and phagocyte cells, and a chronic proliferative phase, in which tissue degeneration and fibrosis occur (Rotelli *et al.*, 2003). Different disease states involve acute and/or chronic inflammatory processes and during the distinct phases of inflammation there are different inflammatory mediators involved that play key roles. For instance, hesperidin has been assessed for its inhibitory effect on lipopolysaccharide (LPS)-induced over-expression of cyclooxygenase-2 (COX-2), inducible nitric oxide synthase (iNOS) proteins, over-production of prostaglandin E₂ (PGE₂) and nitric oxide (NO) using mouse macrophage cells. Treatment with hesperidin suppressed production of PGE₂, nitrogen dioxide (NO₂), and expression of iNOS protein. In the case of COX-2, hesperidin did not affect the protein expression and levels. Thus, hesperidin has been reported to be a COX-2 and iNOS inhibitor, and these mechanisms of action may account for its anti-inflammatory and anti-tumorigenic efficacies (Sakata *et al.*, 2003). Furthermore, hesperetin and hesperidin in the concentration range 250-500 µM have been shown to potently inhibit the LPS-induced expression of the COX-2 gene in RAW 264.7 cells, further highlighting the anti-inflammatory activity of these compounds. The ability of hesperetin and hesperidin to suppress COX-2 gene expression has been suggested to possibly be a consequence of their anti-oxidant activity (Hirata *et al.*, 2005). Other studies have reported that hesperidin downregulates the LPS-

induced expression of different proinflammatory (TNF- α , IL-1 β , IL-6) and anti-inflammatory mediators (IL-12) cytokines as well as cytokines (KC, MCP-1 and MIP-2), while enhancing the production of other anti-inflammatory cytokines (IL-4 and IL-10) (Yeh *et al.*, 2007). Furthermore, hesperidin suppresses the expression of IL-8 on A549 cells and THP-1 cells, the expression of TNF- α , IL-1 β , and IL-6 on THP-1 cells, the expression of ICAM-1 and VCAM-1 (responsible for cell adhesion) on A549 cells. The suppression of these inflammatory mediators is regulated by NF- κ B and AP-1, which are activated by I κ B and MAPK pathways indicating that hesperidin might interact with these pathways to exert its anti-inflammatory activity (Yeh *et al.*, 2007).

Similar observations have been reported for naringenin and its effect on nitric oxide (NO) and prostaglandin E₂ (PGE₂) production induced by lipopolysaccharide (LPS) in the macrophage cell line J774A.1. Naringenin (0.5-50 μ M) was observed to be a significant inhibitor of NO production and this effect was concentration-dependent and significant at 5 and 50 μ M. A similar pattern was observed considering the inhibitory effect of naringenin on LPS-induced PGE₂ release and COX-2 expression. Naringenin markedly decreased PGE₂ release and COX-2 expression in a concentration-dependent manner. Thus, naringenin inhibits iNOS and COX-2 expression and this may be the mechanism of action responsible for their anti-inflammatory effects (Raso *et al.*, 2001). However, naringenin has been reported to have poor or no effect over other various inflammatory mediators *in vitro*. For instance, naringenin was ineffective in inhibiting endothelial adhesion molecule expression or in attenuating expression of E-selectin and intercellular adhesion molecule 1 (ICAM-1), vascular cell adhesion molecule 1 (VCAM-1), and tumor necrosis factor alpha-induced adhesion molecule expression in human aortic endothelial cells (Lotito *et al.*, 2006). In another study, naringenin also exhibited

virtually no effects on cytokines, metabolic activity or on the number of cells in the studied cell populations of stimulated human peripheral blood mononuclear cells (PBMC) by lipopolysaccharide (LPS) (Hougee *et al.*, 2005). Furthermore, the inability of naringenin to inhibit the activity of NOS-2, and induce NOS-2 protein in LPS-treated J774.2 cells using Western blotting techniques has been reported (Olszanecki *et al.*, 2002). However, naringin has also been reported to regulate certain inflammatory mediators and to possess certain anti-inflammatory activity. Naringin (10, 30 and 60 mg/kg i.p.) dose-dependently suppressed LPS-induced production of TNF-alpha in mice. To further examine the mechanism by which naringin suppresses LPS-induced endotoxin shock, an *in vitro* model, RAW 264.7 mouse macrophage cells was utilized. Naringin (1 mM) suppressed LPS-induced production of NO and the expression of inflammatory gene products such as inducible NO synthase (iNOS), TNF-alpha, inducible cyclooxygenase (COX-2) and interleukin-6 (IL-6) as determined by RT-PCR assay. Naringin was also found to have blocked the LPS-induced transcriptional activity of NF-κB in electrophoretic mobility shift assay and reporter assay. These findings suggest that suppression of the LPS-induced mortality and production of NO by naringin is due to inhibition of the activation of NF-κB (Kanno *et al.*, 2006a).

Similarly, eriodictyol extracted from the methanol fraction of the stem bark of *Populus davidiana* demonstrated moderate inhibition against COX-1 only and exhibited suppressive effects on xanthine oxidase (XO) (Zhang *et al.*, 2006a). In addition, eriodictyol extracted from *Thymus broussonetii* Boiss (Labiatae) leaves, a herbal drug used in Moroccan traditional medicine has been assessed using the croton oil ear test in mice and significant anti-inflammatory properties were reported (Ismaili *et al.*, 2002). Furthermore, pretreatment of RAW 264.7 with eriodictyol inhibited TNF-alpha release in lipopolysaccharide (LPS)-

stimulated macrophages. The potency in inhibiting cytokine production was expressed with an IC_{50} of less than 10 μ M for TNF- α release. It was also observed that pretreatment of cells with eriodictyol decreased I κ B- α phosphorylation and reduced the levels of I κ B- α (Xagorari *et al.*, 2001).

Inflammation plays a critical role in different disorders such as gastrointestinal disorders. These types of disorders affect millions of Americans of all ages and the social and economic costs of such disorders are massive. Ulcerative colitis, a chronic inflammatory bowel disease with an unknown etiology, is one disorder in which symptoms can be severe and debilitating. These severe symptoms include diarrhea, rectal bleeding, abdominal cramps, fatigue, and fever. It is often diagnosed based on the presence of ulcerations and inflammation along the colonic wall that are evident following a colonoscopy examination. Current treatments include anti-inflammatory drug therapy, such as 5-aminosalicylic acid (5-ASA), corticosteroids, and immunomodulators, such as azathioprine and 6-mercaptopurine (6-MP). Corticosteroids and immunomodulators, often prescribed for those suffering from the most severe symptoms, are often accompanied by side effects such as weight gain, acne, increased growth of facial hair, hypertension, mood swings, complications including pancreatitis and hepatitis, a reduced white blood cell count, and an increased risk of infection. In incidences that drug therapy fails to yield significant improvement, surgical removal of all or part of the ulcerated colon (proctocolectomy), is suggested. It is estimated that nearly 25 to upwards of 40% of colitis patients will need surgery sometime during the course of their lives (Razack *et al.*, 2007). Colitis sufferers are also at greater risk of developing colorectal cancer at some point in their lifetime (Razack *et al.*, 2007). Diet also plays a critical role in inflammatory bowel diseases because colitis has also been related to how fast pro-inflammatory agents (toxins, carcinogens,

oxidized forms of lipids, etc.) pass through the gastrointestinal tract. Thus, a fiber-rich diet will increase the transit time reducing the time of exposure of the gastrointestinal lumen to these pro-inflammatory agents reducing the contact time, exposure, and chances of an initial inflammatory insult that could drive the development of gastrointestinal disorders such as colitis (Razack *et al.*, 2007). A recent review concludes that nutrition plays a significant role in the pathogenesis and treatment of the two major forms of inflammatory bowel disease: Crohn's disease and ulcerative colitis (Razack *et al.*, 2007). In addition, patients with inflammatory bowel disease are often found to have nutrient deficiencies at the time of diagnosis, whereas other patients develop features of malnutrition over the course of their illness. Therefore, an understanding of the relationship between nutrients and inflammatory bowel disease is important if these patients are to receive optimal care. Epidemiologic and basic research has helped to shed light on the interaction between diet and the pathogenesis of inflammatory bowel disease. Numerous clinical trials utilizing various types of lipids, including fish oil and short chain fatty acids, suggest that fats play an important role in the inflammatory response that characterizes inflammatory bowel disease (Razack *et al.*, 2007). Vitamins and other micronutrients, including flavonoids, involved in nutrient metabolism and modulation of oxidative stress are important since they play a protective role in the prevention and treatment of nutrient deficiencies and in the amelioration of disease activity in individuals with inflammatory bowel disease (Razack *et al.*, 2007). For instance, it has been observed that hesperidin and diosmin have been evaluated in the acute stage of the trinitrobenzenesulfonic acid (TNBS) model of rat colitis. The results obtained demonstrated that pretreatment with diosmin (10 mg/kg) or hesperidin (10 and 25 mg/kg) reduced colonic damage compared to TNBS control rats. This effect was confirmed biochemically by a reduction in colonic

myeloperoxidase activity compared to non-treated colitic animals. Colonic glutathione levels in colitic animals were significantly increased after hesperidin or diosmin treatment. Diosmin decreased colonic MDA production and inhibited LTB₄ synthesis, whereas hesperidin failed to do so. Conversely, only hesperidin improved colonic fluid absorption, which was impaired in colitic animals. In conclusion, both diosmin and hesperidin were able to prevent colonic inflammation, acting via a mechanism in which protection against oxidative insult may play a role (Crespo *et al.*, 1999).

As mentioned above, nutrition plays an important role in the development of gastrointestinal disorders, which is a major health concern in Western countries including America and other developed countries where dietary habits are suboptimal. Obesity (Body Mass Index ≥ 30 kg/m²) has a high prevalence of 15-30% among European and American populations. The co-morbidity can be reduced substantially by a moderate weight loss of 5-15% (Mathus-Vliegen *et al.*, 2007). The main cause of obesity is an imbalance between energy intake and energy expenditure. Therefore, medical treatment starts with an energy restricted diet, a reduction in sedentary lifestyle, increased physical activity, and behavioral therapy to change eating habits. When necessary, this treatment can be followed by pharmacotherapy or surgery. Obesity is related to several health problems such as cardiovascular disease, diabetes, and recently has been involved with colitis even in neonates (Tan *et al.*, 2007). Obesity is biologically characterized at the cellular level by an increase in the number and size of adipocytes differentiated from fibroblastic pre-adipocytes in adipose tissue (Hsu *et al.*, 2006). Various xenobiotics and foods have demonstrated the capacity to inhibit formation of 3T3-L1 pre-adipocytes, as well as to make them undergo apoptosis. It has been reported that hesperidin, naringin, and naringenin inhibit the formation of 3T3-L1 pre-adipocytes by 11.1%, 5.6%, and

28.3% respectively. Apoptosis assays demonstrated that hesperidin, naringin, and naringenin increased apoptotic cells in time- and concentration-dependent manner. Treatment of cells with the three compounds also decreased the mitochondrial membrane potential a time and dose-dependant manner. The cell apoptosis/necrosis assay demonstrated that hesperidin, naringin, and naringenin increased the number of apoptotic cells, but not necrotic cells. Furthermore, each of these three flavanones treatment of cells caused a significant time- and concentration-dependent increase in the caspase-3 activity. Western blot analysis indicates that treatment of hesperidin, naringin, and naringenin also markedly down-regulated PARP and Bcl-2 proteins, and activated caspase-3, Bax, and Bak proteins. These results indicate that hesperidin efficiently inhibits cell population growth and induction of apoptosis in 3T3-L1 pre-adipocytes (Hsu *et al.*, 2006). Furthermore, in the same *in vitro* model hesperidin, naringin, and naringenin have recently been reported to inhibit intracellular triglyceride by $40.2 \pm 3.2\%$, $41.3 \pm 8.4\%$ and $39.4 \pm 7.8\%$ respectively, and also inhibit GPDH activity by $37.9 \pm 4.6\%$, $39.4 \pm 5.6\%$ and $35.7 \pm 1.4\%$ respectively (Hsu *et al.*, 2007).

A causal association between inflammation and cancer has long been suspected. Multiple lines of compelling evidence from clinical, epidemiologic and laboratory studies support that inflammation plays a critical role in the promotion and progression stages of carcinogenesis. Recent progress in our understanding of the molecular biology of cancer highlights the intracellular signal transduction network, including that involved in mediating the inflammatory response, which often functions abnormally during carcinogenesis. One of the key players in inflammatory signaling is cyclooxygenase-2 (COX-2). Aberrant upregulation of COX-2 is frequently observed in various precancerous and malignant tissues (Surh *et al.*, 2007). Pro-inflammatory stimuli trigger the activation of an intracellular signal transduction

network comprising proline-directed serine/threonine kinases, and their downstream transcription factors, resulting in an inappropriate induction of COX-2 (Surh *et al.*, 2007). Therefore, the normalization of inappropriately overamplified signaling cascades implicated in chronic inflammation-associated carcinogenesis by use of COX-2 specific inhibitors has been recognized as a rational and pragmatic strategy in molecular target-based cancer prevention (Surh *et al.*, 2007). One of the critical stages in cancer development is angiogenesis, or generation of new blood vessels from pre-existing vessels. Angiogenesis is an integral part of many physiological or pathological processes, including tumor growth. Physiological angiogenesis is a complex process controlled by different pro-angiogenic as well as anti-angiogenic factors. For angiogenic induction, the balance between these pro- and anti-angiogenic factors in the microenvironment has to shift in favor of proangiogenic factors, either by upregulation of these pro-angiogenic factors or by downregulation of angiogenic inhibitors (Voronov *et al.*, 2007). Proinflammatory cytokines, such as IL-1 and TNF α , were found to be major proangiogenic stimuli of both physiological and pathological angiogenesis. The IL-1 family consists of pleiotropic proinflammatory and immunoregulatory cytokines, namely, IL-1 α and IL-1 β , and one antagonistic protein, the IL-1 receptor antagonist (IL-1R α), which binds to IL-1 receptors without transmitting an activation signal and represents a physiological inhibitor of preformed IL-1. It has also been reported that an important role for microenvironment IL-1 in tumor angiogenesis is mainly IL-1 β (Voronov *et al.*, 2007). Thus, numerous experiments have been conducted over the last decade to determine the anti-cancer potential of flavanone compounds. For instance, hesperidin (100 μ M) has been reported to reduce cell viability $65 \pm 0.05\%$ of human colon cancer cells, SNU-C4 based in 3-(4,5-dimethylthiazol-2-yl)-2,5-diphenyltetrazolium bromide (MTT) assay (Park *et al.*, 2007). It was

proposed that hesperidin treatment decreased the expression of B-cell CLL/lymphoma 2 (BCL2) mRNA, and increased the expression of BCL2-associated X protein (BAX) and of the apoptotic factor caspase3 (CASP3) inducing apoptosis (Park *et al.*, 2007). Another study, less mechanistic in nature, observed that hesperidin and hesperetin at smaller concentrations (1 μ M) inhibit the neoplastic transformation of C3H 10T1/2 murine fibroblasts induced by the carcinogen 3-methylcholanthrene (Franke *et al.*, 1998). In the case of hesperetin, it has been reported to affect the proliferation and growth of a human breast carcinoma cell line, MDA-MB-435 with an IC_{50} of 22.5 μ g/ml and to exhibit low cytotoxicity (> 500 μ g/ml for 50% cell death) (So *et al.*, 1996). Furthermore, hesperetin has also been reported to significantly inhibit cell proliferation of MCF-7 cells in a concentration-dependent manner by causing cell cycle arrest in the G1 phase. In the G1-phase related proteins, hesperetin downregulates the cyclin-dependent kinases (CDKs) and cyclins, while upregulating p21(Cip1) and p27(Kip1) in MCF-7 cells. Hesperetin also decreases CDK2 and CDK4 together with cyclin D. In addition, hesperetin increases the binding of CDK4 with p21(Cip1) but not p27(Kip1) or p57(Kip2), indicating that the regulation of CDK4 and p21(Cip1) may participate in the anti-cancer activity pathway of hesperetin in MCF-7 cells (Choi, 2007).

Naringin and naringenin have been reported to have anti-cancer activities (Kanno *et al.*, 2006a; Kanno *et al.*, 2005; Kanno *et al.*, 2006b; So *et al.*, 1996; van Meeuwen *et al.*, 2007). For instance, naringenin has been reported to induce cytotoxicity in cell lines derived from cancer of the breast (MCF-7, MDA-MB-231), stomach (KATOIII, MKN-7), liver (HepG2, Hep3B, and Huh7), cervix (Hela, Hela-TG), pancreas (PK-1), and colon (Caco-2) as well as leukemia (HL-60, NALM-6, Jurkat, and U937). Naringenin-induced cytotoxicity was low in Caco-2 and high in leukemia cells compared to other cell lines. Naringenin dose-dependently induced

apoptosis, with hypodiploid cells detected in both Caco-2 and HL-60 by flow cytometric analysis (Kanno *et al.*, 2005). Furthermore, naringenin at concentrations higher than 0.71 mM has been reported to inhibit cell proliferation of HT29 colon cancer cells (Frydoonfar *et al.*, 2003). While, naringin has been reported to induce cytotoxicity via apoptosis in mouse leukemia P388 cells, and to slightly increase the activities of anti-oxidant enzymes, catalase and glutathione peroxidase in these cells (Kanno *et al.*, 2004).

Naringin and naringenin have also been assessed for its effects on proliferation and growth of a human breast carcinoma cell line, MDA-MB-435. The concentration at which cell proliferation was inhibited by 50% (IC₅₀) was around 20 µg/ml for naringin and naringenin with low cytotoxicity (> 500 µg/ml for 50% cell death) (So *et al.*, 1996). It has been proposed two possible mechanisms that could modulate breast tumor growth, one via inhibition of aromatase (CYP19), and via interaction with the estrogen receptor (ER). Multiple *in vitro* studies confirmed that naringin and naringenin act as aromatase inhibitors potentially reducing tumor growth. It is thought that in the *in vivo* situation breast epithelial (tumor) cells communicate with surrounding connective tissue by means of cytokines, prostaglandins and estradiol forming a complex feedback mechanism. It has been reported that naringenin affect MCF-7 proliferation with an EC₅₀ value of 287 nM, and act as an aromatase inhibitor with an IC₅₀ value of 2.2 µM. These results show that naringenin can induce cell proliferation or inhibit aromatase in the same concentration range (1-10 µM) (van Meeuwen *et al.*, 2007). The second proposed mechanism is related with the estrogen receptor (ER), and it has been observed that naringenin exerts an anti-proliferative effect only in the presence of ER α or ER β . Moreover, naringenin stimulation induces the activation of p38/MAPK leading to the pro-apoptotic caspase-3 activation and to the poly(ADP-ribose) polymerase cleavage in all cancer cell lines

considered. Notably, naringenin shows an anti-estrogenic effect only in ER α containing cells; whereas in ER β containing cells, naringenin mimics the 17 β -estradiol effects. (Totta *et al.*, 2004). Nevertheless, naringenin mediated growth-arrest in MCF-7 breast cancer cells has been observed. Naringenin was found to inhibit the activity of phosphoinositide 3-kinase (PI3K), a key regulator of insulin-induced GLUT4 translocation, as shown by impaired phosphorylation of the downstream signaling molecule Akt. Naringenin also inhibited the phosphorylation of p44/p42 mitogen-activated protein kinase (MAPK). Inhibition of the MAPK pathway with PD98059, a MAPK kinase inhibitor, reduced insulin-stimulated glucose uptake by approximately 60%. The MAPK pathway therefore appears to contribute significantly to insulin-stimulated glucose uptake in breast cancer cells (Harmon *et al.*, 2004).

In the case of human prostate cancer cells (PC3) stably transfected with activator protein 1 (AP-1) luciferase reporter gene, the maximum AP-1 luciferase induction is of about 3 fold over control after treatment with naringenin (20 μ M). At higher concentrations, naringenin demonstrated inhibition of AP-1 activity. The MTS assay for cell viability at 24 h demonstrated that even at a very high concentration (500 μ M), cell death was minimal for naringenin. Furthermore, induction of phospho-JNK and phospho-ERK activity was observed after two hour incubation of PC3-AP1 cells with naringenin. However no induction of phospho-p38 activity was observed. Furthermore, pretreating the cells with specific inhibitors of JNK reduced the AP-1 luciferase activity that was induced by naringenin while pretreatment with MEK inhibitor did not affect the AP-1 luciferase activity (Gopalakrishnan *et al.*, 2006). It was also observed that naringenin induced apoptosis of human promyeloleukemia HL-60 cells by markedly promoting the activation of caspase-3, and slightly promoting the activation of caspase-9, but with no observed on caspase-8 (Kanno *et al.*, 2006b). The apoptosis-induced

mechanism of naringenin has also been linked with the activation of NF- κ B and the degradation of I κ B α , which has been observed in human promyeloleukemia HL-60 cells (Kanno *et al.*, 2006b), in human colon carcinoma HCT116 cells, and in human liver carcinoma HepG2 cells (Katula *et al.*, 2005). Neoangiogenesis is required for tumor development and progression. Many solid tumors induce vascular proliferation by production of angiogenic factors, prominently vascular endothelial growth factor (VEGF). It has been reported that naringenin has a significant inhibitory activity against VEGF at 0.1 μ M in MDA human breast cancer cells, and that glioma cells were similarly sensitive, with U343 more than U118. Inhibition of VEGF release by naringenin in these models of neoplastic cells suggests a novel mechanism for mammary cancer prevention (Schindler *et al.*, 2006).

Eriodictyol extracted from lemon fruit (*Citrus limon* BURM. f.) was shown to alter the function of DNA fragmentation in HL-60 cells when analyzed by flow cytometry. An apoptotic DNA ladder and chromatin condensation were observed in HL-60 cells when treated with eriodictyol (Ogata *et al.*, 2000). Eriodictyol also was assessed for its protective role against UV-induced apoptosis of human keratinocytes, the principal cell type of epidermis. The results indicated that eriodictyol had a positive effect on cell proliferation of human HaCaT keratinocytes. Treatment with eriodictyol in particular resulted in significant suppression of cell death induced by ultraviolet (UV) light, a major skin-damaging agent. Eriodictyol treatment apparently reduced the percentage of apoptotic cells and the cleavage of poly(ADP-ribose) polymerase, concomitant with the repression of caspase-3 activation and reactive oxygen species (ROS) generation. The anti-apoptotic and anti-oxidant effects of eriodictyol were also confirmed in UV-induced cell death of normal human epidermal keratinocyte (NHEK) cells (Lee *et al.*, 2007). Eriodictyol also protected L-929 cells from TNF-induced cell

death. The magnitude of protection and potentiation by eriodictyol was concentration-dependent and these effects were not altered when eriodictyol was added as much as 2 h after TNF treatment (Habtemariam, 1997). Eriodictyol possess anti-proliferative activities against several tumor and normal human cell lines. Eriodictyol has IC₅₀ of 12, 10, 8.3, and 6.2 μ M in human lung carcinoma (A549), melanin pigment producing mouse melanoma (B16 melanoma 4A5), human T-cell leukemia (CCRF-HSB-2), and metastasized lymph node (TGBC11TKB) respectively (Kawaii *et al.*, 1999a). No studies have examined the anti-cancer activity of the enantiomers of flavanones and no studies systematically studied the glycoside and aglycone forms of these flavanones for their anti-cancer activity.

As described above, flavanones have different positive pharmacological activities for human health and it has been reported that their anti-oxidant capacity is the one that confer them with their therapeutic potential in cardiovascular diseases, gastric or duodenal ulcers, cancer or hepatic pathologies. Also important are the antiviral and anti-allergic actions of flavanones, as well as their anti-thrombotic and anti-inflammatory properties (Gonzalez-Gallego *et al.*, 2007). Therefore, it is important to characterize their anti-oxidant capacity of the selected flavanones. For instance, hesperidin and its aglycone, hesperetin have been assessed in different *in vitro* chemical anti-oxidant models (cell-free bioassay systems). It has been observed that both hesperidin and hesperetin exhibited similar patterns of 1,1-diphenyl-2-picrylhydrazyl (DPPH) radical scavenging activities (Cho, 2006). Similar results have been reported elsewhere for hesperidin anti-oxidant capacity in similar efficacy of Trolox® (positive control) (Wilmsen *et al.*, 2005). Furthermore, hesperetin alone has been reported to effectively scavenge peroxynitrite (ONOO⁻) in a concentration-dependant manner. Peroxynitrite (ONOO⁻) is a reactive oxidant formed from superoxide (*O₂⁻) and nitric oxide (*NO), that can oxidize

several cellular components, including essential protein, non-protein thiols, DNA, low-density lipoproteins (LDL), and membrane phospholipids (Kim *et al.*, 2004). Different *in vitro* chemical and biological assays have reported that naringin and naringenin have considerable anti-oxidant properties. For instance, naringin has been reported to concentration-dependently scavenge the 1,1-diphenyl-2-picrylhydrazyl (DPPH), 2,2'-azinobis-(3-ethyl-benzothiazoline-6-sulfonic acid) (ABTS) and nitric oxide (NO) radicals *in vitro* (Rajadurai *et al.*, 2007a). Furthermore, naringin and naringenin have been assessed in the beta-carotene-linoleic acid, 1,1-diphenyl-2-picryl hydrazyl (DPPH), superoxide, and hamster low-density lipoprotein (LDL) *in vitro* models to measure their anti-oxidant activity. Using the beta-carotene-linoleate model, naringin (10 μ M) and naringenin (10 μ M) exhibited an 8% and 9% inhibition respectively. Whereas, both compounds demonstrated negative free radical scavenging activity using the DPPH method, and a 25% and 30% inhibition of superoxide radicals for naringin and naringenin respectively. Naringin and naringenin increased the lag time of LDL oxidation to 150 min (a 32% increase from baseline levels). Thus, indicating that both compounds have significant *in vitro* anti-oxidant properties (Yu *et al.*, 2005). Furthermore, naringin has been reported to have a positive effect in iron-induced oxidative stress and in a variety of cellular processes like respiration and DNA synthesis. For this, HepG2 cells were treated with 0.5, 1, 2.5, and 5 mM naringin 1 h before exposure to 0.1, 0.25, 0.5, and 1 mM ferric iron. Pretreatment of HepG2 cells with naringin resulted in inhibition of lipid peroxidation, arrested the iron-induced depletion in the GSH concentration, and increased various antioxidant enzymes like glutathione peroxidase (GSHPx), catalase, and superoxide dismutase (SOD) (Jagetia *et al.*, 2004). Similarly, eriocitrin and eriodictyol isolated from lemon (*Citrus limon*) juice exhibited a potent radical scavenging activity for 1,1-diphenyl-2-picrylhydrazyl (DPPH)

and superoxide. Eriocitrin and eriodictyol were found to significantly suppress the expression of intercellular adhesion molecule-1 (ICAM-1) at 10 μ M in human umbilical vein endothelial cells (HUVECs) induced by necrosis factor-alpha (TNF-alpha) (Miyake *et al.*, 2007). Also eriocitrin obtained from peppermint leaves (*Menthae x piperitae folium*) (total eriocitrin 38%) exhibited a strong antiradical activity (determined as DPPH* scavenging features). It also exhibited a strong anti-H₂O₂ activity (Sroka *et al.*, 2005). Similarly eriocitrin extracted from different *Mentha* species, varieties, hybrids, and cultivars was identified as the dominant radical scavengers in these extracts in an on-line high-performance liquid chromatography-1,1-diphenyl-2-picrylhydrazyl (HPLC-DPPH*) method (Kosar *et al.*, 2004).

This chapter describes the *in vitro* anti-inflammatory properties, cyclooxygenase-1 and 2 inhibitory activities, inflammatory bowel disease activity, anti-adipogenic activity, anti-cancer activity, and anti-oxidant capacity of racemic hesperidin, hesperetin, naringin, naringenin, eriocitrin, and eriodictyol. The anti-inflammatory properties were assessed using an osteoarthritis model using canine chondrocytes after inflammatory insult using interleukin-1beta (IL-1 β) and measuring different inflammatory mediators produced in cell culture medium. The cyclooxygenase-1 and -2 inhibitory activities was measured employing a commercially available ELISA kit. The inflammatory bowel activity was measured using a colitis model in colon adenocarcinoma (HT-29) cells after inflammatory insult with tumor necrosis alpha (TNF- α) and measuring prostaglandin E₂ (PGE₂) levels. The anti-adipogenic activity was assessed using 3T3-L1 pre-adipocytes and staining them for their production of fat droplets. The anti-cancer activity was performed in selected cancer cell lines, and the Alamar blue assay was employed to quantify viable cancer cells present following flavanone treatment. Finally, a comprehensive anti-oxidant method was developed to account for the lipophilic,

hydrophilic, glycoside and aglycone fractions of apple samples and of the selected flavanones. Where applicable, the IC₅₀ values of hesperidin, hesperetin, naringin, naringenin, eriocitrin, and eriodictyol in the different *in vitro* models were modeled using WinNonlin[®] pharmacodynamic software.

4.3 METHODS

4.3.1 Anti-Inflammatory Properties

4.3.1.1 Chemicals and Reagents

Racemic hesperidin, hesperetin, naringin, and naringenin were purchased from Sigma Chemicals (St. Louis, MO, USA). Racemic eriocitrin and eriodictyol were purchased from Indofine Chemical Company (Hillsborough, NJ, USA). Canine chondrocytes (CnC) were purchased from Cell Applications, Inc. (San Diego, CA). Trypsin-ethyl diamine tetraacetic acid (EDTA), phosphate-buffered saline (PBS), trypan blue, dithiothreitol (DTT), resazurin, sodium bicarbonate, penicillin-streptomycin, and Dulbecco's modified Eagle's medium/nutrient mixture F-12 Ham (DMEM/F-12) without phenol red, and interleukin-1 β human recombinant expressed in *Escherichia coli* were purchased from Sigma (St. Louis, MO, USA). Fetal bovine serum (FBS) was purchased from Equitech-Bio Inc. (Kerrville, TX).

The nitric oxide (NO) quantitation kit was purchased from Active Motif (Carlsbad CA), the prostaglandin E₂ (PGE₂) ELISA kit was purchased from Amersham Biosciences Corp. (Piscataway, NJ), the sulphated glycosaminoglycans (sGAG) assay kit was purchased from Kamiya Biomedical Company (Seattle, WA), the matrix metalloproteinase-3 (MMP-3) ELISA kit was purchased from RayBiotech Inc. (Norcross, GA), tumor necrosis factor- α (TNF- α) ELISA kit, and anti-oxidant assay kit were purchased from Cayman Chemical Company (Ann Arbor, MI).

4.3.1.2 Cell Culture

The cell line employed in this series of experiments was canine chondrocytes (CnC). This cell line was purchased from Cell Applications, Inc. (San Diego, CA) and was maintained in DMEM/F-12 without phenol red supplemented with 20% heat-inactivated fetal bovine serum (FBS), and penicillin-streptomycin (10mg/L). It was incubated at 37°C in a 5% CO₂ atmosphere.

4.3.1.3 Cell Subculture and Cell Number

Thirty minutes prior to subculturing the cell line, media, phosphate buffered saline (PBS), and a trypsin-ethyl diamine tetetic acid (EDTA) solution comprised of 0.5% trypsin, 0.2% EDTA / 0.9% NaCl diluted in PBS to prepare a 10% working solution were placed in a 37°C water bath. Next, the cell flask was removed from the 5% CO₂ incubator and cells were observed under the light microscope to determine the percent confluence and their general health. The desired percentage of confluence was 85-95%. After confluence was determined, media was aspirated and cells were washed with 5 ml PBS. PBS was aspirated and 2 ml of the trypsin-EDTA working solution was added and the flask was placed in the 5% CO₂ incubator (37°C) for 5 minutes. The flask was then removed from the incubator and gently tapped three times to complete the detachment of cells from the flask. Detached cells were transferred to a 15 ml conical tube containing 8 ml PBS. The conical tube was then centrifuged at 700 rpm for 5 minutes. Following centrifugation, the conical tube was removed and the PBS was aspirated, leaving the cell pellet undisturbed. Cells were resuspended in 6 ml fresh media and 10 µl was removed and diluted with 30 µl of trypan blue. The cell-trypan blue solution was added to a hemacytometer and the number of live cells was counted using a cell counter. The number of

dead cells was also recorded. If it was determined that the number of dead cells surpassed 10% of the total population of healthy cells, the cell line was excluded from future experiments and a new generation of the cell line was thawed.

The total number of cells present in the flask was determined using the following equation:

$$\text{Cells/ml} = (\# \text{ cells}/4) (\text{dilution}) (1 \times 10^4) \quad (\text{Equation 1})$$

Depending on the observed cell number and the desired cell seeding number, the cells and fresh media are added in determined volumes, to a fresh 25 cm² flask. The flask was then placed into 5% CO₂ incubator (37°C). Cell subculture was performed 1-2 times per week depending on the growth rate of the cell line and observed confluence.

The optimal cell seeding numbers for each cell line was determined by preliminary cell seeding number experiments. Cells were seeded in numbers 1 x 10⁴, 2 x 10⁴, 3 x 10⁴ and so on until the final cell seeding number 1 x 10⁵ per well in a 96 well plate (Costar 3595). Cell plates were incubated at 37°C in a 5% CO₂ atmosphere for 72 hours. Following incubation, medium was aspirated and a 10% Alamar blue (resazurin) fluorescent dye solution was diluted in fresh medium and was added to cells. The cell plates were incubated at 37°C in a 5% CO₂ atmosphere for 3 hours. The cell plates were removed from the incubator and were placed at room temperature in a drawer to protect from light for 15 minutes. Next, the cell plates were placed into the Cytofluor[®] 4000 fluorescence multi-well plate reader (Applied Biosystems, USA). Fluorescence was read at an excitation of 485 nm and an emission of 530 nm. Standard curves of cell seeding number and fluorescence were generated. The optimal cell seeding number to be used in this series of experiments was chosen from the linear portion of the

generated standard curve. It was determined that the optimal cell seeding number for canine chondrocytes (CnC) was 5000 cells/well.

4.3.1.4 Anti-Inflammatory Model

The employed model was adapted from previously described methodology (Ahmed *et al.*, 2002) with some modifications. For our model, canine chondrocytes (CnC) were counted and seeded on 96 well plates. The seeded cells were incubated at 37°C in a 5% CO₂ atmosphere for 24 hours.

Racemic hesperidin, hesperetin, naringin, naringenin eriocitrin and eriodictyol were dissolved in DMSO the day of the experiment and were diluted in medium to yield concentrations of 1, 10, 50, 100, and 250 µg/ml. We decided to use a broad concentration range based on previous studies that reported observed pharmacological activity in similar inflammatory mediators using 1-200 µg/ml of different plant extracts and bioactive compounds in human and bovine chondrocytes (Ahmed *et al.*, 2002; Blanco *et al.*, 1995; Garbacki *et al.*, 2002; Mbvundula *et al.*, 2005; Panico *et al.*, 2005). Following aspiration of the medium, cells were treated with 100 µl of interleukin-1β (IL-1 β) (10 ng/ml), the plates were incubated at 37°C in a 5% CO₂ atmosphere for 2 hours. Following incubation, cells were treated with 200 µl flavanone solutions. Additional cells were treated with either DMSO diluted in medium or medium only. Treated and control cells were incubated at 37°C in a 5% CO₂ atmosphere for 72 hours as reported previously (Stadler *et al.*, 1991). After cell plates were removed from the incubator, medium was collected and stored at -80°C until further analysis.

4.3.1.5 Cell Viability

Alamar Blue (resazurin) fluorescent dye is an easy and accurate assay that has recently gained popularity in determining the cytotoxicity of many cell lines (O'Brien *et al.*, 2000). The

resazurin non-fluorescent compound is metabolized into the fluorescent compound resorufin by viable cells. This emission of fluorescence can be quantified using a cell plate reader and the number of viable cells following treatment can be determined. Cells were counted and seeded on 96 well plates. After the collection of the medium as described in the previous section, the medium was replaced with 10% Alamar blue (resazurin) fluorescent dye diluted in fresh medium. Cell plates were incubated at 37°C in a 5% CO₂ atmosphere for an additional 3 hours. Following incubation, cell plates were placed in a darkened environment for 30 minutes at room temperature. Next, the cell plates were placed into the Cytoflour®4000 fluorescence multi-well plate reader (Applied Biosystems, USA). Fluorescence was read at an excitation of 485nm and an emission of 530nm. The viable cell number (as a percent of control) in each cell line exposed to varying concentrations of the flavanones measured.

4.3.1.6 Relevance of the Selected Inflammatory Mediators in the *In Vitro* Model of Osteoarthritis

Osteoarthritis (OA) is a progressive degenerative joint disease that afflicts various humans and various animal species. OA causes an irreversible cycle of degradation, and inflammation accompanied by histological, clinical, biochemical, and biomechanical changes in the articular cartilage and supporting tissues that can lead to joint swelling, stiffness, dysfunction, and signs of algesia (Kuroki *et al.*, 2002). This degenerative process can be summarized by a simultaneous presence of degenerative, oxidative, and inflammatory mechanisms that causes an imbalance between the destructive and reparative processes of articular cartilage. Different inflammatory mediators are involved in the development and progression of OA, among them are the destructive effect of free radicals such as nitric oxide (NO); inflammatory cytokines such as interleukin-6 (IL-6) and tumor necrosis factor- α (TNF-

α); metalloproteinases (MMP) (Cipolletta *et al.*, 1998; Moulton, 1996); and COX-2 dependent prostaglandin E₂ (PGE₂) (Hardy *et al.*, 2002). It has also been shown that cytokines such as interleukin-1 β (IL-1 β) interfere in the extracellular matrix turnover inducing chondrocytes apoptosis, degradation of cartilage matrix (Panico *et al.*, 2005), and enhancing proteases production (Cawston, 1998). Interleukin-1 β (IL-1 β) induces the production of nitric oxide (NO) from L-arginine oxidation by inducible nitric oxide synthase (iNOS or NOS-II) (Amin *et al.*, 1998). The produced NO can rapidly react with strong oxidants such as superoxide anions, hydroxide peroxide, and hydroxyl radicals (Moncada *et al.*, 1991; Nadaud *et al.*, 1995; Panico *et al.*, 2005). Furthermore, excess NO production could be involved in the pathogenesis of osteoarthritis and that NO derived from iNOS has been related with tissue injury in different pathological conditions (Amin *et al.*, 1998; Goggs *et al.*, 2003). IL-1 β also promotes prostaglandin synthesis, bone resorption, matrix metalloproteinase synthesis (Fenton *et al.*, 2002; Morris *et al.*, 1990; Tetlow *et al.*, 2001), and inhibits the concentration of MMP inhibitors (TIMP) in arthritic joints (Goldring *et al.*, 1994). NO also stimulates the chondrocytes to produce proenzymes that are converted into active enzymes (extracellular activation) such as MMP. MMP-3 is the major metalloproteinase in cartilaginous tissue that can induce the cleavage of collagen and proteoglycans causing matrix degradation (Dean *et al.*, 1989).

Nevertheless, elevated levels of IL-1 β have been reported in synovial fluid of arthritic patients supporting its involvement in the pathogenesis of these arthropaties. *In vitro* studies have shown that IL-1 β inhibits proteoglycan and type-II collagen production, inhibits chondrocytes proliferation, and when injected into an animal synovial joints induces loss of cartilage proteoglycan and synovial fluid leukocytosis (Blanco *et al.*, 1995; Hunter, 2000; van

de Loo *et al.*, 1990; van de Loo *et al.*, 1995). It has also reported that chondrocytes isolated from arthritic joints express high amounts of IL-1 receptor (IL-1r), which would make them more susceptible to the inflammatory action of this cytokine. For these reasons, IL-1 β is considered one of the most potent catabolic factors in a variety of arthropaties (Manfield *et al.*, 1996; van der Kraan *et al.*, 2000).

PGE₂ production is intensified during an inflammation insult contributing to the synovial inflammation by increasing local blood flow and by enhancing the action of mediators such as bradykinin that induced vasopermeability (Panico *et al.*, 2005). Moreover, PGE₂ has also been shown to upregulate IL-1 β and inhibit chondrocytes growth (Manfield *et al.*, 1996). Tumor necrosis factor- α (TNF- α) has also been found at elevated concentrations in inflammatory flare-ups inhibiting matrix synthesis and accelerating matrix degradation. Tumor necrosis factor- α (TNF- α) has also been shown to stimulate the synthesis of hydrogen peroxide and nitric oxide in chondrocytes (Garbacki *et al.*, 2002; Stadler *et al.*, 1991). Other cytokines such as interleukin-6 (IL-6), oncostatin M (OSM), and IL-17 have also been shown to induce cartilage breakdown, while protective effects have been observed by IL-4, IL-13, transforming growth factor-1 (TGF- β 1), and insulin-like growth factor-1 (IGF-1) (Cawston *et al.*, 1996; Mbvundula *et al.*, 2005).

There is a current interest in studying novel anti-inflammatory and chondroprotective agents from natural and commercial sources for the treatment of arthropaties in a multitude of inflammatory and autoimmune diseases. The strong anti-oxidant capacities of the selected flavanones may also be effective in the pharmacotherapy of chronic arthropaties. This chondrocyte model may be very useful to reproduce the pathogenesis of cartilage damage

during an inflammatory insult and to determine the effect on the different key biomarkers involved in the arthritic process.

4.3.1.7 Nitric Oxide Determination

The nitric oxide quantitation kit was purchased from Active Motif (Carlsbad, CA), and it allows for a simple and very sensitive assay to monitor nitric oxide production based on the quantitation of nitrate and nitrite levels. This is a two-step assay method that includes the addition of two cofactors to the nitrate reductase reaction. These cofactors accelerate the conversion of nitrate to nitrite while simultaneously degrading excess NADPH to NADP. Thus, the reductase reaction can be completed within 30 minutes and colorimetric determination can be directly measured by the addition of Griess reagent, without the need for lactate dehydrogenase treatment as customary in most of the other commercially available kits. For more information please refer to the instruction in the kit (Nitric Oxide Quantitation Kit from Active Motif - cat. No. 40020).

4.3.1.8 Prostaglandin E₂ Determination

The prostaglandin E₂ (PGE₂) ELISA kit was purchased from Amersham Biosciences Corp. (Piscataway, NJ), it utilizes novel lysis reagents to facilitate the rapid and efficient extraction of PGE₂ from samples obviating the need for removal of extracting reagents providing a faster read-out at 450 nm. For more information please refer to the instruction in the kit (Prostaglandin E₂ Biotrak Enzymeimmunoassay (EIA) System from Amersham Biosciences - cat. No. RPM222).

4.3.1.9 Sulphated Glycosaminoglycan Determination

The sulphated glycosaminoglycans (sGAG) assay kit was purchased from Kamiya Biomedical Company (Seattle, WA); it takes advantage of the high negative charge of GAGs. This assay utilizes the dye Alcian blue, a tetravalent cation with hydrophobic core allows the dye to bind to the negatively charged polymers such as GAGs at high ionic strength allowing the colorimetric measurement (595 nm) of this stable polymer. For more information please refer to the instruction in the kit (Sulphated Glycosaminoglycans Assay Kit from Kamiya Biomedical Company - cat. No. BP-004).

4.3.1.10 Matrix Metalloproteinase-3 Determination

The matrix metalloproteinase-3 (MMP-3) ELISA kit was purchased from RayBiotech Inc. (Norcross, GA), a simple ELISA assay that employs an antibody specific for human MMP-3 coated on a 96-well plate. For more information please refer to the instruction in the kit (RayBio® Human MMP-3 ELISA kit from Ray Biotech, Inc. - cat. No. ELH-MMP3-001).

4.3.1.11 Tumor Necrosis Factor- α Determination

The Tumor Necrosis Factor- α (TNF- α) ELISA kit was purchased from Cayman Chemical Company (Ann Arbor, MI). This assay is based on a double-antibody “sandwich” technique. Each well has been coated with a monoclonal antibody specific for TNF- α (TNF- α capture antibody) that binds to any TNF- α introduced into the well. An acetylcholinesterase:Fab’ Conjugate (AChE:Fab’) is also added to the well, this binds selectively to a different epitope of the TNF- α molecule. These two antibodies form a “sandwich” by binding on opposite sides of the TNF- α molecule. The concentration of TNF- α can be determined by measuring the enzymatic activity of the AChE through the addition of Ellman’s reagent that produces a yellow-colored product that can be measured

spectrophotometrically (412 nm). For more information please refer to the instruction in the kit (Tumor Necrosis Factor- α (human) EIA assay kit from Cayman Chemical - cat. No. 589201).

4.3.1.12 Statistical Analysis

All experiments were minimally repeated in duplicate. All data are expressed as the mean \pm the standard error of the mean (SEM). Comparisons among the control and treatment groups were made using General Linear Model (GLM) ANOVA with Newman-Keuls multiple comparison test using NCSS Statistical and Power Analysis software (NCSS, Kaysville, UT). With all analyses a $P < 0.05$ was considered significant.

4.3.2 Cyclooxygenase-1 and -2 (COX-1 and COX-2) Inhibitory Activity

4.3.2.1 Description of the Assay

Cyclooxygenase (COX, also called Prostaglandin H Synthase or PGHS) enzymes contain both cyclooxygenase and peroxidase activities. COX catalyzes the first step in the biosynthesis of prostaglandins (PGs), thromboxanes, and prostacyclins; the conversion of arachidonic acid to PGH₂. It is now well established that there are two distinct isoforms of COX. Cyclooxygenase-1 (COX-1) is constitutively expressed in variety of cell types and is involved in normal cellular homeostasis. A variety of mitogenic stimuli such as phorbol esters, lipopolysaccharides, and cytokines lead to the induced expression of a second isoform of COX, cyclooxygenase-2 (COX-2). COX-2 is responsible for the biosynthesis of PGs under acute inflammatory conditions (Xie *et al.*, 1991). This inducible COX-2 is believed to be the target enzyme for the anti-inflammatory activity of nonsteroidal anti-inflammatory drugs. The COX Inhibitor Screening Assay directly measures PGF_{2 α} produced by SnCl₂ reduction of COX-derived PGH₂. The prostanoid product is quantified via enzyme immunoassay (EIA) using a broadly specific antibody that binds to all the major prostaglandin compounds. Thus, the Cayman COX assay is more accurate and reliable than an assay based on peroxidase inhibition. The Cayman COX Inhibitor Screening Assay includes both ovine COX-1 and human

recombinant COX-2 enzymes in order to screen isozyme-specific inhibitors. This assay is an excellent tool which can be used for general inhibitor screening, or to eliminate false positive leads generated by less specific methods.

4.3.2.2 COX Inhibitory Screening

4.3.2.2.1 Pre-Assay Preparation

The assay requires the preparation of different reagents and buffers such as: reaction buffer, EIA buffer, wash buffer, arachidonic acid, hydrochloric acid, stannous chloride, prostaglandin standard, prostaglandin screening AchE tracer, and prostaglandin screening antiserum. While, some reagents are ready to use such as: the enzymes COX-1 (ovine), and COX-2 (human recombinant), and heme. For more information and details about the preparation of reagents please refer to the instruction in the kit (COX inhibitor screening Assay Kit from Cayman Chemical - cat. No. 560131).

4.3.2.2.2 COX Reactions

To run the test, different COX reactions need to be performed.

- a. **Background tubes** – Inactivate COX-1 and COX-2 by transferring 20 μ l of each enzyme and placing it in boiling water for 3 minutes. The inactivated enzymes will be used to generate the background values. Then, 970 μ l of reaction buffer, 10 μ l of heme, and 10 μ l of inactive COX-1 or COX-2 are mixed.
- b. **COX-1 100% Initial Activity tubes** – Add 950 μ l of reaction buffer, 10 μ l of heme, and 10 μ l of COX-1 (performed in duplicates).
- c. **COX-1 Samples** – Add 950 μ l of reaction buffer, 10 μ l of heme, and 10 μ l of sample (performed in 6 replicates).

- d. **COX-2 100% Initial Activity tubes** – Add 950 μ l of reaction buffer, 10 μ l of heme, and 10 μ l of COX-1 (performed in duplicates).
- e. **COX-2 Samples** – Add 950 μ l of reaction buffer, 10 μ l of heme, and 10 μ l of sample (performed in 6 replicates).
- f. Add 20 μ l of inhibitor to the COX-1 and -2 inhibitor tubes and 20 μ l of the reaction buffer to the 100% initial activity tubes.
- g. Incubate for 10 minutes at 37°C.
- h. Initiate the reaction by adding 10 μ l of arachidonic acid to all the test tubes. Vortex and incubate for another 2 minutes at 37°C.
- i. Add 50 μ l of 1M HCl to each tube to stop enzyme catalysis.
- j. Add 100 μ l of the saturated stannous chloride solution to each test tube and vortex.
- k. Incubate for 5 minutes at room temperature. The reaction mixture should be cloudy.

4.3.2.2.3 Performing the Assay

To perform the assay, 96-well plates should be employed in which each standard, control, and sample should be run at least in duplicate. The plating is as follows:

- a. **Blank** – Leave empty the corresponding wells.
- b. **EIA Buffer** – Add 100 μ l of EIA buffer to the non-specific binding (NSB) wells. Add 50 μ l of EIA buffer to the maximum binding (B_0) wells.
- c. **Prostaglandin Standard** – Perform 2-fold successive dilutions of the stock solution and add 50 μ l of each dilution to the corresponding wells.
- d. **Background, COX 100% Initial Activity, and COX Samples** – Add 50 μ l of the each sample to the corresponding wells.

- e. **Prostaglandin Screening AChE Tracer** – Add 50 μ l of the tracer to each well except the initial activity and the blank wells.
- f. **Prostaglandin Screening Antiserum** - Add 50 μ l of the tracer to each well except the initial activity, non-specific binding, and the blank wells.

4.3.2.2.4 Plate Incubation, Developing and Reading

Cover the plate with plastic film and incubate for 18 hours at room temperature. To develop, add 200 μ l Ellman's Reagent to each well, and add 5 μ l to the initial activity wells. Cover the plates with plastic film, wrap in aluminum foil, place on an orbital shaker, and incubate after 60 minutes. Read absorbance between 405-420 nm.

4.3.3 Inflammatory Bowel Disease Activity

4.3.3.1 Chemicals and Reagents

Racemic hesperidin, hesperetin, naringin, and naringenin were purchased from Sigma Chemicals (St. Louis, MO, USA). Racemic eriocitrin and eriodictyol were purchased from Indofine Chemical Company (Hillsborough, NJ, USA). Trypsin- ethyl diamine tetetic acid (EDTA), trypan blue, resazurin, sodium bicarbonate, 4-(2-hydroxyethyl)-1-piperazineethanesulfonic acid (HEPES), sodium pyruvate, penicillin-streptomycin, McCoy's 5A medium was purchased from Sigma (St. Louis, MO, USA). Fetal bovine serum (FBS) was purchased from Equitech-Bio Inc. (Kerrville, TX, USA). HT-29 (colorectal adenocarcinoma) was obtained from American Type Culture Collection (ATCC, Manassas, VA, USA). The Prostaglandin E₂ (PGE₂) ELISA kit was purchased from Amersham Biosciences Corp. (Piscataway, NJ, USA).

4.3.3.2 Cell Culture

HT-29 (colorectal adenocarcinoma) cell lines were maintained in McCoy's 5A medium and supplemented with 10% heat-inactivated FBS, penicillin-streptomycin solution (10 ml/L), and HEPES (6.0 g/L). The cell line was incubated at 37°C in a 5% CO₂ atmosphere.

4.3.3.3 Cell Subculture

Thirty minutes prior to subculturing the corresponding medium, phosphate buffered saline (PBS), and trypsin-ethyl diamine tetetic acid (EDTA) solution comprised of 0.5% trypsin, 0.2% EDTA / 0.9% NaCl diluted in PBS to prepare a 10% working solution were placed in a 37°C water bath. Next, the cell flask was removed from the 5% CO₂ incubator and cells were observed under the light microscope to determine the percentage of confluence, and overall appearance and growth. The desired percentage of confluence was 50-75%. After confluence was determined, medium was aspirated and cells were washed with 5 ml PBS. PBS was aspirated and 2 ml of the trypsin-EDTA working solution was added and the flask was placed in the 5% CO₂ incubator (37°C) for 2 minutes. The flask was then removed from the incubator and observed under the microscope to determine full cell detachment. Detached cells were transferred to a 15 ml conical tube containing 8 ml PBS. The conical tube was then centrifuged at 700 rpm for 5 minutes. Following centrifugation, the conical tube was removed and the PBS was aspirated, leaving the cell pellet undisturbed. Cells were resuspended in 6 ml fresh media and 10 µl was removed and diluted 4 times in trypan blue. The cell-trypan blue solution was added to a hemacytometer and the number of live cells was counted using a cell counter. The number of dead cells was also recorded. If it was determined that the number of

dead cells surpassed 10% of the total population of healthy cells, the cell line was excluded from future experiments and a new generation of the cell line was thawed.

The total number of cells present in the flask was determined using the following equation:

$$\text{Cells/ml} = (\# \text{ cells}/4) (\text{dilution}) (1 \times 10^4) \quad (\text{Equation 1})$$

Depending on the observed cell number and the desired cell seeding number, the cells and fresh media were added in determined volumes to a fresh T75 (125 ml capacity) cell culture flask. The flask was then placed into 5% CO₂ incubator (37°C). Cell subculture was performed 1-2 times per week depending on the growth rate of the cell line and observed confluence.

4.3.3.4 Cell Number

The optimal cell seeding number for HT29 cell line was determined by preliminary cell seeding number experiments. Cells were seeded in numbers 1×10^4 , 2×10^4 , 3×10^4 and so on until the final cell seeding number 1×10^5 per well in a 96 well plate. Cell plates were incubated at 37°C in a 5% CO₂ atmosphere for 72 hours. Following incubation, medium was aspirated and Alamar blue (resazurin) fluorescent dye solution was diluted in fresh medium to make a 10% resazurin solution. The 10% solution was added directly to cells. The cell plates were incubated at 37°C in a 5% CO₂ atmosphere for 3 hours. The cell plates were subsequently removed from the incubator and placed at room temperature in a darkened drawer to protect from light for 30 minutes. Next, the cell plates were placed into the Cytofluor[®] 4000 fluorescence multi-well plate reader (Applied Biosystems, USA). Fluorescence was read at an excitation of 485 nm and an emission of 530 nm. Standard curves of cell seeding number against fluorescence were generated. The HT-29 cell line was seeded at 20,000 cells/well.

4.3.3.5 Inflammatory Bowel Disease Model

The *in vitro* inflammatory bowel model was adapted from previous reports (Calatayud *et al.*, 2002; Otani *et al.*, 2006). HT-29 (colorectal adenocarcinoma) cells were counted and seeded on 96 well plates. The seeded cells were incubated at 37°C in a 5% CO₂ atmosphere until they reached monolayer confluency of 60-80% (72 hours). Cells were then serum starved for 24 hours. Hesperidin, hesperetin, naringin, naringenin, eriocitrin, and eriodictyol were dissolved in DMSO the day of the experiment and were diluted in medium to yield concentrations of 1, 10, 50, 100, and 250 µg/ml. To begin the experiment, cells were divided into one of two groups: cells treated with vehicle (DMSO in media) in the presence of TNF- α , and cells treated with the flavanones in presence of TNF- α (1-250 µg/ml). Following aspiration of the medium, cells were treated with either flavanones (1-250 µg/ml) or vehicle. Cells were then also treated with either 50 µl TNF- α (20 ng/ml) or 50 µl of blank media. Media from each well was collected 24 hours later. Prostaglandin E₂ (PGE₂) levels were measured within 72 hours using commercially available ELISA kits. The prostaglandin E₂ (PGE₂) ELISA kit was purchased from Amersham Biosciences Corp. (Piscataway, NJ), it utilizes novel lysis reagents to facilitate the rapid and efficient extraction of PGE₂ from samples obviating the need for removal of extracting reagents providing a faster read-out at 450 nm. For more information please refer to the instruction in the kit (Prostaglandin E2 Biotrak Enzymeimmunoassay (EIA) System from Amersham Biosciences - cat. No. RPM222).

4.3.4 Anti-Adipogenic Activity

4.3.4.1 Description of the Assay

Obesity is a growing concern worldwide and has reached epidemic proportions in the United States (Camp *et al.*, 2002). It is a risk factor in many major chronic diseases that afflict

our society, including cardiovascular disease, diabetes mellitus, and cancer. In recent years, numerous studies have focused on identifying the mechanism of development of obesity, which is a process of either increasing the number of fat cells (fat cell hyperplasia) or enlargement of fat cells with each cell carrying greater amounts of fat (fat cell hypertrophy), or both (Camp *et al.*, 2002; Spiegelman *et al.*, 1996). The ability to regulate the cell cycle and differentiation of adipocytes are key in the development and physiology of obesity and also in the origin of cancer. Understanding of these processes is critical to a rational approach to the treatment of obesity and cancer. Cayman's Adipogenesis Assay Kit provides the reagents required for studying the induction and inhibition of adipogenesis in the established 3T3-L1 model, using the adipogenesis induction procedure. This kit can also be used to screen compounds with potential anti-adipogenic activity. The classic Oil Red O staining for lipid droplets is used in this kit as an indicator of the degree of adipogenesis, and can be quantified with a plate reader after the dye is conveniently extracted from the lipid droplet. For more information please refer to the instruction in the kit (Adipogenesis Kit from Cayman Chemical - cat. No. 40020).

4.3.4.2 Chemicals and Reagents

Racemic hesperidin, hesperetin, naringin, and naringenin were purchased from Sigma Chemicals (St. Louis, MO, USA). Racemic eriocitrin and eriodictyol were purchased from Indofine Chemical Company (Hillsborough, NJ, USA). Trypsin- ethyl diamine tetraacetic acid (EDTA), trypan blue, resazurin, sodium bicarbonate, sodium pyruvate, penicillin-streptomycin, and Dulbecco's modified Eagle's medium (DMEM) medium was purchased from Sigma (St. Louis, MO, USA). Fetal bovine serum (FBS) was purchased from Equitech-Bio Inc. (Kerrville, TX, USA). 3T3-L1 (preadipocyte) cells were obtained from American Type Culture Collection

(ATCC, Manassas, VA, USA). The Adipogenesis Assay kit was purchased from Cayman Chemical Company (Ann Arbor, MI).

4.3.4.3 Cell Culture

3T3-L1 (preadipocyte) cells were maintained in DMEM medium and supplemented with 10% heat-inactivated FBS, and penicillin-streptomycin solution (10 ml/L). The cell line was incubated at 37°C in a 5% CO₂ atmosphere.

4.3.4.4 Cell Subculture

Thirty minutes prior to subculturing the corresponding medium, phosphate buffered saline (PBS), and trypsin-ethyl diamine tetraacetic acid (EDTA) solution comprised of 0.5% trypsin, 0.2% EDTA / 0.9% NaCl diluted in PBS to prepare a 10% working solution were placed in a 37°C water bath. Next, the cell flask was removed from the 5% CO₂ incubator and cells were observed under the light microscope to determine the percentage of confluence, and overall appearance and growth. The desired percentage of confluence was 50-75%. After confluence was determined, medium was aspirated and cells were washed with 5 ml PBS. PBS was aspirated and 2 ml of the trypsin-EDTA working solution was added and the flask was placed in the 5% CO₂ incubator (37°C) for 2 minutes. The flask was then removed from the incubator and observed under the microscope to determine full cell detachment. Detached cells were transferred to a 15 ml conical tube containing 8 ml PBS. The conical tube was then centrifuged at 700 rpm for 5 minutes. Following centrifugation, the conical tube was removed and the PBS was aspirated, leaving the cell pellet undisturbed. Cells were resuspended in 6 ml

fresh media and 10 μ l was removed and diluted 4 times in trypan blue. The cell-trypan blue solution was added to a hemacytometer and the number of live cells was counted using a cell counter. The number of dead cells was also recorded. If it was determined that the number of dead cells surpassed 10% of the total population of healthy cells, the cell line was excluded from future experiments and a new generation of the cell line was thawed.

The total number of cells present in the flask was determined using the following equation:

$$\text{Cells/ml} = (\# \text{ cells}/4) (\text{dilution}) (1 \times 10^4) \quad (\text{Equation 1})$$

Depending on the observed cell number and the desired cell seeding number, the cells and fresh media were added in determined volumes to a fresh T75 (125 ml capacity) cell culture flask. The flask was then placed into 5% CO₂ incubator (37°C). Cell subculture was performed 1-2 times per week depending on the growth rate of the cell line and observed confluence.

4.3.4.5 Differentiation Procedure and Treatment

Preadipocyte cells were seeded in a 96 well plate at 3×10^4 cells/well and grown to confluency in DMEM with 10% FBS. Two days post confluency, the media of the treatment group was replaced with 150 μ l of the induction medium (DMEM supplemented with IMBX, insulin, and dexamethasone) with the selected flavanone dissolved in it. The control group's media was replaced with fresh 150 μ l of fresh DMEM with 10% FBS. Two days after induction, the media of the treatment group was replaced with 150 μ l of the insulin medium (DMEM supplemented with insulin) with the flavanone dissolved in it. The control group's media was replaced with fresh 150 μ l of fresh DMEM with 10% FBS. Two days later, the media of the treatment group was replaced with 150 μ l of fresh insulin medium (DMEM

supplemented with insulin) with the flavanone dissolved in it. The control group's media was replaced with fresh 150 μ l of fresh DMEM with 10% FBS. Two days later, the visible accumulation of lipid droplets was monitored under a microscope (more than 80 % of the cells are usually differentiated by this day).

4.3.4.6 Lipid Droplet Staining and Quantification

The fixative and oil red O working solutions were prepared. The staining procedure consisted of removing most of the medium from the wells by aspiration, adding 75 μ l of fixative working solution, incubating for 15 minutes, and washing with 100 μ l of wash solution. The washing step was repeated after 5 minutes, then the solution was aspirated and the wells were allowed to air dry. Subsequently, 75 μ l of oil red O was added to all wells, incubated for 20 minutes, followed by removal of the oil red O working solution and washing of the cells with distilled water until the water contained no visible pink color. Finally, the wells were washed with 100 μ l of wash solution, and this washing procedure was repeated after 5 minutes. If desired, microscope images can be taken at this point to visualize pink to red the oil droplet staining in differentiated cells. The wells were allowed to completely air dry again, and 100 μ l of dye extraction solution was added and gently mixed for 15-30 minutes on an orbital shaker. Finally, the absorbance was measured at 492 nm (490-520 nm) with typical absorbances determined to be around 0.2-0.4 and control wells around 0.05.

4.3.5 Anti-Cancer Activity

4.3.5.1 Chemicals and Reagents

Racemic hesperidin, hesperetin, naringin, naringenin, trypsin-Ethyl Diamine Tetraacetic Acid (EDTA), trypan blue, phosphate-buffered saline (PBS), resazurin, sodium bicarbonate,

McCoy's 5A medium, Dulbecco's Modified Eagle Medium (DMEM), RPMI 1640 medium, penicillin-streptomycin, and insulin were purchased from Sigma (St. Louis, MO, USA). Racemic eriocitrin and eriodictyol were purchased from Indofine Chemical Company (Hillsborough, NJ, USA). Fetal bovine serum (FBS) was purchased from Equitech-Bio Inc. (Kerrville, TX). Human umbilical vascular endothelial cell line (HUVEC), A-375 (malignant melanoma), HCT-116 (colorectal carcinoma), Hep-G2 (hepatocellular carcinoma), MDA-MB-231 (Estrogen receptor negative breast adenocarcinoma), and PC-3 (prostate adenocarcinoma) cell lines were obtained from American Type Culture Collection (ATCC, Manassas, VA, USA).

4.3.5.2 Enantiomer Separation

Since pure hesperetin, naringenin, and/or eriodictyol enantiomers are not commercially available, pure enantiomeric fractions were manually collected using the stereospecific HPLC methods described in Chapter II. Each enantiomeric fraction was manually collected and re-injected into the HPLC system for verification of purity. This operation was repeated multiple times to obtain enough pure enantiomer. In order to perform the cancer cell viability studies 20 mg of each enantiomer were needed and each manual fraction collection yielded about 0.1 mg. Thus, to obtain these pure fraction is very labor intensive and time consuming and only cancer cell viability studies could be performed utilizing pure flavanone enantiomers.

4.3.5.3 Cell Culture

HUVEC cells were maintained in epithelial growth medium (EGM-2) and endothelial cell growth supplement. A-375 (malignant melanoma) and MDA-MB-231 (Estrogen receptor negative breast adenocarcinoma) cell lines were maintained in Dulbecco's Modified Eagle Medium (D-MEM) and supplemented with 10% heat-inactivated fetal bovine serum (FBS),

penicillin-streptomycin solution (10 ml/L), HEPES (2.4 g/L), and sodium pyruvate (110.4 mg/L). HCT-116 (colorectal carcinoma) cell line was maintained in McCoy's 5A medium and supplemented with 10% heat-inactivated FBS, penicillin-streptomycin solution (10 ml/L), and HEPES (6.0 g/L). Hep-G2 (human hepatoma) cell line was maintained in Dulbecco's Modified Eagle Medium: Nutrient Mixture F-12 (Ham) (DMEM/F-12) and supplemented with 10% heat-inactivated fetal bovine serum (FBS), penicillin-streptomycin solution (10 ml/L), and insulin (4 mg/ml). PC-3 (prostate adenocarcinoma) cell line was maintained in RPMI medium and supplemented with 10% heat-inactivated FBS and penicillin-streptomycin solution (10 ml/L). All cell lines were incubated at 37°C in a 5% CO₂ atmosphere.

4.3.5.4 Cell Subculture

Thirty minutes prior to subculturing the corresponding medium for each cell line, phosphate buffered saline (PBS), and trypsin-ethyl diamine tetetic acid (EDTA) solution comprised of 0.5% trypsin, 0.2% EDTA / 0.9% NaCl diluted in PBS to prepare a 10% working solution were placed in a 37°C water bath. Next, the cell flask was removed from the 5% CO₂ incubator and cells were observed under the light microscope to determine the percentage of confluence, and overall appearance and growth. The desired percentage of confluence was 50-75%. After confluence was determined, medium was aspirated and cells were washed with 5 ml PBS. PBS was aspirated and 2 ml of the trypsin-EDTA working solution was added and the flask was placed in the 5% CO₂ incubator (37°C) for 2 minutes. The flask was then removed from the incubator and observed under the microscope to determine full cell detachment. Detached cells were transferred to a 15 ml conical tube containing 8 ml PBS. The conical tube was then centrifuged at 700 rpm for 5 minutes. Following centrifugation, the conical tube was removed and the PBS was aspirated, leaving the cell pellet undisturbed. Cells were

resuspended in 6 ml fresh media and 10 μ l was removed and diluted 4 times in trypan blue. The cell-trypan blue solution was added to a hemacytometer and the number of live cells was counted using a cell counter. The number of dead cells was also recorded. If it was determined that the number of dead cells surpassed 10% of the total population of healthy cells, the cell line was excluded from future experiments and a new generation of the cell line was thawed.

The total number of cells present in the flask was determined using the following equation:

$$\text{Cells/ml} = (\# \text{ cells}/4) (\text{dilution}) (1 \times 10^4) \quad (\text{Equation 1})$$

Depending on the observed cell number and the desired cell seeding number, the cells and fresh media were added in determined volumes to a fresh T75 (125 ml capacity) cell culture flask. The flask was then placed into 5% CO₂ incubator (37°C). Cell subculture was performed 1-2 times per week depending on the growth rate of the cell line and observed confluence.

4.3.5.5 Cell Number

The optimal cell seeding numbers for each cell line was determined by preliminary cell seeding number experiments. Cells were seeded in numbers 1×10^4 , 2×10^4 , 3×10^4 and so on until the final cell seeding number 1×10^5 per well in a 96 well plate. Cell plates were incubated at 37°C in a 5% CO₂ atmosphere for 72 hours. Following incubation, medium was aspirated and Alamar blue (resazurin) fluorescent dye solution was diluted in fresh medium to make a 10% resazurin solution. The 10% solution was added directly to cells. The cell plates were incubated at 37°C in a 5% CO₂ atmosphere for 3 hours. The cell plates were subsequently removed from the incubator and placed at room temperature in a darkened drawer to protect from light for 30 minutes. Next, the cell plates were placed into the Cytofluor[®] 4000

fluorescence multi-well plate reader (Applied Biosystems, USA). Fluorescence was read at an excitation of 485 nm and an emission of 530 nm. Standard curves of cell seeding number against fluorescence were generated. HUVEC cells were seeded at a density of 15,000 cells/well. MDA-MB-231, Hep-G2, and PC-3 cell lines were seeded at 5,000 cells/well. A-375 cell line was seeded at 1,000 cells/well, while HCT-116 cell line was seeded at 3,000 cells/well.

4.3.5.6 Alamar Blue Assay

Alamar Blue (resazurin) fluorescent dye is a facile and accurate assay to determine the cytotoxicity of many cell lines including the five cancer cell lines used in the present study (O'Brien *et al.*, 2000). The resazurin non-fluorescent compound is metabolized into the fluorescent compound resorufin by intact and viable cells. This emission of fluorescence can be quantified using a cell plate reader and the number of viable cells following treatment can be determined. Cells were counted and seeded on 96 well plates. The seeded cells were incubated at 37°C in a 5% CO₂ atmosphere for 24 hours. The compounds were dissolved in dimethyl sulfoxide (DMSO) the day of the experiment and were diluted in medium to yield concentrations of 1, 10, 50, 100, and 250 µg/ml. Following aspiration of the medium, cells were treated with the flavanones solution. Additional cells were treated with either DMSO diluted in medium or medium only. Treated and control cells were incubated at 37°C in a 5% CO₂ atmosphere for 72 hours. After cell plates were removed from the incubator, medium was aspirated and replaced with 10% Alamar blue (resazurin) fluorescent dye diluted in fresh medium. Cell plates were incubated at 37°C in a 5% CO₂ atmosphere for an additional 3 hours. Following incubation, cell plates were placed in a darkened environment for 30 minutes at room temperature. Next, the cell plates were placed into the Cytoflour[®] 4000 fluorescence

multi-well plate reader (Applied Biosystems, USA), and fluorescence was read at an excitation of 485 nm and an emission of 530 nm. The viable cell number (as a percent of control) in each cell line exposed to varying concentrations of tested compounds was determined.

4.3.5.7 Data Analysis

Data were analyzed as mean percent of viable cells \pm standard deviation in Microsoft Excel[®] and then graphed using Sigma Plot[®] software. Next, the individual mean percent of viable cells was modeled using the inhibitory effect model WinNonlin[®] (version 5.01) pharmacodynamic software to obtain the concentration that inhibits 50% cell viability (IC₅₀) values for each cell line investigated. The IC₅₀ values were obtained using the following equation:

$$E^* = E_{\max}^{**} \left(\frac{1 - C^{***}}{C + IC_{50}} \right)$$

* Viability

** Maximum viability

*** Concentration

Modeled IC₅₀ values were checked using the following equation:

$$IC_{50} = C_{\max}^{****} / C + IC_{50}$$

**** Maximum concentration

Data were expressed as the mean \pm standard error of measurement (SEM) of IC₅₀ values across replicates.

4.3.6 Anti-Oxidant Capacity

4.3.6.1 Chemicals and Reagents

Daidzein, 2,2'-azion-bis-(3-ethylbenzthiazoline-6-sulfonic acid) in the crystallized diammonium salt form (ABTS), 6-hydroxy-2,5,7,8-tetramethylchroman-2-carboxylic acid

(Trolox®), peroxidase type VI from horseradish (HRP) (1067 U/mg), phosphate buffer saline (PBS), ethyl acetate, racemic hesperidin, hesperetin, naringin, naringenin, phloretin, phloridzin, quercetin, quercetin-3-rutinoside (rutin), and quercetin-3-rhamnoside (quercitrin) were purchased from Sigma (St. Louis, MO, USA). Racemic eriocitrin and eriodictyol were purchased from Indofine Chemical Company (Hillsborough, NJ, USA). Hydrogen peroxide (H₂O₂), glacial acetic acid, HPLC grade acetonitrile, methanol, and water were purchased from J. T. Baker (Phillipsburg, NJ, USA). β -glucosidase from almonds (2500 U/mg) was purchased from MP Biomedicals (Solon, OH, USA). Conventional and organic Red Delicious apples were purchased from a local grocery store.

4.3.6.2 Stock Solutions

Methanol stock solutions of daidzein, phloretin, phloridzin, quercetin, quercetin-3-rutinoside (rutin), and quercetin-3-rhamnoside (quercitrin) for LC-MS-ESI analysis were prepared by accurately measuring 10 mg (0.01 g) of each compound and dissolving them completely in 100 ml HPLC grade methanol to make a final stock solution of 100 μ g/ml. β -glucosidase from almonds (2500 U/mg) was prepared by completely dissolving 1.5 mg (0.0015 g) in 5 ml PBS to make a solution of 750 U/ml (Ismail *et al.*, 2005; Zhang *et al.*, 2006b). The stock solutions of ABTS, H₂O₂, HRP, and Trolox® were slightly modified in preparation and concentrations from previously described methodology (Arnao *et al.*, 2001a; Cano *et al.*, 1998). For instance, ABTS was prepared by dissolving 55 mg (0.055 g) in 10 ml HPLC grade methanol to make a final solution of 10 mM ABTS. Hydrogen peroxide (H₂O₂) was prepared by mixing 0.37 ml of stock H₂O₂ (30% of concentration and estimated density of 1.3 g/ml) with 9.63 ml HPLC grade methanol to make a final solution of 350 μ M. Hydrogen peroxide (HRP) (1067 U/mg) was prepared by completely dissolving 16 mg (0.016 g) in 20 ml HPLC

grade water to make a stock solution of 20 μM . Trolox® was prepared by completely dissolving 12.5 mg (0.0125 g) in 10 ml HPLC grade methanol to make a stock solution of 5 mM.

4.3.6.3 Biological Material and Separation of Lipophilic and Hydrophilic Fractions

The red delicious conventional and organic apples were completely peeled and the skin was collected and rapidly frozen under liquid nitrogen. The peeled apples were then cut in half and the seed cavity was rapidly removed and discarded. The apple halves were cut in smaller pieces and also rapidly frozen under liquid nitrogen. The entire procedure took less than 2 minutes per apple; thus, there was minimum browning. Once the skin and the flesh were frozen, they were grounded separately to a fine homogenous powder with excess liquid nitrogen using a mortar and pestle. The fine powders were stored at -80°C . The methodology to obtain the hydrophilic and lipophilic fractions was adapted from Arnao *et al.* (Arnao *et al.*, 2001a) with some modifications. Homogenous apple tissue samples (0.1 g) or polyphenol pure powder (phloridzin, quercetin, quercetin-3-rutinoside (rutin), and quercetin-3-rhamnoside (quercitrin) – 0.001 g) were combined with 0.3 ml PBS (pH 7.4) and 0.7 ml ethyl acetate and ground in a homogenizer (Talboys Engineering Corp., Montrose, PA, USA) for 1 min. The samples were vortexed for 30 seconds; the slurry was then transferred to Eppendorf tubes, and centrifuged at 5,000 rpm for 5 min at room temperature (25°C) (Beckman Microfuge, Beckman Coulter Inc., Fullerton, CA, USA). The aqueous phase was collected to measure hydrophilic anti-oxidant activity (HAA). The organic phase was collected to measure lipophilic anti-oxidant activity (LAA). Any solid residue was collected and dissolved in 1 ml HPLC

grade methanol and if soluble it was employed to measure insoluble anti-oxidant activity (IAA) (Figure 4-1).

The concept of obtaining hydrophilic and lipophilic fractions to assess anti-oxidant activity is relatively new (Alcolea *et al.*, 2002; Arnao *et al.*, 2001a). Previous reports have employed different solvents (methanol, ethanol, hexane, acetone, water, etc.) to extract different biological samples and assess the anti-oxidant activity of these individual fractions (Cai *et al.*, 2004; Pellati *et al.*, 2004; Wang *et al.*, 1999).

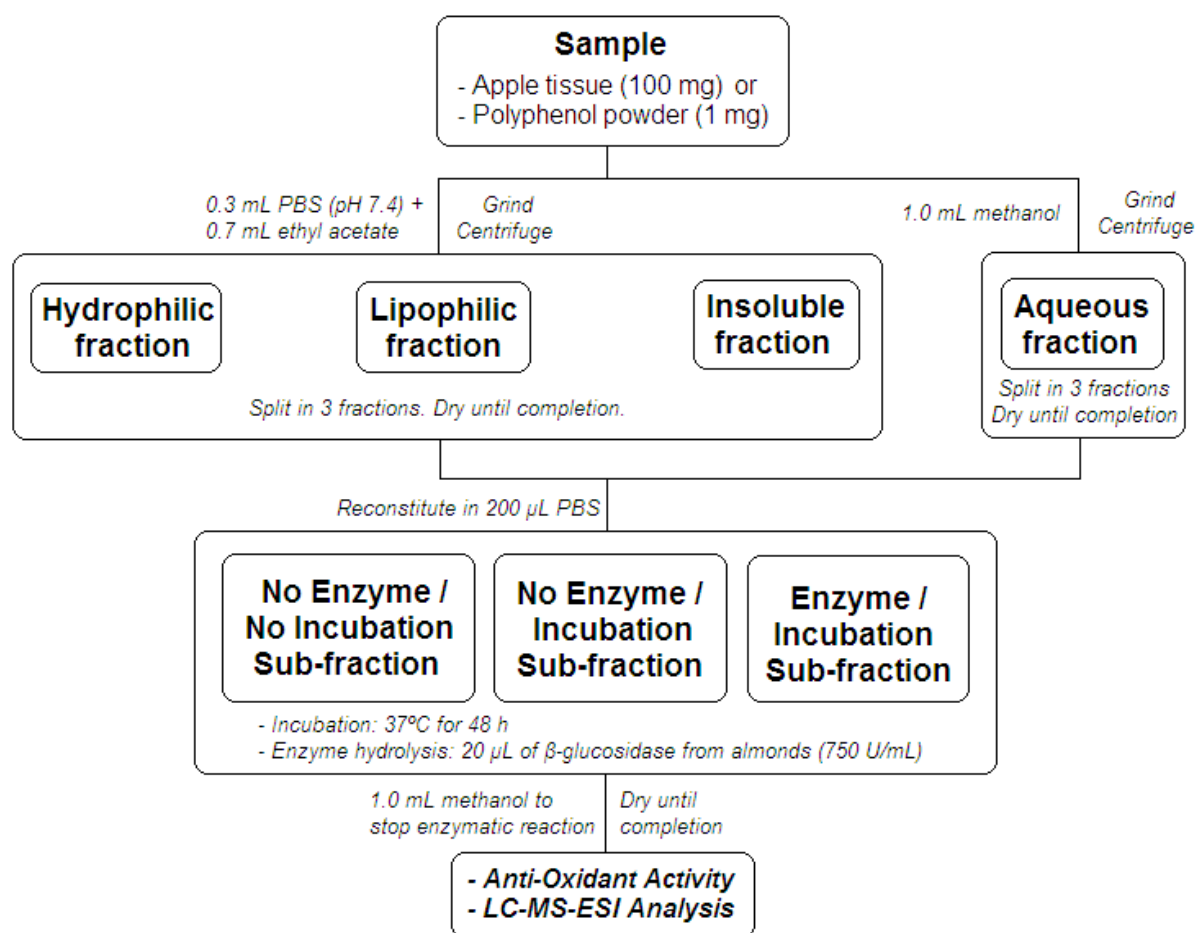


Figure 4-1: Schematic of the methodology of the novel comprehensive anti-oxidant activity method.

The most common fraction utilized for determination of anti-oxidant capacity is the aqueous fraction (water, ethanol, or methanol). Thus, in order to have a control fraction for comparison, the aqueous anti-oxidant activity (AAA) was employed. For this, the same samples (apple tissue and polyphenol powders) and 1 ml HPLC grade methanol were ground in a homogenizer (Talboys Engineering Corp., Montrose, PA, USA) for 1 min. The same methodology as described above was followed (namely vortex, centrifugation). The aqueous phase was collected to measure aqueous anti-oxidant activity (AAA). Any solid residue was discarded (Cai *et al.*, 2004; Pellati *et al.*, 2004; Wang *et al.*, 1999).

All extraction procedures were carried out under subdued light at room temperature, all the fractions were split in 3 equal aliquots (sub-fractions) and were dried until completion under a current flow of compressed nitrogen gas. These 3 sub-fractions allowed the assessment of the glycoside and aglycone compounds contribution to total anti-oxidant capacity. The different sub-fractions were named: No enzyme, no incubation (NE/NI); no enzyme, incubation (NE/I); and enzyme, incubation (E/I). The NE/NI sub-fraction would represent the total anti-oxidant activity provided by the glycosides and aglycones content (aglycone/glycoside ratio) present in the samples as quantified by LC-MS-ESI. The NE/I sub-fraction assess the effect of the incubation temperature and time over the glycoside and aglycone content (aglycone/glycoside ratio) and the total anti-oxidant activity. The E/I sub-fraction assess the effect of the β -glucosidase from almonds in the aglycone/glycoside ratio and the total anti-oxidant activity after the enzymatic hydrolysis of the O-glycosidic bond allowing the conversion of glycosides to aglycones (Ismail *et al.*, 2005; Zhang *et al.*, 2006b) (Figure 4-1).

4.3.6.4 Enzymatic Hydrolysis

The methodology was modified from the report by Ismail and Hayes (Ismail *et al.*, 2005) and Zhang *et al.* (Zhang *et al.*, 2006b). For this, the E/I sub-fractions were reconstituted in 200 μ l PBS and 20 μ l of β -glucosidase from almonds (750 U/ml) were added and incubated under agitation at 37°C for 48 h (Ismail *et al.*, 2005; Zhang *et al.*, 2006b). The reaction was terminated by the addition of 1 ml of HPLC grade methanol (Zhang *et al.*, 2006b). The samples were dried until completion under a current flow of compressed nitrogen gas (Figure 1). β -glucosidase from almonds can specifically hydrolyze β -glycosides into aglycones (Ismail *et al.*, 2005; Zhang *et al.*, 2006b).

4.3.6.5 Anti-Oxidant Capacity using a Modified ABTS Method

Activity was determined using the ABTS/HRP discoloration method (Alcolea *et al.*, 2002; Arnao *et al.*, 2001a; Arnao *et al.*, 2001b; Cano *et al.*, 1998) with some modifications. The different fractions (hydrophilic, lipophilic, insoluble, and aqueous) and sub-fractions (No enzyme, no incubation (NE/NI); no enzyme, incubation (NE/I); and enzyme, incubation (E/I)) were completely dissolved in 30 μ l of their corresponding solvents. Independently of the sub-fraction, the hydrophilic fractions were dissolved in PBS, the lipophilic fractions in ethyl acetate, the insoluble and aqueous fractions in HPLC grade methanol. To perform the test, 25 μ l of 10 mM ABTS was added to each well of a 96-well plate (Costar 3595) followed by the addition of 25 μ l of 350 μ M hydrogen peroxide (H_2O_2), 25 μ l of 15 μ M horseradish peroxidase (HRP), and 162.5 μ l of HPLC grade methanol. The plate was incubated for 1 hour in a microplate shaker without protection from the light to allow $\text{ABTS}^{\cdot+}$ radical generation. Following incubation, the absorbance was read at 730 nm at room temperature and the absorbance values recorded (plate with no samples). Then 15 μ l of each sample was added to each corresponding well, shake for 30 seconds in a microplate shaker, and incubated at room

temperature for 6 minutes. Following incubation, the absorbance was read again at 730 nm at room temperature and the absorbance values recorded (plate with samples). The absorbance values in the plate with samples are expected to decrease due to the discoloration caused by the action of the anti-oxidants present in the samples; thus, reducing the amount of ABTS^{•+} present in each well. Standard curves with Trolox[®] dissolved in the three solvents employed (ethyl acetate, PBS, and methanol) were constructed and the results were expressed as millimolar Trolox[®] equivalents anti-oxidant capacity per 100 g of dry weight sample (mM TEAC/100 g DW). Where possible the IC₅₀ values were calculated, and the anti-radical efficiency (AE) values were calculated by dividing 1000 by the IC₅₀ value (Parejo *et al.*, 2003).

4.3.6.6 LC-MS-ESI Analysis

The separation of phenolic compounds was performed on a Shimadzu LCMS-2010 EV liquid chromatograph mass spectrometer system (Kyoto, Japan) connected to the LC portion consisting of two LC-10AD pumps, a SIL-10AD VP auto injector, a SPD-10A VP UV detector, and a SCL-10A VP system controller was employed. Data analysis was accomplished using Shimadzu LCMS Solutions Version 3 software (Kyoto, Japan). The chromatographic conditions were slightly modified from the report by Schieber *et al.* (Schieber *et al.*, 2001). The columns employed were a Phenomenex Luna (2) C₁₈ column (250 x 4.60 mm, i.d. 5 µm particle size, Torrance CA, USA), and a guard Phenomenex Luna (2) C₁₈ column (30 x 4.60 mm, i.d. 3 µm particle size, Torrance CA, USA). The mobile phase consisted of 2% (v/v) acetic acid in water (eluent A) and of 0.5% acetic acid in water and acetonitrile (50:50, v/v; eluent B). The gradient was as follows: 10% B to 55% B (70 min), 55% B to 100% B (10 min), 100% B to 10% B (10 min). The flow rate was as follows: 0.8 ml/min (55 min), 1 ml/min (45 min). The injection volume for all samples was 5 µl, and the internal standard employed was

daidzein. Simultaneous monitoring was performed at 280 nm (catechins, benzoic acids, and hydroxycinnamic acids) and 370 nm (flavonols). The mass spectrometer conditions consisted of a curved desolvation line (CDL) temperature of 200°C and a block temperature of 200°C. The CDL, interface, and detector voltages were -20.0 V, 4.5 kV, and 1.2 kV, respectively. Vacuum was maintained by an Edwards[®] EM30 rotary vacuum pump (Edwards, UK). Liquid nitrogen (Washington State University Central Stores) was used as a source of nebulizer gas (1.5 L/min). In the negative-specific ion mode (SIM) the monitored single plot transitions (*m/z*) were: gallic acid 170→169, catechin 290→289, chlorogenic acid 354→353, epicatechin 290→289, quercetin-3-rutinoside (rutin) 664→663, quercetin-3-rhamnoside (quercitrin) 448→447, phloridzin 436→435, quercetin 302→301, phloretin 274→273, and daidzein 254→253.

4.3.6.7 Statistical Analysis

Compiled data were presented as mean and standard error of the mean (mean ± SEM). General Linear Model (GLM) Analysis of Variance (ANOVA) with Newman-Keuls multiple comparison test was utilized with a p-value < 0.05 been statistically significant (NCSS Statistical and Power Analysis, Kaysville, UT).

4.4 RESULTS AND DISCUSSION

4.4.1 Anti-Inflammatory Properties

4.4.1.1 Cell Viability

Cell viability was indirectly measured as conversion of Alamar blue (resazurin) to resorufin. The results indicated that hesperidin, hesperetin, naringin, naringenin, eriocitrin and eriodictyol at 1 – 250 µg/ml did not reduce cell viability of canine chondrocytes (Figure 4-2). This was also verified with microscopic examination during the length of the whole study

before cell culture media collection. Similar results have been observed for aqueous extracts of *Capparis spinosa* in a similar osteoarthritis model (Panico *et al.*, 2005).

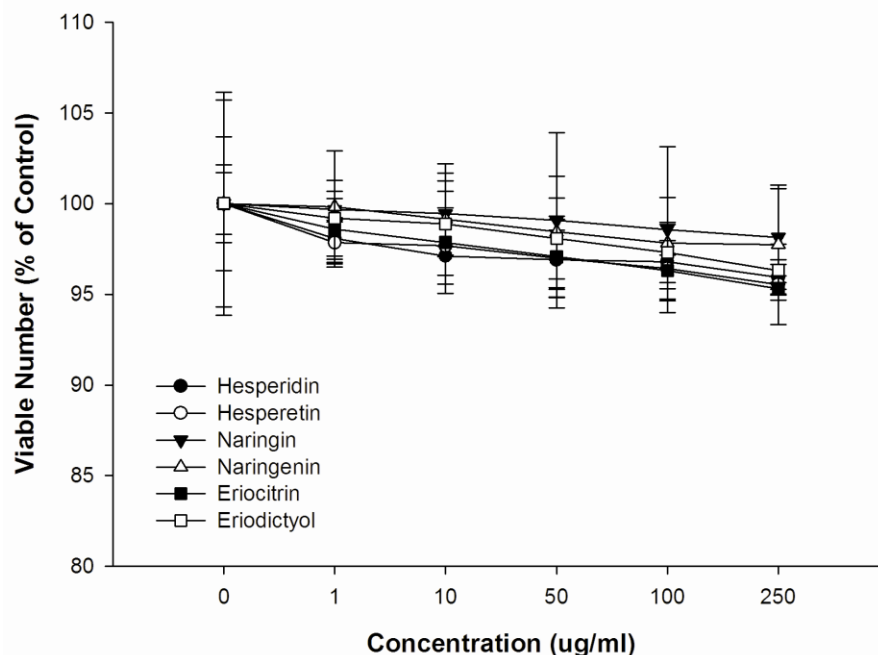


Figure 4-2: The number of viable canine chondrocytes following treatment of the different flavanones (mean \pm SEM, n=4).

4.4.1.2 Nitric Oxide

4.4.1.2.1 Nitrite Levels

The canine chondrocyte controls produced low nitrite levels ($5.48 \mu\text{M} \pm 0.03$) mainly due to the activity of the constitutive nitric oxide synthase compared to cells treated with IL-1 β ($8.68 \mu\text{M} \pm 0.13$) ($P < 0.001$). Canine chondrocytes treated with the different flavanones demonstrated a significant concentration-dependant decrease in nitrite levels similar to baseline levels (chondrocytes without inflammatory insult) (Figure 4-3). It was also observed that some of the flavanones at the highest concentrations (100-250 $\mu\text{g/ml}$) reduced nitrite production to values lower than baseline; however, independent of the concentration all the flavanones

significantly reduced nitrite production compared to the chondrocytes with inflammatory insult (IL-1 β treated samples).

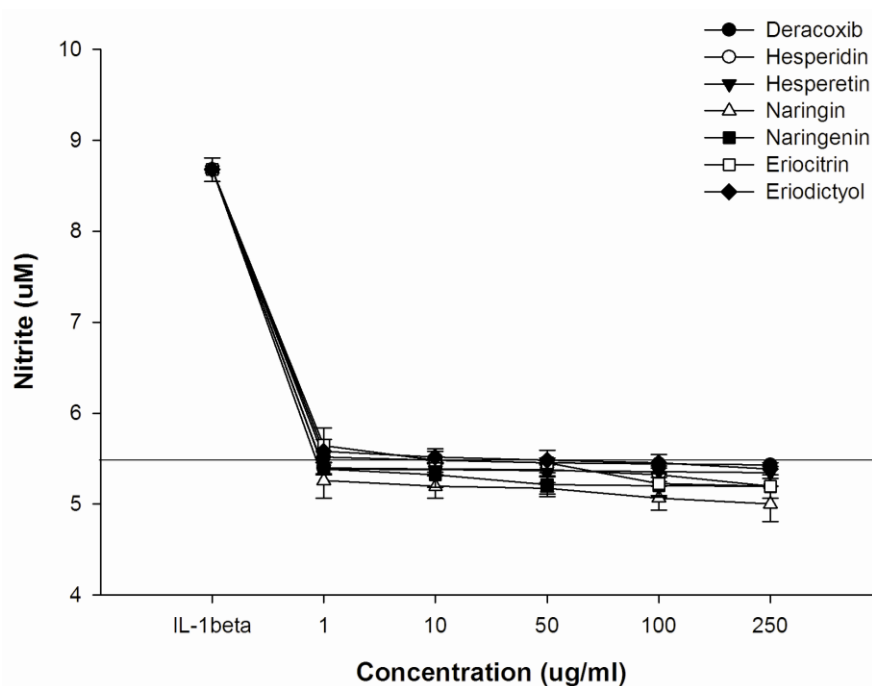


Figure 4-3: Nitrite production (means \pm SEM) in the cell culture medium from canine chondrocytes 72 h after the addition of the different flavanones and deracoxib as positive control at concentrations 1-250 μ g/ml with IL-1 β (100 μ l of 100 ng/ml). Values are expressed as μ M. The line represents the baseline level (chondrocytes without inflammatory insult).

The IC₅₀ values for nitrite reduction were calculated and it was observed that all the flavanones (glycosides and aglycones) exhibited lower IC₅₀ values in μ g/ml than deracoxib (Table 4-1). It was observed that the glycosides (hesperidin, naringin, and eriocitrin) were more active in reducing nitrite than their corresponding aglycones (hesperetin, naringenin, and eriodictyol). The most active glycoside was eriocitrin, followed by naringenin and hesperidin, while the most active aglycone was naringenin, followed by hesperetin and eriodictyol. Thus, it can be observed that there are differences with the glycoside and the aglycone form, and that small chemical changes between flavanones confer different pharmacological activities in the molecules. Eriodictyol is a tetrahydroxyflavanone, while naringenin is a trihydroxyflavanone,

and hesperetin has a methoxy group added. Similar results were observed between the aglycone and glycoside forms, also similar results were obtained for the corrected IC₅₀ values expressed in mM (Table 4-1).

Table 4-1: IC₅₀ values of deracoxib and flavanones for nitrite reduction (mean ± SEM, n=4).
^aSignificantly different from deracoxib (P<0.05).

Compound	IC ₅₀ (µg/ml)	IC ₅₀ (mM)
Deracoxib	814.46 ± 77.37	2.05 ± 0.19
Hesperidin	652.10 ± 56.73 ^a	1.07 ± 0.09 ^a
Hesperetin	782.10 ± 61.79	2.59 ± 0.20 ^a
Naringin	635.19 ± 43.83 ^a	1.09 ± 0.08 ^a
Naringenin	704.07 ± 56.32	2.59 ± 0.21 ^a
Eriocitrin	620.53 ± 56.46 ^a	1.04 ± 0.09 ^a
Eriodictyol	791.53 ± 58.57	2.75 ± 0.20 ^a

4.4.1.2.2 Nitrate Levels

The nitrate results (Figure 4-4) exhibit similar patterns compared to the nitrite levels. The canine chondrocyte controls produced low nitrite levels (1.40 µM ± 0.07) mainly due to the activity of the constitutive nitric oxide synthase compared to cells treated with IL-1β (2.38 µM ± 0.02) (P<0.001). Canine chondrocytes treated with the different flavanones demonstrated a significant concentration-dependant reduction in nitrate levels. Similarly to the nitrite reduction results, it was also observed that some of the flavanones at the highest concentrations (100-250 µg/ml) reduced nitrate production to values lower than baseline; however, independent of the

concentration all the flavanones significantly reduced nitrate production compared to the chondrocytes with inflammatory insult (IL-1 β treated samples).

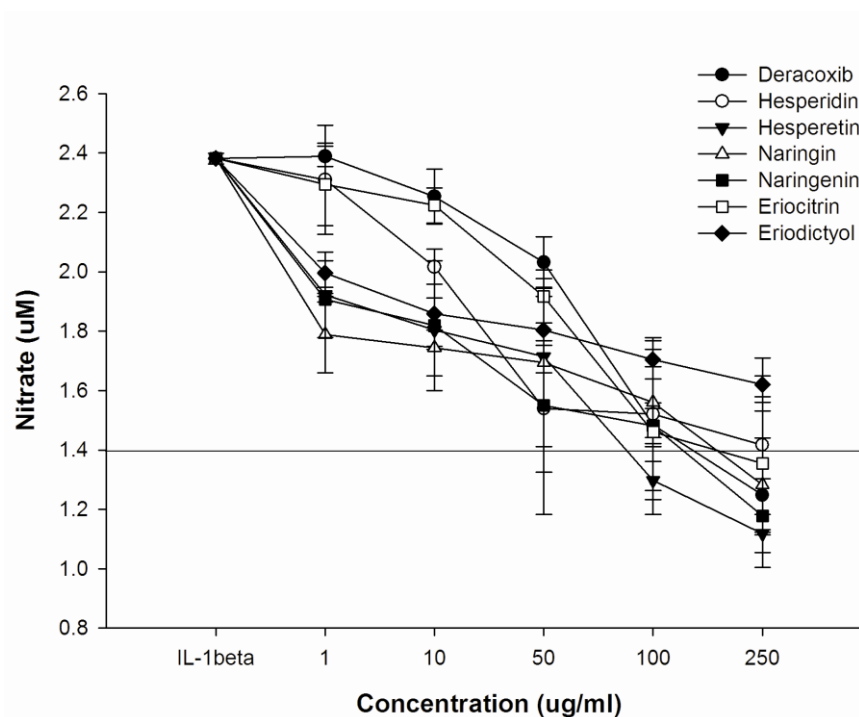


Figure 4-4: Nitrate production (means \pm SEM) in the cell culture medium from canine chondrocytes 72 h after the addition of the different flavanones and deracoxib as positive control at concentrations 1-250 μ g/ml with IL-1 β (100 μ l of 100 ng/ml). Values are expressed as μ M. The line represents the baseline level (chondrocytes without inflammatory insult).

The IC₅₀ values for nitrate reduction were calculated and it was observed that only hesperetin exhibited lower IC₅₀ value in μ g/ml than deracoxib (Table 4-2). Interestingly the aglycones (with the exception of eriodictyol) were more active in reducing nitrate than their corresponding glycosides. The most active glycoside was eriocitrin, followed by hesperidin and naringenin, while the most active aglycone was hesperetin, followed by naringenin and eriodictyol. Similar results were obtained for the corrected IC₅₀ values expressed in mM (Table 4-2). The nitrite and nitrate results correlate with previous observations that indicated that hesperidin (Yeh *et al.*, 2007), and naringin (Kanno *et al.*, 2006a) can significantly reduce nitric

oxide production, and iNOS expression. However, as observed here also eriocitrin and eriodictyol exhibited activity along with the aglycones hesperetin and naringenin.

Table 4-2: IC₅₀ values of deracoxib and flavanones for nitrate reduction (mean ± SEM, n=4).
^aSignificantly different from deracoxib (P<0.05).

Compound	IC ₅₀ (µg/ml)	IC ₅₀ (mM)
Deracoxib	231.81 ± 18.78	0.58 ± 0.05
Hesperidin	280.06 ± 18.20 ^a	0.46 ± 0.03 ^a
Hesperetin	204.60 ± 19.23	0.67 ± 0.06
Naringin	397.57 ± 23.85 ^a	0.69 ± 0.04 ^a
Naringenin	256.96 ± 20.30 ^a	0.94 ± 0.07 ^a
Eriocitrin	248.72 ± 20.89 ^a	0.42 ± 0.03 ^a
Eriodictyol	683.69 ± 62.90 ^a	2.37 ± 0.22 ^a

4.4.1.3 Prostaglandin E₂

Figure 4-5 refers to the results of PGE₂ levels obtained in treated and untreated canine chondrocytes. Canine chondrocytes stimulation with IL-1β (1 ng) significantly increased the production of PGE₂ (56%) when compared to untreated controls (P<0.001). The treatment of canine chondrocytes with deracoxib caused a concentration-dependant decrease in the PGE₂ concentrations to levels lower than baseline at concentrations higher than 10 µg/ml. The treatment with all the flavanones caused an actual increase in PGE₂ levels at the lowest concentration (1 µg/ml) followed by a concentration-dependant decrease.

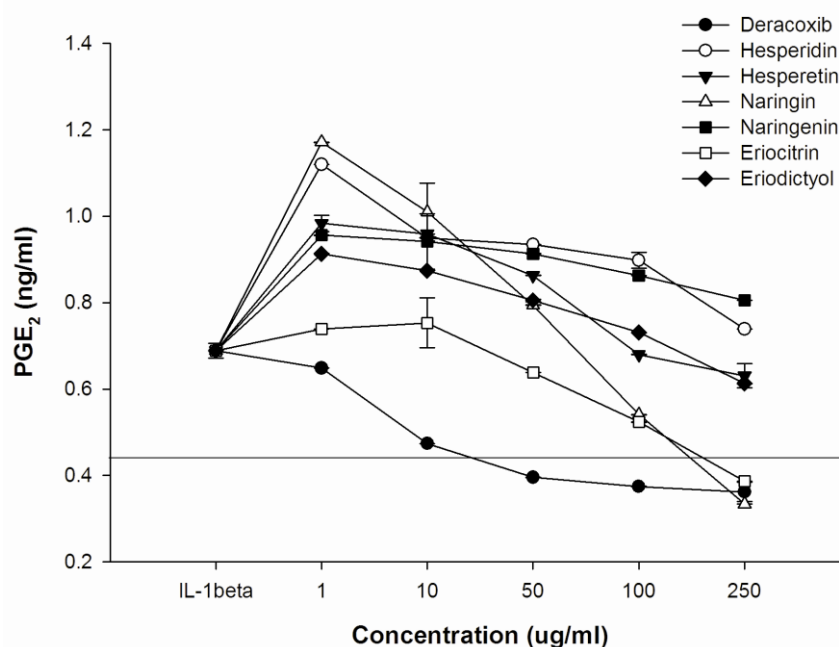


Figure 4-5: Prostaglandin E₂ (PGE₂) production (means \pm SEM) in the cell culture medium from canine chondrocytes 72 h after the addition of the different flavanones and deracoxib as positive control at concentrations 1-250 μ g/ml with IL-1 β (100 μ l of 100 ng/ml). Values are expressed as pg/ml. The line represents the baseline level (chondrocytes without inflammatory insult).

The IC₅₀ values for PGE₂ were calculated and it was observed that only naringin exhibited an IC₅₀ value similar to deracoxib (Table 4-3). It was also observed that naringin and eriocitrin were more active than their aglycones, while the opposite was observed for hesperidin. The most active glycoside was naringin, followed by eriocitrin and hesperidin, while the most active aglycone was hesperetin, followed by eriodictyol and naringenin. Similar results were obtained for the corrected IC₅₀ values expressed in mM (Table 4-3). These results correlate with previous observations that hesperidin suppresses the production of PGE₂ (Sakata *et al.*, 2003), and that hesperetin and hesperidin in the concentration range 250-500 μ M can inhibit the expression of COX-2 gene (Hirata *et al.*, 2005). Similarly, naringenin (0.5-50 μ M) was observed to elicit a concentration-dependant reduction in PGE₂ release and COX-2 expression (Raso *et al.*, 2001).

Table 4-3: IC₅₀ values of deracoxib and flavanones for PGE₂ reduction (mean ± SEM, n=4).
^aSignificantly different from deracoxib (P<0.05).

Compound	IC ₅₀ (µg/ml)	IC ₅₀ (mM)
Deracoxib	162.49 ± 10.24	0.41 ± 0.03
Hesperidin	1040.47 ± 73.87 ^a	1.70 ± 0.12 ^a
Hesperetin	549.40 ± 54.39 ^a	1.82 ± 0.18 ^a
Naringin	144.34 ± 11.98	0.25 ± 0.02 ^a
Naringenin	3099.87 ± 244.89 ^a	11.39 ± 0.90 ^a
Eriocitrin	276.37 ± 23.49 ^a	0.46 ± 0.04
Eriodictyol	611.89 ± 57.52 ^a	2.12 ± 0.20 ^a

4.4.1.4 Sulphated Glycosaminoglycan

Figure 4-6 refers to the concentrations of sulfated glycosaminoglycans (sGAG) obtained in treated and untreated canine chondrocytes. The untreated control samples released 46.25 µg/ml ± 0.02 sGAG in the cell culture medium. When the samples were treated with IL-1β (10 ng/ml), a significant increase (16%) in sGAG production was observed (53.89 µg/ml ± 0.59) (P<0.001). It was observed that hesperetin and naringin increase the sGAG production at the lowest concentration (1 µg/ml). All the flavanones demonstrated higher activity than deracoxib in reducing sGAG release.

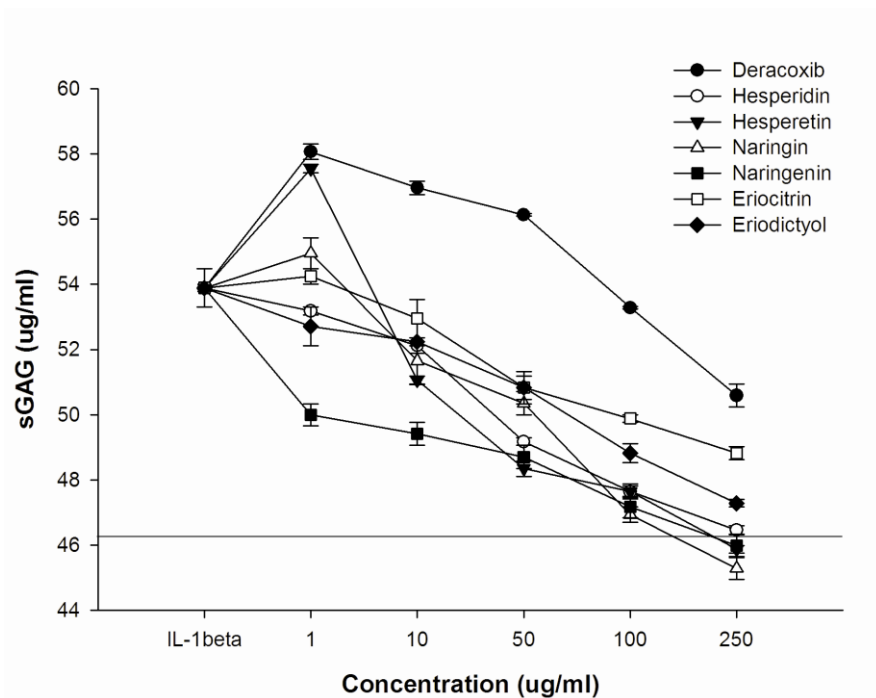


Figure 4-6: Sulfated glycosaminoglycans (sGAG) production (means \pm SEM) in the cell culture medium from canine chondrocytes 72 h after the addition of the different flavanones and deracoxib as positive control at concentrations 1-250 $\mu\text{g/ml}$ with IL-1 β (100 μl of 100 ng/ml). Values are expressed as $\mu\text{g/ml}$. The line represents the baseline level (chondrocytes without inflammatory insult).

Indeed, the flavanones exhibited higher activity (lower IC_{50} values) for sGAG production (Table 4-4). It was observed that hesperetin and eriodictyol were more active than their glycosides, while the opposite was observed for naringenin. Similar results were obtained for the corrected IC_{50} values expressed in mM (Table 4-4).

Table 4-4: IC₅₀ values of deracoxib and flavanones for sGAG reduction (mean ± SEM, n=4).
^aSignificantly different from deracoxib (P<0.05).

Compound	IC ₅₀ (µg/ml)	IC ₅₀ (mM)
Deracoxib	2114.98 ± 177.66	5.32 ± 0.45
Hesperidin	1540.39 ± 143.26 ^a	2.52 ± 0.23 ^a
Hesperetin	1198.22 ± 94.66 ^a	3.96 ± 0.31 ^a
Naringin	1188.15 ± 95.05 ^a	2.05 ± 0.16 ^a
Naringenin	1990.47 ± 183.12	7.31 ± 0.67 ^a
Eriocitrin	2288.00 ± 201.34	3.83 ± 0.34 ^a
Eriodictyol	1895.25 ± 149.72 ^a	6.57 ± 0.52 ^a

4.4.1.5 Matrix Metalloproteinase-3

The reduction in matrix metalloproteinase-3 is presented in figure 4-7. The controls released a low amount of MMP-3 (0.033 ng/ml ± 0.007), while a remarkable increase (>2.5-fold) in the release of MMP-3 was observed after the treatment of samples with IL-1β (0.084 µM ± 0.003) (P<0.001). It was observed that all the flavanones exhibited a significant concentration-dependent reduction in MMP-3 production. Furthermore, hesperidin, hesperetin and eriodictyol were observed to reduce MMP-3 concentrations below baseline levels at concentrations higher than 50 µg/ml.

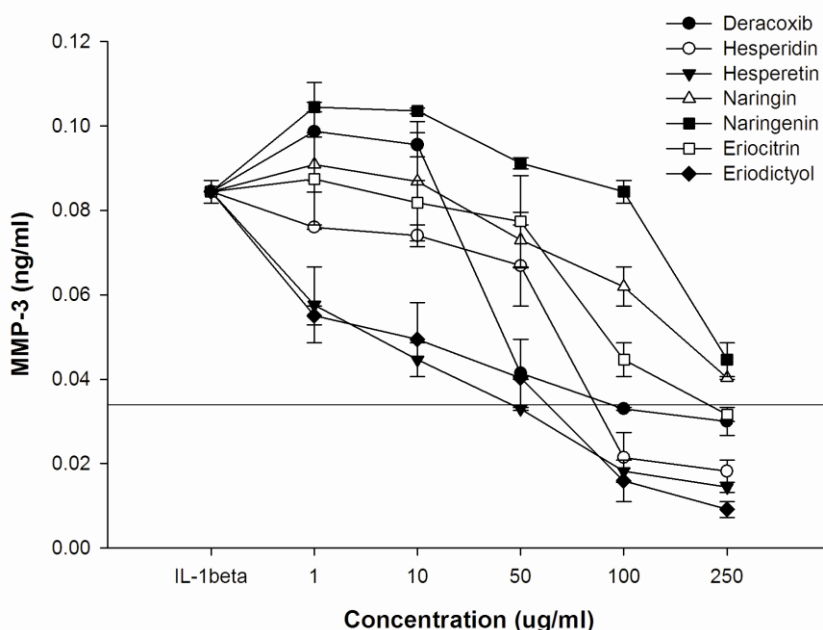


Figure 4-7: Matrix metalloproteinase-3 (MMP-3) production (means \pm SEM) in the cell culture medium from canine chondrocytes 72 h after the addition of the different flavanones and deracoxib as positive control at concentrations 1-250 μ g/ml with IL-1 β (100 μ l of 100 ng/ml). Values are expressed as ng/ml. The line represents the baseline level (chondrocytes without inflammatory insult).

All the flavanones (except naringin and naringenin) exhibited similar IC_{50} values than deracoxib (Table 4-5). It was observed that hesperetin and eriodictyol were more active than their glycosides, while the opposite was observed for naringenin. Similar results were obtained for the corrected IC_{50} values expressed in mM (Table 4-5). These results correlate with previous reports that have observed that hesperidin downregulates various matrix metalloproteinases (MMPs) (Balakrishnan *et al.*, 2007a; Balakrishnan *et al.*, 2007b).

Table 4-5: IC₅₀ values of deracoxib and flavanones for MMP-3 reduction (mean ± SEM, n=4).
^aSignificantly different from deracoxib (P<0.05).

Compound	IC ₅₀ (µg/ml)	IC ₅₀ (mM)
Deracoxib	124.94 ± 11.37	0.31 ± 0.03
Hesperidin	124.14 ± 10.43	0.20 ± 0.02 ^a
Hesperetin	122.44 ± 7.71	0.40 ± 0.02 ^a
Naringin	220.46 ± 17.42 ^a	0.38 ± 0.03
Naringenin	297.05 ± 23.76 ^a	1.09 ± 0.09 ^a
Eriocitrin	148.75 ± 12.20	0.25 ± 0.02
Eriodictyol	123.73 ± 11.88	0.43 ± 0.04 ^a

4.4.1.6 Tumor Necrosis Factor- α

The reduction in tumor necrosis factor- α is presented in figure 4-8. The untreated control samples released 7.45 pg/ml ± 0.28 in the cell culture medium. When the samples were treated with IL-1 β (10 ng/ml), a significant increase (18%) in TNF- α production was observed (8.80 pg/ml ± 0.07) (P=0.004). It was observed that all the flavanones exhibited a significant concentration-dependant reduction in TNF- α production. Furthermore, hesperetin, naringenin, and eriocitrin were observed to reduce TNF- α concentrations below baseline levels at concentrations higher than 50 µg/ml.

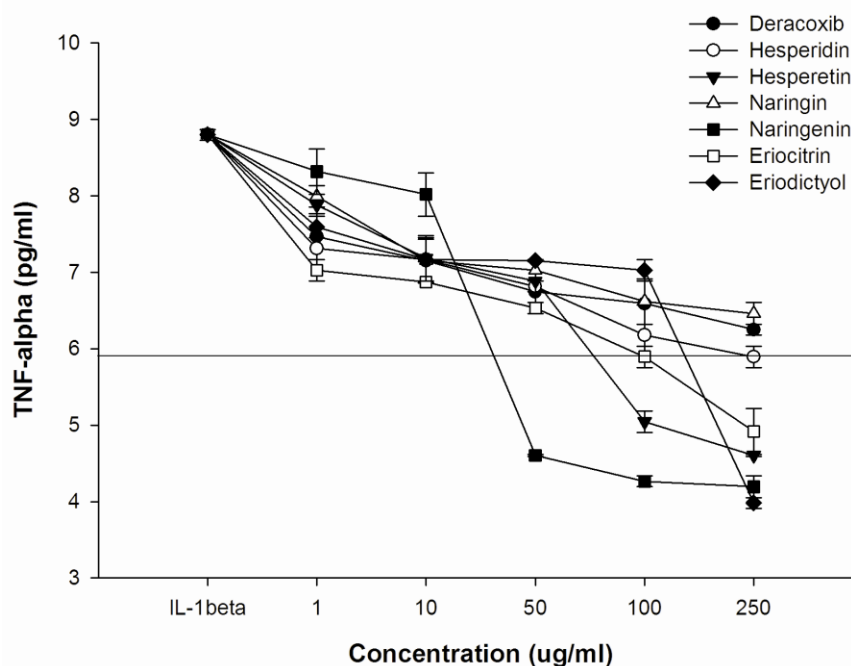


Figure 4-8: Tumor necrosis factor- α (TNF- α) production (means \pm SEM) in the cell culture medium from canine chondrocytes 72 h after the addition of the different flavanones and deracoxib as positive control at concentrations 1-250 μ g/ml with IL-1 β (100 μ l of 100 ng/ml). Values are expressed as pg/ml. The line represents the baseline level (chondrocytes without inflammatory insult).

All the flavanones (except hesperidin and naringin) exhibited lower IC₅₀ values than deracoxib (Table 4-6). It was also observed that the aglycones were more active than their corresponding glycosides. Similar results were obtained for the corrected IC₅₀ values expressed in mM (Table 4-6). These results correlate with previous reports that have observed that hesperidin (Yeh *et al.*, 2007), naringin (Kanno *et al.*, 2006a; Kawaguchi *et al.*, 2004), and eriodictyol (Ismaili *et al.*, 2002) downregulates the LPS-induced expression of different proinflammatory (TNF- α , IL-1 beta, IL-6) *in vivo*. Similar activities have also been observed *in vitro* for hesperidin in A549 cells (Yeh *et al.*, 2007), naringenin (1 mM) in RAW 264.7 mouse macrophage cells (Kanno *et al.*, 2006a), and eriodictyol in RAW 264.7 mouse macrophages as well (Xagorari *et al.*, 2001).

Table 4-6: IC₅₀ values of deracoxib and flavanones for TNF- α reduction (mean \pm SEM, n=4).
^aSignificantly different from deracoxib (P<0.05).

Compound	IC ₅₀ (μ g/ml)	IC ₅₀ (mM)
Deracoxib	506.68 \pm 33.44	1.27 \pm 0.08
Hesperidin	629.91 \pm 46.61 ^a	1.03 \pm 0.08 ^a
Hesperetin	239.73 \pm 20.38 ^a	0.79 \pm 0.07 ^a
Naringin	834.23 \pm 77.58 ^a	1.44 \pm 0.13
Naringenin	117.82 \pm 10.25 ^a	0.43 \pm 0.04 ^a
Eriocitrin	389.47 \pm 37.00 ^a	0.65 \pm 0.06 ^a
Eriodictyol	325.03 \pm 26.65 ^a	1.13 \pm 0.09

4.4.2 Cyclooxygenase-1 and -2 (COX-1 and COX-2) Inhibitory Activity

The selected flavanones were assessed for their COX-1 and COX-2 inhibitory activity using a commercially available ELISA assay. For the COX-1 assay, ibuprofen was employed as a positive control since it has inhibitory activity towards both COX isoforms. For the COX-2 assay, ibuprofen and etodolac were employed since etodolac is a specific COX-2 inhibitor. As shown in Figure 4-9, all the tested flavanones have a concentration-dependant inhibition of COX-1 activity and it can be observed that all the flavanones are more active than ibuprofen in this respect.

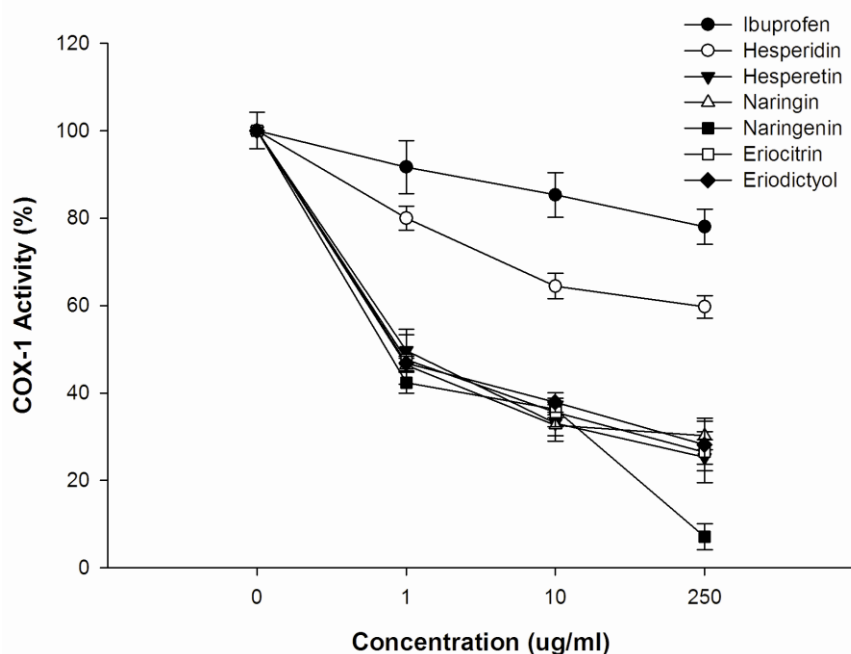


Figure 4-9: Cyclooxygenase-1 (COX-1) activity (means \pm SEM) after the addition of the different flavanones and ibuprofen as positive control at concentrations 1-250 μ g/ml. Values are expressed as percentage (%).

The IC_{50} values were also calculated and as show in Table 4-7, all the flavanones exhibited significantly lower IC_{50} values than ibuprofen indicating that they might be better COX-1 inhibitors than ibuprofen. Furthermore, it was observed that the aglycones were significantly more active than their corresponding glycosides. Similar results were observed when the IC_{50} values were reported as mM. These results are in agreement with previous reports that observed that eriodictyol extracted from the methanol fraction of the stem bark of *Populus davidiana* demonstrated moderate inhibition against COX-1 only and exhibited suppressive effects on xanthine oxidase (XO) (Zhang *et al.*, 2006a).

Table 4-7: IC₅₀ values of ibuprofen and flavanones for COX-1 inhibition (mean ± SEM, n=4).
^aSignificantly different from ibuprofen (P<0.05).

Compound	IC ₅₀ (µg/ml)	IC ₅₀ (mM)
Ibuprofen	1280.39 ± 121.64	6.207 ± 0.589
Hesperidin	608.79 ± 52.96 ^a	0.997 ± 0.086 ^a
Hesperetin	1.71 ± 0.13 ^a	0.006 ± 0.001 ^a
Naringin	148.17 ± 10.22 ^a	0.255 ± 0.018 ^a
Naringenin	35.64 ± 2.85 ^a	0.131 ± 0.010 ^a
Eriocitrin	389.47 ± 37.00 ^a	0.003 ± 0.001 ^a
Eriodictyol	1.66 ± 0.15 ^a	0.352 ± 0.026 ^a

In the case of the COX-2 inhibition assay, it was observed that all the flavanones exhibited similar inhibitory activity than ibuprofen and etodolac, with the exception of hesperidin that actually increased the activity of COX-2 (Figure 4-10). The observation with hesperidin correlates with studies that have observed that hesperidin can suppress the production of PGE₂, nitrogen dioxide (NO₂), and expression of iNOS protein, but it is ineffective in reducing the protein levels of COX-2 (Sakata *et al.*, 2003). However, all the other flavanones exhibited similar inhibitory activity to etodolac. This in agreement with observations that reported that naringenin (0.5-50 µM) can markedly decrease the PGE₂ release and COX-2 expression in a concentration-dependent manner (Raso *et al.*, 2001).

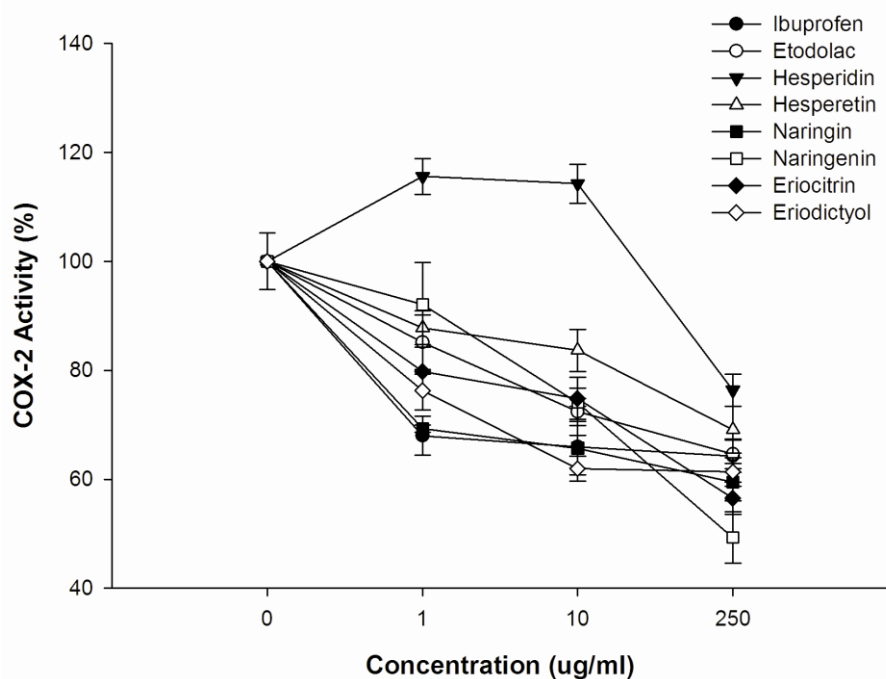


Figure 4-10: Cyclooxygenase-2 (COX-2) activity (means \pm SEM) after the addition of the different flavanones, ibuprofen and etodolac as positive control at concentrations 1-250 μ g/ml. Values are expressed as percentage (%).

The IC_{50} values were also calculated and as show in Table 4-8, all the flavanones exhibited significantly lower IC_{50} values than ibuprofen indicating that they might be better COX-2 inhibitors than ibuprofen. However, only hesperidin, naringenin, and eriocitrin reported lower IC_{50} values than etodolac, a COX-2 specific inhibitor. It was also observed that naringenin was the only aglycone that has higher activity than its glycoside. In the case of hesperidin and eriocitrin, both demonstrated higher activity than their aglycones. Similar results were observed when the IC_{50} values were reported as mM.

Table 4-8: IC₅₀ values of ibuprofen, etodolac, and flavanones for COX-2 inhibition (mean ± SEM, n=4). ^aSignificantly different from ibuprofen (P<0.05), ^bSignificantly different from etodolac (P<0.05).

Compound	IC ₅₀ (µg/ml)	IC ₅₀ (mM)
Ibuprofen	1057.11 ± 85.62 ^b	5.12 ± 0.41 ^b
Etodolac	694.87 ± 62.54 ^a	2.42 ± 0.22 ^a
Hesperidin	571.11 ± 37.12 ^{a,b}	0.93 ± 0.06 ^{a,b}
Hesperetin	765.97 ± 72.00 ^a	2.53 ± 0.24 ^a
Naringin	715.08 ± 42.90 ^{a,b}	1.23 ± 0.07 ^{a,b}
Naringenin	278.38 ± 21.99 ^{a,b}	1.02 ± 0.08 ^{a,b}
Eriocitrin	461.41 ± 38.76 ^{a,b}	0.77 ± 0.06 ^{a,b}
Eriodictyol	749.76 ± 68.98 ^{a,b}	2.60 ± 0.24 ^{a,b}

Furthermore, the COX-2 to COX-1 ratio was calculated in order to observe the preferential inhibitory activity for one of the COX isozymes involved primarily in inflammation. As shown in Figure 4-11, etodolac exhibited selective COX-2 inhibition, while ibuprofen exhibited selective COX-1 inhibition. All the other flavanones exhibited higher inhibition of COX-2 (COX-2 to Cox-1 ration values between 1.5 and 3) but not as high as the inhibition values for etodolac. These results correlate with previous observations that indicate that these compounds have COX-2 inhibitory activity (Raso *et al.*, 2001; Sakata *et al.*, 2003), while only eriodictyol has been reported to partially inhibit COX-1 at high concentrations (Zhang *et al.*, 2006a).

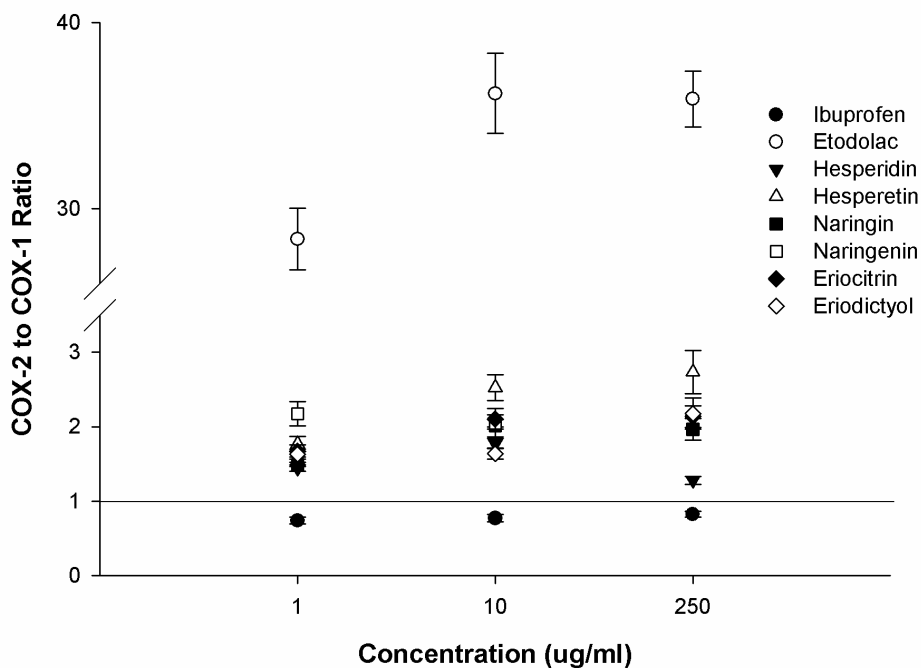


Figure 4-11: Cyclooxygenase-2 (COX-2) to cyclooxygenase-1 (COX-1) ratio (means \pm SEM) of the different flavanones, ibuprofen and etodolac as positive control at concentrations 1-250 $\mu\text{g/ml}$. Values are expressed as percentage (%). The line represents a ratio of 1 that would indicate equal inhibitory activity for both COX isomers.

4.4.3 Inflammatory Bowel Activity

The studied flavanones were assessed for their inflammatory bowel activity in an *in vitro* colitis-induced model. It was observed that all the flavanones exhibited a concentration-dependant reduction in PGE_2 concentrations, and at concentrations higher than 100 $\mu\text{g/ml}$ there is a significant reduction in PGE_2 concentration even below the baseline level (Figure 4-12).

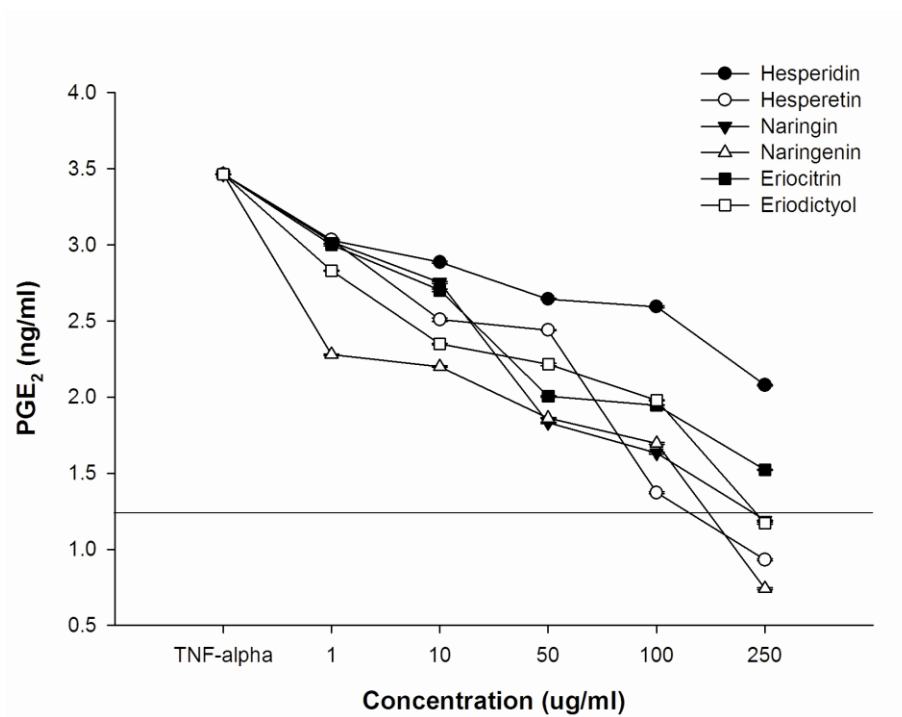


Figure 4-12: Prostaglandin E₂ (PGE₂) production (means \pm SEM) in the cell culture medium from colorectal adenocarcinoma (HT-29) cells after the addition of the different flavanones at concentrations 1-250 μ g/ml with TNF- α (100 μ l of 100 ng/ml). Values are expressed as ng/ml. The line represents the baseline level (HT-29 cells without inflammatory insult).

The IC₅₀ values were also calculated and as shown in Table 4-9 only hesperetin was significantly more active than its glycoside hesperidin. The other glycosides and aglycone demonstrated similar activities in reducing PGE₂ levels. These results correlate to previous observations that hesperidin suppresses the production of PGE₂ (Sakata *et al.*, 2003), and that hesperetin and hesperidin in the concentration range 250-500 μ M can inhibit the expression of COX-2 gene (Hirata *et al.*, 2005). Similarly, naringenin (0.5-50 μ M) was observed to be a cause a concentration-dependant reduction in PGE₂ release and COX-2 expression (Raso *et al.*, 2001).

Table 4-9: IC₅₀ values of the different flavanones for PGE₂ reduction (mean ± SEM, n=4).
^aSignificantly different from its corresponding glycoside (P<0.05).

Compound	IC ₅₀ (µg/ml)	IC ₅₀ (mM)
Hesperidin	457.79 ± 39.39	0.74 ± 0.06
Hesperetin	99.07 ± 7.83 ^a	0.33 ± 0.02 ^a
Naringin	99.35 ± 6.85	0.17 ± 0.01
Naringenin	112.96 ± 9.04	0.41 ± 0.03 ^a
Eriocitrin	166.64 ± 15.16	0.28 ± 0.02
Eriodictyol	161.68 ± 11.96	0.56 ± 0.04 ^a

4.4.4 Anti-Adipogenic Activity

4.4.4.1 Hesperidin and Hesperetin

The effects of hesperidin and hesperetin on oil red O stained material (OROSM) in 3T3-L1 pre-adipocytes are shown in Figure 4-13B. On the 8th day, the mature 3T3-L1 pre-adipocytes accumulated intracellular triglyceride lipids within their cellular structure (Figure 4-13A) that was lysed liberating these intracellular triglycerides that were stained by oil red O. Thus, a reduction on the oil red O stained material (OROSM) would indicate a reduction in intracellular triglyceride formation and accumulation. It can be observed that hesperidin is ineffective, while hesperetin caused a concentration-dependant reduction in intracellular triglycerides. These results are in agreement with other reports that have observed that hesperidin (50-250 µM or 30-150 µg/ml) doesn't reduce the OROSM in the same 3T3-L1 pre-adipocyte model (Hsu *et al.*, 2007).

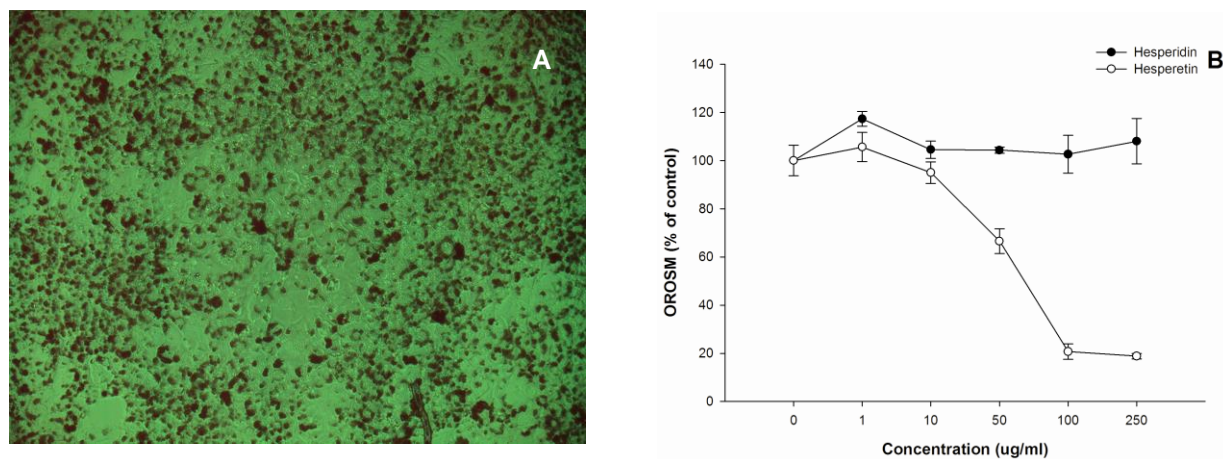


Figure 4-13: Effects of flavanones on oil red O stained material (OROSM) in 3T3-L1 pre-adipocytes. 3T3-L1 pre-adipocytes were harvested 8 days after the initiation of differentiation and were stained with oil red O (A). Cells were treated with 0–250 µg/ml of hesperidin or hesperetin (B) for 72 h at 37°C in a humidified 5% CO₂ incubator. Cells were stained with oil red O (means ± SEM).

4.4.4.2 Naringin and Naringenin

The effects of naringin and naringenin on oil red O stained material (OROSM) in 3T3-L1 pre-adipocytes are shown in Figure 4-14. It can be observed that naringin is ineffective, while hesperetin caused a concentration-dependant reduction in intracellular triglycerides. These results are in agreement with other reports that have observed that naringin (50-250 µM or 30-150 µg/ml) doesn't reduce the OROSM in the same 3T3-L1 pre-adipocyte model (Hsu *et al.*, 2007). However, the same group observed the same lack of effect for naringenin in the same concentration range (Hsu *et al.*, 2007); however, we observed considerable activity for naringenin in inhibiting OROSM (Figure 4-14).

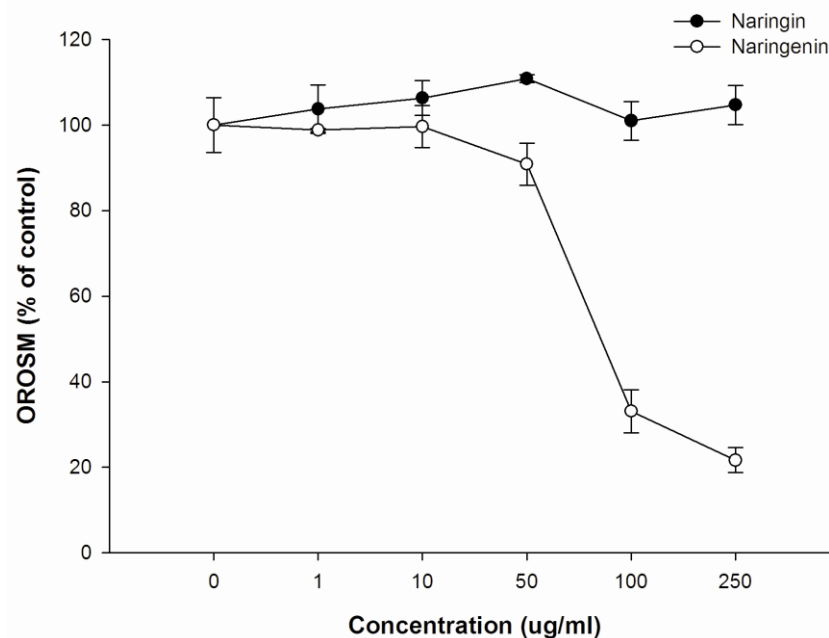


Figure 4-14: Effects of flavanones on oil red O stained material (OROSM) in 3T3-L1 pre-adipocytes. 3T3-L1 pre-adipocytes were harvested 8 days after the initiation of differentiation and were stained with oil red O. Cells were treated with 0–250 $\mu\text{g/ml}$ of naringin or naringenin for 72 h at 37°C in a humidified 5% CO_2 incubator. Cells were stained with oil red O (means \pm SEM).

4.4.4.3 Eriocitrin and Eriodictyol

The effects of eriocitrin and eriodictyol on oil red O stained material (OROSM) in 3T3-L1 pre-adipocytes are shown in Figure 4-15. It can be observed that eriocitrin is ineffective, while eriodictyol caused a concentration-dependant reduction in intracellular triglycerides.

The IC_{50} values for the selected flavanones were also calculated as shown in Table 4-10, and it was observed that hesperetin and eriodictyol were more active than naringenin and because there was no reduction induced by the glycosides, the IC_{50} values could not be determined.

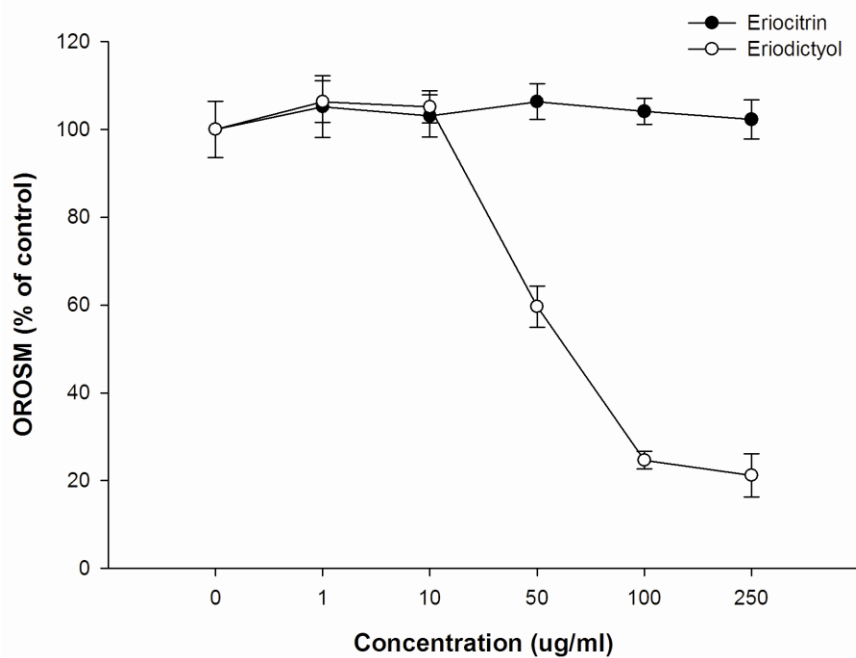


Figure 4-15: Effects of flavanones on oil red O stained material (OROSM) in 3T3-L1 pre-adipocytes. 3T3-L1 pre-adipocytes were harvested 8 days after the initiation of differentiation and were stained with oil red O. Cells were treated with 0–250 $\mu\text{g/ml}$ of eriocitrin or eriodictyol for 72 h at 37°C in a humidified 5% CO_2 incubator. Cells were stained with oil red O (means \pm SEM).

Table 4-10: IC_{50} values of the different flavanones for OROSM reduction (mean \pm SEM, $n=4$). NA = not applicable.

Compound	IC_{50} ($\mu\text{g/ml}$)	IC_{50} (mM)
Hesperidin	NA	NA
Hesperetin	53.69 ± 4.24	0.18 ± 0.01
Naringin	NA	NA
Naringenin	92.56 ± 7.40	0.34 ± 0.03
Eriocitrin	NA	NA
Eriodictyol	53.45 ± 3.95	0.18 ± 0.01

4.4.5 Anti-Cancer Activity

4.4.5.1 Hesperidin and Hesperetin

The cytotoxic effects of hesperidin and hesperetin on different cancer cells lines are presented in Figure 4-16A and 4-16B. It can be observed that uniformly in the different cancer cell lines tested, hesperetin was more active than its corresponding glycoside hesperidin.

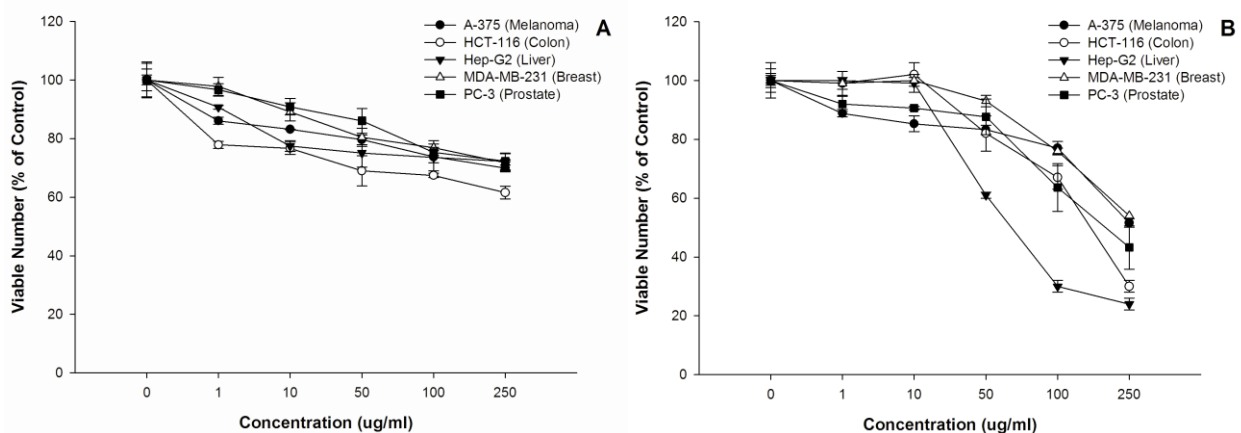


Figure 4-16: Effects of hesperidin (A) and hesperetin (B) in the viability of different cancer cell lines (means \pm SEM).

4.4.5.2 Naringin and Naringenin

The cytotoxic effects of naringin and naringenin on different cancer cells lines are presented in Figure 4-17A and 4-17B. It can be observed that in parallel across the different cancer cell lines tested, naringenin was more active than its corresponding glycoside naringin. However, naringin exhibited similar activity in reducing the number of viable prostate adenocarcinoma (PC-3) cells.

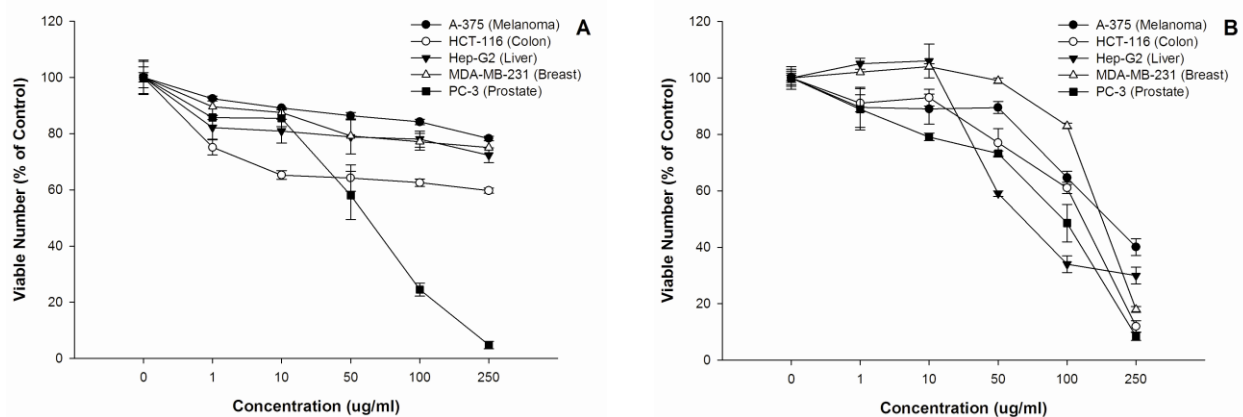


Figure 4-17: Effects of naringin (A) and naringenin (B) in the viability of different cancer cell lines (means \pm SEM).

4.4.5.3 Eriocitrin and Eriodictyol

The cytotoxic effects of eriocitrin and eriodictyol on different cancer cells lines are presented in Figure 4-18A and 4-18B. It can be observed that an analysis of the different cancer cell lines tested demonstrates eriodictyol was more active than its corresponding glycoside eriocitrin.

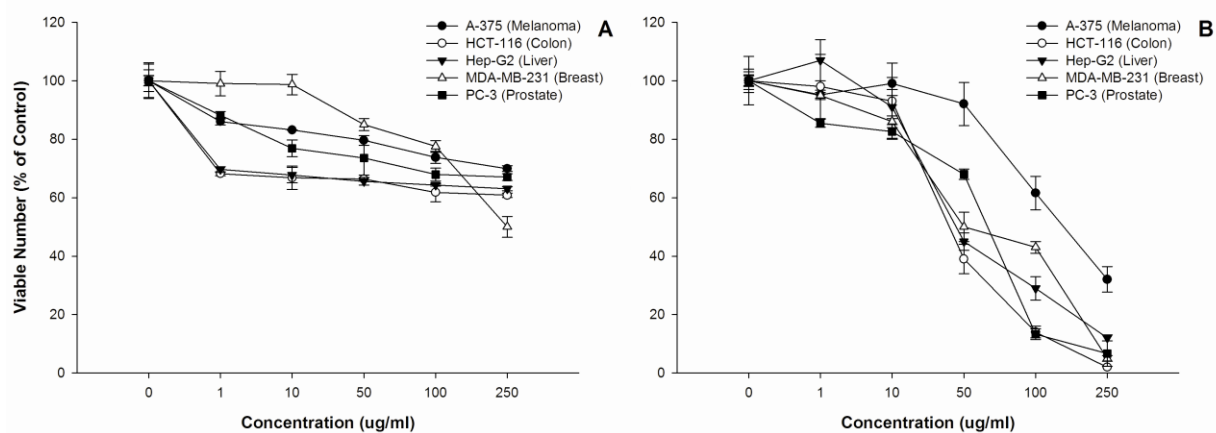


Figure 4-18: Effects of eriocitrin (A) and eriodictyol (B) in the viability of different cancer cell lines (means \pm SEM).

4.4.5.4 Determination of IC₅₀ values

The IC₅₀ values of the racemic flavanones in the different cell lines were calculated as shown in Table 4-11. The IC₅₀ values were compared to 5-fluorouracil (5-FU), a widely used chemotherapeutic agent employed in treatment of different cancers, particularly liver, breast, and colon under the trade name Adrucil® also available in generic. 5-FU was tested and assessed side by side with the flavanones. The different flavanones were assessed in regular canine chondrocytes and human umbilical vein endothelial cells (HUVEC) and no cytotoxicity was observed in the range tested (Figure 2-1). It was observed that 5-FU has very low IC₅₀ values across the different cell lines indicating their potency as a chemotherapeutic agent. The flavanones exhibited higher IC₅₀ values than 5-FU in all the cancer cell lines, except HepG2 in which hesperetin, naringenin, and eriodictyol actually exhibited lower IC₅₀ values than 5-FU indicating better activity. In all the different cell lines, the aglycones exhibited higher activity than their corresponding glycosides. The only exception was observed in prostate adenocarcinoma (PC-3) cells where naringin actually was more active than naringenin.

The obtained IC₅₀ values are in agreement with previous reports. For instance, hesperidin (100 µM or about 60 µg/ml) has been shown to reduce cell viability by $65 \pm 0.05\%$ of human colon cancer cells, SNU-C4 (Park *et al.*, 2007), our results indicate that hesperidin (50 µg/ml) induce a reduction in cell viability of human colon cancer cells, HCT-116 by $68.97\% \pm 5.17\%$. Furthermore, hesperetin has been reported to have an IC₅₀ of 22.5 µg/ml for human breast carcinoma cell line, MDA-MB-435 (So *et al.*, 1996), while we obtained a higher IC₅₀ of 295 ± 41 µg/ml for MDA-MB-231. In the case of naringenin it has been observed to inhibit cell proliferation of HT29 colon cancer cells at concentrations higher than 0.71 mM or about 193

$\mu\text{g/ml}$ (Frydoonfar *et al.*, 2003). Our results indicate that naringenin at 250 $\mu\text{g/ml}$ reduce cell viability by more than 88%.

Furthermore, naringenin have IC_{50} values of 20 $\mu\text{g/ml}$ for the human breast carcinoma cell line, MDA-MB-435 (So *et al.*, 1996). We obtained higher IC_{50} values of 175 ± 22 $\mu\text{g/ml}$ for MDA-MB-231. However, it needs to be mentioned that each cancer cell line within the same type of cancer is different in nature and to make a direct comparison between them is not possible but the previous reports indicate that our results are within the range previously reported.

Similarly, eriodictyol has been reported to have low IC_{50} of 12, 10, 8.3, and 6.2 μM (1-3 $\mu\text{g/ml}$) in human lung carcinoma (A549), melanin pigment producing mouse melanoma (B16 melanoma 4A5), human T-cell leukemia (CCRF-HSB-2), and lymph node metastasized (TGBC11TKB) respectively (Kawaii *et al.*, 1999a). Even though, these cell lines were not tested in all the tested cell lines eriodictyol exhibited the lowest IC_{50} values compared to the other aglycones. This finding is very interesting indeed since eriodictyol was found to be the aglycone with the highest activity and it has 3 hydroxyl (OH) groups, the second most active flavanone is naringenin that has 2 OH groups, and the least effective flavanone, hesperetin, has only one OH group. In this limited sample, a correlation between the number of hydroxyl groups and the anti-cancer activity may be made. The same indirect correlation phenomena can also be observed for the selected flavanone glycosides examines.

4.4.5.5 Flavanone Enantiomers

The cytotoxic effects of collected pure hesperetin, naringenin, and eriodictyol enantiomers in hepatoma (HepG2) cells are presented in Figure 4-19A, 4-19B and 4-19C.

Table 4-11: IC₅₀ values (µg/ml) of the racemic hesperetin, naringenin, and eriodictyol, and 5-FU as positive control across different cancer cell lines (mean ± SEM, n=4). ^aSignificantly different from 5-FU (P<0.05). The values in parenthesis indicate IC₅₀ values in µM.

Compound	Melanoma (A-375)	Colon (HCT-116)	Hepatoma (HepG2)	Breast (MDA-MB-231)	Prostate (PC-3)
5-FU	1.81 ± 0.21 (0.014 ± 0.002)	2.53 ± 0.32 (0.019 ± 0.002)	45.1 ± 2.2 (0.347 ± 0.017)	12.7 ± 1.4 (0.098 ± 0.01)	15.5 ± 3.1 (0.12 ± 0.02)
Hesperidin	810 ± 86 ^a (1.33 ± 0.14) ^a	610 ± 76 ^a (0.99 ± 0.12) ^a	995 ± 117 ^a (1.63 ± 0.19) ^a	899 ± 87 ^a (1.47 ± 0.14) ^a	990 ± 110 ^a (1.62 ± 0.18) ^a
Hesperetin	270 ± 38 ^a (0.89 ± 0.13) ^a	180 ± 25 ^a (0.59 ± 0.08) ^a	74.3 ± 10.1 ^a (0.25 ± 0.03) ^a	295 ± 41 ^a (0.98 ± 0.13) ^a	218 ± 21 ^a (0.72 ± 0.07) ^a
Naringin	920 ± 52 ^a (1.58 ± 0.09) ^a	445 ± 56 ^a (0.77 ± 0.09) ^a	860 ± 43 ^a (1.48 ± 0.07) ^a	889 ± 33 ^a (1.53 ± 0.06) ^a	61 ± 19 ^a (0.10 ± 0.03)
Naringenin	182 ± 43 ^a (0.67 ± 0.16) ^a	130 ± 14 ^a (0.48 ± 0.05) ^a	62 ± 9 ^a (0.23 ± 0.03) ^a	175 ± 22 ^a (0.64 ± 0.08) ^a	93 ± 8 ^a (0.34 ± 0.03) ^a
Eriocitrin	557 ± 45 ^a (0.93 ± 0.07) ^a	470 ± 40 ^a (0.79 ± 0.07) ^a	482 ± 55 ^a (0.81 ± 0.09) ^a	265 ± 31 ^a (0.44 ± 0.05) ^a	495 ± 42 ^a (0.83 ± 0.07) ^a
Eriodictyol	169 ± 28 ^a (0.59 ± 0.09) ^a	43 ± 10 ^a (0.15 ± 0.03) ^a	45 ± 9 (0.16 ± 0.03) ^a	66 ± 23 ^a (0.22 ± 0.08) ^a	68 ± 19 ^a (0.23 ± 0.07) ^a

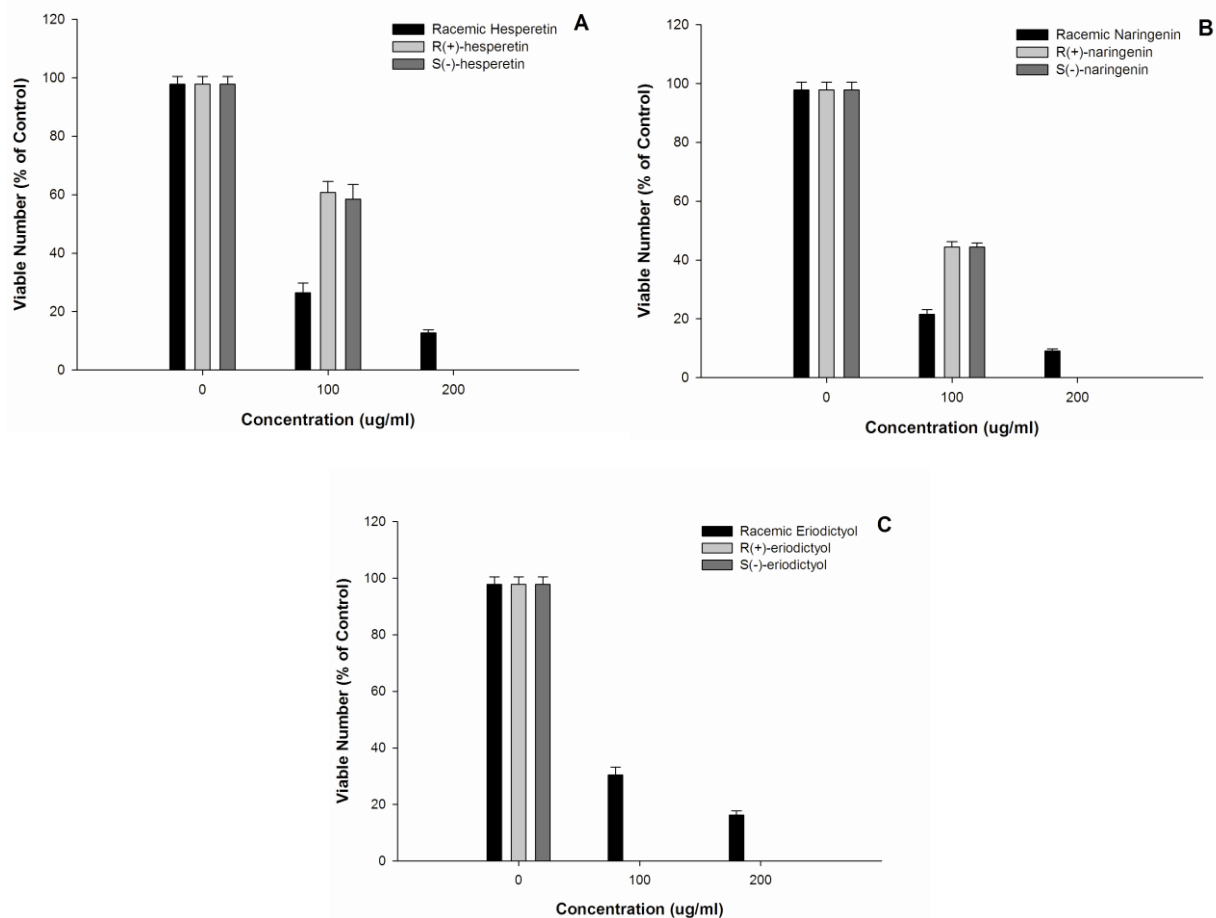


Figure 4-19: Effects of collected hesperetin enantiomers (A), naringenin enantiomers (B), and eriodictyol enantiomers (C) in the viability of hepatoma (HepG2) cells (means \pm SEM). At concentration 100 $\mu\text{g/ml}$, the racemic flavanone is a sum of 50 $\mu\text{g/ml}$ of R(+)-enantiomer and 50 $\mu\text{g/ml}$ of S(-)-enantiomer; while each pure enantiomer was at 100 $\mu\text{g/ml}$. At concentration 200 $\mu\text{g/ml}$, the racemic flavanone is a sum of 100 $\mu\text{g/ml}$ of R(+)-enantiomer and 100 $\mu\text{g/ml}$ of S(-)-enantiomer; while the pure enantiomers were not tested at these concentrations.

In the case of hesperetin (Figure 4-19A), it can be observed that racemic hesperetin provides a concentration-dependant decrease in HepG2 cell viability. Furthermore, the collected pure enantiomers exhibit similar reduction in cell viability. For instance, R(+)-hesperetin reduced the cell viability to $60.76\% \pm 3.76\%$, while the S(-)-enantiomer decreased it to $58.46\% \pm 5.08\%$. This indicates a reduction in cell viability of 39.24% and 41.54% for R(+)- and S(-)-hesperetin respectively. These results are at the concentration of 100 $\mu\text{g/ml}$ for each

enantiomers; thus, a racemic mixture will equal 200 µg/ml. It can be observed that the racemic mixture at 200 µg/ml reduced cell viability by 87.3%. Therefore, it can be observed that hesperetin enantiomers have less activity when they are separate (39.24% and 41.54% reduction for R(+)- and S(-)-hesperetin respectively) than in equivalent racemic mixture (87.3% reduction). Thus, it can be observed that when both enantiomers are in a racemic mixture additive effects may be evident.

Similar effects were observed for naringenin (Figure 4-19B), where it can be observed that racemic naringenin also provides a concentration-dependant decrease in HepG2 cell viability. The collected pure enantiomers exhibit similar reduction in cell viability. For instance, R(+)-naringenin reduced the cell viability to $44.39\% \pm 1.86\%$, while the S(-)-enantiomer decreased it to $44.19 \pm 1.32\%$. This indicates a reduction in cell viability of 55.61% and 55.81% for R(+)- and S(-)-naringenin respectively. These results are at the concentration of 100 µg/ml for each enantiomers; thus, a racemic mixture will equal 200 µg/ml. It can be observed that the racemic mixture at 200 µg/ml reduced cell viability by 90.88%. Therefore, it can be observed that naringenin enantiomers have less activity when they are administered separately (55.61% and 55.81% reduction for R(+)- and S(-)-naringenin respectively) than in equivalent racemic mixture (90.88% reduction). Thus, it can be observed that when both enantiomers are in a racemic mixture there might be some additive effects between enantiomers.

However, in the case of eriodictyol (Figure 4-19C), a different observation was apparent. The collected pure enantiomers exhibit similar reduction in cell viability. For instance, R(+)-eriodictyol reduced the cell viability to $0.051\% \pm 0.001\%$, while the S(-)-enantiomer decreased it to $0.014\% \pm 0.001\%$. This indicates a reduction in cell viability of 99.949% and 99.986% for R(+)- and S(-)-eriodictyol respectively. These results are at the concentration of 100 µg/ml for

each enantiomers; thus, a racemic mixture will equal 200 µg/ml. It can be observed that the racemic mixture at 200 µg/ml reduced cell viability by 83.71%. Therefore, it can be observed that eriodictyol enantiomers have significant more activity when they are separate (99.949% and 99.986% reduction for R(+)- and S(-)-eriodictyol respectively) than in an equivalent racemic mixture (83.71% reduction). Thus, it can be observed that when both enantiomers are in a racemic mixture there might be some antagonistic effects between antipodes.

These observations constitute the first and only evaluation of pure flavanone enantiomers in the literature for their capacity to inhibit cancer cells, in this case hepatoma (HepG2) cells. Since the pure enantiomers are not commercially available, manual collection and purification of pure enantiomers is necessary. This is a very labor intensive and time consuming task that allowed us only to test one concentration in only one cancer cell line. However, our results indicate that there may be differences between enantiomers, when the enantiomers are separate and stereochemically pure and when they are in a racemic mixture. Clearly, further experiments are necessary to assess enantiospecific effects employing different concentrations and in more cancer cell lines and other model systems.

4.4.6 Anti-Oxidant Capacity

4.4.6.1 Hesperidin and Hesperetin

The Trolox® equivalent anti-oxidant capacity (TEAC) of hesperidin and hesperetin is presented in Figure 4-20. It can be observed that there is a concentration-dependant TEAC and that hesperetin is more active in scavenging the ABTS radical than its corresponding glycoside hesperidin.

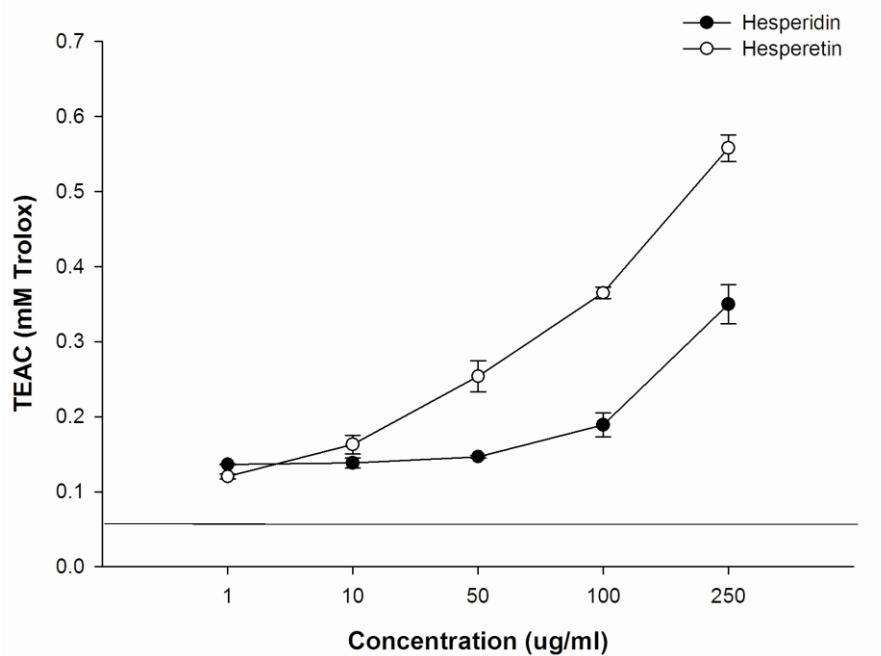


Figure 4-20: Trolox® equivalent anti-oxidant capacity (TEAC) of hesperidin and hesperetin (means \pm SEM).

4.4.6.2 Naringin and Naringenin

The Trolox® equivalent anti-oxidant capacity (TEAC) of naringin and naringenin is presented in Figure 4-21. It can be observed that there is a concentration-dependant TEAC and that naringenin is more active in scavenging the ABTS radical than its corresponding glycoside naringin.

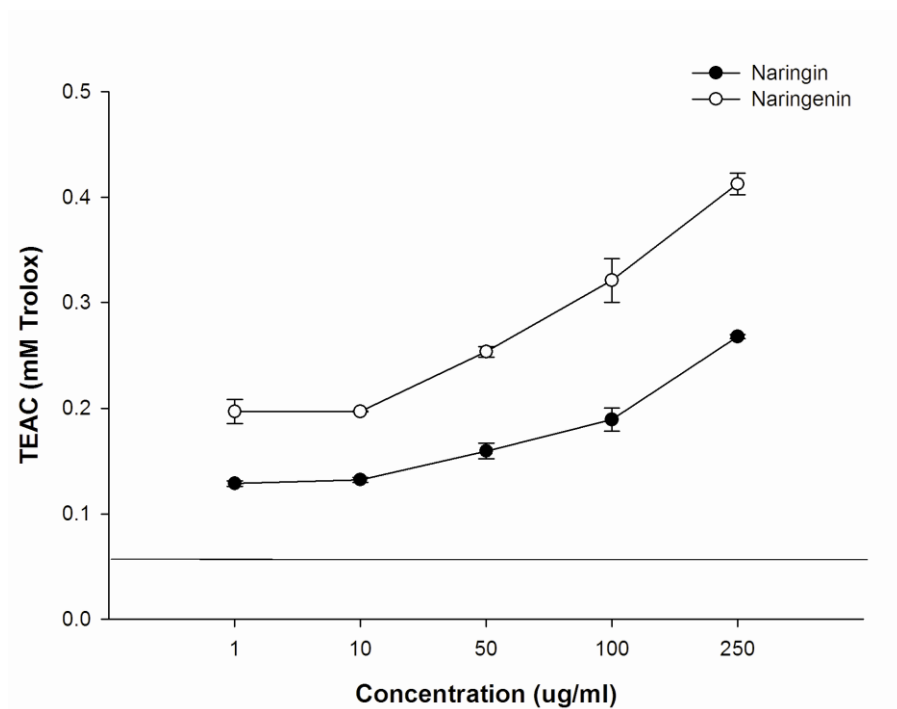


Figure 4-21: Trolox® equivalent anti-oxidant capacity (TEAC) of naringin and naringenin (means \pm SEM).

4.4.6.3 Eriocitrin and Eriodictyol

The Trolox® equivalent anti-oxidant capacity (TEAC) of eriocitrin and eriodictyol is presented in Figure 4-22. It can be observed that there is a concentration-dependant TEAC and that eriodictyol is more active in scavenging the ABTS radical than its corresponding glycoside eriocitrin.

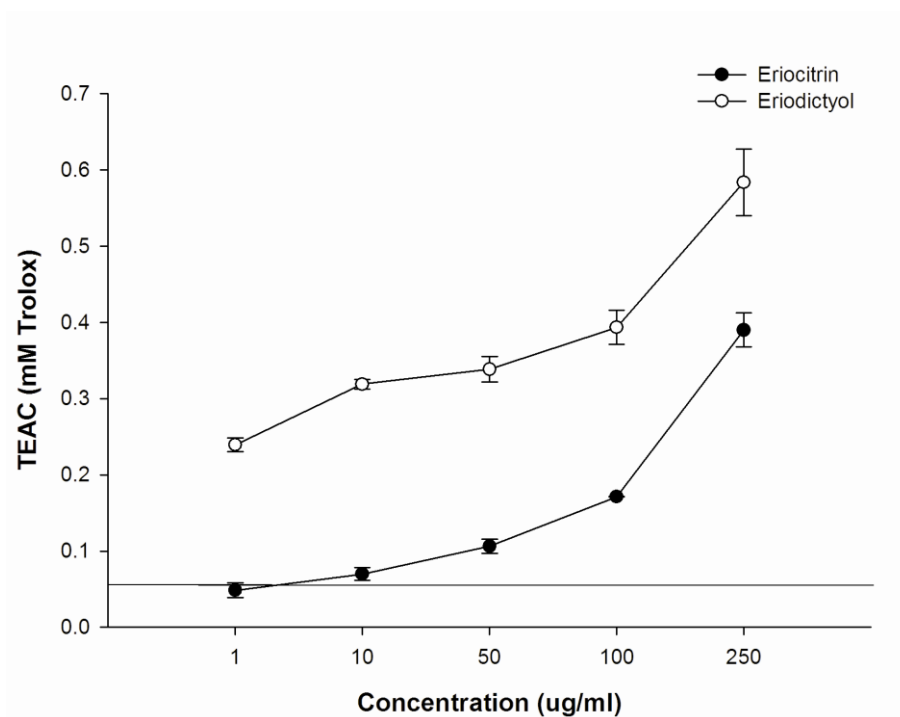


Figure 4-22: Trolox® equivalent anti-oxidant capacity (TEAC) of eriocitrin and eriodictyol (means \pm SEM).

The IC_{50} values of the racemic flavanones to inhibit ABTS radical formation are presented in Table 4-12. The IC_{50} values were compared to α -tocopherol, a widely recognized anti-oxidant. α -tocopherol was tested and assessed side by side with the flavanones. It was observed that the aglycones exhibited higher anti-oxidant capacity than the glycosides and the only flavanone that exhibited higher anti-oxidant capacity than α -tocopherol was eriodictyol. It was observed that eriodictyol was the most active flavanone and that similar structure-activity relationships between the number of hydroxyl groups and anti-oxidant capacity exist, which parallel the observations of the anti-cancer activity. Similar results were observed for the anti-radical efficiency (AE) values.

Table 4-12: IC₅₀ (μg/ml) and anti-radical efficiency values (AE) (μg/ml)⁻¹ values of the racemic hesperetin, naringenin, and eriodictyol, and α-tocopherol as positive control (mean ± SEM, n=4). ^aSignificantly different from α-tocopherol.

Compound	IC ₅₀ value	AE value
α-tocopherol	69.35 ± 3.43	14.42 ± 0.71
Hesperidin	249.69 ± 11.29 ^a	4.00 ± 0.18 ^a
Hesperetin	109.91 ± 5.21 ^a	9.10 ± 0.43 ^a
Naringin	376.45 ± 11.21 ^a	2.66 ± 0.08 ^a
Naringenin	153.25 ± 5.22 ^a	6.52 ± 0.22 ^a
Eriocitrin	217.71 ± 20.13 ^a	4.59 ± 0.42 ^a
Eriodictyol	53.67 ± 2.55 ^a	18.63 ± 0.88 ^a

4.4.6.4 Comprehensive Anti-Oxidant Method

4.4.6.4.1 Percent Hydrolysis of Glycosides

Polyphenols can be found as aglycone and glycosides (with one or more sugars attached). Different analytical techniques such as HPLC and GC alone and coupled to MS can detect either one form or the other or both found simultaneously. Furthermore, different enzymes can be used to hydrolyze the sugar moiety and convert a glycoside to its aglycone form. β-glucosidase from almonds is one of these enzymes that can specifically hydrolyze β-glycosides into aglycones (Ismail *et al.*, 2005; Zhang *et al.*, 2006b). Thus, in order to assess its efficacy in hydrolyzing glycosides, quercitrin, rutin, and phloridzin were hydrolyzed to their corresponding aglycones. Quercitrin is the 3-O-rhamnoside of quercetin, while rutin is the 3-O-rutinoside of quercetin. Phloridzin is the 2'-O-glucoside of phloretin. Thus, three different sugar moieties in different substitution positions were assessed. The concentrations of the

glycosides and the aglycones were monitored simultaneously employing a previously described LC-MS-ESI method (Schieber *et al.*, 2001) with some modifications. It was observed that incubation of the glycosides with 20 μ l of β -glucosidase from almonds (750 U/ml) at 37°C for 48 h (Ismail *et al.*, 2005; Zhang *et al.*, 2006b) caused their significant conversion to their corresponding aglycones. For instance, 82% of phloridzin was converted to phloretin, while 79% of quercitrin and 72% of rutin were converted to quercetin. Similar amounts of conversion using the same enzyme and similar incubation conditions have been reported for isoflavones (Ismail *et al.*, 2005). Thus, the enzyme and incubation conditions were significant to allow significant conversion of the glycosides to their aglycone forms.

4.4.6.4.2 LC-MS-ESI Analysis

The method described by Schieber *et al.* (Schieber *et al.*, 2001) and our modified method allows the separation of 26 phenolic compounds. However, of these polyphenols only 8 phenolic compounds were the main compounds identified in apples. As shown in Figure 4-23A, baseline separation and resolution were achieved for all the compounds. ESI mass spectra were recorded in the negative ion mode having optimal ionization. The limit of detection for all the compounds was 50 ng/ml and the CV% for the different compounds ranged from 7-11%. Figure 4-23B represents the chromatogram of the different phenolic constituents identified in organic red delicious apple skin. All the different apple tissue samples with the different extraction solvents with and without enzymatic hydrolysis exhibited similar chromatograms.

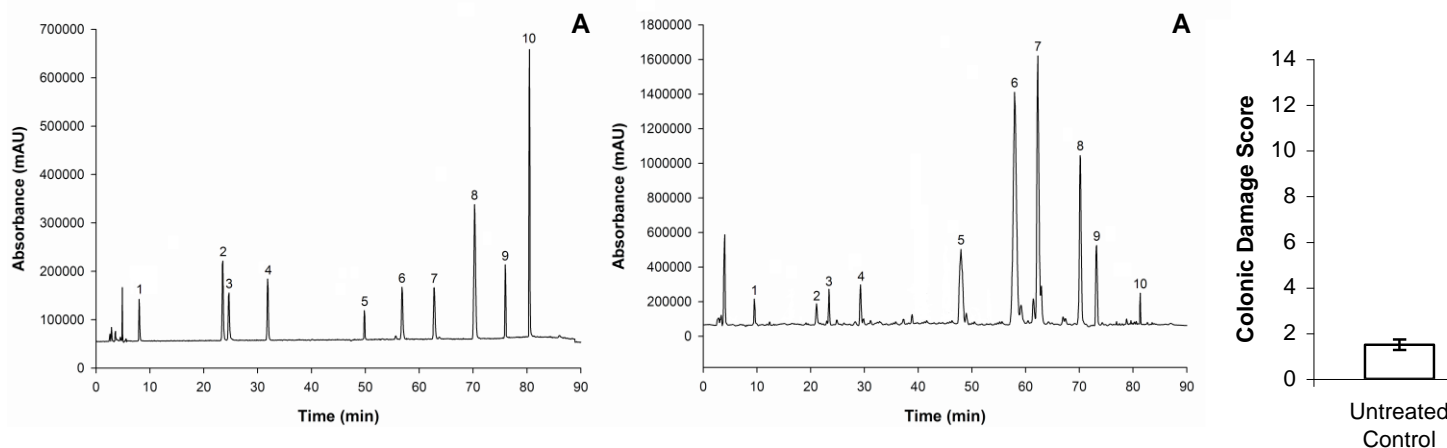


Figure 4-23: Chromatogram of (A) standard mixture of phenolic compounds (10 $\mu\text{g}/\text{ml}$ of each compound) and daidzein (internal standard, IS) by liquid chromatography (LC) (280 nm) (B) red delicious apple skin. 1=Gallic acid, 2=Catechin, 3=Chlorogenic acid, 4=epicatechin, 5=quercetin-3-rutinoside (rutin), 6=quercetin-3-rhamnoside (quercitrin), 7=phloridzin, 8=daidzein (IS), 9=quercetin, and 10=phloretin.

The LC-MS-ESI method was employed to monitor the conversion of the glycosides to the aglycone form. As shown in Figure 4.24A-E, the concentrations of rutin, quercitrin, and phloridzin (glycosides) significantly decrease, while the concentrations of quercetin and phloretin (aglycones) increase after enzymatic hydrolysis in all the apple tissues independently of the fraction assessed. It can also be observed that the percentage of conversion of glycosides into aglycone is not as high as obtained with the pure polyphenols. This might be due to the complexity of the apple matrix that will contain other components such as protein, fiber, carbohydrates, vitamins, and others that might interfere with the hydrolysis and enzyme access to the substrates.

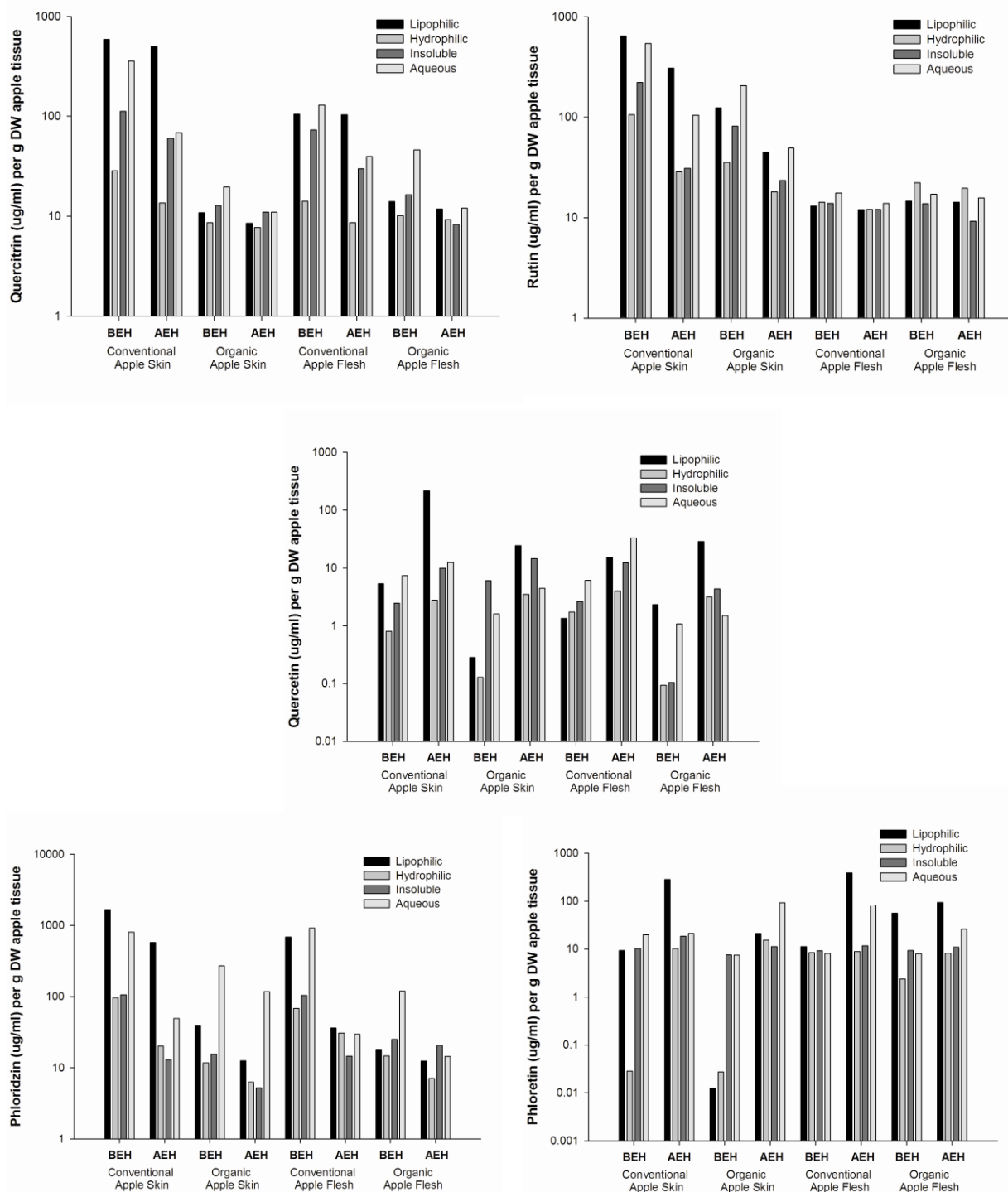


Figure 4-24: Concentrations ($\mu\text{g/ml}$) of (A) quercitrin, (B) rutin, (C) quercetin, (D) phloridzin, and (E) phloretin in conventional and organic apples skin and flesh before enzymatic hydrolysis (BEH) and after enzymatic hydrolysis (AEH), (mean \pm SEM, $n=3$).

4.4.6.4.3 Anti-Oxidant Capacity of Pure Compounds

The developed comprehensive anti-oxidant method allows the assessment of the contribution of the lipophilic, hydrophilic, and insoluble (if available) fractions as well as the fraction after enzymatic hydrolysis to the total anti-oxidant capacity. The anti-oxidant capacity of phloridzin, phloretin, quercitrin, rutin, and quercetin was assessed. As shown in Figure 4-25, the hydrophilic fraction contributes the majority of the Trolox® equivalent anti-oxidant capacity (TEAC) of all the compounds, while the lipophilic fraction still contributes a significant portion of the total TEAC. It is interesting to note the really small contribution of the aqueous fraction (methanol extraction) to the total TEAC since methanol is a solvent widely used in anti-oxidant methodology (Cai *et al.*, 2004; Hu *et al.*, 2000; Panico *et al.*, 2005; Pellati *et al.*, 2004; Proestos *et al.*, 2005; Sudjaroen *et al.*, 2005; Wang *et al.*, 1999). Furthermore, it can be noted that the hydrophilic TEAC significantly increased in all the compounds after enzymatic hydrolysis with the exception of quercitrin and rutin. On the other hand the lipophilic TEAC increased after enzymatic hydrolysis in all the compounds tested, while the aqueous TEAC was not affected by enzymatic hydrolysis (Table 4-13). The changes in hydrophilic and lipophilic TEAC are believed to be due to changes in compound solubility after enzymatic hydrolysis.

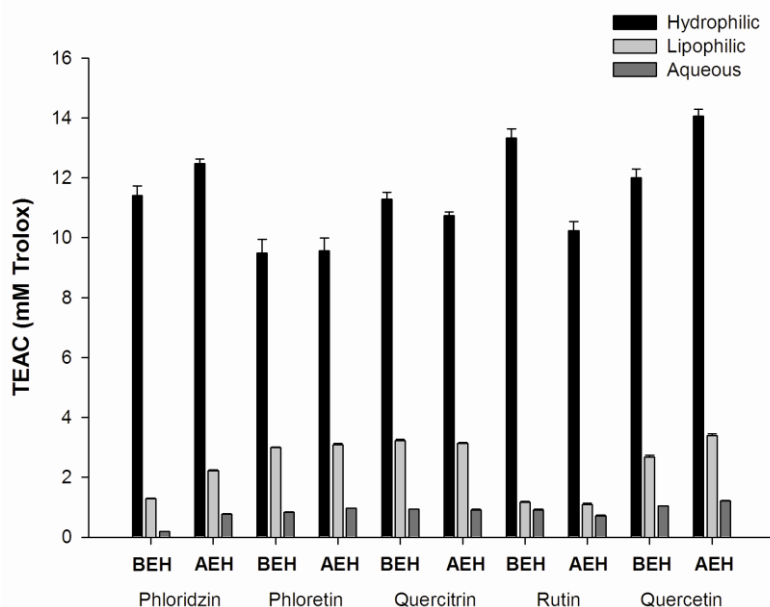


Figure 4-25: Trolox® equivalent anti-oxidant capacity (TEAC) expressed as mM Trolox® of phloridzin, phloretin, quercitrin, rutin, and quercetin before enzymatic hydrolysis (BEH) and after enzymatic hydrolysis (AEH), (mean ± SEM, n=3).

Table 4-13: Trolox® equivalent anti-oxidant capacity (TEAC) expressed as mM Trolox® of phloridzin, phloretin, quercitrin, rutin, and quercetin before enzymatic hydrolysis (BEH) and after enzymatic hydrolysis (AEH) (mean ± SEM, n=4). Total is the sum of the hydrophilic and lipophilic fractions.

Compound	Hydrophilic	Lipophilic	TOTAL	Aqueous
Phloridzin BEH	11.41 ± 0.31	1.28 ± 0.02	12.70 ± 0.33	0.19 ± 0.002
Phloridzin AEH	12.48 ± 0.15	2.22 ± 0.02	14.70 ± 0.17	0.77 ± 0.015
Phloretin BEH	9.49 ± 0.45	2.99 ± 0.02	12.48 ± 0.46	0.84 ± 0.005
Phloretin AEH	9.56 ± 0.43	3.08 ± 0.05	12.65 ± 0.47	0.97 ± 0.002
Quercitrin BEH	11.28 ± 0.23	3.22 ± 0.04	14.50 ± 0.28	0.94 ± 0.002
Quercitrin AEH	10.74 ± 0.12	3.14 ± 0.03	13.88 ± 0.15	0.90 ± 0.028
Rutin BEH	13.33 ± 0.31	1.17 ± 0.02	14.50 ± 0.34	0.91 ± 0.025
Rutin AEH	10.24 ± 0.30	1.09 ± 0.04	11.33 ± 0.34	0.70 ± 0.041
Quercetin BEH	12.00 ± 0.30	2.67 ± 0.07	14.67 ± 0.37	1.04 ± 0.004
Quercetin AEH	14.06 ± 0.23	3.38 ± 0.06	17.45 ± 0.29	1.21 ± 0.007

4.4.6.4.4 Anti-Oxidant Capacity of Apples

The developed comprehensive anti-oxidant method was also applied to the quantification of TEAC in apples tissues. As shown in Figure 4-26, the hydrophilic fraction contributes the majority of the Trolox® equivalent anti-oxidant capacity (TEAC) of all the apple samples, while the lipophilic fraction still contributes a significant portion of the total TEAC and the insoluble fraction has a minor contribution. It is interesting to note the really small contribution of the aqueous fraction (methanol extraction) to the total TEAC since methanol is the preferable solvent in anti-oxidant methodology. Furthermore, it can be noted that all the fractions (hydrophilic, lipophilic, insoluble, and aqueous) TEAC significantly decrease after enzymatic hydrolysis (Table 4-14). The apple contains polyphenols in the glycosylated (glycosides) and non-glycosylated (aglycones) forms as shown in Figure 4-21. Thus, in the samples before enzymatic hydrolysis (BEH) the TEAC is the results of the contribution of both forms, while in the samples after enzymatic hydrolysis (AEH) because the conversion of glycosides to aglycones, the anti-oxidant contribution will derive mainly from the aglycones present. The observed decrease in TEAC in all the fractions would indicate that the reduction in glycosides (converted to aglycones) reduced the total TEAC of samples. This observation appears to contradict the literature dogma that the anti-oxidant capacity of a compound increases with the number of available hydroxyl (OH) groups as would be the case with the aglycones. The glycosylated forms (glycosides) will have one or more OH group attached to a sugar so it is expected that the anti-oxidant capacity is reduced, and when that sugar is removed by enzymatic hydrolysis the OH could become available or could be present as a O⁻ radical. Nevertheless, the removal of the sugar moieties from the glycosides will mean that these sugars are available to react with the environment and as reported previously sugars can affect the

ABTS and DPPH radical scavenging capacity (Parejo *et al.*, 2004). Thus, refinement in the methodology is necessary to be able to remove the sugars after enzymatic hydrolysis to be able to eliminate any interference that might be the cause of the decrease in TEAC.

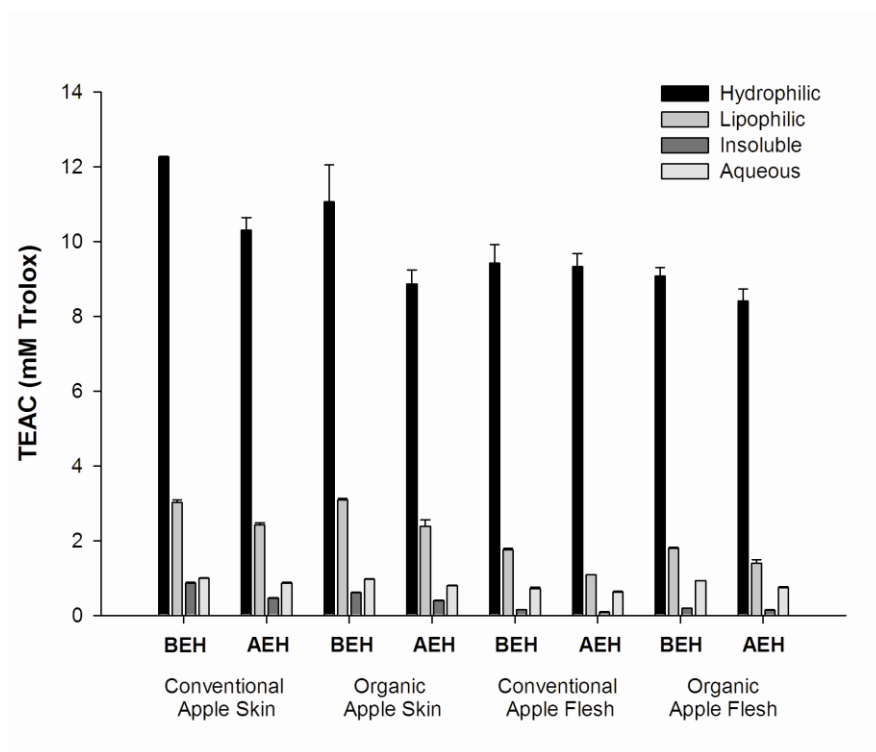


Figure 4-26: Trolox® equivalent anti-oxidant capacity (TEAC) expressed as mM Trolox® of apples before enzymatic hydrolysis (BEH) and after enzymatic hydrolysis (AEH), (mean \pm SEM, n=3).

Table 4-14: Trolox® equivalent anti-oxidant capacity (TEAC) expressed as mM Trolox® of apples before enzymatic hydrolysis (BEH) and after enzymatic hydrolysis (AEH) (mean \pm SEM, n=4). Total is the sum of the hydrophilic, lipophilic, and insoluble fractions.

Compound	Hydrophilic	Lipophilic	Insoluble	TOTAL	Aqueous
Conventional Apple Skin BEH	12.27 \pm 0.01	3.02 \pm 0.07	0.86 \pm 0.03	16.15 \pm 0.11	1.00 \pm 0.01
Conventional Apple Skin AEH	10.30 \pm 0.34	2.42 \pm 0.05	0.46 \pm 0.01	13.18 \pm 0.39	0.86 \pm 0.04
Organic Apple Skin BEH	11.06 \pm 0.99	3.09 \pm 0.04	0.62 \pm 0.01	14.76 \pm 1.03	0.97 \pm 0.01
Organic Apples Skin AEH	8.86 \pm 0.38	2.38 \pm 0.18	0.39 \pm 0.02	11.64 \pm 0.57	0.79 \pm 0.01
Conventional Apple Flesh BEH	9.42 \pm 0.50	1.75 \pm 0.04	0.15 \pm 0.01	11.32 \pm 0.55	0.71 \pm 0.04
Conventional Apple Flesh AEH	9.33 \pm 0.34	1.08 \pm 0.01	0.09 \pm 0.01	10.51 \pm 0.35	0.62 \pm 0.02
Organic Apple Flesh BEH	9.07 \pm 0.23	1.80 \pm 0.02	0.19 \pm 0.01	11.06 \pm 0.25	0.93 \pm 0.01
Organic Apples Flesh AEH	8.41 \pm 0.32	1.40 \pm 0.08	0.14 \pm 0.01	9.95 \pm 0.41	0.74 \pm 0.03

4.5 CONCLUSIONS

These studies have demonstrated that hesperidin, hesperetin, naringin, naringenin, eriocitrin, and eriodictyol are bioactive compounds in different *in vitro* assays. Interestingly, these investigations have revealed that small structural differences translate into significant pharmacokinetic and pharmacodynamic differences (Chapter III and IV) and into significant differences in chromatography and analytical conditions must be employed (Chapter II). For example, eriodictyol, a tetrahydroxyflavanone, demonstrates greater activity anti-cancer activity across all cell lines and greater anti-oxidant capacity compared to naringenin, a

trihydroxyflavanone. The least active compound in these two assays was hesperetin. In this instance, it appears that the addition of a hydroxyl group improves anti-cancer activity and anti-oxidant capacity whereas the addition of a methoxy group (hesperetin) attenuates activity. However, it was not possible to establish structure-activity relationships in the other *in vitro* assays since the different aglycones exhibited similar activities between each other. It needs to be mentioned that the aglycones were more active than the glycosides in all the different *in vitro* assays indicating that the sugar moiety partially hinders the pharmacological activity. Also, eriocitrin exhibited the highest anti-cancer activity and anti-oxidant capacity, followed by naringin and hesperidin.

Also, a novel comprehensive method to assess total anti-oxidant capacity was developed to assess the contribution of the lipophilic, hydrophilic, insoluble fractions before and after enzymatic hydrolysis. This method is potentially more comprehensive than any previous literature methodology. Furthermore, pure enantiomers were collected and for the first time the stereospecific cytotoxic activity of these selected flavanones were assessed in hepatoma (HepG2) cells.

These *in vitro* pharmacodynamic studies indicate that these compounds have concentration-dependant anti-inflammatory properties in our osteoarthritis model indicating that they are effective in reducing various inflammatory mediators such as nitrite, nitrate, prostaglandin E₂ (PGE₂), sulphated glycosaminoglycans (sGAGs), matrix metalloproteinase-3 (MMP-3) and tumor necrosis factor- α . Flavanones also exhibited significant ability to inhibit both COX isoforms (COX-1 and COX-2) with higher activity against the COX-2 enzyme. Furthermore, these compounds also exhibited concentration-dependant activity in reducing PGE₂ levels in a *in vitro* inflammatory bowel disease (colitis) model and the aglycones were

effective in reducing the amounts of intracellular triglycerides in an adipogenesis model using pre-adipocytes (3T3-L1 cells). Concentration-dependant anti-cancer activity and anti-oxidant capacity was also observed, with the aglycone flavanones more active than the glycosides.

CHAPTER V In Vivo Pharmacodynamics of Racemic Hesperidin, Hesperetin, Naringin, and Naringenin in the Experimental Model of Ulcerative Colitis

5.6 INTRODUCTION

This chapter describes the pharmacodynamic activities of racemic hesperidin, hesperetin, naringin, and naringenin in an experimental model of ulcerative colitis with a novel detection method. To induce ulcerative colitis, male Sprague Dawley rats (4 rats/treatment group) were administered 2,4,6-trinitrobenzenesulfonic acid (TNBS) via rectal administration. 20 mg/kg doses of the racemic flavanones were administered 48 h, 24 h, and 1 hour prior to colitis induction, and 24 h post colitis induction via oral gavage. Eriocitrin and eriodictyol were not assessed in this model due to prohibitive financial costs for the amounts required for such *in vivo* studies. The glucocorticoid dexamethasone was added as an additional treatment group and acted as a positive control. Furthermore, another control group was administered with vehicle (10% methanol and saline). Twenty-five hours following TNBS administration, rats were administered 1g phenol red solution via oral gavage to assess colonic permeability. Urine samples were collected 24 hours following phenol red administration. In addition to colonic wall permeability to assess ulcerative damage, each rat was euthanized and the colon was excised for macroscopic inspection and damage scoring. This experimental model of ulcerative colitis and the novel detection methods of assessing colonic damage are presented in detail and its application to the assessment of gastrointestinal protective activities of racemic hesperidin, hesperetin, naringin, and naringenin are described in this chapter.

5.7 BACKGROUND

Gastrointestinal disorders affect millions of Americans of all ages and the social and economic costs of such disorders are massive. Inflammatory bowel diseases (IBD), such as Crohn's disease and ulcerative colitis, are chronic inflammatory diseases of unknown etiology, which are difficult to manage pharmacologically. An inherent problem in the treatment of these diseases is that diagnosis is often difficult and it is usually symptomatic and often involve colonoscopy or a symptom-based activity index. Some of these symptoms include diarrhea, rectal bleeding, severe abdominal cramps, fatigue, and fever. These inflammatory bowel diseases (IBD) are often diagnosed based on the presence of ulcerations and inflammation along the colonic wall that are evident following a colonoscopic examination. There is current need for non-invasive methods in order to assess and diagnose inflammatory bowel diseases in order to reduce colonoscopy cost and the number of patients diagnosed early in the disease progression to increase treatment success and reduce the development of colonic cancer.

Current treatments of IBDs include anti-inflammatory drug therapy, such as 5-aminosalicylic acid (5-ASA), corticosteroids, and immunomodulators, such as azathioprine and 6-mercaptopurine (6-MP) (Kho *et al.*, 2001). Corticosteroids and immunomodulators, often prescribed for those suffering from the most severe symptoms, are often accompanied by side effects such as weight gain, acne, increased growth of facial hair, hypertension, mood swings, complications including pancreatitis and hepatitis, a reduced white blood cell count, and an increased risk of infection. For these reasons, these therapies are not recommended for long-term use. In cases that drug therapy fails to yield significant improvement, surgical removal of all or part of the ulcerated colon (proctocolectomy), is suggested. It is estimated that nearly 25 to 40% of colitis patients will need surgery sometime during the course of their

lives. Colitis sufferers are also at greater risk of developing colorectal cancer at some point in their lifetime due to prolonged bouts of gastrointestinal inflammation that predisposes the epithelium to pro-inflammatory, pro-oxidative, and pro-carcinogen mediators (Vagefi *et al.*, 2005). It is widely recognized that oxidative stress is of substantial clinical importance in the development of GI disorder etiology not only because oxidants are common in inflammation, but also, because disruption of mitochondrial energy metabolism, with reduced ATP synthesis, leads to a breach of the GI barrier function which can lead to mucosal barrier hyperpermeability and, in turn, lead to the initiation and/or perturbation of mucosal inflammation and injury (D'Odorico *et al.*, 2001; Seril *et al.*, 2003; Tuzun *et al.*, 2002). Disturbance of enterocytes may also impair the ability to combat free oxygen radicals which are partly responsible for cell damage involved in colitis. Mitochondrial oxidative damage to intestinal enterocytes may occur in parallel with these permeability changes and be further perturbed by the inflammatory insult. This may be important for the transition from the inactive to active (flare up) phases of inflammation in which intestinal oxidants and pro-inflammatory molecules periodically create a vicious cycle that leads to sustained oxidative stress, increased permeability, inflammation, and tissue damage and pre-disposition to colorectal carcinogenesis (D'Odorico *et al.*, 2001; Seril *et al.*, 2003; Tuzun *et al.*, 2002).

The rat has become an accepted model for the study of colitis-induced adverse effects in the large bowel (Hoffmann *et al.*, 2002). The trinitrobenzene sulfonic acid (TNBS) model is often employed due to its simplicity and susceptibility to pharmacological treatment (Kim *et al.*, 1992; Morris *et al.*, 1989; Neurath *et al.*, 2000; Strober *et al.*, 2004; Whittle *et al.*, 2003; Yanez *et al.*, 2006c). However, the criteria described to quantify colonic damage and histological ulceration usually also involves a scoring system which varies considerably

between investigators, often making comparison between laboratory findings difficult (Kim *et al.*, 1992; Kruschewski *et al.*, 2001; Morris *et al.*, 1989; Rabau *et al.*, 1996; Strober *et al.*, 2004). The degree of GI penetration by passively absorbed molecules is referred to as permeability. Impairment of epithelial barrier function, as seen in ulcerative colitis and Crohn's disease, causes increased permeability of the mucosa (Davies, 1998; Morita *et al.*, 2004; Peeters *et al.*, 1994). Many investigators have demonstrated that an increase in colonic permeability of the large intestine occurs in experimental colitis in patients afflicted with this disease (Arslan *et al.*, 2001; Gitter *et al.*, 2001; Jenkins *et al.*, 1992). Over the last 25 years, substantial efforts have been made to develop non-invasive methods of detecting gastrointestinal (GI) abnormalities. As the intracellular junctions of colonic epithelial cells appear to be susceptible to a variety of agents, they may be the first organelle to suffer when the energy production of the enterocyte is compromised. This disruption of intercellular integrity allows permeation of macromolecules into the GI mucosa. Several non-invasive probes have been previously utilized to examine colonic permeability clinically and in experimental models (Arslan *et al.*, 2001; Gitter *et al.*, 2001; Jenkins *et al.*, 1992). ^{51}Cr -EDTA has been the most frequently employed probe, however, it is not specific in nature because it quantifies total gastrointestinal (GI) tract permeability and lacks the necessary site specificity besides requiring a gamma counter and exposing the animal and researcher to radiation (Arslan *et al.*, 2001; Jenkins *et al.*, 1992). Another method for assessment of intestinal colonic permeability has been inulin-fluorescein allowing the quantification of fluorescence intensity in plasma (Krimsky *et al.*, 2000). In addition, the permeation of an isomolar water-soluble X-ray contrast medium CM iodixanol has been applied as an enema and the excretion in urine has been quantified (Andersen *et al.*, 1996). Another approach has consisted in employing

small carbohydrates such as sucrose, sucralose, or lactulose carbohydrates (Meddings *et al.*, 1998). However, these carbohydrates found in diet and oligosaccharides analysis is often time-consuming and extraction and chromatographic procedures are often prohibitive for routine screening as high performance liquid chromatography (HPLC) with an electrochemical detector is necessary. Therefore, the need for a readily probe that can be quantified rapidly is warranted.

Phenol red is a non-absorbable molecule almost completely ionized at pH above 1. Its excretion probably reflects both the small intestinal and colonic permeability. However, because this probe reaches the colon within 3 hours similar to sucralose, the majority of phenol red absorption would occur within the colon after oral administration (Meddings *et al.*, 1998). Thus, based on its physicochemical and pharmacokinetic properties phenol red might be suitable for assessing colonic permeability. Our laboratory have previously reported the suitability of the rat as a model for non-invasive detection of NSAID induced gastroduodenal and small intestinal permeability (Davies *et al.*, 1995; Davies *et al.*, 1994). The use of phenol red as a marker of intestinal permeability to indomethacin in rats has previously been suggested, however, it seems to require excessively large doses 20-100 mg/kg (Nakamura *et al.*, 1982). Permeability studies in the rat with phenol red have not been extended to colitis. Given the apparent parallels between the occurrence of colitis in rats and humans, it is of interest to examine novel ways of detecting this damage non-invasively in the colon. The first aim of this chapter is to examine the suitability of phenol red excretion and mitochondrial oxidative damage in the rat as relatively simple and novel experimental tools for screening and evaluating experimental colitis.

The second aim is to apply this novel non-invasive model of ulcerative colitis to assess the gastrointestinal protective properties of racemic hesperidin, hesperetin, naringin, and naringenin. As described in Chapter I, these selected flavanones have pharmacological beneficial activities. It has been observed *in vitro* that each selected flavonoid significantly decrease PGE₂ levels in the *in vitro* inflammatory bowel disease model using colon adenocarcinoma (HT29) cells, significantly inhibited COX-2 enzyme, provided activity in an anti-oxidant capacity assay (Chapter IV), and demonstrated anti-inflammatory activities. Furthermore, based on their pharmacokinetic disposition they are mainly excreted via non-renal routes, and undergo phase II metabolism (Chapter III). Thus, these selected flavanones are metabolized in the liver and then return to the gastrointestinal tract to be further eliminated via feces. This is critical because it demonstrates that these compounds transit across the gastrointestinal tract and are in direct contact with the colon from the systemic and luminal sides, which may enable flavanones to exhibit their anti-oxidant, anti-inflammatory, and COX-inhibitory activity in the lower GI tract. Therefore, based on these observations in Chapters III and IV particularly the *in vitro* inflammatory bowel disease results, it is hypothesized that these flavanones may exhibit gastrointestinal actions *in vivo*. The gastrointestinal protective activity *in vivo* has been reported with some similar compounds and micronutrients. For instance, vitamins and other micronutrients, including flavonoids, involved in nutrient metabolism and modulation of oxidative stress are important since they play a protective role in the prevention and treatment of nutrient deficiencies and in the amelioration of disease activity in individuals with inflammatory bowel disease (Razack *et al.*, 2007). Pretreatment with diosmin (10 mg/kg) or hesperidin (10 and 25 mg/kg) reduced colonic damage compared to TNBS control rats. This effect was confirmed biochemically by a reduction in colonic myeloperoxidase activity

compared to non-treated colitic animals. Colonic glutathione levels in colitic animals were significantly increased after hesperidin or diosmin treatment. Diosmin decreased colonic MDA production and inhibited LTB₄ synthesis, whereas hesperidin did not appear to demonstrate these pharmacological actions. Conversely, only hesperidin improved colonic fluid absorption, which was impaired in colitic animals. In conclusion, both diosmin and hesperidin were able to prevent colonic inflammation, acting via a mechanism in which protection against oxidative insult may play a role (Crespo *et al.*, 1999). Similar activity has been also reported for the stilbene resveratrol, which at a dose of 10 mg/kg has been shown to significantly reduce colonic ulceration and inflammation in the model of TNBS-induced ulcerative colitis (Martin *et al.*, 2004).

Therefore, this chapter first examines the suitability of phenol red excretion and mitochondrial oxidative damage in the rat as simple experimental tools for screening and evaluating experimental colitis, and secondly describes the application of this novel non-invasive model of ulcerative colitis to assess the gastrointestinal protective properties of racemic hesperidin, hesperetin, naringin, and naringenin.

5.8 NON-INVASIVE METHOD FOR ASSESSING EXPERIMENTAL COLITIS *IN VIVO* AND *EX VIVO*

5.8.1 Methods

5.8.1.1 Chemicals and Reagents

Phenol red, dexamethasone, diclofenac, indomethacin, 5-acetylsalicylic acid, methylcellulose, racemic hesperidin, hesperetin, naringin, and naringenin were purchased from Sigma Chemicals (St. Louis, MO, USA). DNAeasy® Mini Kit 50 was obtained from Qiagen

Inc (Stanford, CA, USA). 2,4,6-trinitrobenzenesulfonic acid (TNBS) stock solution (1M in water) was purchased from Fluka Chemie GmbH (CH-9471 Buchs, Switzerland). Polyethylene glycol 600 (PEG 600, FCC grade, was purchased from Union Carbide Chemicals and Plastic Company Inc. (Danbury, CT, USA). ⁵¹Cr-EDTA was purchased from NEN Life Sciences Products (Boston, MA, USA). Purina #5001 pelleted rat chow (Lot # 2134-4) containing d-alpha tocopherol succinate for a dose of 2 g/kg was purchased from Dyets Inc. (Bethlehem, Penn, U.S.A.).

5.8.1.2 Preparation of Drugs

TNBS Stock solution (1M) 2.047 ml of was added to a mixture of 2.953 ml water and 5 ml of alcohol to prepare 10 ml of TNBS working solution (60 mg/ml TNBS in 50% ethanol. Dexamethasone was dissolved in PEG 600 to form a solution of 4 mg/ml. 5-ASA and indomethacin were dispersed in 2% methylcellulose.

5.8.1.3 Induction of Colitis and Phenol Red Excretion

Male Sprague-Dawley rats (350 – 450 g,) were obtained from Harlan Sprague Dawley, Inc., Indianapolis, IN, USA) were anesthetized with halothane. Colitis was induced by rectal intraluminal administration of 0.5 ml of (TNBS, 60 mg/ml in 50% ethanol) using a foley catheter (2 mm i.d., Bard Urological Division, C.R. Bard Inc., Covington, GA, USA). On the morning of the permeability study, rats were housed in individual metabolic cages (Techniplast, USA) with wire mesh floors allowing separate quantitative collection of urine and feces. Animals were fed a standard Purina rat chow and allowed free access to food and water for the duration of the experiment. Ethics approval for animal experiments was obtained from Washington State University Institutional Animal Care and Use Committee.

At 24, 48 or 72 h post-induction of colitis, 1 g of phenol red solution was administered

orally or intrarectally to rats (n = 4-5 group) using an 18 gauge 5 cm curved feeding needle attached to a 1 ml syringe. Urine was collected 0 to 8 hours and 8 to 24 hours, and phenol red excretion was examined 24 hours post-dose. Following the test with phenol red, the rats were sacrificed with over-dosed halothane and dissected with the colon removed. The damage of the colon was assessed using a scoring scheme adopted from Appleyard *et al.* (Appleyard *et al.*, 1995), with the total area of colon ulceration recorded (Table 5-1).

Table 5-1: Criteria for macroscopic scoring of colonic damage.

Feature	Score
Normal appearance	0
No adhesions	0
No diarrhea	0
Focal hyperemia, no ulcers	1
Minor adhesions	1
Diarrhea	1
Ulceration without hyperemia or bowel wall thickening	2
Ulceration with inflammation at one site	3
Ulceration/inflammation at two or more sites	4
Major sites of damage extending >1 cm along the length of the colon	5
When an area of damage extended >2 cm along the length of the colon, the score was increased by 1 for each additional cm of involvement	6-10
Plus Maximal bowel wall thickness (x), in mm	x

5.8.1.4 Protective Effect of Dexamethasone

Rats were assessed in parallel in four experimental groups. For the negative control group (n = 5), saline was used instead of TNBS. For the positive control group (n = 5), colitis was induced using 0.5 ml of TNBS, (60 mg/ml in 50% ethanol). For the dexamethasone treated group (n = 5), dexamethasone in PEG 600 was administered to rats (2 mg/kg) subcutaneously

12 and 1 hour before induction of colitis based on previously reported effective doses (Holma *et al.*, 2002; Kankuri *et al.*, 2001). For the control group of dexamethasone, (n = 5) the vehicle, PEG 600 without dexamethasone, was administered to rats subcutaneously 12 and 1 hour before induction of colitis.

5.8.1.5 Protective Effect of 5-ASA

For the 5-ASA treated group (n = 10), rats were orally administered 100 mg/kg 5-ASA in 2% methylcellulose twice daily from 72 h before the induction of colitis for 3 days and then 1 h and 12, 24, 36 h post colitis induction (Galvez *et al.*, 2000; Nakamaru *et al.*, 1994). Forty-eight hours after the induction of colitis, 5 of the rats were sacrificed and their injured colon tissues were taken and stored at -20°C for analysis of oxidative damage. The other 5 rats were dosed phenol red 1 g via oral gavage to investigate the phenol red excretion from urine.

5.8.1.6 Reactivation of Colitis

Six weeks after the initial intracolonic administration of 0.5 ml (60 mg/ml in 50% ethanol), rats were randomized into treatment and control groups and TNBS in 0.9 % saline (5 mg/kg) or saline alone administered intravenously via a tail vein once daily for 3 days (Appleyard *et al.*, 1995; Sun *et al.*, 2001). An hour after the last dose of TNBS, rats were administered 1 g of phenol red orally using an 18 gauge 5 cm curved feeding needle attached to a 1 ml syringe. Urine was collected from 0 to 8 hours and from 8 to 24 hours.

5.8.1.7 Exacerbation of Colitis

Diclofenac was administered 10 mg/kg orally to rats 3 h and every 12 h after induction of colitis (Reuter *et al.*, 1996). An hour after the last dose of diclofenac, rats were administered 1 g of phenol red orally using an 18 gauge 5 cm curved feeding needle attached to a 1 ml syringe. Urine was collected from 0 to 8 hours and from 8 to 24 hours. The rats were sacrificed

72 h after induction of colitis for assessment of colonic damage using criteria described in Table 5-1.

5.8.1.8 Assessment of Colonic Injury and Inflammation

All scoring of colonic damage was performed in a randomized manner. The presence or absence of diarrhea (loose or water stool with perianal fur soiling) was noted, the animal was sacrificed with a halothane overdose and the abdomen was opened and the distal colon excised. The severity (major or minor) and presence of adhesions between the colon and other internal organs was noted. The colon was opened by a longitudinal incision, rinsed with tap water, then pinned onto a wax block and scored for macroscopic damage with the use of criteria in Table 5-1.

5.8.1.9 Assay of Phenol Red

Urine samples (~1.5 ml) are centrifuged in 1.5 ml micro tubes at 15,000 rpm for 3 min using a Beckman Microfuge E™ (Beckman, CT, USA), and 0.5 – 1 ml of supernatant was used for analysis. In culture tubes (10 × 75 mm), 0.375 ml of 2N NaOH was pipetted to each tube and 0.75 ml of distilled water. 0.75 ml of the test sample was mixed and then centrifuged again at 15,000 g for 3 min. The absorbance at 559 nm was measured using a Shimadzu spectrophotometer UV 2100U (Shimadzu, Kyoto, Japan) with 0.375 ml of NaOH 2N in 1.5 ml of H₂O as a reference. When the absorbance exceeds 2, further dilution of sample is required. Phenol red concentration was directly determined from the standard curve and the dilution factor, a typical standard curve is presented in Figure 5-1.

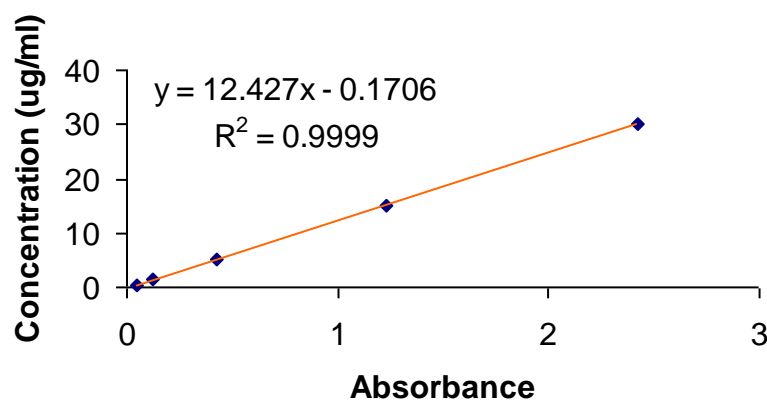


Figure 5-1: Typical calibration curve of phenol red in urine.

5.8.1.10 Indomethacin-⁵¹Cr-EDTA and Phenol Red

Indomethacin in 2% methylcellulose and 2% methylcellulose alone were administered orally to rats (n = 5/group) using an 18 gauge 5 cm curved feeding needle attached to a 1 ml syringe. Phenol red 1 g was administered orally and its excretion was examined 24 hours post-dose. ⁵¹Cr-EDTA in urine was measured by relative permeability determined by calculating the radioactivity present in urine samples as a percentage of the administered dose as previously described (Davies *et al.*, 1995).

5.8.1.11 Mitochondrial Oxidative Damage

A quantitative polymerase chain reaction (QPCR) technique was developed based on previously described work (Ayala-Torres *et al.*, 2000; Santos *et al.*, 2006). DNA was isolated using Qiagen® genomic tip and genomic DNA buffer set kit for mammalian DNA extractions (Qiagen Inc., Valencia, CA, USA). DNA quantitation was performed utilizing the PicoGreen® dsDNA Quantitation Kit (Molecular Probes, Eugene, OR, USA). QPCR involved the use of GeneAmp XL PCR kit (Applied Biosystems, Branchburg, NJ, USA) and dNTPs (Pharmacia, Peapack, NJ, USA). Primers were based on sequences already optimized by Van Houten's

laboratory (Ayala-Torres *et al.*, 2000; Santos *et al.*, 2006) (Table 5-2). Picogreen® was used to quantify dsDNA fragment. Fluorescence was measured using a CytoFluor® 4000 fluorescence multi-well plate reader (applied Biosystems, Foster City, California, USA). After fluorescent readings for all samples were subtracted from the no template controls, relative amplification was calculated in paired samples.

Table 5-2. Primer Sequences for Rat QPCR.

Gene Clusterin (TRPM-2)	Sequence (5' to 3')	Direction	Amplicon Length (base pairs)
5781	AGACGGGTGAGACAGCTGCACCTTTTC	Sense	12.5 kb
18314	CGAGAGCATCAAGTGCAGCGATTAGAG	Anti-sense	12.5 kb
13559	AAAATCCCCGCAAACAATGACCACCC	Sense	13.4 kb
10633	GCGAATAAGAGTGGGATGGAGCCAA	Anti-sense	13.4 kb
14678	CCTCCATTCATTATCGCCGCCCTTGC	Sense	235 bp
14885	GTCTGGGTCTCCTAGTAGGTCTGGGAA	Anti-sense	235 bp

5.8.1.12 Statistical Analysis

All experiments were repeated at least four times. All data are expressed as the mean \pm the standard error of the mean (SEM). Comparisons among the control and treatment groups were made using General Linear Model (GLM) ANOVA with Newman-Keuls multiple comparison test using NCSS Statistical and Power Analysis software (NCSS, Kaysville, UT). With all analyses a $P < 0.05$ was considered significant.

5.9 APPLICATION OF A NON-INVASIVE DETECTION METHOD IN EXPERIMENTAL COLITIS

5.9.1 Methods

5.9.1.1 Stock Solutions Preparation

Stock solution of TNBS (1M) was prepared by adding 2.047 ml of concentrated TNBS to a mixture of 2.953 ml water and 5 ml of alcohol to prepare 10 ml of the TNBS working solution (60 mg/ml TNBS in 50% ethanol). Racemic hesperidin, hesperetin, naringin, and naringenin were suspended in PEG 600.

5.9.1.2 Treatment and Induction of Colitis

Male Sprague-Dawley rats (n=4/group, 300 – 400 g) were randomly assigned to one of four experimental groups. Each group was administered racemic hesperidin (20 mg/kg), hesperetin (20 mg/kg), naringin (20 mg/kg), naringenin (20mg/kg), dexamethasone (10 mg/kg), or vehicle (10% methanol and saline) via oral gavage (18 gauge 5 cm curved feeding needle attached to a 1 ml syringe). Treatments were administered 48h, 24h and 1 h prior to colitis induction. A final dose was administered 24 h post colitis induction.

Colitis was induced via rectal intraluminal administration of 0.5 ml of (TNBS, 60 mg/ml in 50% ethanol) using a foley catheter (2 mm i.d., Bard Urological Division, C.R. Bard Inc., Covington, GA, USA) (Yanez *et al.*, 2006c). On the morning of the colonic wall permeability study, rats were housed in individual metabolic cages (Techniplast, USA) with wire mesh floors allowing separate quantitative collection of urine and feces. Animals were fed a standard Purina rat chow and allowed free access to food and water for the duration of the experiment. Ethics approval for animal experiments was obtained from Washington State University Institutional Animal Care and Use Committee.

5.9.1.3 Phenol Red Excretion

One hour following the final treatment dose, each rat was administered 1 g of the non-absorbable permeability marker phenol red solution dissolved in 0.5 ml of distilled water via oral gavage. Urine was collected at 24 hours following phenol red administration. Urine samples (~1.5 ml) were centrifuged in 1.5 ml eppendorf tubes at 15,000 rpm for 3 min using a Beckman Microfuge E™ (Beckman, CT, USA), and 0.5 – 1 ml of supernatant was used for analysis. In culture tubes (10 × 75 mm), 0.375 ml of sodium hydroxide (NaOH) 2M and 0.75 ml of HPLC water were carefully pipetted to each tube. 0.75 ml of the test sample was vortexed and centrifuged again at 15,00 g for 3 min. The ultraviolet (UV) absorbance of each sample was measured at 559 nm using a Shimadzu spectrophotometer UV 2100U (Shimadzu, Kyoto, Japan). 0.375 ml of NaOH 2N in 1.5 ml of H₂O was used as a reference. A standard curve was constructed for phenol red concentration and absorbance. The phenol red concentration of each urine sample was directly determined from the standard curve (Yanez *et al.*, 2006c).

5.9.1.4 Macroscopic Scoring

Following urine collection for phenol red quantification, the rats were sacrificed with over-dosed halothane. All scoring of colonic damage was performed in a randomized manner. The presence or absence of diarrhea (loose or water stool with perianal fur soiling) was noted, the animal was sacrificed with an overdose of halothane in a glass bell jar and the abdomen was opened and the distal colon excised. The damage of the colon was assessed on a numerical scale with a score of 0 indicating no damage using a scoring scheme adopted from Appleyard *et al.* (Appleyard *et al.*, 1995), with the total area of colon ulceration recorded. The severity (major or minor) and presence of adhesions between the colon and other internal organs was

noted. The colon was opened by a longitudinal incision, rinsed with tap water, then pinned onto a wax block and scored for macroscopic damage with the use of criteria in Table 5-1.

5.9.1.5 Statistical Analysis

All samples were analyzed in duplicate. All data are expressed as the mean \pm the standard error of the mean (SEM). Comparisons among the control and treatment groups were made using General Linear Model (GLM) ANOVA with Newman-Keuls multiple comparison test using NCSS Statistical and Power Analysis software (NCSS, Kaysville, UT). With all analyses a $P < 0.05$ was considered significant.

5.10 RESULTS AND DISCUSSION

5.10.1 Non-Invasive Method for Assessing Experimental Colitis *In Vivo* and *Ex Vivo*

After colitis induction, macroscopic inflammation (Figure 5-2) was assessed using a previously defined criteria (Table 5-1). Inflammatory mucosal lesions were determined 24 h post TNBS enema dose. The size of ulcerative lesions reached its maximum at 48 h and remained increased from baseline thereafter until the end of the 72 h follow-up.

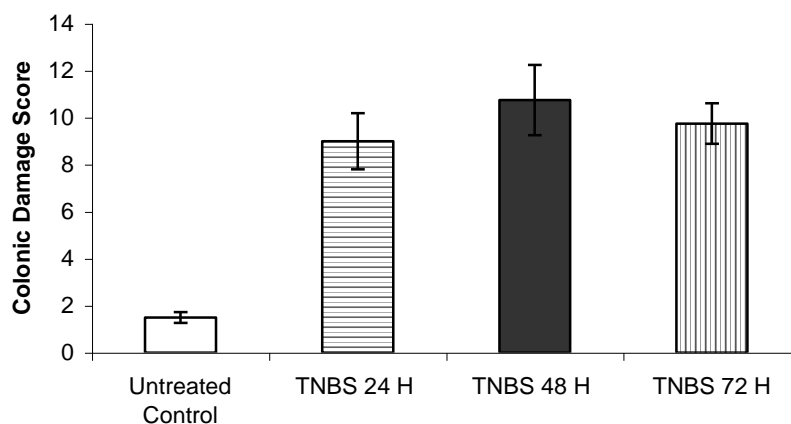


Figure 5-2: Macroscopic colonic damage score after administration of TNBS to rats (n=5, Mean \pm SEM).

The increase in macroscopic damage demonstrated similar time dependency in parallel with the increase in permeability and excretion of phenol red (Figure 5-3).

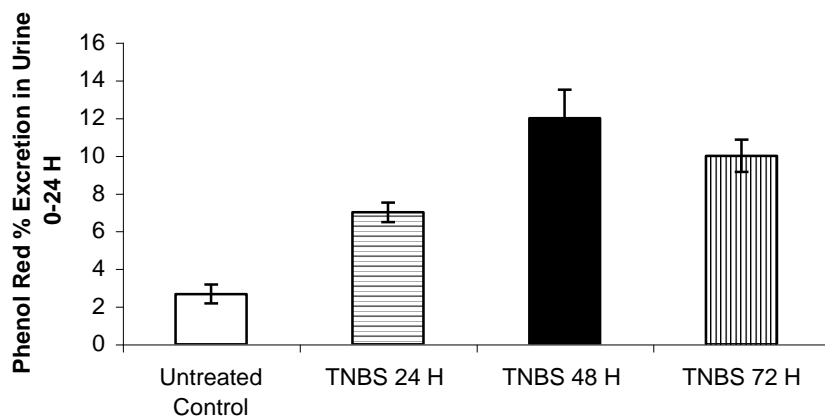


Figure 5-3: Phenol red excretion in urine of rats over time (n=5, Mean \pm SEM).

The intracolonic administration of phenol red 48 h post-colitis demonstrated a significant increase in colonic permeability which was similar to that observed after oral administration (Figure 5-4). Based on these data, 48 h post-colitis induction was chosen as the assessment time point for the studies of drug effects on TNBS induced colitis assessed by phenol red excretion and colonic mitochondrial damage.

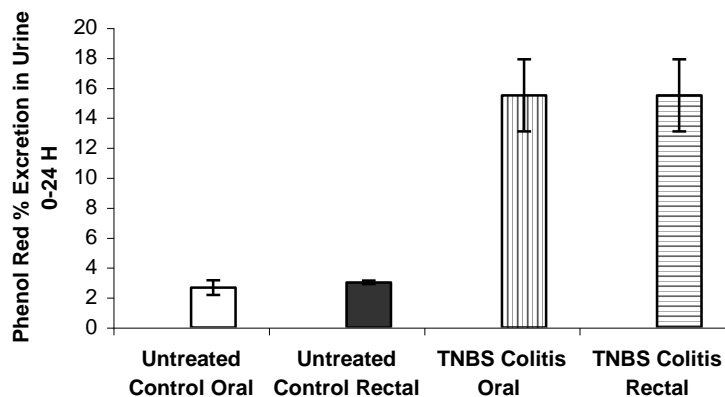


Figure 5-4: Oral and rectal administration of phenol red to rats with colitis (n=5, Mean \pm SEM).

The single dose treatment with indomethacin 10 mg/kg orally caused significant macroscopic ulceration and increased intestinal permeability as measured by ^{51}Cr -EDTA excretion in urine 24 h post-indomethacin compared to control levels (Figure 5-5).

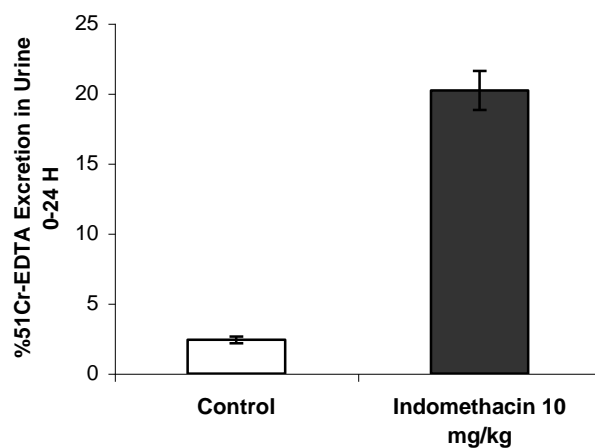


Figure 5-5: Excretion of ^{51}Cr -EDTA in urine of rats treated with indomethacin 10 mg/kg 24 h post-dose (n=5, Mean \pm SEM).

The urinary excretion of phenol red 24 h post-indomethacin was not significantly elevated compared to the control group (Figure 5-6).

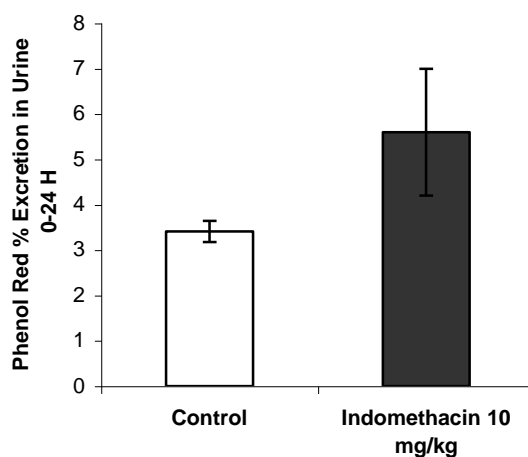


Figure 5-6: Excretion of phenol red in urine of rats treated with indomethacin 10 mg/kg 24 h post-dose (n=5, Mean \pm SEM).

Treatment with dexamethasone, dietary vitamin E succinate and 5-ASA attenuated macroscopic damage in the 48 h model of the acute experimental colitis (Figure 5-7).

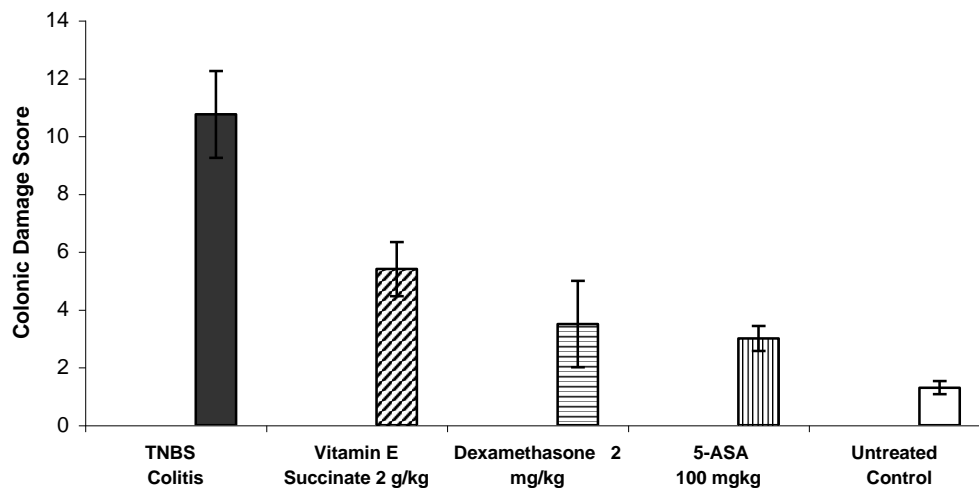


Figure 5-7: Effects of 5-ASA and dexamethasone on macroscopic damage score after acute colitis (n=5, Mean ± SEM).

In a parallel fashion, there was a significant reduction in the excretion of phenol red excretion in urine in the TNBS-colitis group treated with these agents compared to positive TNBS treated controls (Figure 5-8).

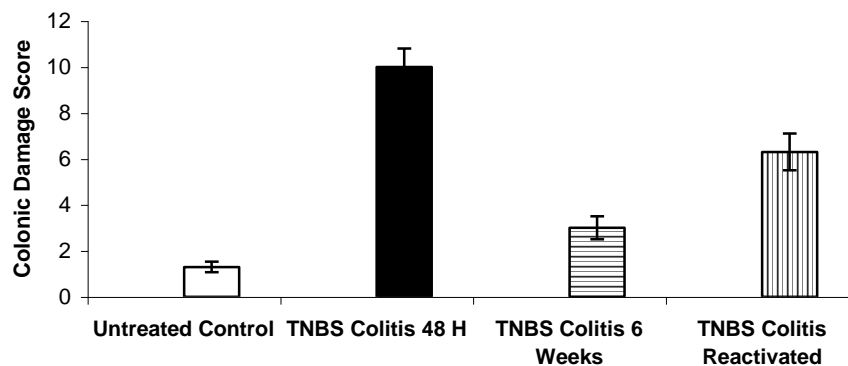


Figure 5-8: Effects of 5-ASA and dexamethasone on phenol red excretion in acute colitis (n=5, Mean ± SEM).

Six weeks after intracolonic administration of TNBS (30 mg in 50% ethanol) to rats, some macroscopically visible inflammation and damage was still evident (Figure 5-9).

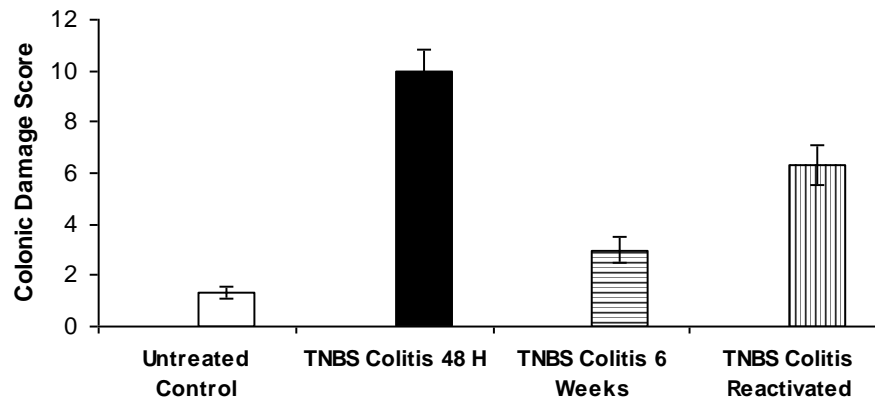


Figure 5-9: Macroscopic colonic damage of colitis in rats (n=5, Mean ± SEM).

Intravenous administration of saline to these TNBS treated rats did not significantly affect the colonic damage score. When, TNBS was administered intravenously to these rats that had been treated intracolonicly with TNBS 6 weeks earlier, the colonic damage scores increased significantly ($p < 0.001$) and the colons from these rats exhibited extensive ulcerations and marked thickening, and adhesions between the colon and other organs were frequently observed and 100% of the rats experienced diarrhea. Colonic permeability of phenol red was increased significantly ($P < 0.05$) in the rats treated intravenously with TNBS (Figure 5-10).

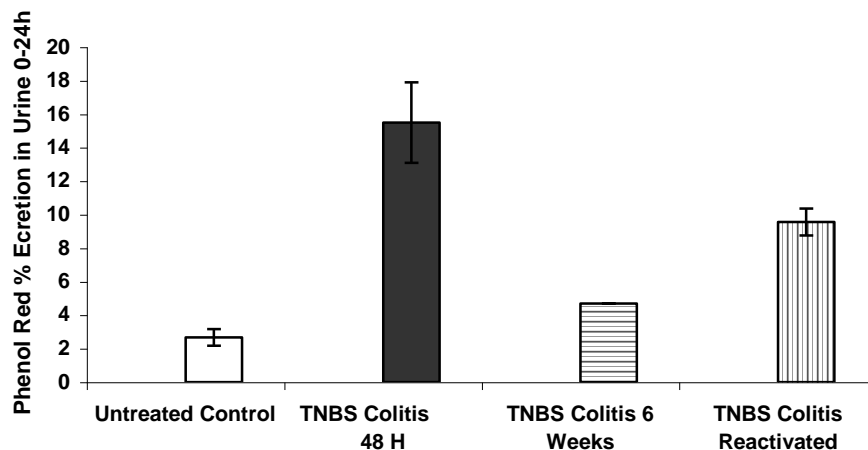


Figure 5-10. Effects of reactivation of experimental colitis on urinary excretion of oral phenol red excretions (n=5, Mean ± SEM).

Rats treated with TNBS and diclofenac were sacrificed after 3 days of drug administration and the colonic damage was scored (macroscopically). The NSAID significantly increased the colonic damage score above that observed in vehicle treated rats with colitis. (Figure 5-11).

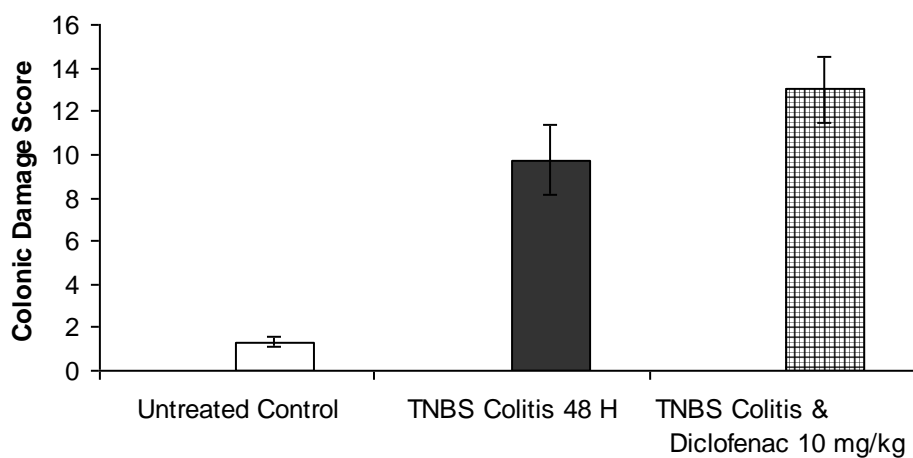


Figure 5-11. Exacerbation of experimental colitis in by diclofenac (n=5, Mean ± SEM).

In addition, the incidence of diarrhea increased from 40% in the vehicle-treated group to 100% in the group treated with diclofenac. In parallel with the macroscopic observations of colonic damage, there was a significant increase in the permeability of phenol red and excretion in urine in the diclofenac treated group (Figure 5-12).

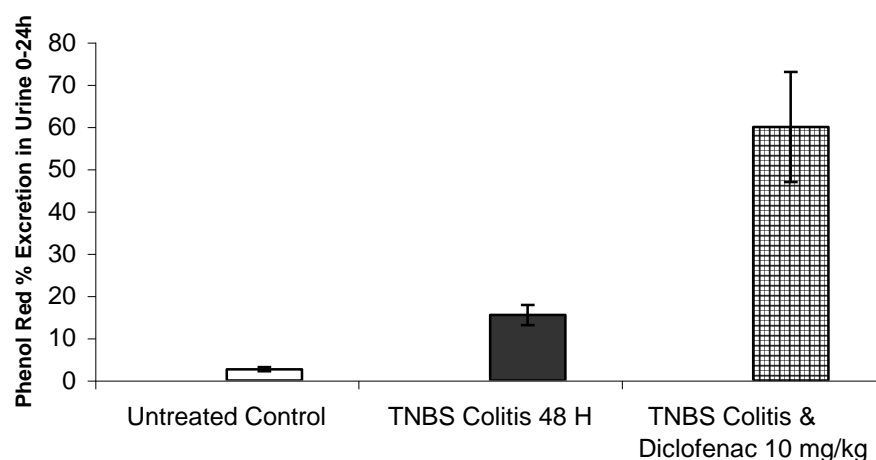


Figure 5-12. Effects of diclofenac on experimental colitis and urinary excretion of oral administered phenol red (n=5, Mean \pm SEM).

Mitochondrial DNA damage was apparent in colonic tissue in rats treated with TNBS 24, 48, and 72 hours after administration. However, no nuclear DNA damage was detected (Figure 5-13). Treatment with dexamethasone, vitamin E succinate and 5-ASA decreased mitochondrial damage in the acute experimental colitis (Figure 5-13).

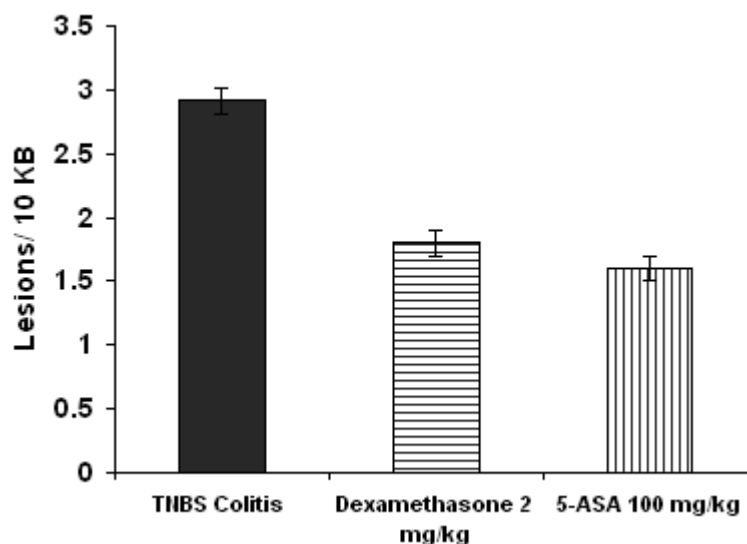


Figure 5-13. Mitochondrial oxidative DNA damage in rat colonic tissue after administration of TNBS and protection with various pharmacological agents (n=3, Mean ± SEM).

Phenol red is a non-absorbable molecule almost completely ionized at pH above 1. Its urinary excretion may reflect both the small intestinal and colonic permeability. However, because this probe reaches the colon within 3 hours similar to sucralose, most phenol red absorption occurs within the damaged colon after oral administration (Meddings *et al.*, 1998; Ogiso *et al.*, 2001). It appears to be more suitable for assessing colonic permeability. Nevertheless, this probe can also be administered directly into the colon, with similar findings to oral administration.

Similar to our previous findings in the rat with NSAIDs (Davies *et al.*, 1995; Davies *et al.*, 1994), the rat appears to be a suitable model for examining colonic permeability after experimental colitis induced with TNBS. Data from the present study demonstrated that the urinary recovery of phenol red is significantly increased when acute colonic damage was produced (Figure 5-2). In addition, in parallel with the observations in the rat using the methods of scoring the damage (Figure 5-5, TNBS induced colitis was reduced by 5-ASA, and dexamethasone as measured by damage score and a reduction in phenol red excretion (Galvez

et al., 2000; Holma *et al.*, 2002; Kankuri *et al.*, 2001; Nakamaru *et al.*, 1994). Therefore, this method can be used as a simple screening test for drugs used in the treatment of colitis.

As shown in Figure 5-9, the healing period of 6 weeks was enough to restore the colonic damage to near baseline. This is correlated well with the data of the urinary recovery of phenol red. From the results described above, this method may be utilized as a simple, useful, an non-invasive screening test for assessment of colonic damage *in vivo*. It is well known that administration of NSAIDs cause gastrointestinal ulceration. Our laboratory in previous investigations demonstrated that indomethacin-induced enteropathy is maximal at 24 hours post-dose as measured by ^{51}Cr -EDTA excretion, or caecal bleeding and intestinal ulceration after a 10 mg/kg dose (Davies *et al.*, 1994; Dillon *et al.*, 2003; Wright *et al.*, 1997). Previous findings also suggest that indomethacin-induced ulceration requires a dose of 20-100 mg/kg to detect appreciable intestinal damage using phenol red (Nakamura *et al.*, 1982). Our present findings are consistent with these previous findings.

Phenol red is an attractive alternative to ^{51}Cr -EDTA for assessing colonic disease, because the latter radioactive probe possesses restrictions for routine or serial tests. It is also an attractive alternative to carbohydrates as it possesses a UV chromophore and multiple samples can be analyzed quickly, accurately and reliably. Such a probe could also conceivably be instilled in patients during a colonoscopy procedure to evaluate colonic permeability.

The results shown in (Figure 5-13) confirm that mitochondrial DNA damage measured in lesions is an event in the pathogenesis of colonic toxicity due to TNBS. These results appear to parallel the findings of urinary excretion of 8-hydroxydeoxyguanosine excretion in TNBS colitis (Dukens *et al.*, 1998). This technique allows the determination that this damage is specific to the mitochondria rather than nuclear cellular DNA and parallels the results obtained

with colonic permeability and gross damage scores. It also parallels previously demonstrated results with cisplatin in leukemia cells (Kalinowski *et al.*, 1992). Mitochondrial DNA damage may also be a useful marker technique in other disease state studies that involve oxidative damage.

Damage to mitochondrial DNA (mtDNA) can be assessed without the need for isolation of mitochondria or mitochondrial DNA. Gene specific DNA damage provides more insight into the role played by oxidative stress in disease and mitochondrial DNA damage appear to be a good biomarker of oxidative stress in epithelial cells (Kalinowski *et al.*, 1992).

Measurement of the phenol red concentration excreted into urine after an oral or a rectal dose is a sensitive index of colonic damage. It has the advantages over a scoring method of being quantitative and allowing the time course of development to be studied non-invasively. Permeability tests are safe, reproducible and easy to perform. The non-invasive nature of this test can be easily applied to diagnostic screening and research, and could replace the need for invasive investigations of colonic disease such as radiology, and colonoscopy. An implicit advantage of this permeability test is that it reflects functional integrity over a major area of the colon. Given the well documented changes in gastrointestinal permeability in various diseases, parallel with an increasing body of knowledge of a mechanistic understanding of gastrointestinal disease process and the importance of oxidative damage in the colon, these techniques may help us in further understanding the pathogenesis of colitis.

5.10.2 Application of the Experimental Colitis Model to Flavanones

Treatment with racemic hesperidin, hesperetin, naringin and naringenin significantly attenuated macroscopic damage in the 24 h time point of the acute experimental colitis model (Figure 5-14). It can be observed that the glucocorticoid dexamethasone significantly reduced

the macroscopic damage compared to the TNBS-colitis group. Furthermore, all the tested flavanones (hesperidin, hesperetin, naringin, and naringenin) also significantly reduced the macroscopic damage to colonic damage scores similar to dexamethasone. In addition using colonic damage score as pharmacodynamic endpoint there were no apparent significant differences between the efficacy of flavanone glycosides and flavanones aglycones (Figure 5-14).

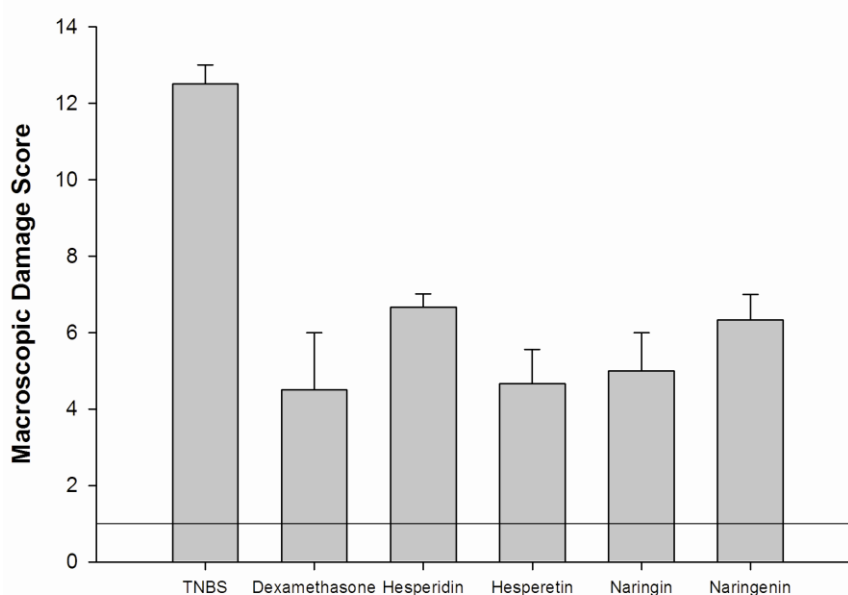


Figure 5-14. Macroscopic colonic damage score of rats treated with dexamethasone (10 mg/kg), or racemic flavanones (20 mg/kg) 24 h post-colitis induction with TNBS (n=5, Mean ± SEM). Line indicates the baseline level of the control without colitis induction.

In a parallel to the macroscopic colonic damage score, there was a significant reduction in the excretion of phenol red excretion in urine in the TNBS-colitis group treated with dexamethasone and each racemic flavanone examined (Figure 5-15). The glucocorticoid dexamethasone significantly reduced the excretion of phenol red compared to the TNBS-colitis group. The treatment with hesperidin and hesperetin also reduced phenol red excretion to

similar concentrations than dexamethasone, and the aglycone exhibited greater activity than hesperidin although statistical significance was not demonstrated. Naringin and naringenin also reduced the excretion of phenol red; however, both compounds reduced the phenol red excretion to baseline levels (group without colitis induction) (Figure 5-15).

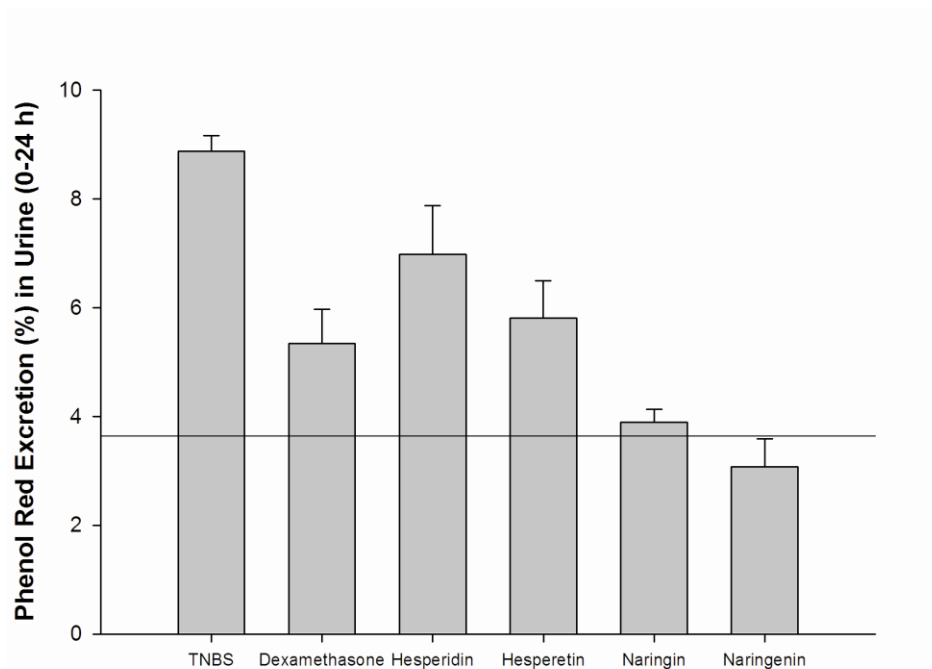


Figure 5-15. Excretion of phenol red in urine of rats treated with dexamethasone (10 mg/kg), or racemic flavanones (20 mg/kg) 24 h post-colitis induction with TNBS (n=5, Mean \pm SEM). Line indicates the baseline level of the control without colitis induction.

These results parallel previous observations that have determined that pretreatment with diosmin (10 mg/kg) or hesperidin (10 and 25 mg/kg) reduced colonic damage compared to TNBS control rats (Crespo *et al.*, 1999). Similar activity has been also reported for the stilbene resveratrol, which at a dose of 10 mg/kg has been shown to significantly reduce colonic ulceration and inflammation in the model of TNBS-induced ulcerative colitis (Martin *et al.*, 2004). These results with racemic flavanones are also in agreement with our *in vitro* results (Chapter IV) suggesting that these racemic flavanones may have activity in ulcerative colitis.

Furthermore, the pharmacokinetic disposition of these racemic flavanones (Chapter III) suggest that they will be cleared via non-renal routes and they will reside in the gastrointestinal tract for their further elimination via feces. In addition, direct contact of the flavanones with the intestinal and colonic lumen as well as the endothelial lining of the liver will enable them to exert their pharmacological actions. Furthermore, these compounds have large volume of distributions (V_{ss}) indicating that they will distribute into tissues, they are medium extraction compounds that undergo extensive biotransformation and in some instances follow enterohepatic recirculation increasing the systemic residence time thus increasing their local and systemic exposure. The novel detection method of evaluating non-invasively colonic damage induced by ulcerative colitis with phenol red urinary excretion was successfully applied to the assessment of selected flavanones and other xenobiotics. The oral administration of these selected flavanones can reduce and protect against colonic damage in this experimental model and flavanones represent attractive candidates for future drug development as therapeutic agents in treating this and other inflammatory gastrointestinal disorders.

CHAPTER VI Conclusions and Future Directions

6.1 SUMMARY

The specific aims of these studies presented in this thesis were:

- 1.) To develop and validate for the first time sensitive, specific, and stereoselective reverse phase high-performance liquid chromatography (RP-HPLC) assays in biological fluids for hesperetin, naringenin, and eriodictyol followed by verification using LC/MS.
- 2.) To characterize for the first time the stereospecific pharmacokinetic parameters of hesperetin, naringenin, and eriodictyol in a rat model and their stereospecific content in selected fruit juices qualitatively and quantitatively using newly developed sensitive, specific and stereoselective reverse phase high-performance liquid chromatography (RP-HPLC) assays and LC/MS for verification.
- 3.) To characterize the *in vitro* pharmacodynamic, namely anti-inflammatory properties by measurement of selected cytokines and other molecule markers of osteoarthritis, cyclooxygenase-1 and -2 inhibitory activity using a commercially available ELISA kit, anti-adipogenic activity using 3T3-L1 pre-adipocytes, gastrointestinal protective activity in an *in vitro* colitis model using HT-29 (colon adenocarcinoma) cells, evaluate their effect on cell viability in different cancer cell lines, evaluate their anti-oxidant capacity using the ABTS method, and develop a novel and improved method for total anti-oxidant capacity determination of racemic hesperidin, hesperetin, naringin, naringenin, eriocitrin, and eriodictyol.

- 4.) To develop a novel detection method of experimental colitis and evaluate the *in vivo* gastrointestinal protective activity of racemic hesperidin, hesperetin, naringin, and naringenin in an experimental model of colitis in the rat.

These studies have demonstrated that hesperidin, hesperetin, naringin, naringenin, eriocitrin, and eriodictyol each has unique pharmacokinetic disposition and content in fruit juice as well as unique activity in different *in vitro* assays as well as in the *in vivo* experimental model of ulcerative colitis. Interestingly, these investigations have revealed that small structural molecular differences in functional group substituents all translate into significant pharmacokinetic and pharmacodynamic differences *in vitro* and *in vivo*. For example, eriodictyol, a tetrahydroxyflavanone, demonstrates greater activity anti-cancer activity across all cell lines and greater anti-oxidant capacity compared to naringenin, a trihydroxyflavanone. The least active compound in these two assays was hesperetin. In this instance, it appears that the addition of a hydroxyl group improves anti-cancer activity and anti-oxidant capacity whereas the addition of a methoxy group (hesperetin) attenuates activity (Chapter IV). However, it was not possible to establish structure-activity relationships in the other *in vitro* and *in vivo* assays since the different aglycones exhibited similar activities between each other (Chapter IV and V). Interestingly, the flavanone aglycones were more active than the glycosides in all the different *in vitro* and *in vivo* assays suggesting that the sugar moiety partially hinders the pharmacological activity. Moreover, eriocitrin with three hydroxyl moieties in its structure exhibited the highest anti-cancer activity and anti-oxidant capacity, followed by naringin and hesperidin.

With the data generated from this thesis and other current and ongoing research in our laboratory it can be seen that small structural functional group differences and glycosylation

patterns can dramatically alter the resulting pharmacological activities and pharmacokinetic disposition of polyphenols. Perhaps these substitution patterns can be exploited further through chemical synthesis of new flavanone compounds to optimize pharmacological activities and pharmacokinetic disposition in specific disease states. For example, flavanones are been employed as potential lead compounds and synthesizing a variety of derivatives such as chiral dihydrofuroflavones (Lantz *et al.*, 2004). More recently, different polyketides have been synthesized from the basic flavonoid structure resulting in significant improvements in the anti-oxidant capacity (Katsuyama *et al.*, 2007). Also, based on the observation that compounds with a higher number of hydroxyl (OH) groups would be more active, different substitution products have been derived by adding OH groups in positions 4', 7, and 6 (Moorthy *et al.*, 2006). Some of these synthesized compounds exhibited improvements in anti-bacterial activity, while maintaining very low toxicity (Moorthy *et al.*, 2006). Polyphenol pharmacokinetics and pharmacodynamics is currently a rapidly evolving area of scientific interest and holds the potential for important discoveries in disease treatment and prevention. Another avenue that must be actively explored with these compounds is formulation optimization because of the lipophilicity of the aglycones. For instance, naringenin has been complexed with a phospholipid demonstrating an increase in plasma concentrations, anti-oxidant capacity, and protection against oxidative damage in the carbon tetrachloride liver toxicity rat model (Maiti *et al.*, 2006). Furthermore, similar compounds, isoflavones such as genistein, genistin, daidzein, and daidzein have shown to increase gramicidin channel lifetime and modulate other ion-channel types after been incorporated into phosphatidylcholine liposomes and sodium dodecyl sulfate (SDS) micelles (Whaley *et al.*, 2006). The issue of chirality of the subclass of flavanones needs to be further examined in terms of

pharmacological actions as does the stability of the isolated stereochemically pure antipodes and the activity of their metabolites.

Flavanones are attractive lead candidates as therapeutic agents in a number of disease states due to their apparent wide margin of safety and their activity in many *in vitro* and *in vivo* systems. However, the importance of fundamental analytical, physicochemical, pharmaceutical, and pharmacokinetic examination of these molecules needs to be undertaken *ab initio* in the development process. There is currently an apparent absence of toxic side effects demonstrated in any species in association with the administration of flavanone compounds. In fact, research has shown that large bolus doses as well as chronic, large dose studies exhibit multiple beneficial effects without any reported toxicities. Flavanones are called “citrus” flavanoids because their predominance in citrus fruits; thus, they are regularly consumed in orange, grapefruit, lemon, and other citrus fruits regularly in our diets and so far no signs of toxicities have been reported for these compounds. For instance, mice fed experimental diets containing naringenin for 21 days exhibit an increase in hepatic fatty acid oxidation mediated by regulation of the expression of several hepatic enzymes, and lowered the levels of serum triglycerides, cholesterol, phospholipids, and fatty acids (Huong *et al.*, 2006). Only a few human clinical trials have been carried out so far with flavanone-containing orange juice or flavanones. In a study consisting of healthy men and women with moderate hypercholesterolemia (elevated plasma cholesterol and LDL-cholesterol but normal triglycerides (TG)), the consumption of 750 ml of orange juice daily for 4 weeks led to an increase in HDL- cholesterol, and to a concomitant decrease in LDL-HDL cholesterol ratio, with no sign of acute toxicities (Kurowska *et al.*, 2000). However, this effect seems to be dose-dependant since a separate study carried with mildly hypercholesterolemic subjects consuming

480 ml daily of orange juice for 10 weeks reported no significant effects on the plasma lipids profile (total cholesterol, total TG, LDL and HDL cholesterol), and no signs of toxicity were reported (Devaraj *et al.*, 2004). Also it has been reported the administration of a water soluble hesperidin derivative, glucosyl-hesperidin or G-hesperidin, to hypertriglyceridemic subjects at 500 mg/day for 24 weeks resulted in a significant decrease of the serum TG levels, and several apolipoproteins, as well as improving the VLDL/LDL ratio (Miwa *et al.*, 2005). Similar results have been observed for naringin capsules at 400 mg/day for 8 weeks (Jung *et al.*, 2003).

In this thesis I have extensively reviewed the available methods to measure and separate chiral flavonoids (Chapter I), I have described the first validated HPLC methods to separate and quantify in biological matrices the selected chiral flavonoids hesperetin, naringenin, and eriodictyol (Chapter III). The validated HPLC methods have also been applied to describe for the first time the stereospecific pharmacokinetics of these selected flavonoids (Chapter III). In addition, I have discovered these citrus flavonoids are also present in apples (*Malus domestica*) for the first time (Chapter III). In order to assess the pharmacological *in vitro* (Chapter IV) and *in vivo* (Chapter V) activities of these selected compounds was also assessed with important and novel contributions to the literature. For instance, a novel *in vitro* osteoarthritis was developed employing canine chondrocytes and flavanones efficacy assessed using different inflammatory mediators (Chapter IV). Also, a novel comprehensive method to assess total anti-oxidant capacity was developed to assess the contribution of the lipophilic, hydrophilic, insoluble fractions before and after enzymatic hydrolysis. Furthermore, pure flavanones enantiomers were collected and for the first time the stereospecific cytotoxic activity of these selected flavanones were assessed in hepatoma (HepG2) cells (Chapter IV). Finally, the *in vivo*

pharmacodynamics of these selected flavonoids was assessed using a novel detection method in a model of ulcerative colitis in the rat (Chapter V).

The stereospecific pharmacokinetic data generated in this thesis demonstrates that these selected flavanones are predominantly cleared in the liver and excreted via non-renal routes. In the case of hesperetin, the R(+)-enantiomers has higher half-life and longer mean residence time (MRT) compared to its counterpart, while naringenin and eriodictyol enantiomers exhibited similar values for these parameters. Also, both enantiomers of the three selected flavanones have high volumes of distribution (V_{ss}) indicating that they distribute from the systemic circulation into tissues. The high volumes of distribution correlate with the lipophilic nature of these compounds (XLogP values of 2.174, 2.211, and 1.837 for hesperetin, naringenin, and eriodictyol, respectively). These compounds were observed to be medium extraction compounds and predominately cleared via hepatic elimination (fraction excreted in urine, f_e of 3%, 7%, and 5-7% for both hesperetin, naringenin and eriodictyol enantiomers, respectively) (assuming that hepatic clearance is equivalent to non-renal clearance). In addition, each flavanone is rapidly glucuronidated upon administration. The total cumulative urinary excretion plots indicate that these three flavonoids undergo significant phase II metabolism due to the significantly higher excretion of glucuronidated metabolites compared to the parent compounds. However, based on the low fraction excreted in urine (f_e values of 3%, 7%, and 5-7% for both hesperetin, naringenin and eriodictyol enantiomers, respectively), it can be presumed that these compounds distributed into tissues (V_{ss} values of 4-9 L/kg), eventually return to the gastrointestinal tract to be eliminated via non-renal routes. Nevertheless, this is a dynamic system in which hesperetin, naringenin, and eriodictyol are rapidly being metabolized to different glucuronides. Despite the difference in solubility and in

the lipophilicity nature of these compounds (parent and glucuronidates compounds) it can be observed that they have similar rates of excretion. This indicates that both forms undergo a similar magnitude of apparent elimination (since their elimination phases are parallel) indicating that the glucuronide conjugates are formation-rate limited and that their half-lives are a reflection of the elimination of the parent flavonoids (Chapter III).

The pharmacokinetic disposition of these compounds indicates that they reside for long periods of time in the body allowing them to exert some of their pharmacological properties. Our *in vitro* pharmacodynamic studies indicate that these compounds have concentration-dependant anti-inflammatory properties in our osteoarthritis model indicating that they are effective in reducing various inflammatory mediators such as nitrite, nitrate, prostaglandin E₂ (PGE₂), sulphated glycosaminoglycans (sGAGs), matrix metalloproteinase-3 (MMP-3) and tumor necrosis factor- α . These selected flavanones exhibit efficacy in inhibiting both COX isoforms (COX-1 and COX-2) with higher activity against COX-2 enzyme. Furthermore, these compounds also exhibited concentration-dependant activity in reducing PGE₂ levels in a *in vitro* inflammatory bowel disease (colitis) model. Flavanone aglycones are effective in reducing the amounts of intracellular triglycerides in an adipogenesis model using pre-adipocytes (3T3-L1 cells). Concentration-dependant anti-cancer activity and anti-oxidant capacity was also observed with the flavanone aglycones more active than the glycosides (Chapter IV). However, similar ability to ameliorate a inflammatory bowel disease were observed for both the flavanone aglycones and glycosides (Chapter V).

6.2 FUTURE DIRECTIONS

Hesperetin, naringenin, eriodictyol, and their corresponding glycosides belong to the flavanone sub-family. As presented in Chapter I, this is a large group of compounds and there

remains a need to separate many enantiomers and study them in details. Currently, other graduate students are developing and validating methods for other flavanones such as homoeriodictyol, taxifolin, sakuranetin, isosakuranetin, and flavanone in the laboratory. The observed pharmacokinetics of these compounds indicate that they could be formulated to improve their delivery. Other experimental models of gastrointestinal disease such as colorectal cancer or hepatic diseases such as hepatitis, cirrhosis, hypercholesterolemia, and hyperlipidemia could be assessed for disease modulation. Our laboratory have developed different polymeric micelles employing amphiphilic block polymers of PEG-block-poly(ϵ -caprolactone) (PEG-b-PCL) to encapsulate poorly water soluble compounds to improve their solubility, delivery, and pharmacokinetics (Forrest *et al.*, 2007; Yanez *et al.*, 2007b). This very same nanocarrier can be employed for delivery and currently the laboratory is working on developing and testing other delivery systems for sustained and controlled-release for oral administration of different flavanoids. These delivery systems will be employed to modify their disposition and/or target specific organs to treat different disease states and passively target inflammation and tumors. There are experimental models of these disease states in our laboratory that can also be induced in the rat model. For example, colorectal cancer (colonic adenocarcinoma) can be induced by administering intraperitoneal injections of azoxymethane (AOM) 15 mg/kg for 4 weeks and assessing the pre-neoplastic lesion (crypt foci) (Miyamoto *et al.*, 2006). Hyperlipidemia can be induced by administering a 1 g/kg dose of Poloxamer 407 (a pluronic) in saline intraperitoneally and different flavanones can be administered orally to examine their anti-hyperlipidemia activity. This can be examined by measuring total triglycerides and total cholesterol in plasma (Megalli *et al.*, 2005; Megalli *et al.*, 2006). Hepatitis can be induced in the rat model by administering a 100 mg/kg dose of alpha-

naphthylisothiocyanate in olive oil intraperitoneally and different flavanones can be administered orally prior to hepatitis induction to quantify hepatic cytoprotection. Protection can be measured by analyzing alanine-aminotransferase concentrations in the serum (Jean *et al.*, 1995).

In addition to investigating the protective activity of flavanones and their formulations, other directions in characterizing flavanone activity include the medicinal clinical chemistry synthesis of new flavanone compounds. Functional groups such as chloro-, bromo-, and fluoro-groups can be easily conjugated to the basic flavanone structure to synthesize novel compounds might further optimize activity while endeavoring to maintain minimal toxicity (Lantz *et al.*, 2004). These new compounds could be also examined in our *in vitro* and *in vivo* model systems. In addition, pharmacokinetic profiles and metabolic pathways of these compounds could be elucidated using the existing techniques and expertise in our laboratory or thorough modifications of these techniques.

In summary, hesperetin, naringenin, eriodictyol, and their corresponding glycosides are flavanones that demonstrated anti-inflammatory, anti-cancer, anti-oxidant, anti-adipogenic, and gastrointestinal protective properties. This thesis describes the development of novel stereospecific HPLC assays to quantify these compounds in biological matrices. The stereospecific pharmacokinetic parameters of these selected flavanones have been thoroughly characterized for the first time. These data have shown that small structural differences and glycosylation patterns translate into significant pharmacological and pharmacokinetic differences and hold the potential for further manipulation in attempt to improve flavanone activity in selected disease states. The pharmaceutical knowledge resulting from these investigations may help to further characterize how this class of compounds, which are

abundant in nature, are metabolized, cleared, eliminated and excreted following ingestion.

Moreover, these important compounds that we, as humans, ingest on a daily basis from a variety of sources, may serve as prototypes for future therapeutic agents in combating a myriad of diseases including cancer, obesity, inflammation, and gastrointestinal disorders.

REFERENCES

Ahmed MS, Galal AM, Ross SA, Ferreira D, ElSohly MA, Ibrahim AS, Mossa JS, El-Ferally FS. A Weakly Antimalarial Biflavanone from *Rhus Retinorrhoea*. *Phytochemistry*. 2001; 58: 599-602.

Ahmed S, Rahman A, Hasnain A, Lalonde M, Goldberg VM, Haqqi TM. Green Tea Polyphenol Epigallocatechin-3-Gallate Inhibits the IL-1 Beta-Induced Activity and Expression of Cyclooxygenase-2 and Nitric Oxide Synthase-2 in Human Chondrocytes. *Free Radic Biol Med*. 2002; 33: 1097-1105.

Alcolea JF, Cano A, Acosta M, Arnao MB. Hydrophilic and Lipophilic Antioxidant Activities of Grapes. *Nahrung*. 2002; 46: 353-356.

Allen DJ, Gray JC, Paiva NL, Smith JT. An Enantiomeric Assay for the Flavonoids Medicarpin and Vestitone Using Capillary Electrophoresis. *Electrophoresis*. 2000; 21: 2051-2057.

Ameer B, Weintraub RA. Drug Interactions with Grapefruit Juice. *Clin Pharmacokinet*. 1997; 33: 103-121.

Ameer B, Weintraub RA, Johnson JV, Yost RA, Rouseff RL. Flavanone Absorption after Naringin, Hesperidin, and Citrus Administration. *Clin Pharmacol Ther*. 1996; 60: 34-40.

Amin AR, Abramson SB. The Role of Nitric Oxide in Articular Cartilage Breakdown in Osteoarthritis. *Curr Opin Rheumatol*. 1998; 10: 263-268.

Andersen R, Hosaka J, Halstensen TS, Stordahl A, Tverdal A, Aabakken L, Laerum F. The X-Ray Contrast Medium Iodixanol Detects Increased Colonic Permeability Equally Well as ⁵¹Cr-Labeled Ethylenediaminetetraacetic Acid in Experimental Colitis of Rats. *Scand J Gastroenterol*. 1996; 31: 140-146.

Appleyard CB, Wallace JL. Reactivation of Hapten-Induced Colitis and Its Prevention by Anti-Inflammatory Drugs. *Am J Physiol.* 1995; 269: G119-125.

Arakawa H, Nakazaki M. Absolute Configuration of (-) Hesperetin and (-) Liquiritigenin. *Chem Ind (Rev).* 1960; 12: 73.

Arayne MS, Sultana N, Bibi Z. Grape Fruit Juice-Drug Interactions. *Pak J Pharm Sci.* 2005; 18: 45-57.

Arnao MB, Cano A, Acosta M. The Hydrophilic and Lipophilic Contribution to Total Antioxidant Activity. *Food Chem.* 2001a; 73: 239-244.

Arnao MB, Cano A, Alcolea JF, Acosta M. Estimation of Free Radical-Quenching Activity of Leaf Pigment Extracts. *Phytochem Anal.* 2001b; 12: 138-143.

Arslan G, Atasever T, Cindoruk M, Yildirim IS. (51)Credta Colonic Permeability and Therapy Response in Patients with Ulcerative Colitis. *Nucl Med Commun.* 2001; 22: 997-1001.

Asztemborska M, Miskiewicz M, Sybilska D. Separation of Some Chiral Flavanones by Micellar Electrokinetic Chromatography. *Electrophoresis.* 2003; 24: 2527-2531.

Asztemborska M, Zukowski J. Determination of Diastereomerization Barrier of Some Flavanones by High-Performance Liquid Chromatography Methods. *J Chromatogr A.* 2006;

Aturki Z, Brandi V, Sinibaldi M. Separation of Flavanone-7-O-Glycoside Diastereomers and Analysis in Citrus Juices by Multidimensional Liquid Chromatography Coupled with Mass Spectrometry. *J Agric Food Chem.* 2004; 52: 5303-5308.

Aturki Z, Sinibaldi M. Separation of Diastereomers of Flavanone-7-O-Glycosides by Capillary Electrophoresis Using Sulfobutyl Ether-B-Cyclodextrin as the Selector. *J Sep Sci.* 2003; 26: 844-850.

Ayala-Torres S, Chen Y, Svoboda T, Rosenblatt J, Van Houten B. Analysis of Gene-Specific DNA Damage and Repair Using Quantitative Polymerase Chain Reaction. *Methods*. 2000; 22: 135-147.

Bae EA, Han MJ, Kim DH. In Vitro Anti-Helicobacter Pylori Activity of Some Flavonoids and Their Metabolites. *Planta Med*. 1999; 65: 442-443.

Bailey DG, Arnold JM, Munoz C, Spence JD. Grapefruit Juice--Felodipine Interaction: Mechanism, Predictability, and Effect of Naringin. *Clin Pharmacol Ther*. 1993a; 53: 637-642.

Bailey DG, Arnold JM, Strong HA, Munoz C, Spence JD. Effect of Grapefruit Juice and Naringin on Nisoldipine Pharmacokinetics. *Clin Pharmacol Ther*. 1993b; 54: 589-594.

Bailey DG, Dresser GK, Kreeft JH, Munoz C, Freeman DJ, Bend JR. Grapefruit-Felodipine Interaction: Effect of Unprocessed Fruit and Probable Active Ingredients. *Clin Pharmacol Ther*. 2000; 68: 468-477.

Bailey DG, Malcolm J, Arnold O, Spence JD. Grapefruit Juice-Drug Interactions. *Br J Clin Pharmacol*. 1998; 46: 101-110.

Balakrishnan A, Menon VP. Antioxidant Properties of Hesperidin in Nicotine-Induced Lung Toxicity. *Fundam Clin Pharmacol*. 2007a; 21: 535-546.

Balakrishnan A, Menon VP. Effect of Hesperidin on Matrix Metalloproteinases and Antioxidant Status During Nicotine-Induced Toxicity. *Toxicology*. 2007b; 238: 90-98.

Balant L, Burki B, Wermeille M, Golden G. Comparison of Some Pharmacokinetic Parameters of (+)-Cyanidanol-3 Obtained with Specific and Non-Specific Analytical Methods. *Arzneimittelforschung*. 1979; 29: 1758-1762.

Bell JR, Donovan JL, Wong R, Waterhouse AL, German JB, Walzem RL, Kasim-Karakas SE. (+)-Catechin in Human Plasma after Ingestion of a Single Serving of Reconstituted Red Wine. *Am J Clin Nutr.* 2000; 71: 103-108.

Benavente-Carcia O, Castillo J, Marin FR, Ortuno A, Del Rio JA. Uses and Properties of Citrus Flavonoids. *J Agric Food Chem.* 1997; 45: 4505-4515.

Berkarda B, Koyuncu H, Soybir G, Baykut F. Inhibitory Effect of Hesperidin on Tumour Initiation and Promotion in Mouse Skin. *Res Exp Med (Berl).* 1998; 198: 93-99.

Blanco FJ, Lotz M. Il-1-Induced Nitric Oxide Inhibits Chondrocyte Proliferation Via Pge2. *Exp Cell Res.* 1995; 218: 319-325.

Bocco A, Cuvelier ME, Richard H, Berset C. Antioxidant Activity and Phenolic Composition of Citrus Peel and Seed Extracts. *J Agric Food Chem.* 1998; 46: 2123-2129.

Bok SH, Lee SH, Park YB, Bae KH, Son KH, Jeong TS, Choi MS. Plasma and Hepatic Cholesterol and Hepatic Activities of 3-Hydroxy-3-Methyl-Glutaryl-Coa Reductase and Acyl Coa: Cholesterol Transferase Are Lower in Rats Fed Citrus Peel Extract or a Mixture of Citrus Bioflavonoids. *J Nutr.* 1999; 129: 1182-1185.

Borradaile NM, Carroll KK, Kurowska EM. Regulation of Hepg2 Cell Apolipoprotein B Metabolism by the Citrus Flavanones Hesperetin and Naringenin. *Lipids.* 1999; 34: 591-598.

Breinholt VM, Offord EA, Brouwer C, Nielsen SE, Brosen K, Friedberg T. In Vitro Investigation of Cytochrome P450-Mediated Metabolism of Dietary Flavonoids. *Food Chem Toxicol.* 2002; 40: 609-616.

Brevik A, Rasmussen SE, Drevon CA, Andersen LF. Urinary Excretion of Flavonoids Reflects Even Small Changes in the Dietary Intake of Fruits and Vegetables. *Cancer Epidemiol Biomarkers Prev.* 2004; 13: 843-849.

Bugianesi R, Catasta G, Spigno P, D'Uva A, Maiani G. Naringenin from Cooked Tomato Paste Is Bioavailable in Men. *J Nutr.* 2002; 132: 3349-3352.

Caccamese S, Caruso C, Parrinello N, Savarino A. High-Performance Liquid Chromatographic Separation and Chiroptical Properties of the Enantiomers of Naringenin and Other Flavanones. *J Chromatogr A.* 2005; 1076: 155-162.

Caccamese S, Manna L, Scivoli G. Chiral Hplc Separation and Cd Spectra of the C-2 Diastereomers of Naringin in Grapefruit During Maturation. *Chirality.* 2003; 15: 661-667.

Cai SS, Hanold KA, Syage JA. Comparison of Atmospheric Pressure Photoionization and Atmospheric Pressure Chemical Ionization for Normal-Phase Lc/Ms Chiral Analysis of Pharmaceuticals. *Anal Chem.* 2007; 79: 2491-2498.

Cai Y, Luo Q, Sun M, Corke H. Antioxidant Activity and Phenolic Compounds of 112 Traditional Chinese Medicinal Plants Associated with Anticancer. *Life Sci.* 2004; 74: 2157-2184.

Calatayud S, Warner TD, Mitchell JA. Modulation of Colony Stimulating Factor Release and Apoptosis in Human Colon Cancer Cells by Anticancer Drugs. *Br J Cancer.* 2002; 86: 1316-1321.

Caldwell J. Importance of Stereospecific Bioanalytical Monitoring in Drug Development. *J Chromatogr A.* 1996; 719: 3-13.

Camp HS, Ren D, Leff T. Adipogenesis and Fat-Cell Function in Obesity and Diabetes. *Trends Mol Med.* 2002; 8: 442-447.

Cano A, Hernandez-Ruiz J, Garcia-Canovas F, Acosta M, Arnao MB. An End-Point Method for Estimation of the Total Antioxidant Activity in Plant Material. *Phytochem Anal.* 1998; 9: 196-202.

Cao G, Sofic E, Prior RL. Antioxidant and Prooxidant Behavior of Flavonoids: Structure-Activity Relationships. *Free Radic Biol Med.* 1997; 22: 749-760.

Carbonnier B, Janus L, Morcellet M. High-Performance Liquid Chromatographic Enantioseparation of Flavanones on 2-Hydroxy- 3-Methacryloyloxypropyl Beta-Cyclodextrin Copolymer Coated Silica Phase. *J Chromatogr Sci.* 2005; 43: 358-361.

Caristi C, Bellocco E, Panzera V, Toscano G, Vadala R, Leuzzi U. Flavonoids Detection by Hplc-Dad-Ms-Ms in Lemon Juices from Sicilian Cultivars. *J Agric Food Chem.* 2003; 51: 3528-3534.

Castrillo JL, Vanden Berghe D, Carrasco L. 3-Methylquercetin Is a Potent and Selective Inhibitor of Poliovirus Rna Synthesis. *Virology.* 1986; 152: 219-227.

Cawston T. Matrix Metalloproteinases and Timps: Properties and Implications for the Rheumatic Diseases. *Mol Med Today.* 1998; 4: 130-137.

Cawston TE, Ellis AJ, Bigg H, Curry V, Lean E, Ward D. Interleukin-4 Blocks the Release of Collagen Fragments from Bovine Nasal Cartilage Treated with Cytokines. *Biochim Biophys Acta.* 1996; 1314: 226-232.

Chan WK, Nguyen LT, Miller VP, Harris RZ. Mechanism-Based Inactivation of Human Cytochrome P450 3a4 by Grapefruit Juice and Red Wine. *Life Sci.* 1998; 62: PL135-142.

Chankvetadze B, Yashima E, Okamoto Y. Dichloro-, Dimethyl-, and Chloromethylphenylcarbamate Derivatives of Cyclodextrins as Chiral Stationary Phases for High-Performance Liquid Chromatography. *Chirality.* 1996; 8402-8407.

Chen J, Montanari AM, Widmer WW. Two New Polymethoxylated Flavones, a Class of Compounds with Potential Anticancer Activity, Isolated from Cold Pressed Dancy Tangerine Peel Oil Solids. *J Agric Food Chem.* 1997; 45: 364-368.

- Cho J. Antioxidant and Neuroprotective Effects of Hesperidin and Its Aglycone Hesperetin. *Arch Pharm Res.* 2006; 29: 699-706.
- Choi EJ. Hesperetin Induced G1-Phase Cell Cycle Arrest in Human Breast Cancer MCF-7 Cells: Involvement of Cdk4 and P21. *Nutr Cancer.* 2007; 59: 115-119.
- Choudhury R, Chowrimootoo G, Srini K, Debnam E, Rice-Evans CA. Interactions of the Flavonoid Naringenin in the Gastrointestinal Tract and the Influence of Glycosylation. *Biochem Biophys Res Commun.* 1999; 265: 410-415.
- Chow HH, Cai Y, Alberts DS, Hakim I, Dorr R, Shahi F, Crowell JA, Yang CS, Hara Y. Phase I Pharmacokinetic Study of Tea Polyphenols Following Single-Dose Administration of Epigallocatechin Gallate and Polyphenon E. *Cancer Epidemiol Biomarkers Prev.* 2001; 10: 53-58.
- Cipolletta C, Jouzeau JY, Gegout-Pottier P, Presle N, Bordji K, Netter P, Terlain B. Modulation of IL-1-Induced Cartilage Injury by NO Synthase Inhibitors: A Comparative Study with Rat Chondrocytes and Cartilage Entities. *Br J Pharmacol.* 1998; 124: 1719-1727.
- Cook NC, Samman S. Flavonoids-Chemistry, Metabolism, Cardioprotective Effects, and Dietary Sources. *J Nutr Biochem.* 1996; 6: 66-76.
- Corpet DE, Pierre F. Point: From Animal Models to Prevention of Colon Cancer. Systematic Review of Chemoprevention in Min Mice and Choice of the Model System. *Cancer Epidemiol Biomarkers Prev.* 2003; 12: 391-400.
- Corpet DE, Tache S. Most Effective Colon Cancer Chemopreventive Agents in Rats: A Systematic Review of Aberrant Crypt Foci and Tumor Data, Ranked by Potency. *Nutr Cancer.* 2002; 43: 1-21.

Crespo ME, Galvez J, Cruz T, Ocete MA, Zarzuelo A. Anti-Inflammatory Activity of Diosmin and Hesperidin in Rat Colitis Induced by Tnbs. *Planta Med.* 1999; 65: 651-653.

Crespy V, Morand C, Besson C, Cotelle N, Vezin H, Demigne C, Remesy C. The Splanchnic Metabolism of Flavonoids Highly Differed According to the Nature of the Compound. *Am J Physiol Gastrointest Liver Physiol.* 2003; 284: G980-988.

Crossley R. The Relevance of Chirality to the Study of Biological Activity. *Tetrahedron.* 1992; 48: 8155-8178.

Cvetnic Z, Vladimir-Knezevic S. Antimicrobial Activity of Grapefruit Seed and Pulp Ethanolic Extract. *Acta Pharm.* 2004; 54: 243-250.

D'Odorico A, Bortolan S, Cardin R, D'Inca R, Martines D, Ferronato A, Sturniolo GC. Reduced Plasma Antioxidant Concentrations and Increased Oxidative DNA Damage in Inflammatory Bowel Disease. *Scand J Gastroenterol.* 2001; 36: 1289-1294.

Daigle DJ, Conkerton EJ, Sanders TH, Mixon AC. Peanut Hull Flavonoids: Their Relationship with Peanut Maturity. *J Agric Food Chem.* 1988; 36: 1179-1181.

Dapkevicius A, van Beek TA, Lelyveld GP, van Veldhuizen A, de Groot A, Linssen JP, Venskutonis R. Isolation and Structure Elucidation of Radical Scavengers from Thymus Vulgaris Leaves. *J Nat Prod.* 2002; 65: 892-896.

Davies B, Morris T. Physiological Parameters in Laboratory Animals and Humans. *Pharm Res.* 1993; 10: 1093-1095.

Davies NM. Review Article: Non-Steroidal Anti-Inflammatory Drug-Induced Gastrointestinal Permeability. *Aliment Pharmacol Ther.* 1998; 12: 303-320.

Davies NM, Corrigan BW, Jamali F. Sucrose Urinary Excretion in the Rat Measured Using a Simple Assay: A Model of Gastroduodenal Permeability. *Pharm Res.* 1995; 12: 1733-1736.

Davies NM, Wright MR, Jamali F. Antiinflammatory Drug-Induced Small Intestinal Permeability: The Rat Is a Suitable Model. *Pharm Res.* 1994; 11: 1652-1656.

Davis BD, Needs PW, Kroon PA, Brodbelt JS. Identification of Isomeric Flavonoid Glucuronides in Urine and Plasma by Metal Complexation and Lc-Esi-MS/MS. *J Mass Spectrom.* 2006; 41: 911-920.

De Clercq E. Potential Antivirals and Antiviral Strategies against Sars Coronavirus Infections. *Expert Rev Anti Infect Ther.* 2006; 4: 291-302.

Dean DD, Martel-Pelletier J, Pelletier JP, Howell DS, Woessner JF, Jr. Evidence for Metalloproteinase and Metalloproteinase Inhibitor Imbalance in Human Osteoarthritic Cartilage. *J Clin Invest.* 1989; 84: 678-685.

Delserone LM, Matthews DE, VanEtten HD. Differential Toxicity of Enantiomers of Maackian and Pisatin to Phytopathogenic Fungi. *Phytochemistry.* 1992; 31: 3813-3819.

Devaraj S, Jialal I, Vega-Lopez S. Plant Sterol-Fortified Orange Juice Effectively Lowers Cholesterol Levels in Mildly Hypercholesterolemic Healthy Individuals. *Arterioscler Thromb Vasc Biol.* 2004; 24: e25-28.

Di Carlo G, Mascolo N, Izzo AA, Capasso F. Flavonoids: Old and New Aspects of a Class of Natural Therapeutic Drugs. *Life Sci.* 1999; 65: 337-353.

Di Rosa M, Giroud JP, Willoughby DA. Studies on the Mediators of the Acute Inflammatory Response Induced in Rats in Different Sites by Carrageenan and Turpentine. *J Pathol.* 1971; 104: 15-29.

Dillon CT, Hambley TW, Kennedy BJ, Lay PA, Zhou Q, Davies NM, Biffin JR, Regtop HL. Gastrointestinal Toxicity, Antiinflammatory Activity, and Superoxide Dismutase Activity of Copper and Zinc Complexes of the Antiinflammatory Drug Indomethacin. *Chem Res Toxicol.* 2003; 16: 28-37.

Donovan JL, Bell JR, Kasim-Karakas S, German JB, Walzem RL, Hansen RJ, Waterhouse AL. Catechin Is Present as Metabolites in Human Plasma after Consumption of Red Wine. *J Nutr.* 1999; 129: 1662-1668.

Dukens JA, Naginski TJ. Urinary 8-Hydroxydeoxyguanosine Excretion as a Non-Invasive Marker of Neutrophil Activation in Animal Models of Inflammatory Bowel Disease. *Scand J Gastroenterol.* 1998; 33: 628-636.

Dwyer JT, Peterson JJ. Measuring Flavonoid Intake: Need for Advanced Tools. *Public Health Nutr.* 2002; 5: 925-930.

Eagling VA, Profit L, Back DJ. Inhibition of the Cyp3a4-Mediated Metabolism and P-Glycoprotein-Mediated Transport of the Hiv-1 Protease Inhibitor Saquinavir by Grapefruit Juice Components. *Br J Clin Pharmacol.* 1999; 48: 543-552.

Edenharder R, Grunhage D. Free Radical Scavenging Abilities of Flavonoids as Mechanism of Protection against Mutagenicity Induced by Tert-Butyl Hydroperoxide or Cumene Hydroperoxide in Salmonella Typhimurium Ta102. *Mutat Res.* 2003; 540: 1-18.

Edwards DJ, Bellevue FH, 3rd, Woster PM. Identification of 6',7'-Dihydroxybergamottin, a Cytochrome P450 Inhibitor, in Grapefruit Juice. *Drug Metab Dispos.* 1996a; 24: 1287-1290.

Edwards DJ, Bernier SM. Naringin and Naringenin Are Not the Primary Cyp3a Inhibitors in Grapefruit Juice. *Life Sci.* 1996b; 59: 1025-1030.

el-Gammal AA, Mansour RM. Antimicrobial Activities of Some Flavonoid Compounds. *Zentralbl Mikrobiol.* 1986; 141: 561-565.

Erlund I, Meririnne E, Alfthan G, Aro A. Plasma Kinetics and Urinary Excretion of the Flavanones Naringenin and Hesperetin in Humans after Ingestion of Orange Juice and Grapefruit Juice. *J Nutr.* 2001; 131: 235-241.

Erlund I, Silaste ML, Alfthan G, Rantala M, Kesaniemi YA, Aro A. Plasma Concentrations of the Flavonoids Hesperetin, Naringenin and Quercetin in Human Subjects Following Their Habitual Diets, and Diets High or Low in Fruit and Vegetables. *Eur J Clin Nutr.* 2002; 56: 891-898.

Exarchou V, Godejohann M, van Beek TA, Gerothanassis IP, Vervoort J. Lc-Uv-Solid-Phase Extraction-Nmr-Ms Combined with a Cryogenic Flow Probe and Its Application to the Identification of Compounds Present in Greek Oregano. *Anal Chem.* 2003; 75: 6288-6294.

FDA. Fda'S Policy Statement for the Development of New Stereoisomeric Drugs. *Chirality*; 1992. p. 338-340.

Fenton JI, Chlebek-Brown KA, Caron JP, Orth MW. Effect of Glucosamine on Interleukin-1-Conditioned Articular Cartilage. *Equine Vet J Suppl.* 2002; 219-223.

Ficarra P, Ficarra R, Bertucci C, Tommasini S, Calabro ML, Costantino D, Carulli M. Direct Enantiomeric Separation of Flavanones by High Performance Liquid Chromatography Using Various Chiral Stationary Phases. *Planta Med.* 1995; 61: 171-176.

Formica JV, Regelson W. Review of the Biology of Quercetin and Related Bioflavonoids. *Food Chem Toxicol.* 1995; 33: 1061-1080.

Forrest ML, Yanez JA, Remsberg CM, Ohgami Y, Kwon GS, Davies NM. Paclitaxel Prodrugs with Sustained Release and High Solubility in Poly(Ethylene Glycol)-B-

Poly(Epsilon-Caprolactone) Micelle Nanocarriers: Pharmacokinetic Disposition, Tolerability, and Cytotoxicity. *Pharm Res.* 2007;

Fotsis T, Pepper MS, Aktas E, Breit S, Rasku S, Adlercreutz H, Wahala K, Montesano R, Schweigerer L. Flavonoids, Dietary-Derived Inhibitors of Cell Proliferation and in Vitro Angiogenesis. *Cancer Res.* 1997; 57: 2916-2921.

Franke AA, Cooney RV, Custer LJ, Mordan LJ, Tanaka Y. Inhibition of Neoplastic Transformation and Bioavailability of Dietary Flavonoid Agents. *Adv Exp Med Biol.* 1998; 439: 237-248.

Franke AA, Custer LJ, Cooney RV, Tanaka Y, Xu M, Dashwood RH. Inhibition of Colonic Aberrant Crypt Formation by the Dietary Flavonoids (+)-Catechin and Hesperidin. *Adv Exp Med Biol.* 2002; 505: 123-133.

Frydoonfar HR, McGrath DR, Spigelman AD. The Variable Effect on Proliferation of a Colon Cancer Cell Line by the Citrus Fruit Flavonoid Naringenin. *Colorectal Dis.* 2003; 5: 149-152.

Fuhr U. Drug Interactions with Grapefruit Juice. Extent, Probable Mechanism and Clinical Relevance. *Drug Saf.* 1998; 18: 251-272.

Fukuda K, Ohta T, Yamazoe Y. Grapefruit Component Interacting with Rat and Human P450 Cyp3a: Possible Involvement of Non-Flavonoid Components in Drug Interaction. *Biol Pharm Bull.* 1997; 20: 560-564.

Gaffield W. Circular Dichroism, Optical Rotatory Dispersion and Absolute Configuration of Flavanones, 3-Hydroxyflavanones and Their Glycosides. *Tetrahedron.* 1970; 26: 4093-4108.

Gaffield W, Lundin RE, Gentili B, Horowitz RH. C-2 Stereochemistry of Naringenin and Its Relation to Taste and Biosynthesis in Maturing Grapefruit. *Bioorgan Chem.* 1975; 4: 259-269.

Galati EM, Monforte MT, Kirjavainen S, Forestieri AM, Trovato A, Tripodo MM. Biological Effects of Hesperidin, a Citrus Flavonoid. (Note I): Antiinflammatory and Analgesic Activity. *Farmaco.* 1994; 40: 709-712.

Galensa R, Herrmann K. Analysis of Flavonoids by High-Performance Liquid Chromatography. *J Chromatogr.* 1980; 189: 217-224.

Galvez J, Garrido M, Merlos M, Torres MI, Zarzuelo A. Intestinal Anti-Inflammatory Activity of Ur-12746, a Novel 5-Asa Conjugate, on Acute and Chronic Experimental Colitis in the Rat. *Br J Pharmacol.* 2000; 130: 1949-1959.

Garbacki N, Angenot L, Bassleer C, Damas J, Tits M. Effects of Prodelphinidins Isolated from Ribes Nigrum on Chondrocyte Metabolism and Cox Activity. *Naunyn Schmiedebergs Arch Pharmacol.* 2002; 365: 434-441.

Garg A, Garg S, Zaneveld LJ, Singla AK. Chemistry and Pharmacology of the Citrus Bioflavonoid Hesperidin. *Phytother Res.* 2001; 15: 655-669.

Geissman TA. The Isolation of Eriodictyol and Homoeriodictyol. An Improved Procedure. *J Am Chem Soc.* 1940; 62: 3258-3259.

Gel-Moreto N, Streich R, Galensa R. Chiral Separation of Diastereomeric Flavanone-7-O-Glycosides in Citrus by Capillary Electrophoresis. *Electrophoresis.* 2003; 24: 2716-2722.

Gel-Moreto N, Streich R, Galensa R. Chiral Separation of Six Diastereomeric Flavanone-7-O-Glycosides by Capillary Electrophoresis and Analysis of Lemon Juice. *J Chromatogr A.* 2001; 925: 279-289.

Gil-Izquierdo A, Riquelme MT, Porras I, Ferreres F. Effect of the Rootstock and Interstock Grafted in Lemon Tree (*Citrus Limon* (L.) Burm.) on the Flavonoid Content of Lemon Juice. *J Agric Food Chem.* 2004; 52: 324-331.

Giorgio E, Parrinello N, Caccamese S, Rosini C. Non-Empirical Assignment of the Absolute Configuration of (-)-Naringenin, by Coupling the Exciton Analysis of the Circular Dichroism Spectrum and the Ab Initio Calculation of the Optical Rotatory Power. *Org Biomol Chem.* 2004; 2: 3602-3607.

Gitter AH, Wullstein F, Fromm M, Schulzke JD. Epithelial Barrier Defects in Ulcerative Colitis: Characterization and Quantification by Electrophysiological Imaging. *Gastroenterology.* 2001; 121: 1320-1328.

Goggs R, Carter SD, Schulze-Tanzil G, Shakibaei M, Mobasheri A. Apoptosis and the Loss of Chondrocyte Survival Signals Contribute to Articular Cartilage Degradation in Osteoarthritis. *Vet J.* 2003; 166: 140-158.

Goldring MB, Birkhead JR, Suen LF, Yamin R, Mizuno S, Glowacki J, Arbiser JL, Apperley JF. Interleukin-1 Beta-Modulated Gene Expression in Immortalized Human Chondrocytes. *J Clin Invest.* 1994; 94: 2307-2316.

Gonzalez-Gallego J, Sanchez-Campos S, Tunon MJ. Anti-Inflammatory Properties of Dietary Flavonoids. *Nutr Hosp.* 2007; 22: 287-293.

Gopalakrishnan A, Xu CJ, Nair SS, Chen C, Hebbar V, Kong AN. Modulation of Activator Protein-1 (Ap-1) and Mapk Pathway by Flavonoids in Human Prostate Cancer Pc3 Cells. *Arch Pharm Res.* 2006; 29: 633-644.

Gorinstein S, Leontowicz H, Leontowicz M, Krzeminski R, Gralak M, Delgado-Licon E, Martinez Ayala AL, Katrich E, Trakhtenberg S. Changes in Plasma Lipid and Antioxidant

Activity in Rats as a Result of Naringin and Red Grapefruit Supplementation. *J Agric Food Chem.* 2005; 53: 3223-3228.

Grundy JS, Eliot LA, Kulmatycki KM, Foster RT. Grapefruit Juice and Orange Juice Effects on the Bioavailability of Nifedipine in the Rat. *Biopharm Drug Dispos.* 1998; 19: 175-183.

Guengerich FP, Kim DH. In Vitro Inhibition of Dihydropyridine Oxidation and Aflatoxin B1 Activation in Human Liver Microsomes by Naringenin and Other Flavonoids. *Carcinogenesis.* 1990; 11: 2275-2279.

Guo LQ, Fukuda K, Ohta T, Yamazoe Y. Role of Furanocoumarin Derivatives on Grapefruit Juice-Mediated Inhibition of Human Cyp3a Activity. *Drug Metab Dispos.* 2000a; 28: 766-771.

Guo LQ, Taniguchi M, Xiao YQ, Baba K, Ohta T, Yamazoe Y. Inhibitory Effect of Natural Furanocoumarins on Human Microsomal Cytochrome P450 3a Activity. *Jpn J Pharmacol.* 2000b; 82: 122-129.

Habtemariam S. Flavonoids as Inhibitors or Enhancers of the Cytotoxicity of Tumor Necrosis Factor-Alpha in L-929 Tumor Cells. *J Nat Prod.* 1997; 60: 775-778.

Harborne JB, Williams CA. Advances in Flavonoid Research since 1992. *Phytochemistry.* 2000; 55: 481-504.

Hardy MM, Seibert K, Manning PT, Currie MG, Woerner BM, Edwards D, Koki A, Tripp CS. Cyclooxygenase 2-Dependent Prostaglandin E2 Modulates Cartilage Proteoglycan Degradation in Human Osteoarthritis Explants. *Arthritis Rheum.* 2002; 46: 1789-1803.

Harmon AW, Patel YM. Naringenin Inhibits Glucose Uptake in MCF-7 Breast Cancer Cells: A Mechanism for Impaired Cellular Proliferation. *Breast Cancer Res Treat.* 2004; 85: 103-110.

Hashimoto K, Shirafuji T, Sekino H, Matsuoka O, Sekino H, Onnagawa O, Okamoto T, Kudo S, Azuma J. Interaction of Citrus Juices with Pranidipine, a New 1,4-Dihydropyridine Calcium Antagonist, in Healthy Subjects. *Eur J Clin Pharmacol.* 1998; 54: 753-760.

Haslam E. Practical Polyphenolics. From Structure to Molecular Recognition and Physiological Action. Cambridge, UK: Cambridge University Press; 1998.

Hertog MG, Feskens EJ, Hollman PC, Katan MB, Kromhout D. Dietary Antioxidant Flavonoids and Risk of Coronary Heart Disease: The Zutphen Elderly Study. *Lancet.* 1993; 342: 1007-1011.

Hirata A, Murakami Y, Shoji M, Kadoma Y, Fujisawa S. Kinetics of Radical-Scavenging Activity of Hesperetin and Hesperidin and Their Inhibitory Activity on Cox-2 Expression. *Anticancer Res.* 2005; 25: 3367-3374.

Ho PC, Saville DJ, Coville PF, Wanwimolruk S. Content of Cyp3a4 Inhibitors, Naringin, Naringenin and Bergapten in Grapefruit and Grapefruit Juice Products. *Pharm Acta Helv.* 2000; 74: 379-385.

Hoffmann JC, Pawlowski NN, Kuhl AA, Hohne W, Zeitz M. Animal Models of Inflammatory Bowel Disease: An Overview. *Pathobiology.* 2002; 70: 121-130.

Holma R, Juvonen P, Asmawi MZ, Vapaatalo H, Korpela R. Galacto-Oligosaccharides Stimulate the Growth of Bifidobacteria but Fail to Attenuate Inflammation in Experimental Colitis in Rats. *Scand J Gastroenterol.* 2002; 37: 1042-1047.

Hougee S, Sanders A, Faber J, Graus YM, van den Berg WB, Garssen J, Smit HF, Hoijer MA. Decreased Pro-Inflammatory Cytokine Production by Lps-Stimulated PbmC Upon in Vitro Incubation with the Flavonoids Apigenin, Luteolin or Chrysin, Due to Selective Elimination of Monocytes/Macrophages. *Biochem Pharmacol.* 2005; 69: 241-248.

Hsiu SL, Huang TY, Hou YC, Chin DH, Chao PD. Comparison of Metabolic Pharmacokinetics of Naringin and Naringenin in Rabbits. *Life Sci.* 2002; 70: 1481-1489.

Hsu CL, Yen GC. Effects of Flavonoids and Phenolic Acids on the Inhibition of Adipogenesis in 3T3-L1 Adipocytes. *J Agric Food Chem.* 2007; 55: 8404-8410.

Hsu CL, Yen GC. Induction of Cell Apoptosis in 3T3-L1 Pre-Adipocytes by Flavonoids Is Associated with Their Antioxidant Activity. *Mol Nutr Food Res.* 2006; 50: 1072-1079.

Hu C, Kitts DD. Studies on the Antioxidant Activity of Echinacea Root Extract. *J Agric Food Chem.* 2000; 48: 1466-1472.

Hungria M, Johnston AW, Phillips DA. Effects of Flavonoids Released Naturally from Bean (*Phaseolus Vulgaris*) on Nod-Regulated Gene Transcription in *Rhizobium Leguminosarum Bv. Phaseoli*. *Mol Plant Microbe Interact.* 1992; 5: 199-203.

Hunter T. Signaling--2000 and Beyond. *Cell.* 2000; 100: 113-127.

Huong DT, Takahashi Y, Ide T. Activity and mRNA Levels of Enzymes Involved in Hepatic Fatty Acid Oxidation in Mice Fed Citrus Flavonoids. *Nutrition.* 2006; 22: 546-552.

Hvattum E. Determination of Phenolic Compounds in Rose Hip (*Rosa Canina*) Using Liquid Chromatography Coupled to Electrospray Ionisation Tandem Mass Spectrometry and Diode-Array Detection. *Rapid Commun Mass Spectrom.* 2002; 16: 655-662.

Ishii K, Furuta T, Kasuya Y. Mass Spectrometric Identification and High-Performance Liquid Chromatographic Determination of a Flavonoid Glycoside Naringin in Human Urine. *J Agric Food Chem.* 2000; 48: 56-59.

Ismail B, Hayes K. Beta-Glycosidase Activity toward Different Glycosidic Forms of Isoflavones. *J Agric Food Chem.* 2005; 53: 4918-4924.

Ismaili H, Sosa S, Brkic D, Fkih-Tetouani S, Ildrissi A, Touati D, Aquino RP, Tubaro A. Topical Anti-Inflammatory Activity of Extracts and Compounds from *Thymus Broussonettii*. *J Pharm Pharmacol.* 2002; 54: 1137-1140.

Jagetia A, Jagetia GC, Jha S. Naringin, a Grapefruit Flavanone, Protects V79 Cells against the Bleomycin-Induced Genotoxicity and Decline in Survival. *J Appl Toxicol.* 2007; 27: 122-132.

Jagetia GC, Reddy TK, Venkatesha VA, Kedlaya R. Influence of Naringin on Ferric Iron Induced Oxidative Damage in Vitro. *Clin Chim Acta.* 2004; 347: 189-197.

Jagetia GC, Venkatesha VA. Treatment of Mice with Stem Bark Extract of *Aphanamixis Polystachya* Reduces Radiation-Induced Chromosome Damage. *Int J Radiat Biol.* 2006; 82: 197-209.

Jamali F, Alballa RS, Mehvar R, Lemko CH. Longer Plasma Half-Life for Procainamide Utilizing a Very Sensitive High Performance Liquid Chromatography Assay. *Ther Drug Monit.* 1988; 10: 91-96.

Jean PA, Roth RA. Naphthylisothiocyanate Disposition in Bile and Its Relationship to Liver Glutathione and Toxicity. *Biochem Pharmacol.* 1995; 50: 1469-1474.

Jenkins AP, Nukajam WS, Menzies IS, Creamer B. Simultaneous Administration of Lactulose and 51cr-Ethylenediaminetetraacetic Acid. A Test to Distinguish Colonic from Small-Intestinal Permeability Change. *Scand J Gastroenterol.* 1992; 27: 769-773.

Jung UJ, Kim HJ, Lee JS, Lee MK, Kim HO, Park EJ, Kim HK, Jeong TS, Choi MS. Naringin Supplementation Lowers Plasma Lipids and Enhances Erythrocyte Antioxidant Enzyme Activities in Hypercholesterolemic Subjects. *Clin Nutr.* 2003; 22: 561-568.

Kalinowski DP, Illenye S, Van Houten B. Analysis of DNA Damage and Repair in Murine Leukemia L1210 Cells Using a Quantitative Polymerase Chain Reaction Assay. *Nucleic Acids Res.* 1992; 20: 3485-3494.

Kanaze FI, Bounartzi MI, Georgarakis M, Niopas I. Pharmacokinetics of the Citrus Flavanone Aglycones Hesperetin and Naringenin after Single Oral Administration in Human Subjects. *Eur J Clin Nutr.* 2007; 61: 472-477.

Kankuri E, Vaali K, Korpela R, Paakkari I, Vapaatalo H, Moilanen E. Effects of a Cox-2 Preferential Agent Nimesulide on Tnbs-Induced Acute Inflammation in the Gut. *Inflammation.* 2001; 25: 301-310.

Kanno S, Shouji A, Hirata R, Asou K, Ishikawa M. Effects of Naringin on Cytosine Arabinoside (Ara-C)-Induced Cytotoxicity and Apoptosis in P388 Cells. *Life Sci.* 2004; 75: 353-365.

Kanno S, Shouji A, Tomizawa A, Hiura T, Osanai Y, Ujibe M, Obara Y, Nakahata N, Ishikawa M. Inhibitory Effect of Naringin on Lipopolysaccharide (Lps)-Induced Endotoxin Shock in Mice and Nitric Oxide Production in Raw 264.7 Macrophages. *Life Sci.* 2006a; 78: 673-681.

Kanno S, Tomizawa A, Hiura T, Osanai Y, Shouji A, Ujibe M, Ohtake T, Kimura K, Ishikawa M. Inhibitory Effects of Naringenin on Tumor Growth in Human Cancer Cell Lines and Sarcoma S-180-Implanted Mice. *Biol Pharm Bull.* 2005; 28: 527-530.

Kanno S, Tomizawa A, Ohtake T, Koiwai K, Ujibe M, Ishikawa M. Naringenin-Induced Apoptosis Via Activation of Nf-Kappab and Necrosis Involving the Loss of Atp in Human Promyeloleukemia HI-60 Cells. *Toxicol Lett.* 2006b; 166: 131-139.

Katsuyama Y, Funa N, Miyahisa I, Horinouchi S. Synthesis of Unnatural Flavonoids and Stilbenes by Exploiting the Plant Biosynthetic Pathway in Escherichia Coli. *Chem Biol.* 2007; 14: 613-621.

Katula KS, McCain JA, Radewicz AT. Relative Ability of Dietary Compounds to Modulate Nuclear Factor-Kappab Activity as Assessed in a Cell-Based Reporter System. *J Med Food.* 2005; 8: 269-274.

Kaul TN, Middleton E, Jr., Ogra PL. Antiviral Effect of Flavonoids on Human Viruses. *J Med Virol.* 1985; 15: 71-79.

Kawaguchi K, Kikuchi S, Hasunuma R, Maruyama H, Ryll R, Kumazawa Y. Suppression of Infection-Induced Endotoxin Shock in Mice by a Citrus Flavanone Naringin. *Planta Med.* 2004; 70: 17-22.

Kawaii S, Tomono Y, Katase E, Ogawa K, Yano M. Antiproliferative Activity of Flavonoids on Several Cancer Cell Lines. *Biosci Biotechnol Biochem.* 1999a; 63: 896-899.

Kawaii S, Tomono Y, Katase E, Ogawa K, Yano M. Quantitation of Flavonoid Constituents in Citrus Fruits. *J Agric Food Chem.* 1999b; 47: 3565-3571.

Kelm MA, Hammerstone JF, Schmitz HH. Identification and Quantitation of Flavanols and Proanthocyanidins in Foods: How Good Are the Datas? *Clin Dev Immunol.* 2005; 12: 35-41.

Kho YH, Pool MO, Jansman FG, Harting JW. Pharmacotherapeutic Options in Inflammatory Bowel Disease: An Update. *Pharm World Sci.* 2001; 23: 17-21.

Kim HJ, Choi JS. Effects of Naringin on the Pharmacokinetics of Verapamil and One of Its Metabolites, Norverapamil, in Rabbits. *Biopharm Drug Dispos.* 2005; 26: 295-300.

Kim HS, Berstad A. Experimental Colitis in Animal Models. *Scand J Gastroenterol.* 1992; 27: 529-537.

Kim JY, Jung KJ, Choi JS, Chung HY. Hesperetin: A Potent Antioxidant against Peroxynitrite. *Free Radic Res.* 2004; 38: 761-769.

Kimura M, Umegaki K, Kasuya Y, Sugisawa A, Higuchi M. The Relation between Single/Double or Repeated Tea Catechin Ingestions and Plasma Antioxidant Activity in Humans. *Eur J Clin Nutr.* 2002; 56: 1186-1193.

Klinge CM, Risinger KE, Watts MB, Beck V, Eder R, Jungbauer A. Estrogenic Activity in White and Red Wine Extracts. *J Agric Food Chem.* 2003; 51: 1850-1857.

Knekt P, Jarvinen R, Seppanen R, Helleovaara M, Teppo L, Pukkala E, Aromaa A. Dietary Flavonoids and the Risk of Lung Cancer and Other Malignant Neoplasms. *Am J Epidemiol.* 1997; 146: 223-230.

Koru O, Toksoy F, Acikel CH, Tunca YM, Baysallar M, Uskudar Guclu A, Akca E, Ozkok Tuylu A, Sorkun K, Tanyuksel M, Salih B. In Vitro Antimicrobial Activity of Propolis Samples from Different Geographical Origins against Certain Oral Pathogens. *Anaerobe.* 2007; 13: 140-145.

Kosar M, Dorman HJ, Can Baser KH, Hiltunen R. Screening of Free Radical Scavenging Compounds in Water Extracts of Mentha Samples Using a Postcolumn Derivatization Method. *J Agric Food Chem.* 2004; 52: 5004-5010.

Krause M, Galensa R. Analysis of Enantiomeric Flavanones in Plant Extracts by High-Performance Liquid Chromatography on a Cellulose Triacetate Based Chiral Stationary Phase. *Chromatographia.* 1991a; 32: 69-72.

Krause M, Galensa R. Direct Enantiomeric Separation of Racemic Flavanones by High-Performance Liquid Chromatography Using Cellulose Triacetate as a Chiral Stationary Phase. *J Chromatogr.* 1988; 441: 417-422.

Krause M, Galensa R. High-Performance Liquid Chromatography of Diastereometric Flavanone Glycosides in Citrus on A-Cyclodextrin-Bonded Stationary Phase (Cyclobond I). *J Chromatogr.* 1991b; 588: 41-45.

Krause M, Galensa R. Hplc-Trennung Von Racemischen Flavanonen an Chiralen Phasen. *Lebensmittelchemie und gerichtliche Chemie.* 1989; 43: 12-13.

Krause M, Galensa R. Improved Chiral Stationary Phase Based on Cellulose Triacetate Supported on Non-Macroporous Silica Gel Diol for the High-Performance Liquid Chromatographic Separation of Racemic Flavanones and Diastereomeric Flavanone Glycosides. *J Chromatogr.* 1990a; 502: 287-296.

Krause M, Galensa R. Optical Resolution of Flavanones by High-Performance Liquid Chromatography on Various Chiral Stationary Phases. *J Chromatogr.* 1990b; 514: 147-159.

Krimsky M, Dagan A, Aptekar L, Ligumsky M, Yedgar S. Assessment of Intestinal Permeability in Rats by Permeation of Inulin-Fluorescein. *J Basic Clin Physiol Pharmacol.* 2000; 11: 143-153.

Kruschewski M, Foitzik T, Perez-Canto A, Hubotter A, Buhr HJ. Changes of Colonic Mucosal Microcirculation and Histology in Two Colitis Models: An Experimental Study Using Intravital Microscopy and a New Histological Scoring System. *Dig Dis Sci.* 2001; 46: 2336-2343.

Kuroki K, Cook JL, Kreeger JM. Mechanisms of Action and Potential Uses of Hyaluronan in Dogs with Osteoarthritis. *J Am Vet Med Assoc.* 2002; 221: 944-950.

Kurowska EM, Spence JD, Jordan J, Wetmore S, Freeman DJ, Piche LA, Serratore P. Hdl-Cholesterol-Raising Effect of Orange Juice in Subjects with Hypercholesterolemia. *Am J Clin Nutr.* 2000; 72: 1095-1100.

Kusuno A, Mori M, Satoh T, Miura M, Kaga H, Kakuchi T. Enantioseparation Properties of (1 \rightarrow 6)-Alpha-D-Glucopyranan and (1 \rightarrow 6)-Alpha-D-Mannopyranan Tris(Phenylcarbamate)S as Chiral Stationary Phases in Hplc. *Chirality.* 2002; 14: 498-502.

Lai XH, Ng SC. Enantioseparation on Mono(6a-N-Allylamino-6a-Deoxy)Permethyated 3-Cyclodextrin Covalently Bonded Silica Gel. *J Chromatogr A.* 2004; 1059: 53-59.

Lantz AW, Rozhkov RV, Larock RC, Armstrong DW. Enantiomeric Separation of Neutral Hydrophobic Dihydrofuroflavones by Cyclodextrin-Modified Micellar Capillary Electrophoresis. *Electrophoresis.* 2004; 25: 2727-2734.

Le Gall G, DuPont MS, Mellon FA, Davis AL, Collins GJ, Verhoeyen ME, Colquhoun IJ. Characterization and Content of Flavonoid Glycosides in Genetically Modified Tomato (*Lycopersicon Esculentum*) Fruits. *J Agric Food Chem.* 2003; 51: 2438-2446.

Lea AGH, Bridle P, Timberlake CF, Singleton VL. The Procyanidins of White Grapes and Wines. *AM J Enol Vitic.* 1979; 30 289-300.

Lee ER, Kim JH, Kang YJ, Cho SG. The Anti-Apoptotic and Anti-Oxidant Effect of Eriodictyol on Uv-Induced Apoptosis in Keratinocytes. *Biol Pharm Bull.* 2007; 30: 32-37.

Lee MJ, Maliakal P, Chen L, Meng X, Bondoc FY, Prabhu S, Lambert G, Mohr S, Yang CS. Pharmacokinetics of Tea Catechins after Ingestion of Green Tea and (-)-Epigallocatechin-3-Gallate by Humans: Formation of Different Metabolites and Individual Variability. *Cancer Epidemiol Biomarkers Prev.* 2002; 11: 1025-1032.

Lee MJ, Wang ZY, Li H, Chen L, Sun Y, Gobbo S, Balentine DA, Yang CS. Analysis of Plasma and Urinary Tea Polyphenols in Human Subjects. *Cancer Epidemiol Biomarkers Prev.* 1995; 4: 393-399.

Leenen R, Roodenburg AJ, Tijburg LB, Wiseman SA. A Single Dose of Tea with or without Milk Increases Plasma Antioxidant Activity in Humans. *Eur J Clin Nutr.* 2000; 54: 87-92.

Li C, Homma M, Ohkura N, Oka K. Stereochemistry and Putative Origins of Flavanones Found in Post-Administration Urine of the Traditional Chinese Remedies Shosaiko-to and Daisaiko-To. *Chem Pharm Bull (Tokyo).* 1998a; 46: 807-811.

Li C, Homma M, Oka K. Characteristics of Delayed Excretion of Flavonoids in Human Urine after Administration of Shosaiko-to, a Herbal Medicine. *Biol Pharm Bull.* 1998b; 21: 1251-1257.

Li C, Homma M, Oka K. Chiral Resolution of Four Major Flavanones in Post-Administrative Urine of Chinese Herbal Medicines by Hplc on Macroporous Silica Gel Coated with Cellulose Tris(3,5-Dimethylphenylcarbamate). *Biomed Chromatogr.* 1998c; 12: 199-202.

Lotito SB, Frei B. Dietary Flavonoids Attenuate Tumor Necrosis Factor Alpha-Induced Adhesion Molecule Expression in Human Aortic Endothelial Cells. Structure-Function Relationships and Activity after First Pass Metabolism. *J Biol Chem.* 2006; 281: 37102-37110.

Lown KS, Bailey DG, Fontana RJ, Janardan SK, Adair CH, Fortlage LA, Brown MB, Guo W, Watkins PB. Grapefruit Juice Increases Felodipine Oral Availability in Humans by Decreasing Intestinal Cyp3a Protein Expression. *J Clin Invest.* 1997; 99: 2545-2553.

Lyu SY, Rhim JY, Park WB. Antiherpetic Activities of Flavonoids against Herpes Simplex Virus Type 1 (Hsv-1) and Type 2 (Hsv-2) in Vitro. *Arch Pharm Res.* 2005; 28: 1293-1301.

Maiti K, Mukherjee K, Gantait A, Saha BP, Mukherjee PK. Enhanced Therapeutic Potential of Naringenin-Phospholipid Complex in Rats. *J Pharm Pharmacol.* 2006; 58: 1227-1233.

Manach C, Morand C, Gil-Izquierdo A, Bouteloup-Demange C, Remesy C. Bioavailability in Humans of the Flavanones Hesperidin and Narirutin after the Ingestion of Two Doses of Orange Juice. *Eur J Clin Nutr.* 2003; 57: 235-242.

Manach C, Williamson G, Morand C, Scalbert A, Remesy C. Bioavailability and Bioefficacy of Polyphenols in Humans. I. Review of 97 Bioavailability Studies. *Am J Clin Nutr.* 2005; 81: 230S-242S.

Manfield L, Jang D, Murrell GA. Nitric Oxide Enhances Cyclooxygenase Activity in Articular Cartilage. *Inflamm Res.* 1996; 45: 254-258.

Marin FR, Martinez M, Uribealago T, Castillo S, Frutos MJ. Changes in Nutraceutical Composition of Lemon Juices According to Different Industrial Extraction Systems. *Food Chem.* 2002; 78: 319-324.

Martin AR, Villegas I, La Casa C, de la Lastra CA. Resveratrol, a Polyphenol Found in Grapes, Suppresses Oxidative Damage and Stimulates Apoptosis During Early Colonic Inflammation in Rats. *Biochem Pharmacol.* 2004; 67: 1399-1410.

Mathus-Vliegen EM, Nikkel D, Brand HS. Oral Aspects of Obesity. *Int Dent J.* 2007; 57: 249-256.

Matsumoto H, Ikoma Y, Sugiura M, Yano M, Hasegawa Y. Identification and Quantification of the Conjugated Metabolites Derived from Orally Administered Hesperidin in Rat Plasma. *J Agric Food Chem.* 2004; 52: 6653-6659.

Mbvundula EC, Bunning RA, Rainsford KD. Effects of Cannabinoids on Nitric Oxide Production by Chondrocytes and Proteoglycan Degradation in Cartilage. *Biochem Pharmacol.* 2005; 69: 635-640.

McKay DL, Blumberg JB. A Review of the Bioactivity and Potential Health Benefits of Peppermint Tea (*Mentha Piperita* L.). *Phytother Res.* 2006; 20: 619-633.

Meddings JB, Gibbons I. Discrimination of Site-Specific Alterations in Gi Permeability in the Rat. *Gastroenterology.* 1998; 114: 83-92.

Megalli S, Aktan F, Davies NM, Roufogalis BD. Phytopreventative Anti-Hyperlipidemic Effects of *Gynostemma Pentaphyllum* in Rats. *J Pharm Pharm Sci.* 2005; 8: 507-515.

Megalli S, Davies NM, Roufogalis BD. Anti-Hyperlipidemic and Hypoglycemic Effects of *Gynostemma Pentaphyllum* in the Zucker Fatty Rat. *J Pharm Pharm Sci.* 2006; 9: 281-291.

Meier R, Schuler W, Desaulles P. Zur Frage Des Mechanismus Der Hemmung Des Bindegewebswachstums Durch. *Cortisone Experientia.* 1950; VI/12: 469-471.

Meng X, Lee MJ, Li C, Sheng S, Zhu N, Sang S, Ho CT, Yang CS. Formation and Identification of 4'-O-Methyl-(-)-Epigallocatechin in Humans. *Drug Metab Dispos.* 2001; 29: 789-793.

Merken HM, Beecher GR. Liquid Chromatographic Method for the Separation and Quantification of Prominent Flavonoid Aglycones. *J Chromatogr A.* 2000; 897: 177-184.

Middleton E, Jr. Effect of Plant Flavonoids on Immune and Inflammatory Cell Function. *Adv Exp Med Biol.* 1998; 439: 175-182.

Middleton E, Kandaswami C. The Impact of Plant Flavonoids in Mammalian Biology: Implications for Immunity, Inflammation and Cancer. In: Harborne J, editor. *The Flavonoids: Advances in Research since 1986.* London: Chapman & Hall; 1994. p. 619-652.

Miles CO, Main L. The Kinetics and Mechanism, and the Equilibrium Position as a Function of Ph, of the Isomerization of Naringin and the 4'-Rhamnoglucoside of 2',4,4',6'-Tetrahydroxychalcone. *J Chem Soc Perkin Trans II.* 1988; 195-198.

Minato K, Miyake Y, Fukumoto S, Yamamoto K, Kato Y, Shimomura Y, Osawa T. Lemon Flavonoid, Eriocitrin, Suppresses Exercise-Induced Oxidative Damage in Rat Liver. *Life Sci.* 2003; 72: 1609-1616.

Miniscalco A, Lundahl J, Regardh CG, Edgar B, Eriksson UG. Inhibition of Dihydropyridine Metabolism in Rat and Human Liver Microsomes by Flavonoids Found in Grapefruit Juice. *J Pharmacol Exp Ther.* 1992; 261: 1195-1199.

Minoggio M, Bramati L, Simonetti P, Gardana C, Iemoli L, Santangelo E, Mauri PL, Spigno P, Soressi GP, Pietta PG. Polyphenol Pattern and Antioxidant Activity of Different Tomato Lines and Cultivars. *Ann Nutr Metab.* 2003; 47: 64-69.

Miwa Y, Mitsuzumi H, Sunayama T, Yamada M, Okada K, Kubota M, Chaen H, Mishima Y, Kibata M. Glucosyl Hesperidin Lowers Serum Triglyceride Level in Hypertriglyceridemic Subjects through the Improvement of Very Low-Density Lipoprotein Metabolic Abnormality. *J Nutr Sci Vitaminol (Tokyo)*. 2005; 51: 460-470.

Miyagi Y, Om AS, Chee KM, Bennink MR. Inhibition of Azoxymethane-Induced Colon Cancer by Orange Juice. *Nutr Cancer*. 2000; 36: 224-229.

Miyake Y, Mochizuki M, Okada M, Hiramitsu M, Morimitsu Y, Osawa T. Isolation of Antioxidative Phenolic Glucosides from Lemon Juice and Their Suppressive Effect on the Expression of Blood Adhesion Molecules. *Biosci Biotechnol Biochem*. 2007; 71: 1911-1919.

Miyake Y, Sakurai C, Usuda M, Fukumoto S, Hiramitsu M, Sakaida K, Osawa T, Kondo K. Difference in Plasma Metabolite Concentration after Ingestion of Lemon Flavonoids and Their Aglycones in Humans. *J Nutr Sci Vitaminol (Tokyo)*. 2006; 52: 54-60.

Miyake Y, Shimoi K, Kumazawa S, Yamamoto K, Kinae N, Osawa T. Identification and Antioxidant Activity of Flavonoid Metabolites in Plasma and Urine of Eriocitrin-Treated Rats. *J Agric Food Chem*. 2000; 48: 3217-3224.

Miyake Y, Yamamoto K, Osawa T. Metabolism of Antioxidant in Lemon Fruit (Citrus Limon Burm. F.) by Human Intestinal Bacteria. *J Agric Food Chem*. 1997; 45: 3738-3742.

Miyake Y, Yamamoto K, Tsujihara N, Osawa T. Protective Effects of Lemon Flavonoids on Oxidative Stress in Diabetic Rats. *Lipids*. 1998; 33: 689-695.

Miyamoto S, Kohno H, Suzuki R, Sugie S, Murakami A, Ohigashi H, Tanaka T. Preventive Effects of Chrysin on the Development of Azoxymethane-Induced Colonic Aberrant Crypt Foci in Rats. *Oncol Rep*. 2006; 15: 1169-1173.

Mizushima Y, Tsukada W, Akimoto T. A Modification of Rat Adjuvant Arthritis for Testing Antirheumatic Drugs. *J Pharm Pharmacol*. 1972; 24: 781-785.

Moncada S, Palmer RM, Higgs EA. Nitric Oxide: Physiology, Pathophysiology, and Pharmacology. *Pharmacol Rev*. 1991; 43: 109-142.

Montanari A, Chen J, Widmer W. Citrus Flavonoids: A Review of Plant Biological Activity against Disease. Discovery of New Flavonoids from Dancy Tangerine Cold Pressed Oil Solids and Leaves. In: Manthey J, Buslig B, editors. *Flavonoids in the Living System (Advances in Experimental Medicine and Biology)*. New York: Plenum; 1998. p. 103-116.

Moon YJ, Wang X, Morris ME. Dietary Flavonoids: Effects on Xenobiotic and Carcinogen Metabolism. *Toxicol In Vitro*. 2006; 20: 187-210.

Moorthy NS, Singh RJ, Singh HP, Gupta SD. Synthesis, Biological Evaluation and in Silico Metabolic and Toxicity Prediction of Some Flavanone Derivatives. *Chem Pharm Bull (Tokyo)*. 2006; 54: 1384-1390.

Morita T, Tanabe H, Sugiyama K, Kasaoka S, Kiriya S. Dietary Resistant Starch Alters the Characteristics of Colonic Mucosa and Exerts a Protective Effect on Trinitrobenzene Sulfonic Acid-Induced Colitis in Rats. *Biosci Biotechnol Biochem*. 2004; 68: 2155-2164.

Morris EA, McDonald BS, Webb AC, Rosenwasser LJ. Identification of Interleukin-1 in Equine Osteoarthritic Joint Effusions. *Am J Vet Res*. 1990; 51: 59-64.

Morris GP, Beck PL, Herridge MS, Depew WT, Szewczuk MR, Wallace JL. Hapten-Induced Model of Chronic Inflammation and Ulceration in the Rat Colon. *Gastroenterology*. 1989; 96: 795-803.

Moulton PJ. Inflammatory Joint Disease: The Role of Cytokines, Cyclooxygenases and Reactive Oxygen Species. *Br J Biomed Sci*. 1996; 53: 317-324.

Muthyala RS, Ju YH, Sheng S, Williams LD, Doerge DR, Katzenellenbogen BS, Helferich WG, Katzenellenbogen JA. Equol, a Natural Estrogenic Metabolite from Soy Isoflavones: Convenient Preparation and Resolution of R- and S-Equols and Their Differing Binding and Biological Activity through Estrogen Receptors Alpha and Beta. *Bioorg Med Chem.* 2004; 12: 1559-1567.

Nadaud S, Soubrier F. Biologie Moleculaire Et Genetique Des No-Synthetases. *C R Soc Biol.* 1995; 189: 1025–1038.

Nakamaru K, Sugai T, Hongyo T, Sato M, Taniguchi S, Tanaka Y, Kawase S. [Effect of Mesalazine Microgranules on Experimental Colitis]. *Nippon Yakurigaku Zasshi.* 1994; 104: 303-311.

Nakamura J, Takada S, Ohtsuka N, Heya T, Yamamoto A, Kimura T, Sezaki H. An Assessment of Gastrointestinal Mucosal Damage in Vivo: Enhancement of Urinary Recovery after Oral Administration of Phenolsulfonphthalein in Ulcer Rats. *Chem Pharm Bull (Tokyo).* 1982; 30: 2291-2293.

Narvaez-Mastache JM, Novillo F, Delgado G. Antioxidant Aryl-Prenylcoumarin, Flavan-3-Ols and Flavonoids from *Eysenhardtia Subcoriacea*. *Phytochemistry.* 2007;

Neurath M, Fuss I, Strober W. Tnbs-Colitis. *Int Rev Immunol.* 2000; 19: 51-62.

Ng SC, Ong TT, Fu P, Ching CB. Enantiomer Separation of Flavour and Fragrance Compounds by Liquid Chromatography Using Novel Urea-Covalent Bonded Methylated Beta-Cyclodextrins on Silica. *J Chromatogr A.* 2002; 968: 31-40.

Nielsen SE, Breinholt V, Justesen U, Cornett C, Dragsted LO. In Vitro Biotransformation of Flavonoids by Rat Liver Microsomes. *Xenobiotica.* 1998; 28: 389-401.

Nielsen SE, Freese R, Kleemola P, Mutanen M. Flavonoids in Human Urine as Biomarkers for Intake of Fruits and Vegetables. *Cancer Epidemiol Biomarkers Prev.* 2002; 11: 459-466.

O'Brien J, Wilson I, Orton T, Pognan F. Investigation of the Alamar Blue (Resazurin) Fluorescent Dye for the Assessment of Mammalian Cell Cytotoxicity. *Eur J Biochem.* 2000; 267: 5421-5426.

Ogata S, Miyake Y, Yamamoto K, Okumura K, Taguchi H. Apoptosis Induced by the Flavonoid from Lemon Fruit (Citrus Limon Burm. F.) and Its Metabolites in HI-60 Cells. *Biosci Biotechnol Biochem.* 2000; 64: 1075-1078.

Ogiso T, Kasutani M, Tanaka H, Iwaki M, Tanino T. Pharmacokinetics of Epinastine and a Possible Mechanism for Double Peaks in Oral Plasma Concentration Profiles. *Biol Pharm Bull.* 2001; 24: 790-794.

Okamoto Y, Aburatani R, Fukumoto T, Hatada K. Useful Chiral Stationary Phases for Hplc. Amylose Tris(3,5-Dimethylphenylcarbamate) and Tris(3,5-Dichlorophenylcarbamate) Supported on Silica Gel. *Chem Lett.* 1987a; 1857-1860.

Okamoto Y, Aburatani R, Miura S, Hatada K. Chiral Stationary Phases for Hplc: Cellulose Tris(3,5-Dimethylphenylcarbamate) and Tris(3,5-Dichlorophenylcarbamate) Chemically Bonded to Silica Gel. *J Liq Chromatogr.* 1987b; 10: 1613-1628.

Okamoto Y, Kawashima M, Hatada K. Controlled Chiral Recognition of Cellulose Triphenylcarbamate Derivatives Supported on Silica Gel. *J Chromatogr.* 1986a; 363: 173-176.

Okamoto Y, Sakamoto H, Hatada K, Irie M. Resolution of Enantiomers by Hplc on Cellulose Trans- and Cis-Tris(4-Phenylazophenylcarbamate). *Chem Lett.* 1986b; 983-986.

Olszanecki R, Gebaska A, Kozlovski VI, Gryglewski RJ. Flavonoids and Nitric Oxide Synthase. *J Physiol Pharmacol*. 2002; 53: 571-584.

Otani T, Yamaguchi K, Scherl E, Du B, Tai HH, Greifer M, Petrovic L, Daikoku T, Dey SK, Subbaramaiah K, Dannenberg AJ. Levels of Nad(+)-Dependent 15-Hydroxyprostaglandin Dehydrogenase Are Reduced in Inflammatory Bowel Disease: Evidence for Involvement of Tnf-Alpha. *Am J Physiol Gastrointest Liver Physiol*. 2006; 290: G361-368.

Paiva NL, Sun Y, Dixon RA, VanEtten HD, Hrazdina G. Molecular Cloning of Isoflavone Reductase from Pea (*Pisum Sativum* L.): Evidence for a 3r-Isoflavanone Intermediate in (+)-Pisatin Biosynthesis. *Arch Biochem Biophys*. 1994; 312: 501-510.

Panasiak W, Wleklík M, Oraczewska A, Luczak M. Influence of Flavonoids on Combined Experimental Infections with Emc Virus and *Staphylococcus Aureus* in Mice. *Acta Microbiol Pol*. 1989; 38: 185-188.

Panico AM, Cardile V, Garufi F, Puglia C, Bonina F, Ronsisvalle G. Protective Effect of *Capparis Spinosa* on Chondrocytes. *Life Sci*. 2005; 77: 2479-2488.

Paredes A, Alzuru M, Mendez J, Rodriguez-Ortega M. Anti-Sindbis Activity of Flavanones Hesperetin and Naringenin. *Biol Pharm Bull*. 2003; 26: 108-109.

Parejo I, Viladomat F, Bastida J, Rosas-Romero A, Saavedra G, Murcia MA, Jimenez AM, Codina C. Investigation of Bolivian Plant Extracts for Their Radical Scavenging Activity and Antioxidant Activity. *Life Sci*. 2003; 73: 1667-1681.

Parejo I, Viladomat F, Bastida J, Schmeda-Hirschmann G, Burillo J, Codina C. Bioguided Isolation and Identification of the Nonvolatile Antioxidant Compounds from Fennel (*Foeniculum Vulgare* Mill.) Waste. *J Agric Food Chem*. 2004; 52: 1890-1897.

Park H, Jung S. Separation of Some Chiral Flavonoids by Microbial Cyclosophoraoses and Their Sulfated Derivatives in Micellar Electrokinetic Chromatography. *Electrophoresis*. 2005; 26: 3833-3838.

Park HJ, Kim MJ, Ha E, Chung JH. Apoptotic Effect of Hesperidin through Caspase3 Activation in Human Colon Cancer Cells, Snu-C4. *Phytomedicine*. 2007;

Peeters M, Ghoois Y, Maes B, Hiele M, Geboes K, Vantrappen G, Rutgeerts P. Increased Permeability of Macroscopically Normal Small Bowel in Crohn's Disease. *Dig Dis Sci*. 1994; 39: 2170-2176.

Pellati F, Benvenuti S, Magro L, Melegari M, Soragni F. Analysis of Phenolic Compounds and Radical Scavenging Activity of Echinacea Spp. *J Pharm Biomed Anal*. 2004; 35: 289-301.

Philp HA. Hot Flashes--a Review of the Literature on Alternative and Complementary Treatment Approaches. *Altern Med Rev*. 2003; 8: 284-302.

Pietta PG. Flavonoids as Antioxidants. *J Nat Prod*. 2000; 63: 1035-1042.

Proestos C, Chorianopoulos N, Nychas GJ, Komaitis M. Rp-Hplc Analysis of the Phenolic Compounds of Plant Extracts. Investigation of Their Antioxidant Capacity and Antimicrobial Activity. *J Agric Food Chem*. 2005; 53: 1190-1195.

Proksch P, Budzikiewicz H, Tanowitz BD, Smith DM. Flavonoids from the External Leaf Resin of Four Hemizonza Species (Asteraceae). *Phytochemistry*. 1984; 23: 679-680.

Rabau M, Eyal A, Dayan D. Histomorphometric Evaluation of Experimentally Induced Colitis with Trinitrobenzene-Sulphonic Acid in Rats. *Int J Exp Pathol*. 1996; 77: 175-179.

Rajadurai M, Prince PS. Preventive Effect of Naringin on Isoproterenol-Induced Cardiotoxicity in Wistar Rats: An in Vivo and in Vitro Study. *Toxicology*. 2007a; 232: 216-225.

Rajadurai M, Stanely Mainzen Prince P. Preventive Effect of Naringin on Cardiac Markers, Electrocardiographic Patterns and Lysosomal Hydrolases in Normal and Isoproterenol-Induced Myocardial Infarction in Wistar Rats. *Toxicology*. 2007b; 230: 178-188.

Ramesh N, Viswanathan MB, Saraswathy A, Balakrishna K, Brindha P, Lakshmanaperumalsamy P. Phytochemical and Antimicrobial Studies on *Drynaria Quercifolia*. *Fitoterapia*. 2001; 72: 934-936.

Rapavi E, Kocsis I, Feher E, Szentmihalyi K, Lugasi A, Szekely E, Blazovics A. The Effect of Citrus Flavonoids on the Redox State of Alimentary-Induced Fatty Liver in Rats. *Nat Prod Res*. 2007; 21: 274-281.

Rapavi E, Szentmihalyi K, Feher E, Lugasi A, Szekely E, Kurucz T, Pallai Z, Blazovics A. Effects of Citrus Flavonoids on Redox Homeostasis of Toxin-Injured Liver in Rat. *Acta Biol Hung*. 2006; 57: 415-422.

Raso GM, Meli R, Di Carlo G, Pacilio M, Di Carlo R. Inhibition of Inducible Nitric Oxide Synthase and Cyclooxygenase-2 Expression by Flavonoids in Macrophage J774a.1. *Life Sci*. 2001; 68: 921-931.

Razack R, Seidner DL. Nutrition in Inflammatory Bowel Disease. *Curr Opin Gastroenterol*. 2007; 23: 400-405.

Remsberg CM, Yanez JA, Ohgami Y, Vega-Villa KR, Rimando AM, Davies NM. Pharmacometrics of Pterostilbene: Pre-Clinical Pharmacokinetics and Metabolism, Anti-

Cancer, Anti-Inflammatory, Anti-Oxidant, and Analgesic Activity. *Phytother Res.* 2007; In Press.

Reuter BK, Asfaha S, Buret A, Sharkey KA, Wallace JL. Exacerbation of Inflammation-Associated Colonic Injury in Rat through Inhibition of Cyclooxygenase-2. *J Clin Invest.* 1996; 98: 2076-2085.

Rice-Evans CA, Miller NJ, Paganga G. Structure-Antioxidant Activity Relationships of Flavonoids and Phenolic Acids. *Free Radic Biol Med.* 1996; 20: 933-956.

Richelle M, Tavazzi I, Enslin M, Offord EA. Plasma Kinetics in Man of Epicatechin from Black Chocolate. *Eur J Clin Nutr.* 1999; 53: 22-26.

Ritschel WA, Kearns GL. Handbook of Basic Pharmacokinetics... Including Clinical Applications. 6th ed: APhA Publications; 2004.

Rotelli AE, Guardia T, Juarez AO, de la Rocha NE, Pelzer LE. Comparative Study of Flavonoids in Experimental Models of Inflammation. *Pharmacol Res.* 2003; 48: 601-606.

Roupe KA, Yanez JA, Teng XW, Davies NM. Pharmacokinetics of Selected Stilbenes: Rhapontigenin, Piceatannol and Pinosylvin in Rats. *J Pharm Pharmacol.* 2006; 58: 1443-1450.

Runkel M, Bourian M, Tegtmeier M, Legrum W. The Character of Inhibition of the Metabolism of 1,2-Benzopyrone (Coumarin) by Grapefruit Juice in Human. *Eur J Clin Pharmacol.* 1997; 53: 265-269.

Rusznayk S, Szent-Györgyi A. Vitamin P: Flavonols as Vitamins. *Nature.* 1936; 138: 27.

Sakata K, Hirose Y, Qiao Z, Tanaka T, Mori H. Inhibition of Inducible Isoforms of Cyclooxygenase and Nitric Oxide Synthase by Flavonoid Hesperidin in Mouse Macrophage Cell Line. *Cancer Lett.* 2003; 199: 139-145.

Samman S, Wall PM, Cook NC. Flavonoids and Coronary Heart Disease: Dietary Perspectives. In: Manthey J, Buslig B, editors. *Flavonoids in the Living System (Advances in Experimental Medicine and Biology)*. New York: Plenum Press; 1999. p. 469-481.

Sanchez-Rabaneda F, Jauregui O, Casals I, Andres-Lacueva C, Izquierdo-Pulido M, Lamuela-Raventos RM. Liquid Chromatographic/Electrospray Ionization Tandem Mass Spectrometric Study of the Phenolic Composition of Cocoa (*Theobroma Cacao*). *J Mass Spectrom*. 2003; 38: 35-42.

Santos JH, Meyer JN, Mandavilli BS, Van Houten B. Quantitative Pcr-Based Measurement of Nuclear and Mitochondrial DNA Damage and Repair in Mammalian Cells. *Methods Mol Biol*. 2006; 314: 183-199.

Santos KF, Oliveira TT, Nagem TJ, Pinto AS, Oliveira MG. Hypolipidaemic Effects of Naringenin, Rutin, Nicotinic Acid and Their Associations. *Pharmacol Res*. 1999; 40: 493-496.

Scalbert A, Manach C, Morand C, Remesy C, Jimenez L. Dietary Polyphenols and the Prevention of Diseases. *Crit Rev Food Sci Nutr*. 2005; 45: 287-306.

Schieber A, Keller P, Carle R. Determination of Phenolic Acids and Flavonoids of Apple and Pear by High-Performance Liquid Chromatography. *J Chromatogr A*. 2001; 910: 265-273.

Schindler R, Mentlein R. Flavonoids and Vitamin E Reduce the Release of the Angiogenic Peptide Vascular Endothelial Growth Factor from Human Tumor Cells. *J Nutr*. 2006; 136: 1477-1482.

Schmiedlin-Ren P, Edwards DJ, Fitzsimmons ME, He K, Lown KS, Woster PM, Rahman A, Thummel KE, Fisher JM, Hollenberg PF, Watkins PB. Mechanisms of Enhanced Oral Availability of Cyp3a4 Substrates by Grapefruit Constituents. Decreased Enterocyte Cyp3a4

Concentration and Mechanism-Based Inactivation by Furanocoumarins. *Drug Metab Dispos.* 1997; 25: 1228-1233.

Schramm DD, Karim M, Schrader HR, Holt RR, Kirkpatrick NJ, Polagruto JA, Ensunsa JL, Schmitz HH, Keen CL. Food Effects on the Absorption and Pharmacokinetics of Cocoa Flavanols. *Life Sci.* 2003; 73: 857-869.

Seril DN, Liao J, Yang GY, Yang CS. Oxidative Stress and Ulcerative Colitis-Associated Carcinogenesis: Studies in Humans and Animal Models. *Carcinogenesis.* 2003; 24: 353-362.

Setchell KD, Clerici C, Lephart ED, Cole SJ, Heenan C, Castellani D, Wolfe BE, Nechemias-Zimmer L, Brown NM, Lund TD, Handa RJ, Heubi JE. S-Equol, a Potent Ligand for Estrogen Receptor Beta, Is the Exclusive Enantiomeric Form of the Soy Isoflavone Metabolite Produced by Human Intestinal Bacterial Flora. *Am J Clin Nutr.* 2005; 81: 1072-1079.

Shah VP, Midha KK, Dighe S, McGilveray IJ, Skelly JP, Yacobi A, Layloff T, Viswanathan CT, Cook CE, McDowall RD, et al. Analytical Methods Validation: Bioavailability, Bioequivalence and Pharmacokinetic Studies. Conference Report. *Eur J Drug Metab Pharmacokinet.* 1991; 16: 249-255.

Shahidi F, Wanasundara PK. Phenolic Antioxidants. *Crit Rev Food Sci Nutr.* 1992; 32: 67-103.

Shargel L, Wu-Pong S, Yu ABC. Applied Biopharmaceutics & Pharmacokinetics 5th ed: McGraw-Hill Medical; 2004.

Shin YW, Bok SH, Jeong TS, Bae KH, Jeoung NH, Choi MS, Lee SH, Park YB. Hypocholesterolemic Effect of Naringin Associated with Hepatic Cholesterol Regulating Enzyme Changes in Rats. *Int J Vitam Nutr Res.* 1999; 69: 341-347.

Siewek VF, Galensa R, Ara V. Hochleistungsflussigkeitschromatographischer Nachweis Von Orangen Un Grapefruitsaftverfälschungen. *Die industrielle obst un gemu severwertung*. 1985; 70: 11-12.

Smith CJ. Non-Hormonal Control of Vaso-Motor Flushing in Menopausal Patients. *Chic Med*. 1964; 67: 193-195.

So FV, Guthrie N, Chambers AF, Moussa M, Carroll KK. Inhibition of Human Breast Cancer Cell Proliferation and Delay of Mammary Tumorigenesis by Flavonoids and Citrus Juices. *Nutr Cancer*. 1996; 26: 167-181.

Soldner A, Christians U, Susanto M, Wachter VJ, Silverman JA, Benet LZ. Grapefruit Juice Activates P-Glycoprotein-Mediated Drug Transport. *Pharm Res*. 1999; 16: 478-485.

Spiegelman BM, Flier JS. Adipogenesis and Obesity: Rounding out the Big Picture. *Cell*. 1996; 87: 377-389.

Srinivas NR. Evaluation of Experimental Strategies for the Development of Chiral Chromatographic Methods Based on Diastereomer Formation. *Biomed Chromatogr*. 2004; 18: 207-233.

Sroka Z, Fecka I, Cisowski W. Antiradical and Anti-H₂O₂ Properties of Polyphenolic Compounds from an Aqueous Peppermint Extract. *Z Naturforsch [C]*. 2005; 60: 826-832.

Stadler J, Stefanovic-Racic M, Billiar TR, Curran RD, McIntyre LA, Georgescu HI, Simmons RL, Evans CH. Articular Chondrocytes Synthesize Nitric Oxide in Response to Cytokines and Lipopolysaccharide. *J Immunol*. 1991; 147: 3915-3920.

Stefani ED, Boffetta P, Deneo-Pellegrini H, Mendilaharsu M, Carzoglio JC, Ronco A, Olivera L. Dietary Antioxidants and Lung Cancer Risk: A Case-Control Study in Uruguay. *Nutr Cancer*. 1999; 34: 100-110.

Stevens JC, Fayer JL, Cassidy KC. Characterization of 2-[[4-[[2-(1h-Tetrazol-5-Ylmethyl)Phenyl]Methoxy]Methyl]Quinoline N-Glucuronidation by in Vitro and in Vivo Approaches. *Drug Metab Dispos.* 2001; 29: 289-295.

Stewart AJ, Bozonnet S, Mullen W, Jenkins GI, Lean ME, Crozier A. Occurrence of Flavonols in Tomatoes and Tomato-Based Products. *J Agric Food Chem.* 2000; 48: 2663-2669.

Strober W, Fuss I, Boirivant M, Kitani A. Insights into the Mechanism of Oral Tolerance Derived from the Study of Models of Mucosal Inflammation. *Ann N Y Acad Sci.* 2004; 1029: 115-131.

Sudjaroen Y, Haubner R, Wurtele G, Hull WE, Erben G, Spiegelhalter B, Changbumrung S, Bartsch H, Owen RW. Isolation and Structure Elucidation of Phenolic Antioxidants from Tamarind (*Tamarindus Indica* L.) Seeds and Pericarp. *Food Chem Toxicol.* 2005; 43: 1673-1682.

Sugishita E, Amagaya S, Ogihara Y. Anti-Inflammatory Testing Methods: Comparative Evaluation of Mice and Rats. *J Pharmacobiodyn.* 1981; 4: 565-575.

Sun FF, Lai PS, Yue G, Yin K, Nagele RG, Tong DM, Krzesicki RF, Chin JE, Wong PY. Pattern of Cytokine and Adhesion Molecule Mrna in Hapten-Induced Relapsing Colon Inflammation in the Rat. *Inflammation.* 2001; 25: 33-45.

Surh YJ, Kundu JK. Cancer Preventive Phytochemicals as Speed Breakers in Inflammatory Signaling Involved in Aberrant Cox-2 Expression. *Curr Cancer Drug Targets.* 2007; 7: 447-458.

Suzgec S, Mericli AH, Houghton PJ, Cubukcu B. Flavonoids of *Helichrysum Compactum* and Their Antioxidant and Antibacterial Activity. *Fitoterapia.* 2005; 76: 269-272.

Szent-Györgyi A. From Vitamin C to Vitamin P. *Current Science.* 1936; 285-286.

Tan TY, Amor DJ. Obesity, Hypothyroidism, Craniosynostosis, Cardiac Hypertrophy, Colitis, and Developmental Delay: A Novel Syndrome. *Am J Med Genet A*. 2007; 143: 114-118.

Tanaka T, Kohno H, Murakami M, Shimada R, Kagami S, Sumida T, Azuma Y, Ogawa H. Suppression of Azoxymethane-Induced Colon Carcinogenesis in Male F344 Rats by Mandarin Juices Rich in Beta-Cryptoxanthin and Hesperidin. *Int J Cancer*. 2000; 88: 146-150.

Tanaka T, Makita H, Kawabata K, Mori H, Kakumoto M, Satoh K, Hara A, Sumida T, Fukutani K, Tanaka T, Ogawa H. Modulation of N-Methyl-N-Amylnitrosamine-Induced Rat Oesophageal Tumourigenesis by Dietary Feeding of Diosmin and Hesperidin, Both Alone and in Combination. *Carcinogenesis*. 1997a; 18: 761-769.

Tanaka T, Makita H, Kawabata K, Mori H, Kakumoto M, Satoh K, Hara A, Sumida T, Tanaka T, Ogawa H. Chemoprevention of Azoxymethane-Induced Rat Colon Carcinogenesis by the Naturally Occurring Flavonoids, Diosmin and Hesperidin. *Carcinogenesis*. 1997b; 18: 957-965.

Tereschuk ML, Baigori MD, De Figueroa LI, Abdala LR. Flavonoids from Argentine Tagetes (Asteraceae) with Antimicrobial Activity. *Methods Mol Biol*. 2004; 268: 317-330.

Tetlow LC, Adlam DJ, Woolley DE. Matrix Metalloproteinase and Proinflammatory Cytokine Production by Chondrocytes of Human Osteoarthritic Cartilage: Associations with Degenerative Changes. *Arthritis Rheum*. 2001; 44: 585-594.

Tirkey N, Pilkhwal S, Kuhad A, Chopra K. Hesperidin, a Citrus Bioflavonoid, Decreases the Oxidative Stress Produced by Carbon Tetrachloride in Rat Liver and Kidney. *BMC Pharmacol*. 2005; 5: 2.

Torres CA, Andrews PK, Davies NM. Physiological and Biochemical Responses of Fruit Exocarp of Tomato (*Lycopersicon Esculentum* Mill.) Mutants to Natural Photo-Oxidative Conditions. *J Exp Bot.* 2006; 57: 1933-1947.

Torres CA, Davies NM, Yanez JA, Andrews PK. Disposition of Selected Flavonoids in Fruit Tissues of Various Tomato (*Lycopersicon Esculentum* Mill.) Genotypes. *J Agric Food Chem.* 2005; 53: 9536-9543.

Totta P, Acconcia F, Leone S, Cardillo I, Marino M. Mechanisms of Naringenin-Induced Apoptotic Cascade in Cancer Cells: Involvement of Estrogen Receptor Alpha and Beta Signalling. *IUBMB Life.* 2004; 56: 491-499.

Treutter A, Galensa R, Feucht W, Schmid PPS. Flavanone Glucosides in Callus and Phloem of *Prunus Avium*: Identification and Stimulation of Their Synthesis. *Physiol Plant.* 1985; 65: 95-101.

Tuzun A, Erdil A, Inal V, Aydin A, Bagci S, Yesilova Z, Sayal A, Karaeren N, Dagalp K. Oxidative Stress and Antioxidant Capacity in Patients with Inflammatory Bowel Disease. *Clin Biochem.* 2002; 35: 569-572.

Uchiyama N, Kim IH, Kawahara N, Goda Y. Hplc Separation of Hesperidin and the C-2 Epimer in Commercial Hesperidin Samples and Herbal Medicines. *Chirality.* 2005; 17: 373-377.

Ullmann U, Haller J, Decourt JP, Girault N, Girault J, Richard-Caudron AS, Pineau B, Weber P. A Single Ascending Dose Study of Epigallocatechin Gallate in Healthy Volunteers. *J Int Med Res.* 2003; 31: 88-101.

USDA. Usda Database for the Flavonoid Content of Selected Foods. 2003 March 25, 2003 [cited April 9, 2007]; Available from:

<http://www.nal.usda.gov/fnic/foodcomp/Data/Flav/flav.html>

Uzel A, Sorkun K, Oncag O, Cogulu D, Gencay O, Salih B. Chemical Compositions and Antimicrobial Activities of Four Different Anatolian Propolis Samples. *Microbiol Res.* 2005; 160: 189-195.

Vagefi PA, Longo WE. Colorectal Cancer in Patients with Inflammatory Bowel Syndrome. *Clinical Colorectal Cancer.* 2005; 4: 313-319.

van Acker FA, Schouten O, Haenen GR, van der Vijgh WJ, Bast A. Flavonoids Can Replace Alpha-Tocopherol as an Antioxidant. *FEBS Lett.* 2000; 473: 145-148.

Van Amelsvoort JM, Van Hof KH, Mathot JN, Mulder TP, Wiersma A, Tijburg LB. Plasma Concentrations of Individual Tea Catechins after a Single Oral Dose in Humans. *Xenobiotica.* 2001; 31: 891-901.

van de Loo AA, van den Berg WB. Effects of Murine Recombinant Interleukin 1 on Synovial Joints in Mice: Measurement of Patellar Cartilage Metabolism and Joint Inflammation. *Ann Rheum Dis.* 1990; 49: 238-245.

van de Loo FA, Joosten LA, van Lent PL, Arntz OJ, van den Berg WB. Role of Interleukin-1, Tumor Necrosis Factor Alpha, and Interleukin-6 in Cartilage Proteoglycan Metabolism and Destruction. Effect of in Situ Blocking in Murine Antigen- and Zymosan-Induced Arthritis. *Arthritis Rheum.* 1995; 38: 164-172.

van den Broucke CO, Dommisse RA, Esmans EL, Lemli JA. Three Methylated Flavones from *Thymus Vulgaris*. *Phytochemistry.* 1982; 21: 2581-2583.

van der Kraan PM, van den Berg WB. Anabolic and Destructive Mediators in Osteoarthritis. *Curr Opin Clin Nutr Metab Care*. 2000; 3: 205-211.

van het Hof KH, Kivits GA, Weststrate JA, Tijburg LB. Bioavailability of Catechins from Tea: The Effect of Milk. *Eur J Clin Nutr*. 1998; 52: 356-359.

van Meeuwen JA, Korthagen N, de Jong PC, Piersma AH, van den Berg M. (Anti)Estrogenic Effects of Phytochemicals on Human Primary Mammary Fibroblasts, MCF-7 Cells and Their Co-Culture. *Toxicol Appl Pharmacol*. 2007; 221: 372-383.

Vanamala J, Leonardi T, Patil BS, Taddeo SS, Murphy ME, Pike LM, Chapkin RS, Lupton JR, Turner ND. Suppression of Colon Carcinogenesis by Bioactive Compounds in Grapefruit. *Carcinogenesis*. 2006; 27: 1257-1265.

Vega-Villa KR, Yanez JA, Remsberg CM, Ohgami Y, Davies NM. Stereospecific High-Performance Liquid Chromatographic Validation of Homoeriodictyol in Serum and Yerba Santa (*Eriodictyon glutinosum*). *J Pharm Biomed Anal*. 2007;

Vinegar R, Truax JF, Selph JL. Quantitative Studies of the Pathway to Acute Carrageenan Inflammation. *Fed Proc*. 1976; 35: 2447-2456.

Vinegar R, Truax JF, Selph JL, Voelker FA. Pathway of Onset, Development, and Decay of Carrageenan Pleurisy in the Rat. *Fed Proc*. 1982; 41: 2588-2595.

Voronov E, Carmi Y, Apte RN. Role of IL-1-Mediated Inflammation in Tumor Angiogenesis. *Adv Exp Med Biol*. 2007; 601: 265-270.

Wang H, Nair MG, Strasburg GM, Booren AM, Gray JJ. Antioxidant Polyphenols from Tart Cherries (*Prunus cerasus*). *J Agric Food Chem*. 1999; 47: 840-844.

Wang HK, Xia Y, Yang ZY, Natschke SL, Lee KH. Recent Advances in the Discovery and Development of Flavonoids and Their Analogues as Antitumor and Anti-Hiv Agents. *Adv Exp Med Biol.* 1998; 439: 191-225.

Wang XL, Hur HG, Lee JH, Kim KT, Kim SI. Enantioselective Synthesis of S-Equol from Dihydrodaidzein by a Newly Isolated Anaerobic Human Intestinal Bacterium. *Appl Environ Microbiol.* 2005a; 71: 214-219.

Wang XL, Shin KH, Hur HG, Kim SI. Enhanced Biosynthesis of Dihydrodaidzein and Dihydrogenistein by a Newly Isolated Bovine Rumen Anaerobic Bacterium. *J Biotechnol.* 2005b; 115: 261-269.

Whaley WL, Rummel JD, Kastropeli N. Interactions of Genistein and Related Isoflavones with Lipid Micelles. *Langmuir.* 2006; 22: 7175-7184.

Whittle BJ, Cavicchi M, Lamarque D. Assessment of Anticolitic Drugs in the Trinitrobenzene Sulfonic Acid (Tnbs) Rat Model of Inflammatory Bowel Disease. *Methods Mol Biol.* 2003; 225: 209-222.

Wilcox LJ, Borradaile NM, Huff MW. Antiatherogenic Properties of Naringenin, a Citrus Flavonoid. *Cardiovasc Drug Rev.* 1999; 17: 160-178.

Wilmsen PK, Spada DS, Salvador M. Antioxidant Activity of the Flavonoid Hesperidin in Chemical and Biological Systems. *J Agric Food Chem.* 2005; 53: 4757-4761.

Wistuba D, Trapp O, Gel-Moreto N, Galensa R, Schurig V. Stereoisomeric Separation of Flavanones and Flavanone-7-O-Glycosides by Capillary Electrophoresis and Determination of Interconversion Barriers. *Anal Chem.* 2006; 78: 3424-3433.

Wright MR, Davies NM, Jamali F. Toxicokinetics of Indomethacin-Induced Intestinal Permeability in the Rat. *Pharmacol Res.* 1997; 35: 499-504.

Xagorari A, Papapetropoulos A, Mauromatis A, Economou M, Fotsis T, Roussos C. Luteolin Inhibits an Endotoxin-Stimulated Phosphorylation Cascade and Proinflammatory Cytokine Production in Macrophages. *J Pharmacol Exp Ther.* 2001; 296: 181-187.

Xie WL, Chipman JG, Robertson DL, Erikson RL, Simmons DL. Expression of a Mitogen-Responsive Gene Encoding Prostaglandin Synthase Is Regulated by Mrna Splicing. *Proc Natl Acad Sci U S A.* 1991; 88: 2692-2696.

Yamada M, Tanabe F, Arai N, Mitsuzumi H, Miwa Y, Kubota M, Chaen H, Kibata M. Bioavailability of Glucosyl Hesperidin in Rats. *Biosci Biotechnol Biochem.* 2006; 70: 1386-1394.

Yanez JA, Andrews PK, Davies NM. Methods of Analysis and Separation of Chiral Flavonoids. *J Chromatogr B Analyt Technol Biomed Life Sci.* 2007a; 848: 159-181.

Yanez JA, Davies NM. Stereospecific High-Performance Liquid Chromatographic Analysis of Naringenin in Urine. *J Pharm Biomed Anal.* 2005a; 39: 164-169.

Yanez JA, Forrest ML, Ohgami Y, Kwon GS, Davies NM. Pharmacometrics and Delivery of Novel Nanoformulated Peg-B-Poly(Epsilon-Caprolactone) Micelles of Rapamycin. *Cancer Chemother Pharmacol.* 2007b;

Yanez JA, Fukuda C, Davies NM. Naringenin and Naringin: Anti-Cancer Activity and Stereospecific Disposition in Rats, Humans, and Fruit Juices American Association of Pharmaceutical Sciences (AAPS) Annual Meeting; 2005b; Nashville, TN: AAPS Journal; 2005b. p. T3262.

Yanez JA, Fukuda C, Roupe KA, Davies NM. Hesperetin and Hesperidin: Anti-Cancer Activity and Stereospecific Disposition in Rats, Humans, and Citrus Fruit Juices. American

Association of Pharmaceutical Sciences (AAPS) Annual Meeting; 2005c; Nashville, TN:
AAPS Journal; 2005c. p. T3264.

Yanez JA, Miranda ND, Remsberg CM, Ohgami Y, Davies NM. Stereospecific High-Performance Liquid Chromatographic Analysis of Eriodictyol in Urine. *J Pharm Biomed Anal.* 2006a;

Yanez JA, Miranda ND, Remsberg CM, Ohgami Y, Davies NM. Stereospecific High-Performance Liquid Chromatographic Analysis of Eriodictyol in Urine. *J Pharm Biomed Anal.* 2007c; 43: 255-262.

Yanez JA, Miranda ND, Villa-Romero KS, Ohgami Y, Davies NM. Stereospecific Disposition and Anti-Cancer/Anti-Oxidant Activity of the Chiral Flavonoids Eriocitrin and Eriodictyol. In: (IUPHAR) IUoP, editor. The 15th World Congress of Pharmacology; 2006b; Beijing, China: Acta Pharmacologica Sinica; 2006b. p. 219.

Yanez JA, Teng XW, Roupe KA, Davies NM. Alternative Methods for Assessing Experimental Colitis in Vivo and Ex Vivo. *Journal of Medical Sciences.* 2006c; 6: 356-365.

Yanez JA, Teng XW, Roupe KA, Davies NM. Stereospecific High-Performance Liquid Chromatographic Analysis of Hesperetin in Biological Matrices. *J Pharm Biomed Anal.* 2005d; 37: 591-595.

Yang CY, Tsai SY, Chao PDL, Yen HF, Chien TM, Hsiu SL. Determination of Hesperetin and Its Conjugate Metabolites in Serum and Urine. *Journal of Food and Drug Analysis.* 2002; 10: 143-148.

Yang M, Tanaka T, Hirose Y, Deguchi T, Mori H, Kawada Y. Chemopreventive Effects of Diosmin and Hesperidin on N-Butyl-N-(4-Hydroxybutyl)Nitrosamine-Induced Urinary-Bladder Carcinogenesis in Male Icr Mice. *Int J Cancer.* 1997; 73: 719-724.

Yeh CC, Kao SJ, Lin CC, Wang SD, Liu CJ, Kao ST. The Immunomodulation of Endotoxin-Induced Acute Lung Injury by Hesperidin in Vivo and in Vitro. *Life Sci.* 2007; 80: 1821-1831.

Yeum CH, Choi JS. Effect of Naringin Pretreatment on Bioavailability of Verapamil in Rabbits. *Arch Pharm Res.* 2006; 29: 102-107.

Young JM, De Young LM. Cutaneous Models of Inflammation for the Evaluation of Topical and Systemic Pharmacological Agents. In: Spector J, Back N, editors. *Pharmacological Methods in the Control of Inflammation.* New York: Liss; 1989. p. 215–231.

Yu J, Wang L, Walzem RL, Miller EG, Pike LM, Patil BS. Antioxidant Activity of Citrus Limonoids, Flavonoids, and Coumarins. *J Agric Food Chem.* 2005; 53: 2009-2014.

Zhang H, Wong CW, Coville PF, Wanwimolruk S. Effect of the Grapefruit Flavonoid Naringin on Pharmacokinetics of Quinine in Rats. *Drug Metabol Drug Interact.* 2000; 17: 351-363.

Zhang J, Brodbelt JS. Screening Flavonoid Metabolites of Naringin and Narirutin in Urine after Human Consumption of Grapefruit Juice by Lc-Ms and Lc-Ms/Ms. *Analyst.* 2004; 129: 1227-1233.

Zhang X, Hung TM, Phuong PT, Ngoc TM, Min BS, Song KS, Seong YH, Bae K. Anti-Inflammatory Activity of Flavonoids from *Populus Davidiana*. *Arch Pharm Res.* 2006a; 29: 1102-1108.

Zhang X, Thuong PT, Min BS, Ngoc TM, Hung TM, Lee IS, Na M, Seong YH, Song KS, Bae K. Phenolic Glycosides with Antioxidant Activity from the Stem Bark of *Populus Davidiana*. *J Nat Prod.* 2006b; 69: 1370-1373.

Zheng Q, Hirose Y, Yoshimi N, Murakami A, Koshimizu K, Ohigashi H, Sakata K, Matsumoto Y, Sayama Y, Mori H. Further Investigation of the Modifying Effect of Various Chemopreventive Agents on Apoptosis and Cell Proliferation in Human Colon Cancer Cells. *J Cancer Res Clin Oncol*. 2002; 128: 539-546.

Zhou L, Li D, Wang J, Liu Y, Wu J. Antibacterial Phenolic Compounds from the Spines of *Gleditsia Sinensis* Lam. *Nat Prod Res*. 2007; 21: 283-291.

Zhu BT, Taneja N, Loder DP, Balentine DA, Conney AH. Effects of Tea Polyphenols and Flavonoids on Liver Microsomal Glucuronidation of Estradiol and Estrone. *J Steroid Biochem Mol Biol*. 1998; 64: 207-215.